Vanadium and Molybdenum Complexes with Amino Acid Functionalized Ligands

DISSERTATION

zur Erlangung des akademischen Grades doctor rerum naturalium

(Dr. rer. nat.)

vorgelegt dem Rat der Chemisch-Geowissenschaftlichen Fakultät der

Friedrich-Schiller Universität Jena

von Food Chemist Manjola Mancka

geboren am 17.04.1978

in Devoll, Albania

Gutachter

1. Prof. Dr. Winfried Plass

2. Prof. Dr. Matthias Westernhausen

Tag der öffentlichen Verteidigung: October 18^{th} 2006

For my beloved parents and my Family

Acknowledgements

- I would like to express my heartfelt gratitude to my supervisor Prof. Dr. Winfried Plass for giving me the opportunity to work in this interesting field, I thank him for support, advises and guidance.

- I also thank to Dr. Axel Buchholz, for many valuable suggestions, for much help in the single crystal analysis, and for his help in the arrangement of the thesis.

- I am grateful to our research group with whom I had the pleasure of working, for their friendship, helpful discussions, and the good co-operative atmosphere. I also thank to my colleague Arne Roth for helping me in solving LaTeX problems. I would like to thank Ines Seidel for many valuable discussions about the kinetic experiments.

- I moreover thank all Technical assistants of the Institut für Anorganische und Analytische Chemie (IAAC) and NMR department for analyses of the samples: Dr. Popitz, Frau Schönau und Frau Heineck (MS), Frau Rambach und Dr. Friedrich (NMR, EPR), Frau Lentvogt und Frau Schönfeld (CHN).

- Many thanks to Lotte Neupert for the HPLC measurements.

- I am especially pleased to acknowledge Dr. Helmar Görls for measuring my X-ray crystal structures.

- Finally, I would like to thank my parents Seri and Hava, my sisters Anila and Amoleza, as well as my brother Ardi, especially my husband, Anton, for their continued moral support, patience and encouragement. They are the most important people in my life and they have been with me every step of the way.

Contents

Chapter 1

Introduction

1.1 History of vanadium

Vanadium was first discovered in 1801 by Andrés Manuel del Rio, a Spanish professor of mineralogy working in Mexico City. He originally named the element panchromium after the various color of its salts, but later renamed it erythronium because of the red color generated upon heating. Unfortunately, del Rio lost confidence in his discovery, thinking that he had found the element chromium, which had recently been discovered by the Frenchman Fourcroy. Vanadium was rediscovered in 1831 by the Swede Nils Gabriel Sefström. Its present name is derived from the Vanadis, the goddess of love and beauty of Norse mythology. Metallic vanadium was not isolated until 1867 when Sir Henry Enfield Roscoe, Professor of Chemistry at Owens College (later the University of Manchester), reduced vanadium chloride (VCl_5) with gaseous hydrogen to give vanadium metal and HCl. Natural vanadium is a mixture of two isotopes, ^{51}V (99.76%) and ^{50}V (0.24%), the latter being slightly radioactive with a half-life of $>3.9 \times 10^{17}$ years. Important sources of the metal are the minerals carnotite [$K_2(UO_2)_2(VO_4)_2$] and vanadinite [$Pb(VO_4)_3Cl$]. It is also present in some crude oils in the form of organic complexes. Vanadium occurs with an abundance of 0.014% in the earths crust and is widespread. The element is the second most abundant transition metal in the oceans (50 nM). Some aquatic organisms are known to accumulate vanadium. However, the actual function of vanadium and the nature of the vanadium compounds present in these organisms remains unclear.[1]

In 1983, a naturally occurring vanadium-containing enzyme, vanadium bromoperoxidase

Figure 1.1: A tunicate (*Clavelina Puertosecensis*) discovered near Discovery Bay, Jamaica.[2]

(V-BrPO), was discovered in the marine brown alga *Ascophyllum nodosum*.[3] Since then, several vanadium haloperoxidases have been isolated and studied, many of these enzymes have been detected in brown and red seaweeds.[4,5] However, the accumulation of vanadium is not restricted to marine organisms, since vanadium containing haloperoxidases have also been isolated from terrestrial fungi *Curvularia Inaequalis*[6] and a vanadium compound of low molecular weight (amavadin) has been isolated from the toadstool *Amanita muscaria*.[7]

The chemistry of vanadium is characterized by multiple oxidation state ranging from -3 to +5, but with the exception of –2. Of the common oxidation states only the three highest, i.e. +3, +4 and +5, are important in biological systems.[8] Under ordinary conditions, the +4 and +5 oxidation states are the most stable ones. The majority of vanadium(IV) compounds contain the VO^{2+} unit (vanadyl ion). These complexes typically have square planar pyrimidal or bipyrimidal geometries with an axial oxo ligand. The coordination chemistry of vanadium(V) compounds is dominated by oxo complexes, containing the VO^{3+} or the VO_2^+ moiety. V^{4+} and V^{5+} ions are very small with radii of 0.61 Å, and 0.59 Å, respectively. Due to the d^1 configuration of vanadium(IV) ions, these are easily identified by EPR spectroscopy. Typical eight-line patterns are observed due to hyperfine interaction of the ^{51}V nucleus (I = 7/2). V(V) is EPR silent due to its d^0 state. Vanadium(V) complexes are therefore diamagnetic, which makes them appropriate for NMR analyses. Especially ^{51}V NMR is a useful tool in the characterisation

of vanadium(V) complexes, since the chemical shifts are very sensitive to the nature of the coordination sphere of the metal.[9,10]

1.2 Vanadium haloperoxidases

Three classes of haloperoxidases have been identified. One of these consists of enzymes without a prosthetic group and as such have been detected in a number of bacteria.[11] The remaining two classes are heme-containing haloperoxidases exemplified by the ClPOs from the fungus *Caldariomyces fumago*[12] or myeloperoxidase which is present in white blood cells[13] and the vanadium-containing haloperoxidases. Enzymes representing these two classes not only differ in the nature of their prosthetic group but also in at least two other aspects: catalytic mechanism and stability. Heme-containing peroxidases catalyze the formation of the hypohalous acid by a redox mechanism, whereas in vanadate containing haloperoxidases the transition metal does not change its redox state[14,15] but may function as a Lewis acid. Vanadium haloperoxidases are enzymes that catalyse the oxidation of a halide by hydrogen peroxide to the corresponding hypohalous acids (or to a related two-electron oxidised halogenating intermediate such as OX^-, X_3^- and X^+). In the presence of suitable nucleophilic acceptors, halogenated compounds are formed according to :

$$H_2O_2 + X^- + H^+ \longrightarrow H_2O + HOX$$
$$HOX + \text{Org-H} \longrightarrow \text{Org-X} + H_2O$$

Vanadate containing haloperoxidases not only posses a very high stability[16] but they also resist a high concentration of their substrate (H_2O_2) and their product (HOX)[16] that would readily inactivate the heme-containing peroxidases. In addition they are much more resistant toward heat, detergent, and solvent denaturation. The major drawback of all haloperoxidases including the stable V-HPOs is that they are mainly active at mildly acidic pH values, whereas for many applications activity at mildly alkaline pH values is required.

The enzymes are named after the most electronegative halide ion they are able to oxidize. Thus vanadium chloroperoxidases (V-ClPOs) can oxidize chloride, bromide and iodide, while vanadium bromoperoxidases (V-BrPOs) can oxidize bromide and iodide. Iodoperoxidase merely catalyses the oxidation of iodide. Hydrogen peroxide does not have the driving force to oxidize fluoride, however a fluorinating enzyme, fluorinase, has recently been isolated and is proposed to act by an S_N2 mechanism.[17]

Vanadium chloroperoxidase enzymes are the most studied vanadium-containing enzymes and crystal structure determination of the azide-substituted form, the apo-form (metal free) and the tungstate-containing enzyme are available.[18] These have been found in the terrestrial fungi *Curvularia inaequalis*.

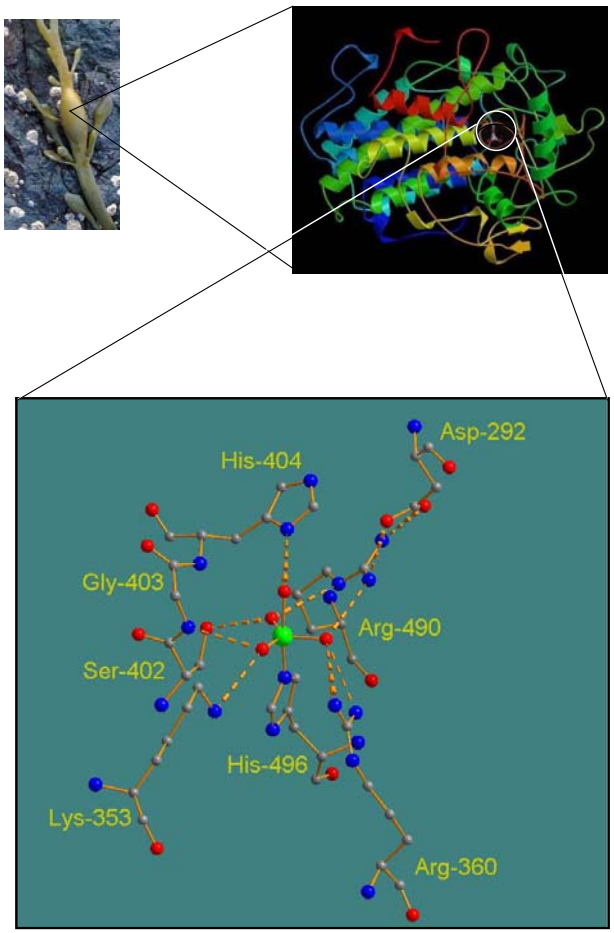

Figure 1.2: Schematic representation of the structure and active site of the V-ClPO isolated from the terrestrial fungi *Curvularia inaequalis*.

The first crystal structure of the native form of the enzyme was reported in 1996 by Messerschmidt and Wever (Figure 1.2).[19] The X-ray structure revealed vanadate as the prosthetic group linked to the protein through only one covalently bond to the imidazole of the histidine residue (His496). It was proposed that, vanadium(V) has a trigonal bipyramidal geometry with three non-proteinous oxygen atoms in the equatorial plane and the fourth one at the apical position postulated as OH group (V–O 193 pm). An extensive hydrogen bonding interaction is observed, that is capable of fixing the vanadate in the protein shell. The equatorial oxygen atoms of the prosthetic group are in hydrogen bonding contact with positively charged amino acid residues, such as Lys353, Arg360 and Arg490. The lysine and one arginine amino acid are also used to compensate for the negative charge of the vanadate moiety. Moreover, the Arg490 residue is further stabilized and kept close to the active binding site by the formation of a salt-bridge with an aspartate residue, namely Asp292. Other key residues in the active site are Gly403 and Ser402, also forming hydrogen bonds with the equatorial oxygen atoms. Furthermore the His404 residue is the single amino acid hydrogen bonded to the apical hydroxyl group.

The active site of vanadium chloroperoxidase (V-ClPO), revealed the vanadate coordinated at the top of one of the two four–helix bundles in a broad channel, which is lined on one half with predominantly polar residues and several main-chain carbonyl oxygens. The other half of the channel is hydrophobic, containing Pro-47, Pro-211, Trp-350, Phe-393, Pro-395, Pro-396, and Phe-397 (see Figure 1.3).
All these amino acids play a very important role in the chloroperoxidase activity.

The vanadate as the prosthetic group of vanadium haloperoxidases, has been found to be vital for the catalytic reaction, since its removal or reduction leads an inactive apoprotein derivate.[4,14] Replacement of vanadate with molybdate did not restore the haloperoxidase activity of the enzyme,[14] although the protein environment of the V-HPO enzymes was capable to bind molybdate.[18]

Besides the X-ray structure of the native enzyme, the structure of the peroxide intermediate in V-ClPO was also determined.[19] The trigonal-bipyrimidal arrangement is converted to tetragonal-pyrimidal upon addition of H_2O_2 (Figure 1.4). The oxo group is now placed in the apical position, whereas the peroxo ligand is located in the tetragonal plane. Also in the peroxide form an extensive hydrogen-bonding network is present. One

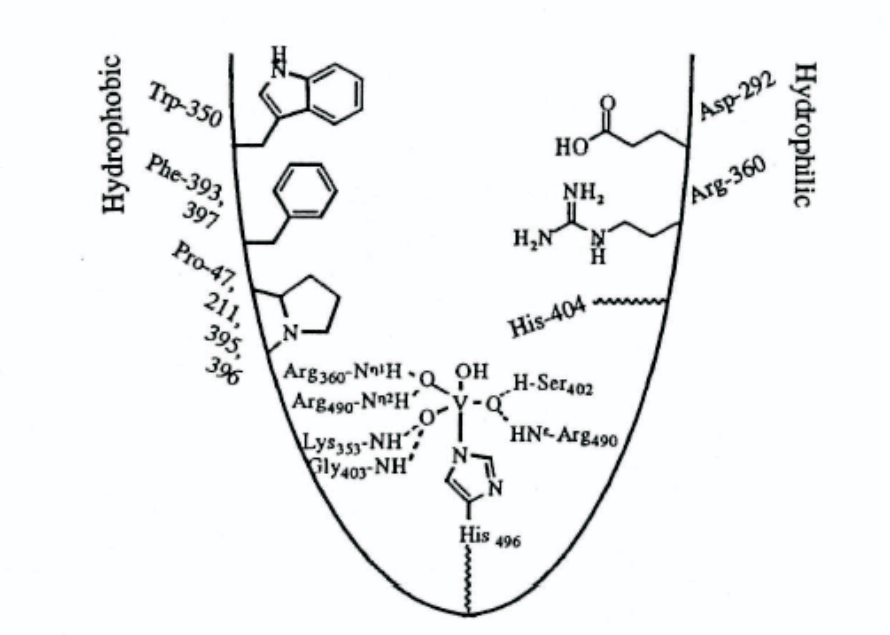

Figure 1.3: Active side channel of V-HPO enzyme

oxygen of the peroxo group is hydrogen-bonded to the nitrogen of Lys-353 and to the amide nitrogen of Gly-403.

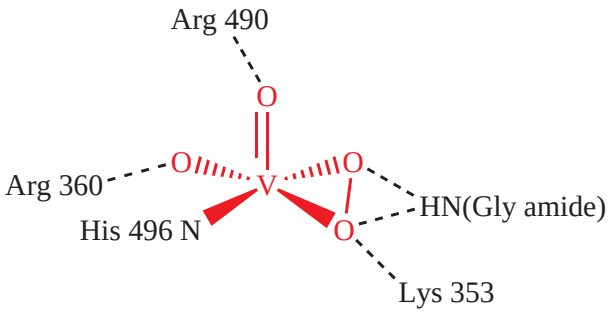

Figure 1.4: The peroxo vanadium site in V-ClPO.[19]

The second peroxo oxygen is also linked to this glycine nitrogen. The other oxygens form hydrogen bonds to Ser-402 and Arg-490, respectively, and to the arginine residues Arg-360 and Arg-490, respectively. A catalytic mechanism has been proposed by Messerschmidt and Wever[19] which is depicted in Figure 1.5. The apical hydroxy unit is hydrogen bonded to a histidine residue (His404) in a protein environment. This hydrogen bond makes the –OH group more nucleophilic. When a peroxide molecule approaches the active site,

the –OH unit is protonated and $–H_2O$ is generated. The weakly ligated water molecule dissociates from the vanadium ion and a side-on bound peroxide intermediate is formed after the departure of another water molecule.

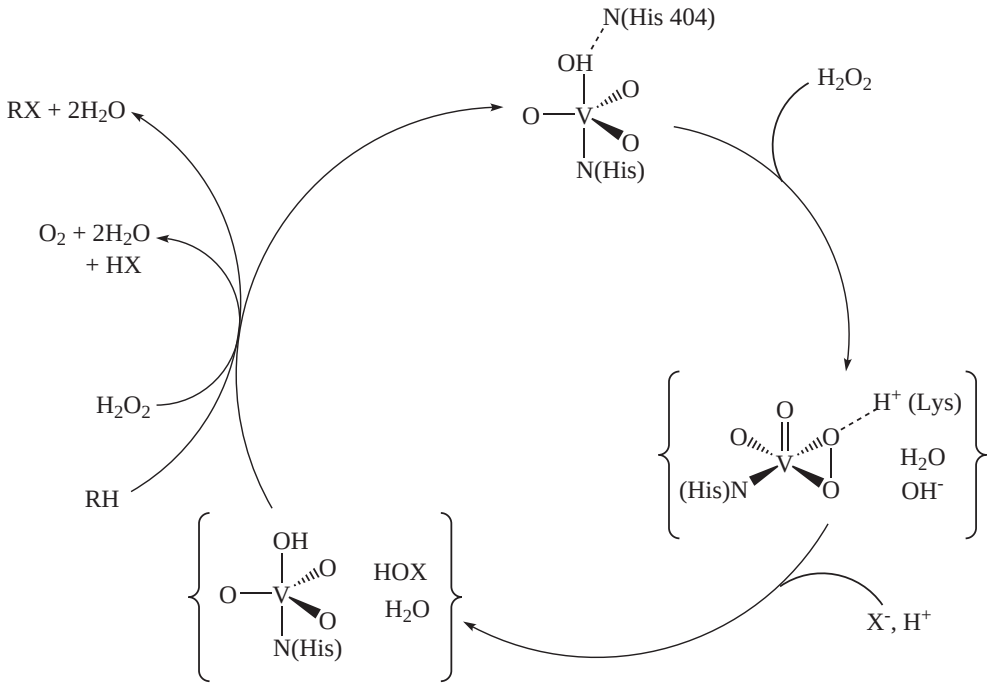

Figure 1.5: Proposed catalytic mechanism of V-ClPO.

Subsequently, attack of a halide ion at one of the peroxo atoms and the uptake of a proton from a surrounding water molecule leads to the generation of hypohalous acid (HOX) and restoration of the native state. At higher acid concentrations, the halogenation activity was inhibited. It was assumed that this is due to protonation of His404.[20] As a result, the formation of the peroxide form does not occur, since it is now impossible for the histidine residue to form a hydrogen bond to the apical OH group. As a consequence, this hydroxy unit loses its ability to activate the H_2O_2 by deprotonation and therefore the peroxide can not be bound to the vanadium ion.

Vanadium haloperoxidases have been shown to catalyse the bromination of various organic substrates[21,22], including monochlorodimedone (MCD, 2-chloro-5,5-dimethyl-1,3-dimedone), which is the standard assay used to evaluate haloperoxidase activity (Figure 1.6). The halogenation of MCD is followed spectrophotometrically at 290 nm which monitors the loss of MCD in the enol form. In addition, phenol red can be used

as organic substrate for oxidative bromination, resulting in the formation of bromphenol blue.[23,24]

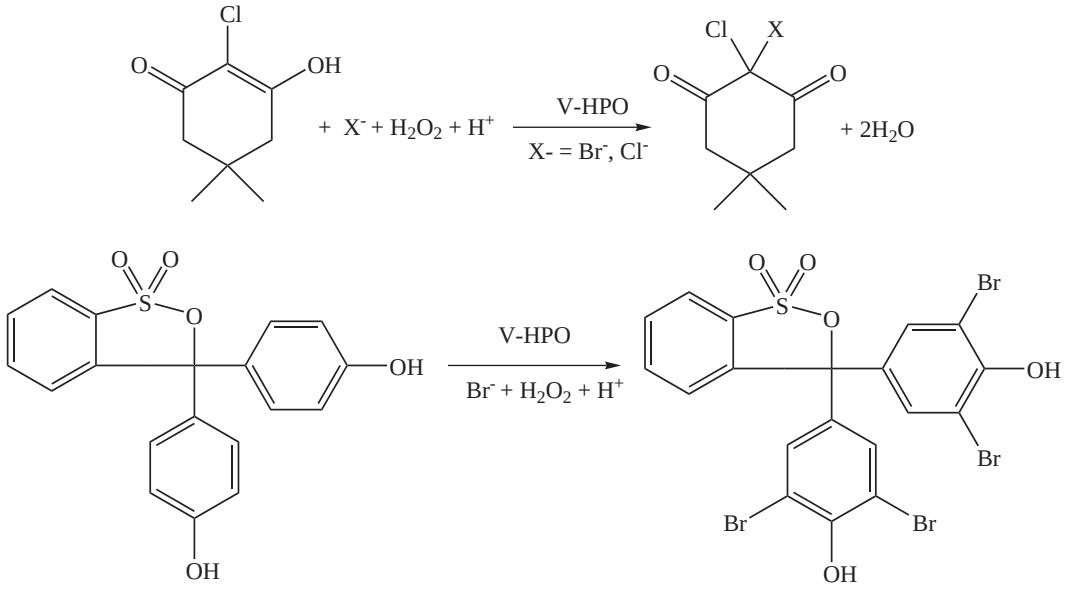

Figure 1.6: Halogenation of MCD (upper reaction) or phenol red (lower reaction) from by V-HPOs. These are used as standard substrate in haloperoxidase activity determinations.

Vanadate-dependent haloperoxidases are also capable of recognizing substrates with a specific chirality: it has been demonstrated that these enzymes mediate enantioselective sulfoxidation by hydrogen peroxide.[25–27] Thus, the asymmetric oxidation of bicyclic aromatic sulfides with hydrogen peroxide as oxidant by bromoperoxidase from the seaweed *Corallina officinalis* yields the corresponding (S)–sulfoxides with high enantiomeric excess (ee), while this enzyme is not able to oxidize methyl phenyl sulfide at all.[25,27] If, however, this reaction is mediated by the bromoperoxidase from the brown seaweed *Ascophyllum nodosum*, the R–enantiomer of the sulfoxide is in 91% ee, under slightly acidic conditions.[28] The sulfoxide with the opposite configuration was obtained (30% ee, 45% yield) in the oxidation mediated by the bromoperoxidase from the red seaweed *Corallina pilulifera*.[26] In contrast, use of the chloroperoxidase from the mold *Curvularia inaequalis* or of recombinant chloroperoxidases led to racemic mixtures.[26] This difference in reactivity suggests a specific orientation of the substrate in the vicinity of the active sites,[29] even though the molecular structures of the chloroperoxidase from *Curvularia inaequalis*[19] and the bromoperoxidase from *Ascophyllum nodosum*[30] revealed a high

degree of amino acid homology in the active sites, with the only difference being the replacement of His411 by Phe397.

1.3 Phosphate-Vanadate-Analogy

The wide spread physiological effects of vanadium are mainly attributed to the similarity between its anionic form, vanadate(V), and phosphate. But there are also important differences between these two anions. At physiological pH values monovanadate is found as doubly protonated $[VO_2(OH)_2]$ species, whereas phosphate occurs in the monoprotonated form HPO_4^{2-}. This is also important for possible mechanisms of the transport systems for these two anions.[31] In addition vanadium is easily reduced under physiological conditions to yield cationic species. The third difference is given by the pronounced ability of vanadium to adopt higher coordination numbers. The higher coordinative flexibility of vanadium can deliberately be used for the structural characterization of phosphate metabolizing enzymes. The crystal structures of several stable enzyme aggregates of phosphatases with vanadate as transition state analog have been reported. An interesting example are the protein tyrosine phosphatases,[32,33] which are involved in signal transduction mechanisms for controlling and regulating intracellular processes (e.g. the insulin receptor system), in this context it is worth noting that vanadate complexes show insulin-enhancing effects. In these aggregates the vanadate is in a trigonal bipyramidal coordination gwomwtry and linked to the protein with a single axial bound cysteine residue, whereas the oxygen atoms of the vanadate moiety are involved in a hydrogen bonding network.

A similar structure is found for the active site of rat prostatic acid phosphatase with the complexed transition state analog vanadate (Figure 1.7).[34] In this case the vanadate is linked to the protein through an axial bound histidine residue. Striking similarities are observed for the vanadium haloperoxidases - e.g. the chloroperoxidase of the fungus *Curvularia inaequalis*.[18,19] As in the case of the rat prostatic acid phosphatase the vanadate is directly linked to the protein only through the axial bound histidine residue and is embedded in the protein via an extensive hydrogen bonding network.

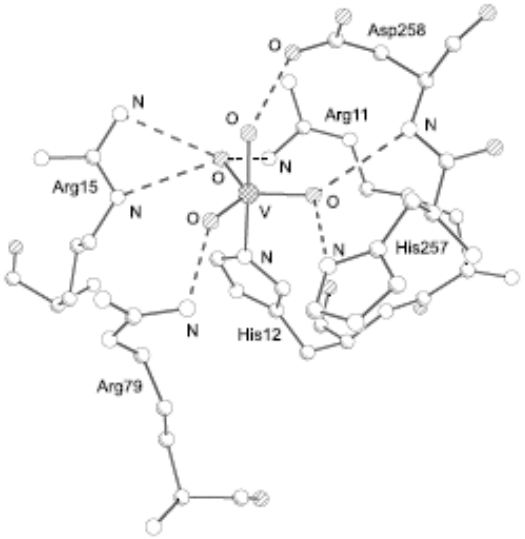

Figure 1.7: Structure of the active site of the rat prostatic acid phosphatase with complexed vanadate. Hydrogen bonds are shown as broken lines.[34]

1.4 Structural models for vanadium-dependent haloperoxidases

As already described in the previous sections, many functional models for V-HPO have been developed since their discovery. In spite of spectroscopic studies carried out on the native enzyme, the coordination environment around the vanadium(V) center was unknown initially. Therefore, functional mimics were developed to obtain more insight in the structural and electronic aspects of the enzyme. Later on, model systems were also designed examine which structural features are important for the catalytic properties of these enzymes, and a variety of structural models for the vanadium-dependent haloperoxidases were developed.[1,35] The latter complexes were designed to mimic the coordination environment of the vanadium center in the active site of the enzyme regardless of their activity in the presence of H_2O_2.

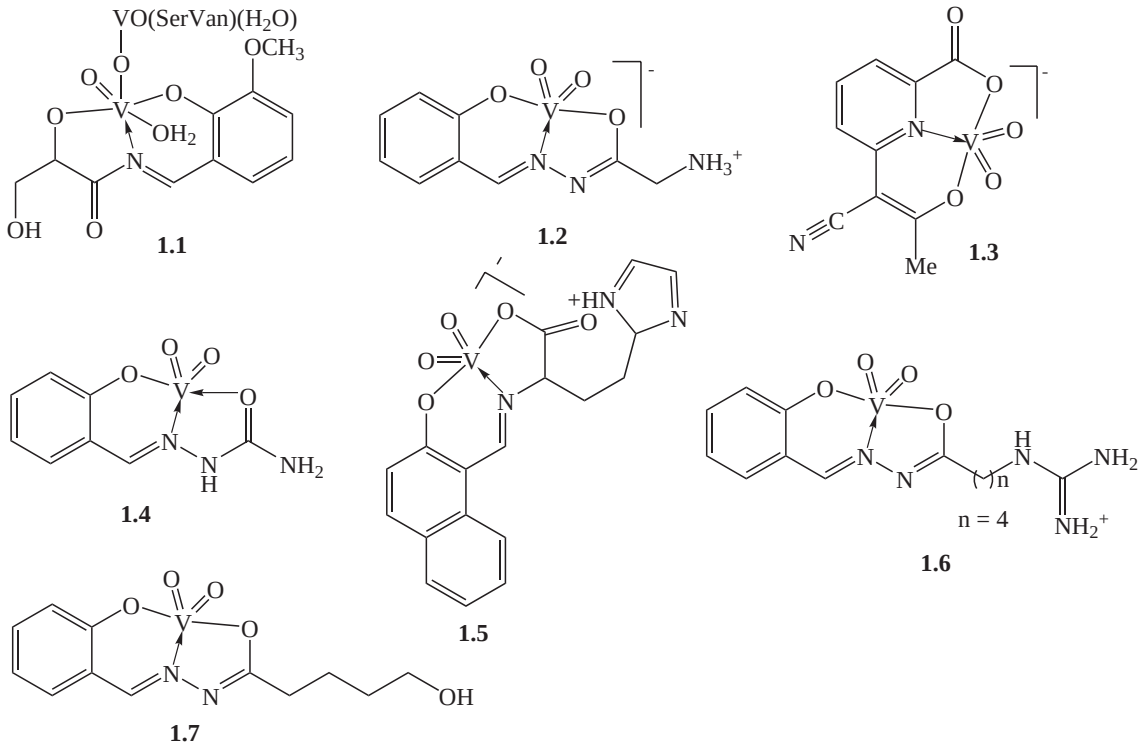

Figure 1.8: Structural models for the active site of vanadium dependent haloperoxidases; **1.1**[36], **1.2**[37], **1.3**[38], **1.4**[39], **1.5**[40], **1.6**[41], **1.7**[42].

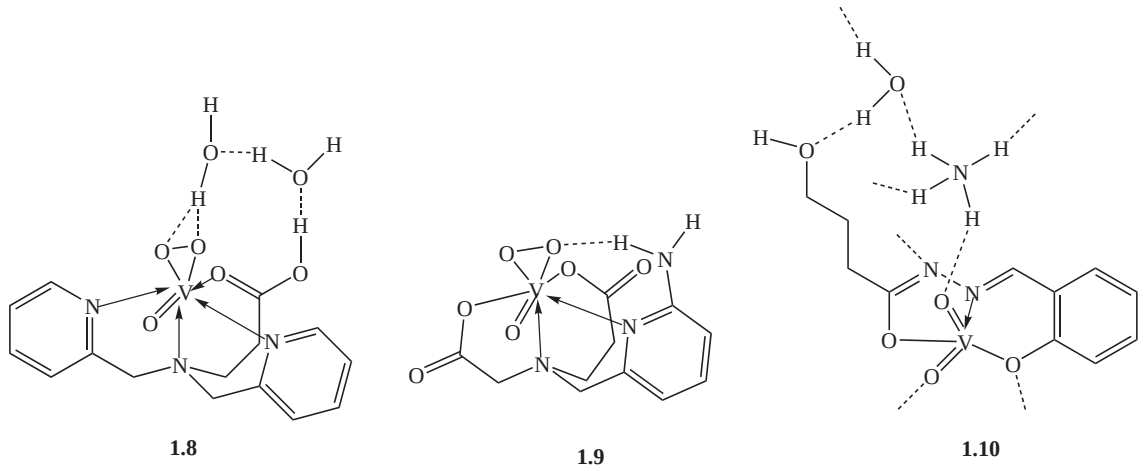

Figure 1.9: Schematic representation of the vanadium complexes modelling the hydrogen bonding interactions in V-HPO; **1.8**[43], **1.9**[44], and **1.10**[45].

In the model complexes shown in Figure 1.8 vanadium is in the oxidation state +5. All ligands consist of oxygen donor sites. Often one or two oxo groups are present at the vanadium center. The non-oxo oxygens stem from alkoxide and phenolate moieties or from a water molecule. Another class of model compounds includes the vanadium complexes which mimic the hydrogen bonding interactions in V-HPO. Only a limited number of this complexes are known so far, which are depicted in Figure 1.9. In the first model complex, **1.8**, the peroxo-oxygen atom is in hydrogen bonding contact with a water molecule, while the second one, **1.9**, contains an intramolecular hydrogen bonding interaction established by a pendant amine functionality and the oxygen atom of the peroxide group. The third one, **1.10**, is the ammonium salt of the *cis*-dioxovanadium(V) complex with hydroxyl substituted aliphatic side chain. The hydroxyl functionality is in hydrogen bonding contact with one water molecule, which establishes further an intramolecular hydrogen bonding interaction with the ammonium cation. The ammonium cation completes this hydrogen bonding network by hydrogen bonding interactions with the oxygen atom.

1.5 Design of new ligand system

Based on the reported crystal structure of vanadium chloroperoxidase, we have focused our attention on the synthesis of vanadium complexes with the Schiff base ligands derived from salicylaldehyde itself or one of its ring substituted derivative and amino acid hydrazides (see Figure 1.10). Starting from protected amino acids, free (unprotected) different amino acids will be introduced. This achievement has the role to probe the importance of the amino acid residues which are in hydrogen bonding interaction with the equatorial oxygen atoms of the prosthetic group in vanadium containing haloperoxidases. Although much knowledge is available about the complex formation between vanadium and amino acids,[40,46–58] to the best of our knowledge, no work has been reported on the complexation of dioxovanadium(V) complexes with *N*-Salicylidene amino acid hydrazide ligands. The interesting information found in the literature is the complexation of vanadate ion by a dipeptide, glycyl-tyrosine, system.[59]

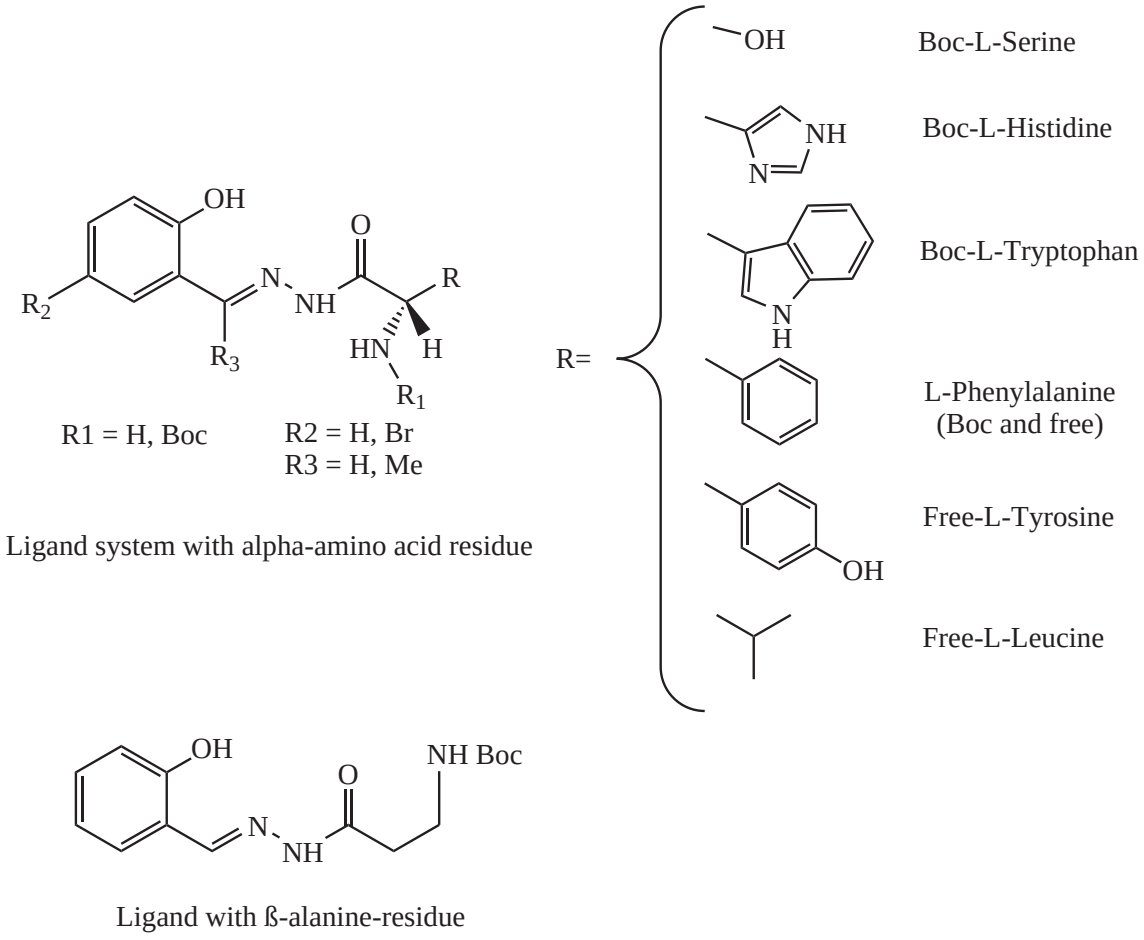

Figure 1.10: Design of the ligand system as model for vanadium haloperoxidase enzymes

1.6 History and occurrence of molybdenum

Molybdenum (from the Greek *molybdos* meaning "lead-like") is not found free in nature, and the compounds that can be found were, until the late 18^{th} century, confused with compounds of other elements, such as carbon or lead. In 1778 Carl Wilhelm Scheele was able to determine that molybdenum was separate from graphite and lead, and isolated the oxide of the metal from molybdenite. In 1782 Hjelm isolated an impure extract of the metal by reducing the oxide with carbon. Molybdenum was little used and remained in the laboratory until the late 19^{th} century. Subsequently, a French company, Schneider and Co, tried molybdenum as an alloying agent in steel armor plate and noted its useful properties. Though molybdenum is found in such minerals as wulfenite ($PbMoO_4$) or powellite ($CaMoO_4$), the main commercial source of molybdenum is molybdenite (MoS_2).

Molybdenum is mined directly, and is also recovered as a byproduct of copper mining. Molybdenum is present in ores from 0.01% to about 0.5%.

Molybdenum has been found to have a role in biology of all classes of organisms. There are many molybdenum-containing enzymes distributed throughout the biosphere.[60] The availability of molybdenum to biological systems is due to the high water solubility of oxidized forms of the metal. The molybdenum containing enzymes can be distinguished according to their amino acid sequences, spectroscopic properties, active site structures and catalyzed reactions. However, based on the rapidly growing number of X-ray crystal structures a classification based on structural homology of the active sites became appropriate. Considering this the molybdopterin containing enzymes can be grouped into three principal families all containing a pyranopterin (ppt) as cofactor element: the active sites consisting of (ppt)MoOS(OH) (the molybdenum hydroxylases), (ppt)MoO_2(S-Cys) (the eukaryotic oxotransferases) and $(ppt)_2$MoOX (the bacterial oxotransferases) (see Figure 1.11).[6, 60]

The molybdenum hydroxylases catalyse the reactions differently to other hydroxylase enzymes, with water rather than molecular oxygen as the ultimate source of the oxygen atom incorporated into product, and with the generation rather than consumption of reducing equivalents. The active sites possess a catalytically labile Mo-OH (or possibly Mo-OH_2) group that is transferred to substrate in the course of the hydroxylation reaction. These enzymes invariably have other redoxactive centres. The eukaryotic oxotransferases consist of the sulphite oxidases and plant nitrate reductases.[61] They catalyse the transfer of an oxygen atom to or from nitrate in a manner that involves formal oxidation-state changes of the molybdenum. As with the molybdenum hydroxylases, the ultimate source of oxygen is water rather than molecular oxygen. The bacterial oxotransferases and related enzymes differ from the other two groups of molybdenum enzymes in having two equivalents of the ppt cofactor co-ordinated to the metal. This family is quite diverse, as reflected in the fact that serine, cysteine or selenocysteine may be found co-ordinated to the molybdenum, depending on the enzyme. As in the case of the molybdenum hydroxylases, both eukaryotic and bacterial oxotransferases utilize water as the source of the oxygen atom incorporated into product, although for these enzymes, the catalytically labile oxygen in the active site is an Mo=O group rather than

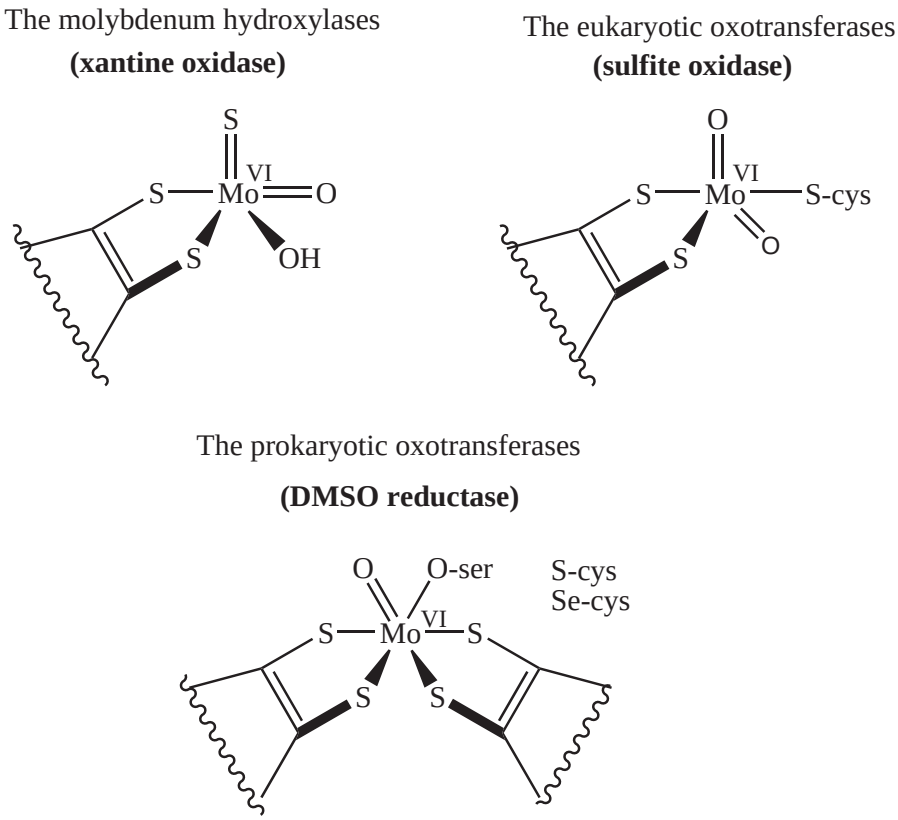

Figure 1.11: Structures of the active sites of the three principal families of molybdenum enzymes. Here, ppt represents a unique ppt cofactor (pyranopterin) that co-ordinates to the metal, and X is a metalliganded serine, cysteine or selenocysteine.

an Mo-OH.

The existence of molybdenum in oxotransferase enzymes had increased the interest for the reactivity and coordination chemistry of *cis*-dioxomolybdenum complexes.[62,63] Moreover, various molybdenum(VI) complexes have been reported as efficient catalysts for epoxidation and hydroxylation of olefines,[64–67] oxidation of sulfides[68] and alcohols[69] and as catalysts of oxygen transferring reaction.[70,71] In addition, $MoO_3(aq)$[72,73] and $[MoO(O_2)_2(oxalate)]^{2-}$[74] are known as functional mimics for V-HPOs enzyme, being capable to catalyze the oxidation of halides by hydrogen peroxide. At this point should be mentioned that, molybdate showed a higher catalytic activity, compared to vanadate. The reported turnover rate for the catalytic bromide oxidation reaction is *ca.* 180 $\mathrm{mol}_{\text{Br-TMB}}\mathrm{h}^{-1}\mathrm{mol}_{\text{Mo}}^{-1}$ which is about 45 times faster than vanadate.[73] However, the

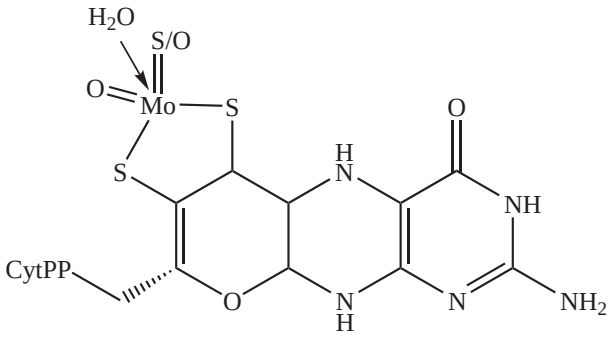

Figure 1.12: Schematic representation of the molybdopterin cytosin cofactor of aldehyde-oxidoreductase.

number of molybdenum-based catalyst for the haloperoxidase catalytic reaction is very reduced and there are reports of coordination molybdenum compounds as analogs of vanadium complexes, which were incapable to mediate the catalytic halide oxidation.[75]

Chapter 2

Vanadium(v) complexes with protected L-α-amino-acid residue ligands

The oxidation chemistry of vanadium(V) complexes has attracted renewed attention with the discovery of naturally occurring vanadium containing haloperoxidase.[5,6,18,19,76,77] To get a better understanding of the working mechanism of the enzyme, many vanadium(V) complexes have been prepared and studied as functional enzyme mimics.[41,45,78–81] Furthermore, the coordination chemistry of vanadium related to its biological functions has been extensively explored.[1,82] Several papers discuss results for vanadium(IV) complexes of amino acids ligands.[40,46–58] However, only a limited number of vanadium complexes with amino acid hydrazide ligands have been investigated as oxidation catalysts so far. It was our intention to develop and study a number of different types of vanadium complexes. In order to design a new ligand system capable of enhancing the hydrogen bonding interaction of vanadate moiety from the natural system with amino acid residues, we have included in this chapter Boc-L-α-serine, Boc-L-α-tryptophan, Boc-L-α-histidine, and Boc-L-α-phenylalanine amino acids. To gain insight in the catalytic properties of these compounds, we studied their catalytic properties in bromination reactions and used them as catalysts in sulfoxidation reaction.

2.1 Synthesis and Reactions

The synthesis of *N*-salicylidene amino acid hydrazide ligands follows the pathway depicted in Figure 2.1. Boc-L-α-serine, Boc-L-α-histidine, Boc-L-α-tryptophan, and Boc-L-α-phenylalanine were used as amino acids. The first step is the esterification of Boc-L-α-amino acids to form the methyl esters. In the second step Boc-L-α-amino acid methyl esters react with two equivalents of hydrazine hydrate, resulting in the nearly quantitative formation of the corresponding Boc-L-α-amino acid hydrazides. The amino acid hydrazides were crystallized from the ethyl acetate as colorless solids, whereas the excess of hydrazine remains in the solution. Subsequent reaction with salicylaldehyde itself or one of its ring substituted derivative results in the formation of the desired Schiff base ligands. The protection of amino functionality of amino acids prevents the second Schiff base condensation reaction between the aldehyde and amino group.

The stoichiometric reactions of these new Schiff base ligands with ammonium or potassium vanadate in refluxing methanol results in the formation of the corresponding salts of the anionic *cis*-dioxovanadium(V) complexes, or the neutral complexes (see Table 2.1). They have a very good solubility in polar organic solvents like DMSO or methanol and are soluble in water. Single crystals of the complex $K[VO_2(BrsalhyBocser)]\cdot 2H_2O$ (**3**) were grown by slow evaporation from methanolic solution. Reaction between equimolar amounts of the Schiff base ligands with Boc-L-α-phenylalanine residue and tri-isopropylatvanadium(V) oxide ($VO(OiPr)_3$) in dry isopropanol under argon atmosphere yields the corresponding mono-oxovanadium(V) complexes (see Figure 2.2).

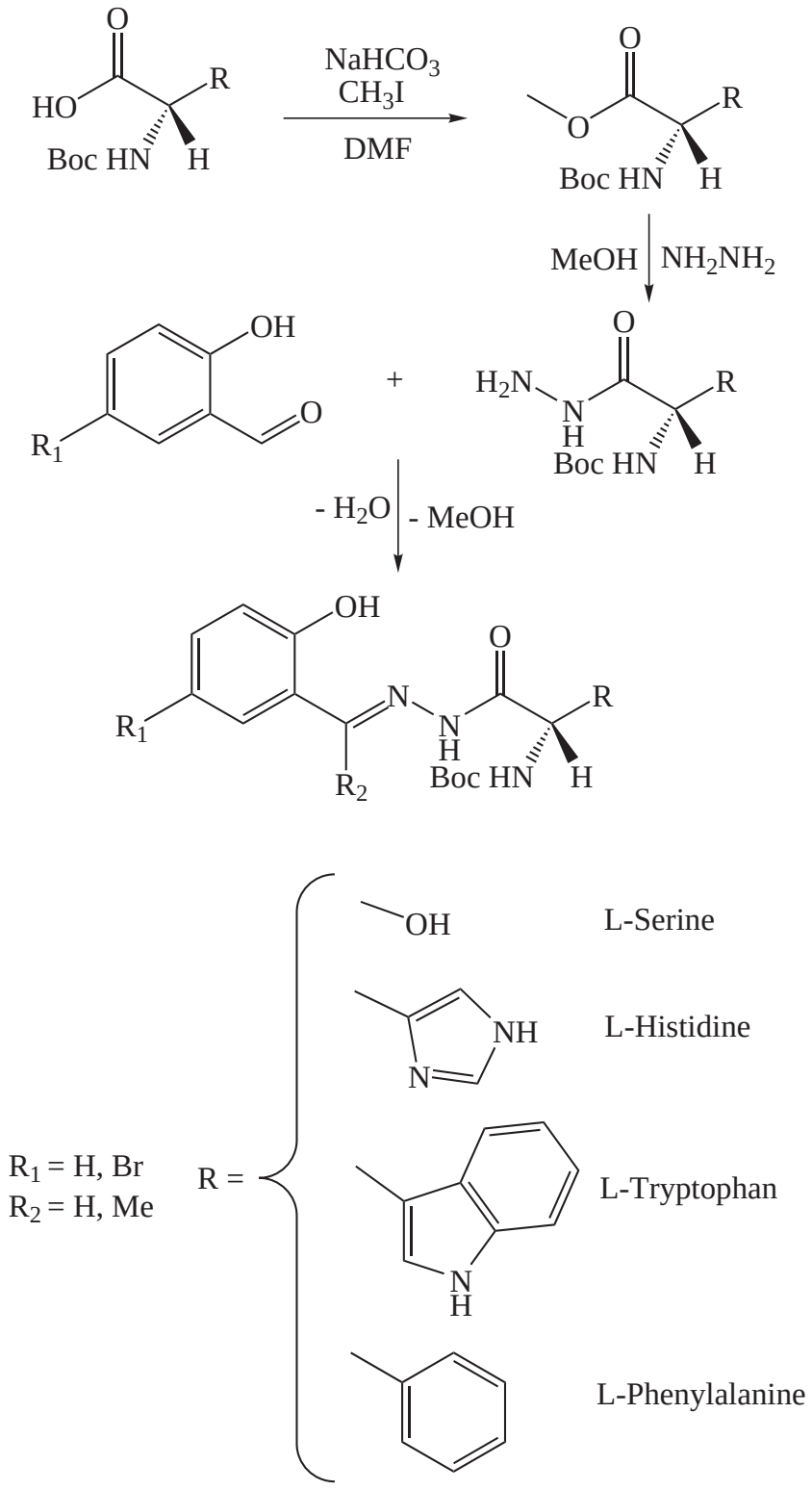

Figure 2.1: Schematic representation of the synthesis of *N*-Salicylidenehydrazide ligands with Boc-protected amino acid substitutions.

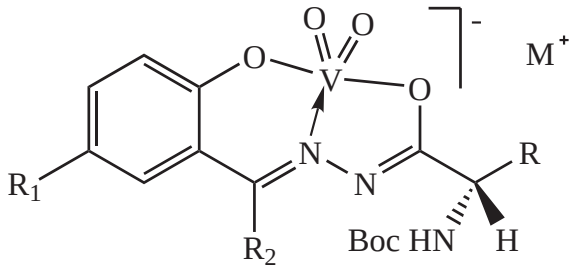

Amino acid residue	R_1	R_2	M^+	Complex	Formula
L-α-serine	H	H	K^+	**1**	$K[VO_2(salhyBocser)]\cdot H_2O$
	H	H	NH_4^+	**2**	$NH_4[VO_2(salhyBocser)]\cdot EtOH\cdot H_2O$
	Br	H	K^+	**3**	$K[VO_2(BrsalhyBocser)]\cdot 2H_2O$
	Br	H	NH_4^+	**4**	$NH_4[VO_2(BrsalhyBocser)]\cdot MeOH$
L-α-histidine	H	H	H^{+a}	**5**	$[VO_2(HsalhyBochis)]$
L-α-tryptophan	H	H	K^+	**6**	$K[VO_2(salhyBoctrp)]\cdot H_2O$
	H	H	H^{+a}	**7**	$[VO_2(HsalhyBoctrp)]\cdot MeOH$
L-α-phenylalanine	H	H	K^+	**8**	$K[VO_2(salhyBocphe)]\cdot H_2O$
	H	H	NH_4^+	**9**	$NH_4[VO_2(salhyBocphe)]\cdot H_2O$
	Br	H	K^+	**10**	$K[VO_2(BrsalhyBocphe)]\cdot H_2O$
	H	Me	K^+	**11**	$K[VO_2(MesalhyBocphe)]$
	H	Me	NH_4^+	**12**	$NH_4[VO_2(MesalhyBocphe)]$

[a]neutral complex

Table 2.1: Schematic representation of *cis*-dioxo-vanadium(V) complexes with Boc-amino acid residues.

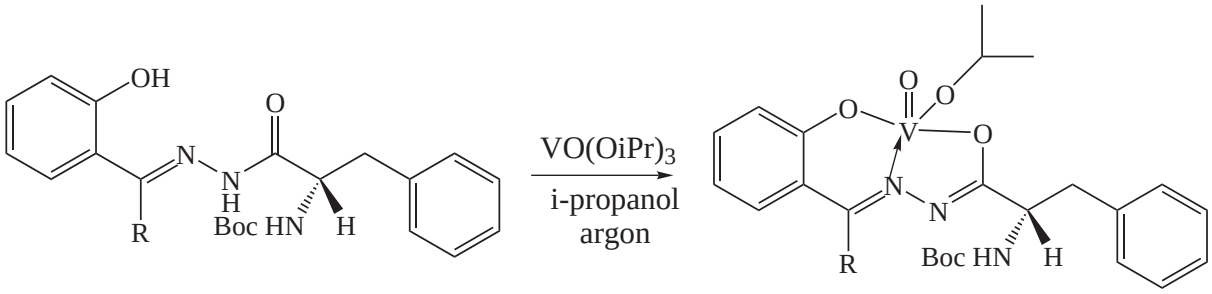

Figure 2.2: Synthesis of oxo-vanadium(V) complexes **13** (R = H), and **14** (R = Me), with Boc-L-α-phenylalanine residue.

2.2 Structural characterization

In the molecular structure of the complex anion $[VO_2(BrsalhyBocser)]^-$ (**3**) of the potassium salt, the vanadium(V) atom is coordinated by the phenolate oxygen atom O3, the imine nitrogen atom N1, amide oxygen atom O4 and the two oxo groups O1 and O2, in a square pyramidal coordinated environment (see Figure 2.3). The ligand acts as a tridentate ligand. The τ^1 value is 0.15 which is slightly distorted from the ideal square-pyramidal geometry. The distortion to an ideal-square pyramidal geometry of the vanadium atom in the complex $K[VO_2(BrsalhyBocser)]\cdot 2H_2O$ (**3**) is very similar and comparable to the distortion found in our other dioxovanadium complexes, with *N*-salicylidene hydrazides published previously.[42,45,84] The V=O distances V–O1 (161.8(6) pm) and V–O2 (165.4(6) pm) are typical for dioxovandium groups.[42,85] The angles in the basal plane of the distorted pyramid are O3–V–O4 150.6(2)° and O3–V–N1 83.0(3)°, which are quite similar to those previously reported for the *cis*-VO_2 moiety in other complexes.[39,42,84,86] (see Table 2.2) The anionic nature of the complex and therefore the presence of the iminolate form of the ligand is consistent with the observed V–O4 and O4–C8 bond lengths. The O4–C8 bond distance, which is the most significant parameter for differentiating between the iminol and keto form of the amide functionality, exhibits value of 130.0(9) pm and is nearer to a C–O single bond than to a C=O double bond distance. The bond lengths N1–N2, N1–C7 of the coordinated ligand system are in good agreement with the

[1] 0 for ideal square-pyramidal and 1 for ideal bipyramidal arrangements[83]

data found for similar dioxovanadium complexes.[42,84] The adjacent C8–N2 bond display a typical double bond distance of 129.7(11) pm, and a concomitant lengthening of the N2-N1 bond of 141.1(10) pm is also apparent. The N1–C7 bond distance of 127.9(11) pm is pretty close to the usual C=N length (see Table 2.2).[84]

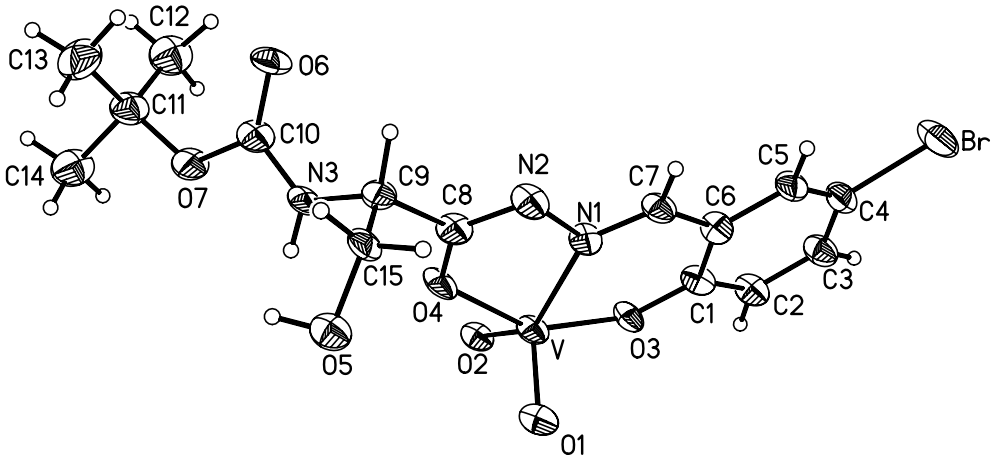

Figure 2.3: Molecular structure of the anionic dioxovanadium(V) complex $[VO_2(BrsalhyBocser)]^-$ in crystals of $K[VO_2(BrsalhyBocser)]\cdot 2H_2O$ (**3**) (thermal ellipsoids are drawn at the 50% probability level).

In the native form of vanadium-chloroperoxidase, interstitial water molecules were found near the the Ser402 residue as well as in the vicinity of the apical oxygen atom of the vandate moiety. In complex $K[VO_2(BrsalhyBocser)]\cdot 2H_2O$ (**3**) water molecules form a long hydrogen bonding water channel. As depicted in Figure 2.4, both oxo groups of the *cis*-dioxovanadium(V) moiety are participating in the hydrogen bonding network. In addition, two water molecules form intermolecular hydrogen bonds with each other, and also involved in the build-up of the hydrogen bonding networks with six neighboring molecules. The oxo group O2 forms two hydrogen bonds, of which one is to atom N3 (O2···N3B 293.8(2) pm) of the Boc group of one neighboring molecule and the other is to the oxygen atom of the serine O5 (O2···O5A 308.9(2) pm) of another neighboring dioxovanadium(V) moiety. This hydrogen bonding resembling the interaction discussed for the native vanadium haloperoxidase enzymes between the vanadate and the serine residue located at the active site (for VClPO: Ser402).[19] The apical oxygen O1 forms intermolecular hydrogen bond with one of the water molecules O1W (O1···O1W 294.1(2) pm),

which in turn is hydrogen bonded to a second water molecule, connects to the hydrazide nitrogen atom N2 (O2W···N2E 298.0(2) pm) and the oxygen atom O6 (O2W···O6C 290.4 pm) of the Boc group of two neighboring molecules. The hydroxy function of the serine moiety does not take part in the coordination of the vanadium, but is hydrogen bonded to the oxo group of the vanadate O2D (O5···O2D 308.9(3) pm), and to a water molecule O1W (O5···O1WC 282.9(3) pm) of the two neighboring molecules. This situation is of specific interest in the light of presence of serine close to the active center in the haloperoxidases.

In the molecular structure of $K[VO_2(BrsalhyBocser)]\cdot 2H_2O$ (**3**) the potassium cation is coordinated to the water molecule of crystallization O1W (270.2 pm), the oxo group O1 (291.8 pm), amide oxygen atom O4 (303.3 pm), and the oxygen atom of the serine moiety O5 (283.1 pm) (see Figure 2.5). Moreover, the coordination sphere of the potassium ion includes an oxo group O2D (269.0 pm), an alcoholic oxygen donor atom O3D (279.4 pm), which belong to the same neighboring molecule, and also an oxo group of another neighboring molecule O2C (269.2 pm), which it is in a μ_2-bridging position with a neighboring potassium cation KB. In addition, there is a weak interaction with amide oxygen of adjacent molecule O4D (314.6 pm).

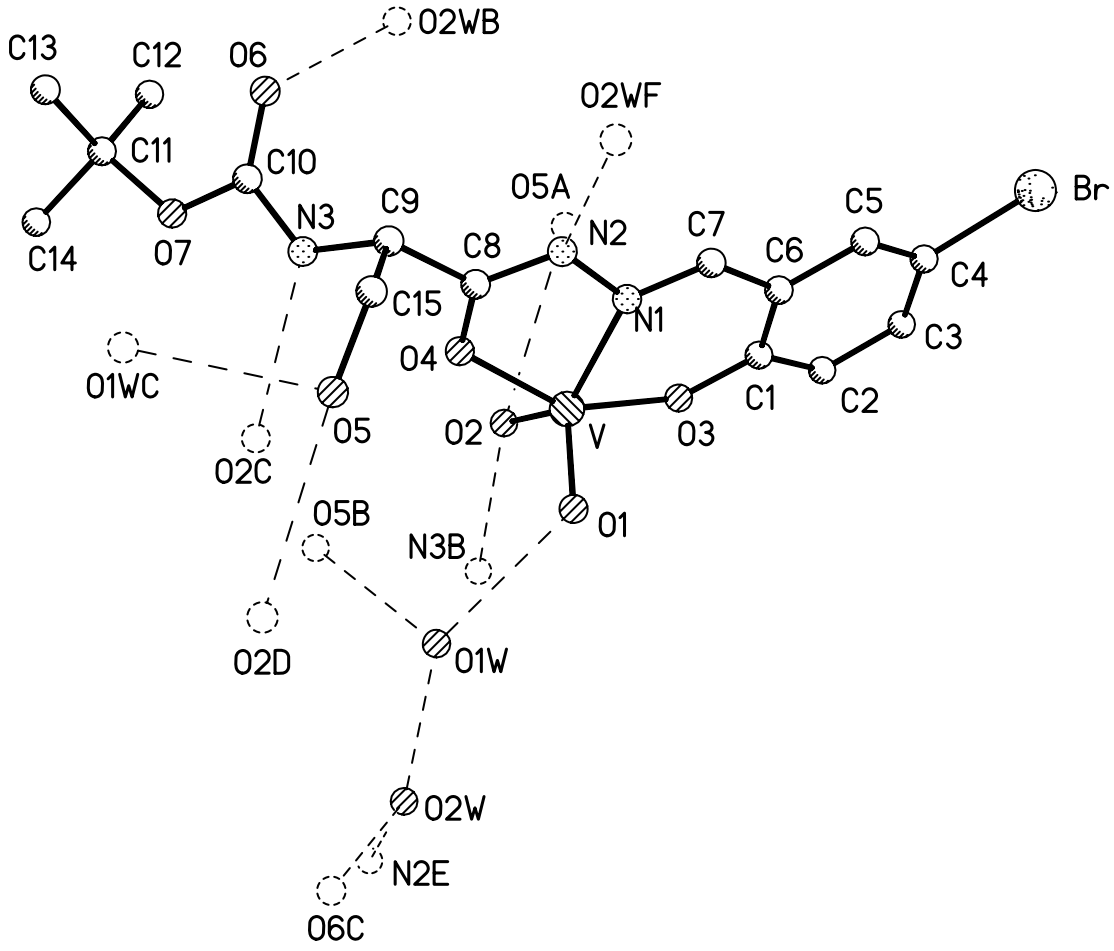

Figure 2.4: Hydrogen bonding network in $K[VO_2(BrsalhyBocser)]\cdot 2H_2O$ (**3**). Hydrogen atoms are omitted for clarity. Broken lines represent hydrogen bonding interactions. Relevant distances (in pm): O1···O1W 294.1(2), O2···N3B 293.8(2), O5···O1WC 282.9(3), O5···O2D 308.9(2), O6···O2WB 290.4(3), N2···O2WF 298.0(2); Dashed circles represent symmetry equivalent atoms (symmetry operators: A: – 1 + x, y, z; B: $-\frac{1}{2}+x, \frac{5}{2}-y,$ – z; C: $\frac{1}{2}+x, \frac{5}{2}-y,$ – z; D: 1 + x, y, z; E: x, 1 + y, z; F: x, –1 + y, z).

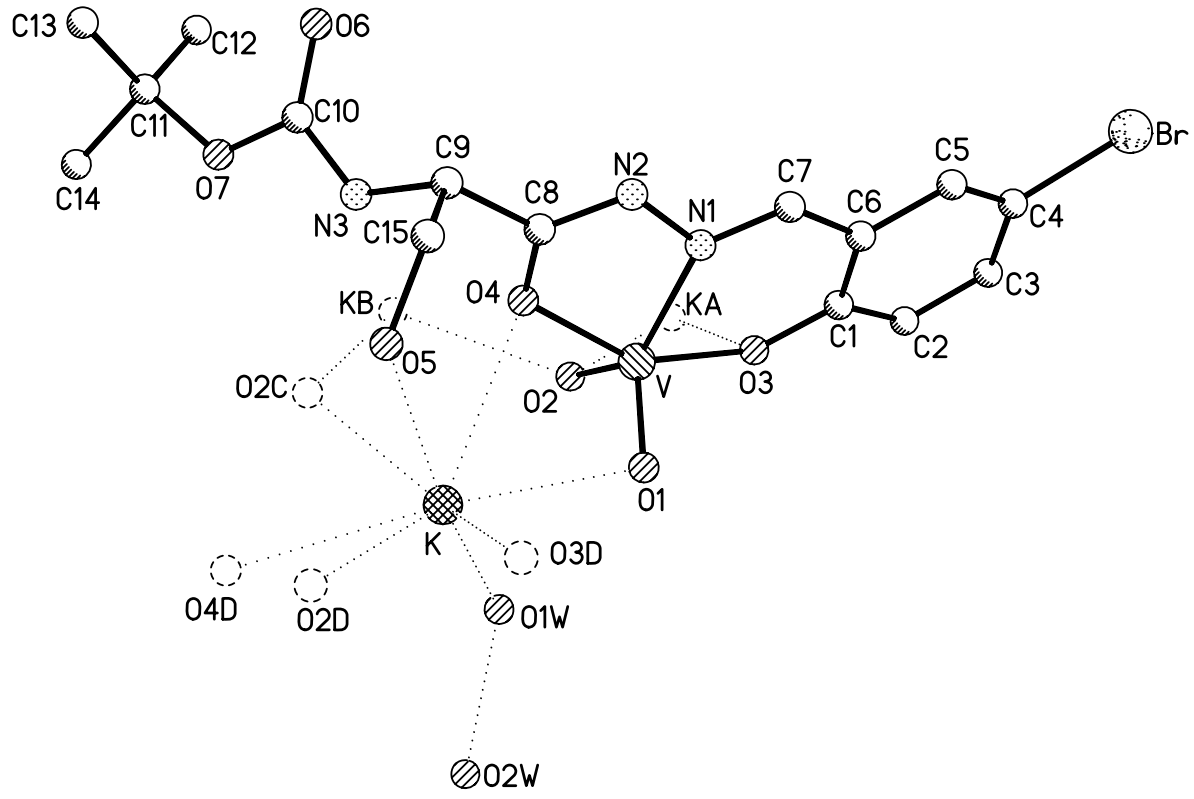

Figure 2.5: Depiction of the K^+ environment in crystals of $K[VO_2(BrsalhyBocser)]\cdot 2H_2O$ (**3**). Potassium contacts are shown as doted lines. Relevant distances (in pm): K···O1W 270.2, K···O1 291.8, K···O4 303.3, K···O5 283.1, K···O2D 269.0, K···O3D 279.4, K···O4D 314.6.

Table 2.2: Selected bond lengths (pm) and angles (°) for $K[VO_2(BrsalhyBocser)]\cdot 2H_2O$ (**3**).

Bond lengths			
V–O1	161.8(6)	O4–C8	130.0(9)
V–O2	165.4(6)	N1–N2	141.1(10)
V–O3	189.3(6)	N1–C7	129.7(11)
V–O4	199.0(6)	N2–C8	127.9(11)
V–N1	214.1(7)		
Bond angles			
O1–V–O2	108.4(3)	O3–V–O4	150.6(3)
O1–V–O3	104.9(3)	O1–V–N1	109.3(3)
O1–V–O4	99.5(3)	O2–V–N1	141.2(3)
O2–V–O3	96.1(3)	O4–V–N1	73.5(3)
O2–V–O4	91.6(3)	O3–V–N1	83.0(3)

2.3 Spectroscopic Characterization

The formation of the *cis*-dioxovanadium(V) complexes is confirmed by aaapearance of strong bands in the IR spectra, corresponding to the $\nu(VO^{2+})$ group. Details are summarized in the experimental section and given in Table 2.3. The infrared spectra of the ligands exhibit a broad band in the 3220–3300 cm^{-1} range due to ν(NH), and a strong band at 1661–1675 cm^{-1} range assigned to ν(C=O) stretches. However, in the spectra of the vanadium complexes appears a broad band around 3372 cm^{-1}, the ν(NH) stretching vibration of the amino acid residues. A medium band at 1692 cm^{-1} is attributed to the ν(C=O) stretching vibration of the Boc group of amino acids in the ligands as well as in the complexes. The strong band in the 1661–1675 cm^{-1} range in the IR spectra of the ligands, due to the carbonyl moiety ν(C=O) stretching vibration, are not observed in the complexes. Instead a strong band is observed around 1617 cm^{-1}, which can be attributed to the stretching vibration of the conjugate –C=N–N=C– grouping.[84] This

Table 2.3: Characteristics IR bands [cm^{-1}] for the complexes .

Formula	Complex	ν(C=N–N=C)	$\nu(VO_2)$
$K[VO_2(salhyBocser)]\cdot H_2O$	**1**	1616	908, 949
$NH_4[VO_2(salhyBocser)]\cdot EtOH\cdot H_2O$	**2**	1614	908, 932
$K[VO_2(BrsalhyBocser)]\cdot 2H_2O$	**3**	1617	904, 949
$NH_4[VO_2(BrsalhyBocser)]\cdot MeOH$	**4**	1616	900, 917
$K[VO_2(salhyBoctrp)]\cdot H_2O$	**6**	1615	906, 912
$[VO_2(HsalhyBoctrp)]\cdot MeOH$	**7**	1610	909, 981
$K[VO_2(salhyBocphe)]$	**8**	1617	908, 940
$NH_4[VO_2(salhyBocphe)]\cdot H_2O$	**9**	1616	908, 937
$K[VO_2(BrsalhyBocphe)]\cdot H_2O$	**10**	1617	907, 941
$K[VO_2(MesalhyBocphe)]$	**11**	1616	901, 949
$NH_4[VO_2(MesalhyBocphe)]$	**12**	1601	873, 944

band is characteristic for the coordination of the iminolate form of the ligand to the dioxovanadium(V) moiety.

A medium/strong band at 1560 cm^{-1}, may originate from the vibration of the (Ph–C–C=N) bond[87] and typifies complexes derived from salicylaldehyde.[49,87,88] An additional band observed for the complexes at 1273 cm^{-1} is assigned to the ν(C–O) (iminol) mode. Also, the complexes show two strong bands between 873 and 949 cm^{-1} assigned to the stretching vibrations of the *cis*-VO_2 moiety of the complexes, which are in a good agreement with the other results.

Further evidence for the coordination mode of the ligands was obtained from the ^{1}H– and ^{13}C–NMR spectra, and ^{51}V–NMR spectra of the complexes in DMSO-d_6, which are summarized in the experimental section. The ^{1}H–NMR integrations and signal multiplicities agree with the proposed formula. The ^{1}H–NMR spectra of the ligands derived from salicylaldehyde, and its bromo substituted residues reveal the presence of two isomers in a ratio as given in the experimental section. The spectra of the free ligands exhibit an OH

(phenolic) proton resonance at 11.79 and 11.36 ppm respectively for two isomers. The absence of this signals in the complexes is in accordance with iminolisation and subsequent replacement of H by the metal ion. When the metal is coordinated, the deshielding effect of the metal atom is apparent in some protons, causing a downfield shift of the corresponding ^{1}H–NMR peaks. A significant downfield shift of ca. 0.39 ppm for the azomethine (CH=N) proton signal in the complexes with respect to the corresponding free ligands confirms the coordination of the azomethine nitrogen atom. The aromatic protons of ligands and complexes as well as the α-CH, β-CH_2, and hydroxy group of amino acids, appear in the expected region, with slight shifts in their positions. A net difference between the potassium and the ammonium salts of the *cis*-dioxovanadium(V) complexes is observed in their ^{1}H–NMR. A broad resonance at ca. 7.10 ppm is observed in the ^{1}H–NMR of the ammonium salt of the *cis*-dioxovanadium(V) complexes and is attributed to NH_4^+ protons. This resonance is absent in the ^{1}H–NMR of the corresponding potassium or neutral *cis*-dioxo- complexes which exhibit instead the specific resonance of the NH proton at this region. We have also recorded ^{13}C–NMR of ligands and complexes to provide diagnostic tools for the elucidation of the structures. Assignments were based on the chemical shift and intensity patterns, and on the coordination-induced shift $\Delta\delta = \delta_{\text{complex}} - \delta_{\text{free-ligand}}$ of the signals for the carbon atoms in the vicinity of the coordinating atoms.[89] A comparison between the ^{13}C–NMR patterns of the free ligand and the corresponding ^{13}C–NMR spectra of complexes proved the coordination mode of the ligands. The most indicative resonance is the down field shift at ca. 155 ppm of the imine carbon atom (CH=N), that resonate around 140–147 ppm, in the free ligands. To characterize the compounds further in solution, ^{51}V–NMR spectra of complexes were also recorded. The dioxovanadium(V) complexes in DMSO-d_6 solution, show one strong resonance at ca. -531 ppm, which is typical for the shift of dioxovanadium(V) complexes containing a mixed O/N donor set.[10,84,90,91] The resonances have line widths at half-height between 950 and 1300 Hz.

2.4 Reactivity of the complexes

2.4.1 Bromination reaction of TMB/MCD

In order to examine halide oxidation catalyzed by dioxovanadium complexes, they were tested in bromination reaction of 1,3,5-trimethoxybenzene (TMB) and monochlorodimedone (MCD), which were frequently used as model substrates.[42,79,92–94] Hydrogen peroxide was used as the oxidant and sodium bromide (NaBr) as the bromide source. Reactions were performed in acetonitrile solution in a quartz cuvette of 10,00 mm optical path, thermostat at 20,0 °C. For each vanadium complex three standard solutions were prepared and the reactions were performed in triplicate. TMB, MCD, and NaBr were premixed in acetonitrile in a ratio of 3:3:9:44. In a typical experiment 6 μM catalyst was added to the mixture of TMB/MCD/NaBr/acetonitrile with the concentration of 0.12, 0.05, and 0.24 mM respectively. Hydrogen peroxide was then added (0.53 mM). The reaction was initiated by addition of $HClO_4$ (0.24 mM) and followed by UV at 258 nm, the characteristic absorption of MCD.[21] Since TMB is much more reactive than MCD, it reacted preferentially with little change of UV at 258 nm during its bromination. The increasing of UV intensity at 258 nm before the bromination of MCD is due to the formation of Br_3^- (λ = 268 nm in acetonitrile). As soon as the bromination of TMB was completed, MCD was brominated as indicated by the decreasing UV intensity at 258 nm. Hence, the period of UV-insensitive time corresponds to the total reaction time of TMB bromination. $(nBu_4N)_2HVO_4$ (vanadate) is used as standard for this reaction.[94] Therefore the turnover frequencies reached by dioxovanadium(V) complexes described here, were compared with those found for $(nBu_4N)_2HVO_4$ published previously.[94] The results are summarized in Table 2.4. The bromination of TMB took 480 s when the reaction was catalyzed by vanadate alone; this reaction time was shortened to 276 s (turn over = 263 $mol_{Br\text{-}TMB}h^{-1}mol^{-1}_{catalyst}$) in the presence of $NH_4[VO_2(BrsalhyBocser)]\cdot MeOH$ (**4**), which indicates that, the catalyst is 1.7 times more reactive with respect to the catalytic bromination of TMB. The turnover frequencies lay in the range 133 – 263 $mol_{Br\text{-}TMB}h^{-1}mol^{-1}_{catalyst}$. No big difference in activity was observed by changing the amino acid residues, but nevertheless a slightly increase in reactivity was observed in the direction Trp < Phe < Ser. Thus the dioxovanadium complexes with serine residue ap-

pear to be the most reactive catalysts (Figure 2.6). This may be due to the fact that the hydroxy functionality of the serine residue is involved in hydrogen bonding interactions with the vanadate moiety. To investigate the influence of electron withdrawing and/or electron donating groups on the aromatic ring on the the reactivity of the model complexes, we have introduced bromo, and Me substituted aldehyde. The results show that, the bromo-substituted vanadium complexes are more reactive than the unsubstituted one, as illustrated in Table 2.4.

Table 2.4: Catalytic oxidative bromination of TMB/MCD by *cis*-dioxovanadium complexes with Boc-L-α-amino acid side chain ligands

Formula	Complex	Time (s)	TOF[(a)]
$K[VO_2(salhyBocser)]\cdot H_2O$	**1**	330	218
$NH_4[VO_2(salhyBocser)]\cdot EtOH\cdot H_2O$	**2**	360	201
$K[VO_2(BrsalhyBocser)]\cdot 2H_2O$	**3**	282	256
$NH_4[VO_2(BrsalhyBocser)]\cdot MeOH$	**4**	276	263
$K[VO_2(salhyBoctrp)]\cdot H_2O$	**6**	456	158
$[VO_2(HsalhyBoctrp)]\cdot MeOH$	**7**	540	133
$K[VO_2(salhyBocphe)]\cdot H_2O$	**8**	408	175
$K[VO_2(BrsalhyBocphe)]\cdot H_2O$	**10**	390	186
$K[VO_2(MesalhyBocphe)]$	**11**	330	218
$NH_4[VO_2(MesalhyBocphe)]$	**12**	330	218

(a) Turnover frequencies ($mol_{Br\text{-}TMB} h^{-1} mol^{-1}_{catalyst}$)

2.4.2 Catalytic oxidation of sulfides catalyzed by *cis*-dioxovanadium(v) complexes

Vanadium haloperoxidase enzymes are also capable to catalyze the oxidation of sulfides to sulfoxides, varying from an enantioselective behavior in the case of vanadium bromoperoxidases to a non-selective reaction when vanadium chloroperoxidase has been used to

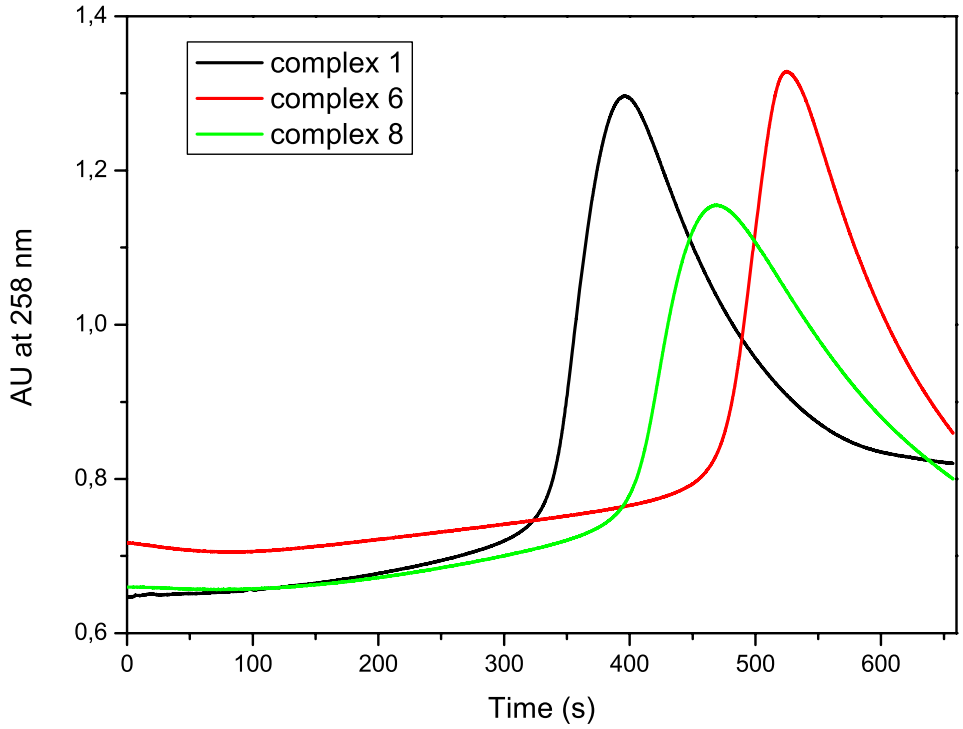

Figure 2.6: Comparison of the catalytic activity of the *cis*-dioxovanadium complexes with three different amino acid residue: complex **1** serine, complex **6** tryptophan, and complex **8** with phenylalanine residue, towards the catalytic bromination of TMB/MCD, followed by UV at 258 nm.

mediate the reaction.[26,28] Various vanadium complexes have been also reported[95,96] as catalysts for sulfides oxidation reaction with the complexes involving mainly Schiff base ligands. The capability of the new chiral *cis*-dioxovanadium(V) complexes to function as catalysts for the oxidation of methyl phenyl sulfide by hydrogen peroxide was investigated. In a standard procedure, 1 mol-% catalyst has been used for the reaction and a slight excess (1.2 equivalents) of hydrogen peroxide, in a mixture CH_2Cl_2/CH_3OH 7:3. Methanol was necessary due to the bad solubility of the complex in non-polar solvents and moreover, for a better miscibility of the aqueous oxidant with the halogenated solvent. After defined intervals of time, aliquots were taken from the reaction mixture and the product analyzed

by NMR (determination of the yield) and HPLC (determination of the ee). The outcomes of the catalytic reaction are summarized in Table 2.5 for the *cis*-dioxovanadium(V) complexes with Boc-amino acid residues. After 1 hour 22% of the corresponding sulfoxide was obtained when complex **6**, with tryptophan residue, whereas 86% conversion was established after 3 hours. For the catalyst **11**, with phenylalanine residue, after 1 hour 55% of sulfoxide was obtained, whereas 98% conversion was established within 3 hours. The catalysts containing serine residue show to have the highest efficient catalytic activity of the herein described complexes. The catalytic reaction was completed in less than three hours when the complexes containing serine residue were used as catalyst. The enantioselectivity of the *cis*-dioxovanadium(V) complexes with Boc-amino acid residue ligands was very low, this indicates that the chiral center is too far away from the vanadate moiety. Nevertheless complex **10** with phenylalanine residue shows to have ee value of 9.34%, which is the highest ee of the herein described *cis*-dioxovanadium complexes. The enantioslective sulfoxidation reaction has been reported.[95–98] Reports of vanadium-catalyzed sulfur oxidation reactions range from 58 to 92% conversion in the period of time of 14-16 hours when oxo- or *cis*-dioxovanadium(V) complexes were used as catalysts. The yields of the catalytic reaction raise to 60% conversion of sulfide within two hours, when peroxovanadium(V) complexes catalyzed the reaction.[99] Efficient vanadium-based catalyst for the sulfide oxidation reaction was reported as salen-type oxovanadium(IV) complex which accomplished 80% conversion after two hours of reaction.[95]

Table 2.5: Summary of the results of the catalyzed asymmetric oxidation of methyl phenyl sulfide by *cis*-dioxovanadium complexes with Boc-L-α-amino acid residue ligands

Formula	Complex	Time (h)	Yield[a] (%)	ee [b] (%)	Configuration[c]
$K[VO_2(salhyBocser)]\cdot H_2O$	**1**	3	100	n.d[d]	–
$K[VO_2(BrsalhyBocser)]\cdot 2H_2O$	**3**	3	100	n.d	–
$NH_4[VO_2(BrsalhyBocser)]\cdot MeOH$	**4**	3	100	n.d	–
$K[VO_2(salhyBoctrp)]\cdot H_2O$	**6**	1	22	5	S
$K[VO_2(salhyBoctrp)]\cdot H_2O$	**6**	3	86	4.7	S
$K[VO_2(salhyBocphe)]\cdot H_2O$	**8**	1	n.d	–	–
$K[VO_2(salhyBocphe)]\cdot H_2O$	**8**	3	70	6.6	S
$NH_4[VO_2(salhyBocphe)]\cdot H_2O$	**9**	1	n.d.	–	–
$NH_4[VO_2(salhyBocphe)]\cdot H_2O$	**9**	3	80	4.12	S
$K[VO_2(BrsalhyBocphe)]\cdot H_2O$	**10**	1	n.d.	–	–
$K[VO_2(BrsalhyBocphe)]\cdot H_2O$	**10**	3	59	0.35	S
$K[VO_2(MesalhyBocphe)]$	**11**	1	55	9.32	S
$K[VO_2(MesalhyBocphe)]$	**11**	3	98	3.02	S
$NH_4[VO_2(MesalhyBocphe)]$	**12**	1	n.d	–	–
$NH_4[VO_2(MesalhyBocphe)]$	**12**	3	85	6.7	S

All reactions were carried out at 0 °C with vanadium complexes loading to 1 mol-% and (1.2 equivalents) of hydrogen peroxide (8.24 M), in a mixture CH_2Cl_2/CH_3OH 7:3.
[a] isolated yield determined by ^{1}H–NMR (400 MHz) using 1,3,5-trimethoxybenzene as internal standard. [b] Determined by HPLC using a (S,S)-WHELK-01 chiral column (25 cm × 4.6 mm). The column was eluted with hexane:2-propanol (90:10), at a flow rate of 2.0 mL/min. [c] Absolute configuration of the major product was determined to be S, by comparison of the chromatogram in HPLC with the authentic sample. [d] n.d. not determined.

2.5 Conclusions

The new *cis*-dioxovanadium complexes with amino acid functionallized ligands have been synthesized and characterized. The ligands were obtained by the condensation of salicylaldehyde itself or one of its ring substituted derivatives with amino acid hydrazides. Boc-L-α-serine, Boc-L-α-histidine, Boc-L-α-tryptophan, and Boc-L-α-phenylalanine were used as amino acid sources. The ligands coordinate in their iminolate form. The compounds exhibit an overall coordination sphere constituting an O_4N donor set. For the vanadium atom a distorted square pyramidal coordination is found. Two water molecules are involved in the buildup of the hydrogen bonding network found in the case of $K[VO_2(BrsalhyBocser)]\cdot 2H_2O$ (**3**). The amino acids in the complexes introduced here are directly involved in coordination. The hydroxy function of amino acids do not take part in the coordination of the vanadium, but they participate to the hydrogen bonding network, as shown from X-ray data of $K[VO_2(BrsalhyBocser)]\cdot 2H_2O$ (**3**). These hydrogen bonding resembling the interaction discussed for the native vanadium haloperoxidase enzymes between the vanadate and the serine residue located at the active site (for VClPO: Ser402). These complexes can be regarded as structural model for the enzymatic system due to the relevant hydrogen bonding interactions which involves the oxygen atoms of the vanadate moiety. The results of catalytic experiments show that the complexes reported here catalyze the oxidation of bromide by hydrogen peroxide in acidic solution, and thus are functional mimics of vanadium haloperoxidases. We have also demonstrated that these vanadium complexes are capable of catalyzing the conversion of an organic sulfide to an organic sulfoxide in the presence of hydrogen peroxide.

2.6 Experimental Part

2.6.1 Synthesis of the Schiff base ligands with Boc-L-α-serine residue

Boc-L-α-serine-methylester

To a suspension of $NaHCO_3$ (0.33 g, 3.9 mmol, 1.1 eq.) in DMF (15 ml) was added Boc-L-α-serine (0.73 g, 3.55 mmol, 1 eq.) and methyl iodide (0.24 mL, 3.9 mmol, 1.1 eq). The mixture was stirred at room temperature for 20 hours. Distilled water (100 mL) was added and the product extracted with ethyl acetate (3 x 50 mL). The combined organic layers were washed with distilled water and than dried over Na_2SO_4, and concentrated *in vacuum* to obtain the product as a pale yellow oil. This yellow oil was purified by column chromatography (eluent: ethyl acetate /hexane 1:1).

Total yield: 0.5 g (2.28 mmol, 61%).

^{1}**H-NMR** (400 MHz, DMSO-d_6): $\delta =$ 1.4 (s, 9H, C(C**H**$_3$)$_3$), 3.7 (m, 5H, β-C**H**$_2$, C**H**$_3$-ester), 4.1 (m, 1H, α-C**H**), 4.8 (s, 1H, O**H**-amino acid), 6.7 (s, 1H, N**H**Boc).

^{13}**C-NMR** (100 MHz, DMSO-d_6): $\delta =$ 28 (C(**C**H$_3$)$_3$), 52 (**C**H$_3$-ester), 56.3 (α-**C**H), 62 (β-**C**H$_2$), 78 (O-**C**(CH$_3$)$_3$), 155 (**C**=OBoc), 172 (**C**ONH).

Boc-L-α-serine hydrazide

Hydrazine hydrate (0.74 mL, 14 mmol) was added to a solution of Boc-L-α-serine-methylester (1 g, 4.56 mmol) in methanol and the mixture was stirred at room temperature for 24 hours. The solvent was removed under vacuum. Recrystallization of the residual from ethyl acetate gave the product as a colorless crystalline solid. mp 128 °C.

Total yield: 0.92 g (4.2 mmol, 93%).

Elemental analysis for $C_8H_{17}N_3O_4$ (219.2 g/mol): calculated C: 43.82%, H: 7.82%, N: 19.17%; found C: 43.87%, H: 7.62%, N: 19.44%.

^{1}**H-NMR** (200 MHz, MeOD-d_4): $\delta =$ 1.44 (s, 9H, C(C**H**$_3$)$_3$), 3.7 (d, 2H, ^{3}J = 5.4 Hz, β-C**H**$_2$), 4.09 (t, ^{3}J = 6.7 Hz, 1H, α-C**H**), 4.84 (s, 5H, O**H**-amino acid, (N**H**)$_2$, N**H**$_2$)

ppm.

^{13}**C-NMR** (50 MHz, MeOD-d_4): $\delta =$ 28 (C(**C**H_3)$_3$), 57 (α-**C**H), 63 (β-**C**H_2), 81 (O-**C**$(CH_3)_3$), 158 (**C**=OBoc), 172 (**C**=ONHN) ppm.

EI–MS: (m/z) = 220 ($M^{+\cdot}$ 20%), 164 ($M^{+\cdot}$ - $C(CH_3)_3$ 40%), 119 ($M^{+\cdot}$ - $C(CH_3)_3$ - CO_2 80%), 104 ($M^{+\cdot}$ - $C(CH_3)_3$ - CO_2 - NH 10%), 88 ($M^{+\cdot}$ - $C(CH_3)_3$ - CO_2 - NH - NH_2 12%), 60 (100%).

N-Salicylidene-Boc-L-α-serine-hydrazide (HsalhyBocser)

Boc-L-α-serine-hydrazide (0.82 g, 3.74 mmol) was dissolved in methanol (30 mL). Salicylaldehyde (0.39 mL, 3.7 mmol) was added dropwise under constant stirring. After 10 minutes the reaction mixture turned its color to yellow. The resulting reaction mixture was stirred for 6 hours. A colorless precipitate formed during the reaction period. It was filtrated off, recrystallized from methanol and dried in vacuum. The NMR data confirm the presence of product as two isomers in ratio 2.9:1. mp 191 °C.

Total yield: 0.99 g (3.06 mmol, 82%).

Elemental analysis for $C_{15}H_{21}N_3O_5$ (323.34 g/mol): calculated C: 55.72%, H: 6.55%, N: 13.00%; found C: 55.16%, H: 6.64%, N: 12.78%.

^{1}**H-NMR** (400 MHz, DMSO-d_6): $\delta =$ 1.37 (s, 9H, C(C**H**$_3$)$_3$), 3.64 (m, 2H, β-C**H**$_2$), 4.05 (m, 1H, α-C**H**), 4.99 (1H, s, O**H**–Amino acid), 6.90 (m, 3H, N**H**Boc + Ph), 7.21 (m, 1H, Ph), 7.51 (m, 1H, Ph), 8.43 and 8.63 (s, 1H, C**H**=N), 10.00, 11.12 and 11.30, 11.70 (s, 1H, O**H**, N**H**) ppm.

^{13}**C-NMR** (100 MHz, DMSO-d_6): $\delta =$ 28 (C(**C**H_3)$_3$), 56.00, 54.00 (α-**C**H), 61.17, 61.54 (β-**C**H_2), 78.00, 78.34 (O**C**$(CH_3)_3$), 116.11, 116.36 (Ph), 118.30 and 118.63, 119.34 and 120.00 (Ph), 126.28, 129.38 (Ph), 131.05, 131.33 (Ph), 140.00, 147.00 (**C**H=N), 156.12, 156.32 (Ph), 155.24, 157.33 (**C**=OBoc), 167.13, 171.34 (O=**C**NHN) ppm.

IR data $\tilde{\nu}/\mathrm{cm}^{-1}$: 3372 (OH), 3261 (NH), 1675 (C=O).

5-Bromo-2-hydroxy-salicylidene-L-α-serine-hydrazide (BrsalhyBocser)

To a solution of Boc-L-α-serine hydrazide (1.15 g, 5.25 mmol) in methanol was added slowly by stirring a solution of 5-bromo-2-hydroxy-benzaldehyde (1.06 g, 5.46 mmol) in methanol resulting in a yellow solution and colorless crystalline solid precipitated. The reaction mixture was stirred at room temperature for 4 hours. The separated colorless compound was collected by filtration, recrystallized from methanol and dried in vacuum. The NMR data confirm the presence of product as two isomers in ratio 1:2.3. mp 216 °C.

Total yield: 1.25 g (3.09 mmol, 59.2%).

Elemental analysis for $C_{12}H_{20}N_3O_5Br$ (402.24 g/mol): calculated C: 44.79% H: 5.01% N: 10.45%; found C: 44.78%, H: 4.81%, N: 10.36%.

^{1}**H-NMR** (400 MHz, DMSO-d_6): $\delta =$ 1.37 (s, 9H, C(C**H**$_3$)$_3$), 3.53–3.68 (m, 2H, β-C**H**$_2$), 4.03 (m, 1H, α-C**H**), 4.99 (s, 1H, O**H**–Amino acid), 6.72 (br, 1H, N**H**Boc), 6.83–6.93 (m, 1H, Ph), 7.34–7.41 (m, 1H, Ph), 7.73–7.89 (m, 1H, Ph), 8.21 and 8.39 (s, 1H, C**H**=N), 10.3, 11.15 and 11.34, 11.79 (s, 1H, O**H**, N**H**) ppm.

^{13}**C-NMR** (100 MHz, DMSO-d_6): $\delta =$ 28 (C(**C**H$_3$)$_3$), 53.83, 55.93 (α-**C**H), 61.15, 61.51 (β-**C**H$_2$), 78.07, 78.33 (O**C**(CH$_3$)$_3$), 110.42, 10.87 (Ph – Br), 118.38, 118.63 (Ph), 121.24, 122.68 (Ph), 127.64, 130.38 (Ph), 133.30, 133.50 (Ph), 138.10, 144.74 (**C**H=N), 155.22, 155.50 (Ph), 156.31 (**C**=OBoc), 167 (O=**C**NHN) ppm.

IR data $\tilde{\nu}$/cm^{-1}: 3372 (OH), 3261 (NH), 1674–1689 (C=O).

2.6.2 Synthesis of *N*-salicylidene-Boc-L-α-histidine-hydrazide (HsalhyBochis)

To a solution of Boc-L-α-histidine-hydrazide (1g, 3.7 mmol) in methanol (20 mL), salicylaldehyde (4.52 mg, 3.7 mmol, 0.4 mL) was added slowly dropwise with stirring at 4 °C (ice bath) for 1 hour, and then at room temperature for another 3 hours. The resulting yellow solution was additionally refluxed for 1 hour. The reaction was followed by TLC (diethyl ether: hexane/5:1) until all starting material was completely reacted. The solvent was removed in vacuo. The remaining yellow solid was purified by column

chromatography (eluent Et_2O:hexane/5:1) to obtain the product as a colorless solid.

Total yield: 820 mg (2.2 mmol, 60%).

2.6.3 Synthesis of the Schiff base ligands with Boc-L-α-tryptophan residue

Boc-L-α-tryptophan-methyl-ester

Using the method described for Boc-L-α-serine-methyl-ester, Boc-L-α-tryptophan (5 g, 16.4 mmol) was converted to the title compound as a colorless solid. mp 47 °C.

Total yield: 3.74 g (11.7 mmol, 71.5%).

Elemental analysis for $C_{17}H_{22}N_2O_4$ (318.37 g/mol): calculated C: 64.13%, H: 6.97%, N: 8.80%; found C: 64.43%, H: 6.69%, N: 8.78%.

^{1}H-NMR (200 MHz, DMSO-d_6): $\delta =$ 1.32 (s, 9H, C(C**H**$_3$)$_3$), 2.92–3.32 (m, 2H, β-C**H**$_2$), 3.59 (s, 1H, C**H**$_3$–ester), 4.18–4.25 (m, 1H, α-C**H**), 6.95–6.99 (m, 1H, N**H**Boc), 7.04–7.08 (m, 2H, Ph), 7.14–7.18 (m, 1H, Ph), 7.34 (m, 1H, Ph), 7.48 (m, 1H, Ph), 10.83 (s, 1H, N**H**–Ph) ppm.

^{13}C-NMR (50 MHz, DMSO-d_6): $\delta =$ 26.79 (β-**C**H$_2$), 28.10 (**C**H$_3$)$_3$), 51.69 (**C**H$_3$), 54.64 (α-**C**H), 78.20 (O(**C**(CH$_3$)$_3$), 109.71 (Ph), 111.40 (Ph), 117.95 (Ph), 118.35 (Ph), 120.90 (Ph), 123.69 (Ph), 127.02 (Ph), 136.06 (Ph), 155.3 (NH**C**=OOC(CH$_3$)$_3$), 172.89 (O=**C**NHNC) ppm.

Boc-L-α-tryptophan-hydrazide

Using the method described for Boc-L-α-serine-hydrazide, Boc-L-α-tryptophan-methyl-ester (3.29 g, 10.33 mmol) was converted to the title compound as a colorless solid. mp 63 °C.

Total yield: 2.37 g (7.44 mmol, 72%).

Elemental analysis for $C_{16}H_{22}N_4O_3$ (318.37 g/mol): calculated C: 60.36%, H: 6.97 %, H: 17.60 %; found C: 60.66%, H: 6.96%, N: 17.55%.

^{1}H-NMR (400 MHz, DMSO-d_6): δ = 1.3 (s, 9H, C(C**H**$_3$)$_3$), 2.85 – 2.91 (dd, ^{3}J = 9.2 Hz, ^{2}J = 14.47 Hz, 1H, β-C**H**$_2$), 2.98 – 3.02 (dd, ^{3}J = 5.0 Hz, ^{2}J = 14.47 Hz, 1H, β-C**H**$_2$), 4.16 (m, 1H, α-C**H**), 6.73–6.75 (br, 1H, N**H**Boc), 6.95–6.98 (m, 1H, Ph), 7.03 – 7.06 (m, 1H, Ph), 7.11 (s, 1H, Ph), 7.29–7.32 (1H, m, Ph), 7.57 – 7.59 (m, 1H, Ph), 9.12 (1H, s, N**H**–NH$_2$), 10.78 (s, 1H, N**H**–Ph) ppm.

^{13}C-NMR (50 MHz, DMSO-d_6): δ = 27.75 (β-**C**H$_2$), 28.16 (**C**H$_3$)$_3$), 54.21 (α-**C**H), 77.86 ((O(**C**(CH$_3$)$_3$), 110.16 (Ph), 110.82 (Ph), 118.16 (Ph), 118.49 (Ph), 120.78 (Ph), 123.64 (Ph), 127.31 (Ph), 136.02 (Ph), 155.04 (NH**C**=OOC(CH$_3$)$_3$), 171.35 (O=**C**NHNC) ppm.

EI-MS: (**MeOH**) m/z = 318 (20% [M$^+$.]), 262 (10%), 245 (2%), 201 (22%), 170 (12%), 130 (100%).

***N*-Salicylidene-Boc-L-α-tryptophan-hydrazide (HsalhyBoctrp)**

Salicylaldehyde (0.33 mL, 3.14 mmol) was slowly added dropwise to a solution of Boc-L-α-tryptophan-hydrazide (1g, 3.14 mmol) in methanol (30 mL). The reaction mixture turned its color to yellow once the salicylaldehyde was added. The mixture was stirred at room temperature for 12 hours. The product was obtained as a colorless solid. (The reaction was followed by TLC). The NMR data confirm the presence of product as two isomers in ratio 2.5:1. mp 157 °C.

Total yield: 1.12 g (2.68 mmol, 85.5%)

Elemental analysis for $C_{23}H_{26}N_4O_4$ (422.48 g/mol): calculated C: 65.39 %, H: 6.20 %, N: 13.26 %; found C: 65.40 %, H: 6.31 %, N: 13.26 %.

^{1}H-NMR (400 MHz, DMSO-d_6): δ = 1.31 (s, 1H, C(C**H**$_3$)$_3$), 2.94–3.1 (m, 2H, β-C**H**$_2$), 4.3 and 5.2 (q, ^{3}J = 5.99 Hz, 7.23 Hz, 1H, α-C**H**), 6.84–6.92 (m, 2H, Ph; N**H**Boc), 6.97–7.07 (m, 2H, Ph), 7.18 (s, 1H, Ph), 7.24–7.34 (2H, m, Ph), 7.49–7.51 (m, 1H, Ph), 7.62–7.72 (m, 2H, Ph), 8.36 and 8.42 (s, 1H, C**H**=N), 10.03, 10.78 and 11.11, 11.28 (s, 1H, O**H**, N**H**), 11.76 (s, 1H, O**H**) ppm.

^{13}C-NMR (100 MHz, DMSO-d_6): δ = 27.55 (β-**C**H$_2$), 28.15 **C**H$_3$)$_3$), 51.66 and 54.21 (α-**C**H), 77.82 and 78.12 (O(**C**(CH$_3$)$_3$), 109.78 (Ph), 110.27 (Ph), 111.30 (Ph), 116.11 (Ph), 116.31 (Ph), 118.06 (Ph), 118.19 (Ph), 118.39 (Ph), 118.48 (Ph), 118.63 (Ph), 119.28

(Ph),120.37 (Ph), 120.87 (Ph), 123.90 (Ph), 126 .6 (Ph), 127.16 (Ph), 129.28 (Ph), 131.07 (Ph), 131.28 (Ph), 136.04 (Ph), 140.83 (**C**H=N), 147.33 (**C**–NH), 155.29 (Ph), 156.35 (Ph), 157.28 (N=**C**–OH), 168.56 (NH**C**=OOC$(CH_3)_3$), 173.51 (O=**C**NHNC) ppm.

IR data $\tilde{\nu}/cm^{-1}$: 3335 (OH), 3256 (NH), 1669 (C=O), 1616 (C=N).

ESI-MS (positive mode): m/z = 422 ([M + H^+] 8%).

2.6.4 Synthesis of the Schiff base ligands with Boc-L-α-phenylalanine residue

Boc-L-α-phenylalanine-methyl-ester

Using the method described for Boc-L-α-serine-methyl-ester, Boc-L-α-Phenylalanine (6.5 g, 24.5 mmol) was converted to the title compound as an orange oil.

Total yield: 6.34 g (23 mmol, 93%)

^{1}**H-NMR** (200 MHz, MeOD-d_4): δ = 1.36 (s, 9H, C(C**H**$_3$)$_3$), 3.04–3.14 (dd, ^3J = 5.84 Hz, ^2J = 13.63 Hz, 2H, β-C**H**$_2$), 3.66 (s, 1H, C**H**$_3$–ester), 4.33–4.40 (m, 1H, α-C**H**), 4.83 (s, 1H, N**H**Boc), 7.17–7.30 (m, 5H, Ph) ppm.

^{13}**C-NMR** (50 MHz, MeOD-d_4): δ = 28.64 (C(**C**H$_3$)$_3$), 38.66 (β-**C**H$_2$), 52.57 (**C**H$_3$–ester), 56.47 (α-**C**H), 80.51 (O**C**(CH$_3$)$_3$), 127.75 (Ph), 129.39 (Ph), 130.21 (Ph), 138.32 (Ph), 157.64 (**C**=OBoc), 174.11 (O=**C**NHNC) ppm.

Boc-L-α-phenylalanine-hydrazide

Using the method described for Boc-L-α-serine-hydrazide, Boc-L-α-Phenylalanine-methyl-ester (6 g, 21.5 mmol) was converted to the title compound as a colorless solid.

mp 127 °C.

Total yield: 5.69 g (21.1 mmol, 98.5%).

Elemental analysis for $C_{14}H_{21}N_3O_3$ (279.34 g/mol): calculated C: 60.20%, H: 7.58%, N: 15.04%; found C: 60.23%, H: 7.54%, N: 15.20%.

^{13}**C-NMR** 400 MHz, $CDCl_3$): δ = 1.36 (s, 9H, C(C**H**$_3$)$_3$), 2.99–3.02 (m, 2H, β-C**H**$_2$),

3.57 (br, 2H, N**H**$_2$–hydrazide), 4.33 (m, 1H, α-C**H**), 5.23 (br, 1H, N**H**–hydrazide), 7.13–7.27 (m, 5H, Ph) ppm.

^{13}**C-NMR** (100 MHz, $CDCl_3$): δ = 28.25 (C(**C**H$_3$)$_3$), 38.59 (β-**C**H$_2$), 54.57 (α-**C**H), 80.27 (O(**C**(CH$_3$)$_3$), 126.97 (Ph), 128.62 (Ph), 129.17 (Ph), 136.44 (Ph), 155.36 (**C**=OBoc), 172 (O=**C**NHNC) ppm.

N-Salicylidene-Boc-L-α-phenylalanine-hydrazide (HsalhyBocphe)

A sample of Boc-L-α-Phenylalanine-hydrazide (1.5 g, 5.37 mmol) was dissolved in methanol (50 mL). Salicylaldehyde (0.7 g, 5.73 mmol) was added dropwise under constant stirring and stirring was continued overnight. Removing of the solvent under reduced pressure yielded the product as a white-yellowish solid, which was dried under vacuum. The NMR data confirm the presence of product as two isomers in ratio 2:1. mp 91 °C.

Total yield: 2.03 g (5.30 mmol, 98.8%).

Elemental analysis for $C_{21}H_{25}N_3O_4$ (383.45 g/mol): calculated C: 65.78%, H: 6.57%, N: 10.96%; found C: 65.43%, H: 6.45%, N: 10.59%.

^{1}**H-NMR** (400 MHz, DMSO-d$_6$): δ = 1.29 (s, 9H, C(C**H**$_3$)$_3$), 2.78 – 2.87 (m, 1H, β-C**H**$_2$), 2.96 – 3 (m, 1H, β-C**H**$_2$), 4.22 (m, 1H, α-C**H**), 6.86 (m, 2H, Ph), 7.24 (m, 5H, Ph, N**H**Boc), 7.51 (m, 1H, Ph), 7.67 (m, 1H, Ph), 8.31 and 8.44 (s, 1H, C**H**=N), 10.05, 11.06 and 11.29, 11.75 (s, 1H, O**H**, N**H**) ppm.

^{13}**C-NMR** (50 MHz, DMSO-d$_6$): δ = 28, 30.62 (C(**C**H$_3$)$_3$), 36.40, 37.20, (β-**C**H$_2$), 53.18, 55 (α-**C**H), 77.91, 78.14 (O(**C**(CH$_3$)$_3$), 115.35 (Ph), 116.15 (Ph), 116.30 (Ph), 117.19 (Ph), 118.62 (Ph), 119.28 (Ph), 120.20 (Ph), 122.24 (Ph), 126.29 (Ph), 127.04 (Ph),128.05 (Ph), 129.06 (Ph), 129.18 (Ph), 131.06 (Ph), 131.30 (Ph), 136.36 (Ph), 137.80 (Ph), 138.26 (Ph), 140.97, 147.95 (**C**H=N), 155.33 (Ph), 156.35 (Ph), 157.24 (Ph), 160.68 (**C**=OBoc), 168.15, 172.83 (O=**C**NHNC) ppm.

EI–MS (positive mode): m/z = 383 (M + H$^+$ 24%), 327 (50%), 310 (15%), 256 (2%), 192 (44%), 120 (82%), 57 (100%).

IR data $\tilde{\nu}$/cm^{-1}: 3341 (br, OH), 3219 (br, NH), 1665 (C=O), 1610 (C=N).

o-Hydroxy-acetophenone-Boc-L-α-phenylalanine-hydrazide (MesalhyBocphe)

To a solution of Boc-L-α-Phenylalanine-hydrazide (0.48 g, 1.72 mmol) in methanol (30 mL), was added dropwise 2-hydroxyacetophenone (0.24 g, 1.73 mmol) and the reaction mixture was refluxed for 8 hours. The reaction mixture was taken to dryness by means of a rotary evaporator, and the remaining yellow solid was crystallized from ethanol, to obtain the product as a colorless solid which was finally dried in vacuum.
mp 179 °C.

Total yield: 0.35 g (0.88 mmol, 51%).

Elemental analysis for $C_{22}H_{27}N_3O_4$ (397.48 g/mol): calculated C: 66.48%, H: 6.85%, N: 10.57%; found C: 66.45%, H: 6.86%, N: 10.52%.

^{1}**H-NMR** (200 MHz, DMSO-d_6): $\delta =$ 1.31 (s, 9H, C(C**H**$_3$)$_3$), 2.47 (s, 3H, C**H**$_3$), 2.85 – 2.94 (m, 2H, β-C**H**$_2$), 4.5 (m, 1H, α-C**H**), 6.83 – 6.9 (m, 2H, Ph), 7.19 – 7.31 (m, 6H, Ph; N**H**Boc), 7.55 – 7.60 (m, 1H, Ph), 11.04 (s, 1H, N**H**C=O), 13.12 (s, 1H, Ph–O**H**) ppm.

^{13}**C-NMR** (50 MHz, DMSO-d_6): $\delta =$ 13.61 (**C**H$_3$), 28.14 (C(**C**H$_3$)$_3$), 40.75 (β-**C**H$_2$), 54.30 (α-**C**H), 78.19 (O**C**(CH$_3$)$_3$), 117.2 (Ph), 118.49 (Ph), 119.25 (Ph), 126.32 (Ph), 128.02 (Ph), 128.38 (Ph), 129.27 (Ph), 131.12 (Ph), 137.73 (Ph), 155.45 (**C**=N), 155.86 (Ph), 158.49 (**C**=OBoc), 169 (O=**C**NHNC) ppm.

IR data $\tilde{\nu}$/cm^{-1}: 3392 (OH), 3300 (NH), 1698, 1661 (C=O), 1606 (C=N).

EI-MS (positive mode): 398 (M + H$^+$ 60%), 341 (36%), 206 (50%), 177 (100%), 120 (52%), 57 (94%).

5-Bromo-2-hydroxy-salicylidene-Boc-L-α-phenylalanine-hydrazide (BrsalhyBocphe)

To a solution of Boc-L-α-phenylalanine-hydrazide (1.5 g, 5.37 mmol) in methanol (10 mL) was added a solution of 5-bromo-2-hydroxy-benzaldehyde (1.1 g, 5.47 mmol) in methanol (50 mL). The reaction mixture was stirred at room temperature overnight. Then the reaction mixture was filtrated and the filtrate was cooled at 0 °C for an overnight period.

The colorless crystalline precipitate thus obtained was filtrated, and dried in vacuum. The NMR data confirm the presence of product as two isomers in ratio 1.1:1. mp 169 °C.

Total yield: 0.90 g (1.95 mmol, 36%).

Elemental analysis for $C_{21}H_{24}BrN_3O_4$ (462.34 g/mol): calculated C: 54.55%, H: 5.23%, N: 9.09%; found C: 54.42%, H: 5.35%, N: 9.16%.

^{1}**H-NMR** (200 MHz, DMSO-d$_6$): $\delta =$ 1.31 (s, 9H, C(C**H**$_3$)$_3$), 2.77 – 2.99 (m, 2H, β-C**H**$_2$), 4.19 and 4.99 (m, 1H, α-C**H**), 6.85–6.89 (m, 1H, Ph), 7.10–7.43 (m, 7H, Ph; N**H**Boc), 7.74–8.87 (m, 1H, Ph), 8.22, 8.37 (s, 1H, C**H**=N), 10.36, 11.09 (s, 1H, O**H**, N**H**), 11.37, 11.81 (s, 1H, Ph–O**H**) ppm.

^{13}**C-NMR** (50 MHz, DMSO-d$_6$): $\delta =$ 28.38 (C(**C**H$_3$)$_3$), 38.42 (β-**C**H$_2$), 53.16, 55.05 (α-**C**H), 77.91, 78.12 (O**C**(CH$_3$)$_3$), 110.38 (Ph), 110.61 (Ph), 110.71 (Ph), 118.43 (Ph), 118.56 (Ph), 121.22 (Ph), 122.77 (Ph), 126.08 (Ph), 127.54 (Ph), 128.06 (Ph), 128.99 (Ph), 129.15 (Ph), 130.20 (Ph), 133.14 (Ph), 133.47 (Ph), 137.76 (Ph), 138.36 (Ph), 138.54 (**C**H=N), 144.62 (**C**=N), 155.31 (Ph), 155.43 (Ph), 156.22 (Ph), 168.37 (**C**=OBoc), 173.25 (O=**C**NHNC) ppm.

IR data $\tilde{\nu}$/cm^{-1}: 3341 (OH), 3260 (NH), 1690, 1665 (C=O), 1611 (C=N).

2.6.5 Synthesis of *cis*-dioxovanadium(v)-complexes with Boc-L-α-serine residue ligands

K[VO$_2$(salhyBocser)]·H$_2$O (1)

To a solution of the ligand HsalhyBocser (70 mg, 0.22 mmol) in methanol (20 mL) was added KVO_3 (30 mg, 0.22 mmol). The reaction mixture was heated at reflux for 3 hours yielding a yellow solution. The hot reaction mixture was filtrated to remove the unreacted KVO_3. The product was collected as a yellow microcrystalline powder by slow concentration of the reaction mixture at room temperature. mp 164 °C.

Total yield: 90 mg (0.19 mmol, 89%).

Elemental analysis for $C_{15}H_{21}KN_3O_8V$ (461.38 g/mol): calculated C: 39.05%, H: 4.59%, N: 9.11%; found C 38.84%, H 4.70%, N 8.99%.

^{1}H-NMR (400 MHz, DMSO-d_6): δ = 1.39 (s, 9H, C(C**H**$_3$)$_3$), 3.33 (s, 2H, **H**$_2$O), 3.56–3.62 (m, 2H, β-C**H**$_2$), 4.22 (s, 1H, α-C**H**), 4.71 (s, 1H, O**H**–Amino acid), 6.50–6.52 (d, ^{3}J = 8.20 Hz, 1H, N**H**Boc), 6.74–6.89 (m, 2H, Ph), 7.17 (m, 1H, Ph), 7.49–7.50 (m, 1H, Ph), 8.78 (s, 1H, C**H**=N) ppm.

^{13}C-NMR (100 MHz, DMSO-d_6): δ = 28.22 (C(**C**H$_3$)$_3$), 54.35 (α-**C**H), 62.42 (β-**C**H$_2$), 77.85 (O**C**(CH$_3$)$_3$), 116.55 (Ph), 119.41 (Ph), 119.68 (Ph), 132.43 (Ph), 132.94 (Ph), 155.03 (Ph), 155.49 (**C**=N), 164.61 (NH**C**=OBoc), 173.91 (O–**C**NNC) ppm.

^{51}V-NMR (105 MHz, DMSO-d_6): δ = - 531 ppm ($\nu_{1/2}$ = 831 Hz) ppm.

IR data $\tilde{\nu}$/cm^{-1}: 3413 (s, br; OH), 1616 (s, br; C=N–N=C), 949 (s, VO_2), 908 (s, VO_2).

ESI-MS (negative ion mode, in methanol): m/z = 404 ([VO_2(salhyBocser)] – H^+).

NH_4[VO_2(salhyBocser)]·EtOH·H_2O (2)

To a solution of the ligand HsalhyBocser (150 mg, 0.46 mmol) in methanol (20 mL) was added NH_4VO_3 (54 mg, 0.46 mmol). The reaction mixture was heated at reflux for 30 minutes when all vanadate has been reacted, yielding a dark brown solution. The hot reaction mixture was filtrated, the solvent was removed to dryness and the residue is recrystallized from ethanol to obtain the product as a brown solid.

Total yield: 174 mg (0.358 mmol, 78%).

Elemental analysis for $C_{17}H_{31}N_4O_9V$ (486.39 g/mol): calculated C: 41.98%, H: 6.42%, N: 11.52%; found C: 41.78%, H: 5.75%, N: 11.38%.

^{1}H-NMR (400 MHz, DMSO-d_6): δ = 1.06 (t, ^{3}J = 7 Hz, 3H, EtOH), 1.37 (s, 9H, C(C**H**$_3$)$_3$), 3.33 (s, 2H, **H**$_2$O), 3.56 – 3.61 (m, 2H, β-C**H**$_2$ overlapping with ethanol), 4.22 (br, 1H, α-C**H**), 4.72 (br, 1H, O**H**–Amino acid), 6.56 (m, 1H, Ph), 7.08 (br, 5H, N**H**Boc + N**H**$_4^+$), 7.41 (m, 1H, Ph), 7.74 (s, 1H, Ph), 8.70 (s, 1H, C**H**=N) ppm.

^{13}C-NMR (100 MHz, DMSO-d_6): δ = 18.51 (EtOH), 28.27 (C(**C**H$_3$)$_3$), 48.59 (**C**H$_3$CH$_2$OH), 54.46 (α-**C**H), 56.06 (EtOH), 62.37 (β–**C**H$_2$), 77.89 (O**C**(CH$_3$)$_3$), 114.89 (Ph), 115.28 (Ph), 115.80 (Ph), 129.30 (Ph), 131.35 (Ph), 132.05 (Ph), 155.07 (**C**=N), 163.00 (NH**C**=OBoc), 169.40 (O–**C**NNC) ppm.

^{51}V-NMR (105 MHz, DMSO-d_6): δ = - 530.89 ppm ($\nu_{1/2}$ = 1057 Hz) ppm.

IR data $\tilde{\nu}$/cm^{-1}: 3372 (s, OH), 3190 (br, NH), 1649 (C=OBoc), 1614 (s, C=N–N=C),

932 (s, VO_2), 908 (s, VO_2).

K[VO_2(BrsalhyBocser)]·2H_2O (3)

To a solution of the ligand BrsalhyBocser (80 mg, 0.25 mmol) in methanol (20 mL) was added KVO_3 (40 mg, 0.25 mmol). The reaction mixture was heated at reflux for 5 h yielding a yellow solution. The hot reaction mixture was filtrated to remove the unreacted KVO_3. Upon standing at 5 °C, yellow colored single crystals suitable for X-ray studies formed within one month.

Total yield: 83 mg (0.14 mmol, 60%).

Elemental analysis for $C_{15}H_{22}BrKN_3O_9V$ (558.29 g/mol): calculated C: 32.27%, H: 3.97%, N: 7.53%; found C: 33.06%, H: 4.03%, N: 7.48%.

^{1}**H-NMR** (400 MHz, DMSO-d_6): $\delta =$ 1.39 (s, 9H, C(C**H**$_3$)$_3$), 3.33 (s, 4H, **H**$_2$O), 3.56-3.61 (m, 2H, β-C**H**$_2$), 4.22 (br, 1H, α-C**H**), 4.72 (br, 1H, O**H**–Amino acid), 6.54 (d, ^{3}J = 8.4 Hz, 1H, N**H**Boc) 6.72 (m, 1H, Ph), 7.40 (m, 1H, Ph), 7.72 (s, 1H, Ph), 8.79 (s, 1H, C**H**=N) ppm.

^{13}**C-NMR** (100 MHz, DMSO-d_6): $\delta =$ 28.22 (C(**C**H$_3$)$_3$), 54.43 (α-**C**H), 62.37 (β–**C**H$_2$), 77.86 (O**C**(CH$_3$)$_3$), 106.83 (Ph), 121.61 (Ph), 121.80 (Ph), 133.85 (Ph), 135.06 (Ph), 154.29 (**C**=N), 155.02 (Ph), 163.51 (NH**C**=OBoc), 174.55 (O–**C**NNC) ppm.

^{51}**V-NMR** (105 MHz, DMSO-d_6): $\delta =$ - 531.1 ppm ($\nu_{1/2}$ = 950 Hz) ppm.

IR data $\tilde{\nu}$/cm^{-1}: 3372 (s, br; OH), 1617 (s, br; C=N–N=C), 949 (s, VO_2), 904 (s, VO_2).

UV/Vis (DMF solution, λ_{max} in nm (ε in 10^3 M^{-1} cm^{-1})): 287 (10.8), 386 (5).

ESI-MS (negative ion mode, in methanol): m/z = 482 ([VO_2(BrsalhyBocser)] – H^+).

NH_4[VO_2(BrsalhyBocser)]·MeOH (4)

To a solution of the ligand BrsalhyBocser (1.10 g, 2.76 mmol) in methanol (20 mL) was added NH_4VO_3 (0.37 g, 2.76 mmol). The reaction mixture was heated at reflux for 3 hours yielding a dark brown solution. The hot reaction mixture was filtrated off, and left to cool at room temperature to give a yellow precipitate, which was recrystallized from $CHCl_3$.

Total yield: 0.66 g (1.24 mmol, 45%).

Elemental analysis for $C_{16}H_{26}BrN_4O_8V$ (533.25 g/mol): calculated C: 36.04%, H: 4.91%, N: 10.51%; found C: 36.25%, H: 4.48%, N: 9.75%.

^{1}**H-NMR** (400 MHz, DMSO-d_6): $\delta =$ 1.35 (s, 9H, C(C**H**$_3$)$_3$), 3.56 – 3.61 (m, 2H, β-C**H**$_2$ + C**H**$_3$OH), 4.22 (br, 1H, α-C**H**), 4.73 (br, 2H, O**H**–Amino acid + CH$_3$O**H**), 6.56 (m, 1H, Ph), 7.08 (br, 5H, N**H**Boc + N**H**$_4^+$), 7.41 (m, 1H, Ph), 7.74 (s, 1H, Ph), 8.80 (s, 1H, C**H**=N) ppm.

^{13}**C-NMR** (100 MHz, DMSO-d_6): $\delta =$ 28.27 (C(**C**H$_3$)$_3$), 48.59 (**C**H$_3$OH), 54.46 (α-**C**H), 62.37 (β–**C**H$_2$), 77.89 (O**C**(CH$_3$)$_3$), 106.97 (Ph), 121.63 (Ph), 121.80 (Ph), 133.95 (Ph), 135.16 (Ph), 154.29 (**C**=N), 155.07 (Ph), 163.51 (NH**C**=OBoc), 174.55 (O–**C**NNC) ppm.

^{51}**V-NMR** (105 MHz, DMSO-d_6): $\delta =$ - 532.20 ppm ($\nu_{1/2}$ = 1308 Hz) ppm.

IR data $\tilde{\nu}$/cm^{-1}: 3325 (s, OH), 1690 (s, C=OBoc), 1616 (s, C=N–N=C), 917 (s, VO_2), 900 (s, VO_2).

2.6.6 Synthesis of *cis*-dioxovanadium(v)-complexes with Boc-L-α-histidine residue ligands

2.6.7 [VO_2(HsalhyBochis)] (5)

To a solution of Schiff base ligand HsalhyBochis (300 mg, 0.80 mmol) in dry methanol (35 mL) was added NH_4VO_3 (94 mg, 0.80 mmol) to give a brown colored mixture. The resulting mixture was refluxed for 6 hours when a clear solution was obtained. The hot dark brown mixture was filtrated off and the volume of the solution was reduced to about half of its original volume, under reduce pressure and left overnight at room temperature to give a yellow precipitate.

Total yield: 182 mg (0.4 mmol, 50%).

Elemental analysis for $C_{18}H_{22}N_5O_6V$ (455.1 g/mol): calculated C: 47.48%, H: 4.87%, N: 15.38%; found C: 47.22%, H: 4.71%, N: 15.10%.

^{1}**H-NMR** (400 MHz, DMSO-d_6): $\delta =$ 1.32 (s, 9H, C(C**H**$_3$)$_3$), 3.00 (m, 2H,β-C**H**$_2$), 4.50 (s, 1H, α-C**H**), 6.77 (m, 1H, His-Ph), 6.90 (m, 2H, Ph), 7.16 (m, 1H, Ph), 7.30 (m, 1H, Ph), 7.50 (m, 1H, His-Ph), 8.67 (s, 1H, N**H**), 8.79 (s, 1H, C**H**=N) ppm.

^{13}**C-NMR** (100 MHz, DMSO-d$_6$): $\delta =$ 28.13 (C(**C**H$_3$)$_3$), 28.55 (β-**C**H$_2$), 51.29 (α-**C**H), 78.05 (O**C**(CH$_3$)$_3$), 116.68 (Ph), 117.19 (Ph), 118.60 (**C**^{4}), 119.32 (Ph), 119.57 (Ph), 129.24 (Ph), 133.24 (Ph), 154.98 (**C**H=N), 156.08 (**C**=OBoc), 171.34 (O=**C**NHN) ppm.

^{51}**V-NMR** (105 MHz, DMSO-d$_6$): $\delta =$ - 530.30 ppm ($\nu_{1/2}$ = 1321 Hz) ppm.

ESI-MS (negative ion mode, in methanol): m/z = 454 ([VO$_2$(salhyBochis)] – H$^+$).

2.6.8 Synthesis of *cis*-dioxovanadium(v)-complexes with Boc-L-α-tryptophan residue ligands

K[VO$_2$(salhyBoctrp)]·H$_2$O (6)

To a stirred solution of ligand (HsalhyBoctrp) (0.49 g, 1.16 mmol) in methanol (20 mL) was added (0.16 g, 1.16 mmol) of KVO$_3$. The resulting yellow solution was heated at 65 °C for 1 day. The hot reaction mixture was filtrated off and then left to cool at room temperature. The yellow product was obtained within a few days on slow evaporation of the solvent in air. mp 206 °C.

Total yield: 0.58 g (1.03 mmol, 89%).

Elemental analysis for C$_{23}$H$_{26}$KN$_4$O$_7$V (560.62 g/mol): calculated C: 49.28%, H: 4.68%, N: 10.00%; found C: 49.01%, H: 4.56%, N: 10.11%.

^{1}**H-NMR** (400 MHz, DMSO-d$_6$): $\delta =$ 1.34 (s, 9H, C(C**H**$_3$)$_3$), 3.02 – 3.2 (m, 2H, β-C**H**$_2$), 3.31 (s, 2H, **H**$_2$O), 4.42 (m, 1H, α-C**H**), 6.48 – 6.52 (br, 1H, N**H**Boc), 6.73 – 6.78(m, 2H, Ph), 6.93 – 7.06 (m, 3H, Ph), 7.26 – 7.3(m, 2H, Ph), 7.44 – 7.54 (m, 2H, Ph), 8.75 (s, 1H, C**H**=N), 10.74 (s, 1H, N**H**) ppm.

^{13}**C-NMR** (50 MHz, DMSO-d$_6$): $\delta =$ 28.19 (C(**C**H$_3$)$_3$), 30.64 (β-**C**H$_2$), 52.73 (α-**C**H), 77.72 O(**C**(CH$_3$)$_3$), 110.28 (Ph), 111.25 (Ph), 116.49 (Ph), 118.10 (Ph), 118.24 (Ph), 119.41 (Ph), 119.63 (Ph), 120.58 (Ph), 123.57 (Ph), 127.73 (Ph), 132.40 (Ph), 132.98 (Ph), 135.86 (Ph), 154.73 (**C**H=N), 155.52 (Ph), 164.47 (**C**=OBoc), 174.78 (O–**C**NNC) ppm.

^{51}**V-NMR** (105 MHz, DMSO-d$_6$): $\delta =$ -530.37 ppm.

IR data $\tilde{\nu}$/cm^{-1}: 3414 (NH), 1615 (C=N–N=C), 912 (s, VO$_2$), 906 (s,VO$_2$).

UV/Vis (DMF solution, λ_{max} in nm (ε in 10^3 M^{-1} cm^{-1})): 311 (7.2), 387 (5).

UV/Vis (Acetonitrile solution, λ_{max} in nm (ε in 10^3 M^{-1} cm^{-1})): 223 (29.6), 280 (14.4), 386 (5.9).

ESI-MS(negative mode): m/z = 503.2 ([VO_2(salhyBoctrp)] – H^+).

[VO_2(HsalhyBoctrp)]·MeOH (7)

To a solution of Schiff base ligand HsalhyBoctrp (180 mg, 0.427 mmol) in methanol (20 mL) was added NH_4VO_3 (49 mg, 0.426 mmol). The resulting mixture was refluxed for 3.5 hours until all vanadate was reacted, filtrated off, and the solution was allowed to stand at room temperature, to evaporate slowly the solvent to obtain the dark brown solid which was filtered off, and dried in air.

Total yield: 70 mg (0.13 mmol, 30%).

Elemental analysis for $C_{24}H_{29}N_4O_7V$ (536.45 g/mol): calculated C: 53.73%, H: 5.45%, N: 10.46%; found C: 53.99%, H: 5.31%, N: 9.56%.

^{51}V-NMR (105 MHz, DMSO-d_6): δ = -531.39 ppm.

IR data $\tilde{\nu}$/cm^{-1}: 3409 (NH), 1697 (C=OBoc), 1610 (C=N–N=C), 981 (s, VO_2), 909 (s, VO_2).

2.6.9 Synthesis of *cis*-dioxovanadium(v)-complexes with Boc-L-α-phenylalanine residue ligands

K[VO_2(salhyBocphe)]·H_2O (8)

To a solution of HsalhyBocphe (0.5 g, 1.3 mmol) in methanol (40 mL) was added KVO_3 (0.18 g, 1.3 mmol). The solution changed its color from yellow to orange. The reaction mixture was heated at 65 °C for 1 day to obtain a dark orange solution then filtrated off and the filtrate was kept at ambient temperature to allow for slow evaporation of the solvent. A few days later, yellow crystalline solid appeared at the bottom of the flask which was isolated by filtration and dried in vacuo. mp 185 °C.

Total yield: 0.61 mg (1.21 mmol, 93%).

Elemental analysis for $C_{21}H_{25}KN_3O_7V$ (521.48 g/mol): calculated C: 48.37%, H: 4.83%, N: 8.06)%; found C: 48.50%, H: 5.05%, N: 8.19%.

^{1}H-NMR (200 MHz, DMSO-d_6): δ = 1.31 (s, 9H, C(C**H**$_3$)$_3$), 2.81 – 2.92 (dd, ^{3}J = 8.8 Hz, ^{2}J = 13.53 Hz, 1H, β-C**H**$_2$), 3.02 – 3.09 (dd, ^{3}J = 5.12 Hz, ^{2}J = 13.53 Hz, 2H, β-C**H**$_2$), 3.31 (s, 2H, **H**$_2$O), 4.36 – 4.38 (m, 1H, α-C**H**), 6.71 – 6.78 (m, 2H, Ph), 7.20 – 7.35 (m, 5H, Ph, N**H**Boc), 7.50 (m, 1H, Ph), 8.77 (s, 1H, C**H**=N) ppm.

^{13}C-NMR (50 MHz, DMSO-d_6): δ = 28.17 (C(**C**H$_3$)$_3$), 38 (β-**C**H$_2$), 53.19 (α-**C**H), 77.70 (O**C**(CH$_3$)$_3$), 116.53 (Ph), 119.45 (Ph), 119.65 (Ph), 125.98 (Ph), 127.87 (Ph), 129.28 (Ph), 132.45 (Ph), 133.02 (Ph), 138.28 (Ph), 154.83 (Ph), 155.65 (**C**H=N), 164.48 (**C**=OBoc), 174.63 (O–**C**NNC) ppm.

^{51}V-NMR (105 MHz, DMSO-d_6): δ = -530.78 ppm ($\nu_{1/2}$ = 957 Hz) ppm.

IR data $\tilde{\nu}$/cm^{-1}: 3420 (br, H_2O), 1617 (s, C=N–N=C), 940 (s, VO_2), 908 (s, VO_2).

UV/Vis (MeOH solution, λ_{max} in nm (ε in 10^3 M^{-1} cm^{-1})): 279 (10.9), 381 (2.7).

ESI-MS (negative ion mode, in methanol): m/z = 464 ([VO_2(salhyBocPhe)] – H^+).

NH_4[VO_2(salhyBocphe)]·H_2O (9)

To a solution of Schiff base ligand HsalhyBocphe (0.5 g, 1.3 mmol) in methanol (40 mL) was added NH_4VO_3 (0.15 g, 1.31 mmol). The resulting mixture was heated under reflux for 3 days. The hot reaction mixture was filtrated to remove the unreacted NH_4VO_3. The filtrate was kept at ambient temperature to allow for slow evaporation of the solvent. A few days later, brown precipitate appeared at the bottom of the flask which was isolated by filtration and dried in vacuo. mp 138 °C.

Total yield: 0.55 g (1.14 mmol, 88%).

Elemental analysis for $C_{21}H_{29}N_4O_7V$ (500.42 g/mol): calculated C: 50.40%, H: 5.84%, N: 11.20%; found C: 50.63%, H: 5.65%, N: 10.92%.

^{1}H-NMR (400 MHz, DMSO-d_6): δ = 1.31 (s, 9H, C(C**H**$_3$)$_3$), 2.84 – 3.16 (m, 2H, β-C**H**$_2$), 3.34 (s, 2H, **H**$_2$O), 4.37 (m, 1H, α-C**H**), 6.75 (m, 2H, Ph), 7.15 (m, 10H, Ph, N**H**$_4^+$, N**H**boc), 8.78 (s, 1H, C**H**=N) ppm.

^{13}C-NMR (50 MHz, DMSO-d_6): δ = 28.15 (C(**C**H$_3$)$_3$), 38 (β-**C**H$_2$), 53.03 (α-**C**H), 77.71

(O**C**$(CH_3)_3$), 116.72 (Ph), 119.53 (Ph), 125.56 (Ph), 126 (Ph), 127.88 (Ph), 128.06 (Ph), 129.25 (Ph), 133.13 (Ph), 138.24 (Ph), 154.82 (**C**H=N), 155.37 (Ph), 168 (**C**=OBoc), 174.32 (O–**C**NNC) ppm.

^{51}**V-NMR** (105 MHz, DMSO-d_6): $\delta =$ -531.07 ppm ($\nu_{1/2} = 1050$ Hz).

IR data $\tilde{\nu}/cm^{-1}$: 3424 (br, H_2O), 1616 (s, C=N–N=C), 937 (s, VO_2), 908 (s, VO_2).

UV/Vis (MeOH solution, λ_{max} in nm (ε in 10^3 M^{-1} cm^{-1})): 279 (14.9), 381 (4.3).

ESI-MS (negative ion mode, in methanol): m/z = 464 ([VO_2(salhybocphe)] – H^+).

K[VO_2(BrsalhyBocphe)]·H_2O (10)

To a solution of Schiff base ligand BrsalhyBocphe (0.4 g, 0.86 mmol) in methanol (40 mL) was added KVO_3 (0.2 mg, 0.86 mmol). The resulting dark yellow solution was heated at 60 °C for 1 day until the majority of KVO_3 was reacted. The color of the reaction mixture became orange. It was filtrated and the filtrate volume was reduced to ca. 5 mL by rotary evaporation and finally cooled at room temperature. A few days later, yellow crystalline precipitate formed, which was isolated by filtration and dried in vacuo.

mp 196 °C.

Total yield: 0.4 g (0.68 mmol, 79%).

Elemental analysis for $C_{21}H_{24}BrKN_3O_7V$ (598.99 g/mol): calculated C: 42.01%, H: 4.03%, N: 7.00%; found C: 41.96%, H 3.88%, N 6.94%.

^{1}**H-NMR** (400 MHz, DMSO-d_6): $\delta =$ 1.30 (s, 9H, C(C**H**$_3$)$_3$), 2.86 (dd, ^{3}J = 8.79 Hz, ^{2}J = 13.7 Hz, 1H, β-C**H**$_2$), 3.05 (dd, ^{3}J = 5.4 Hz, ^{2}J = 13.7 Hz, 1H, β-C**H**$_2$), 3.32 (s, 2H, **H**$_2$O), 4.38 (m, 1H, α-C**H**), 6.73 (d, ^{2}J = 8.9 Hz, 1H, Ph), 6.80 (m, 1H, N**H**Boc), 7.16 – 7.20 (m, 5H, Ph), 7.41 (m, 8.8 Hz, 1H, Ph), 7.73 (m, 1H, Ph), 8.78 (s, 1H, C**H**=N) ppm.

^{13}**C-NMR** (100 MHz, DMSO-d_6): $\delta =$ 28.16 (C(**C**H$_3$)$_3$), 38.23 (β-**C**H$_2$), 53.24 (α-**C**H), 77.70 (O**C**$(CH_3)_3$), 106.83 (Ph), 121.57 (Ph), 121.82 (Ph), 125.99 (Ph), 127.87 (Ph), 129.24 (Ph), 133.87 (Ph), 135.11 (Ph), 138.24 (Ph), 154.54 (Ph), 154.85 (**C**H=N), 163.51 (**C**=OBoc), 175.40 (O–**C**NNC) ppm.

^{51}**V-NMR** (105 MHz, DMSO-d_6): $\delta =$ -530.47 ppm ($\nu_{1/2} = 983$ Hz).

IR data $\tilde{\nu}/cm^{-1}$: 3420 (br, H_2O), 1617 (s, C=N–N=C), 941 (s, VO_2), 907 (s, VO_2).

UV/Vis (MeOH solution, λ_{max} in nm (ε in 10^3 M^{-1} cm^{-1})): 290 (12), 390 (3.6).

ESI-MS (negative ion mode, in methanol): m/z = 544 ([VO_2(Brsalhybocphe)] – H^+).

K[VO_2(MesalhyBocphe)] (11)

To a solution of the ligand MesalhyBocphe (0.46 g, 1.16 mmol) in methanol (40 mL) was added KVO_3 (0.16 g, 1.16 mmol). The resulting mixture was heated to 60 °C for 2 days. The hot mixture was filtrated and the resulting solution was reduced in vacuum to about half of its original volume. After standing overnight a crystalline material in the form of yellow plates can be isolated. mp 185 °C.

Total yield: 0.56 g (1.08 mmol, 93%).

Elemental analysis for $C_{22}H_{25}KN_3O_6V$ (517.49 g/mol): calculated C: 51.06%, H: 4.87%, N: 8.12%; found C: 49.91%, H: 4.86%, N: 7.96%.

^{1}**H-NMR** (400 MHz, DMSO-d_6): $\delta =$ 1.31 (s, 9H, C(C**H**$_3$)$_3$), 2.67 (s, 3H, C**H**$_3$), 2.85 – 2.91 (dd, ^{3}J = 9.6 Hz, ^{2}J = 13.4 Hz, 1H, β-C**H**$_2$), 3.07 – 3.1 (dd, ^{3}J = 4.4 Hz, ^{2}J = 13.4 Hz, 1H, β-C**H**$_2$), 4.53 (m, 1H, α-C**H**), 6.75 – 6.79 (m, 3H, Ph, N**H**boc), 7.23 – 7.29 (m, 5H, Ph), 7.66 – 7.70 (m, 1H, Ph) ppm.

^{13}**C-NMR** (100 MHz, DMSO-d_6): $\delta =$ 15.90 (**C**H$_3$), 28.17 (C(**C**H$_3$)$_3$), 38.19 (β-**C**H$_2$), 53.76 (α-**C**H), 77.62 (O**C**(CH$_3$)$_3$), 116.83 (Ph), 119.85 (Ph), 122.80 (Ph), 125.90 (Ph), 127.84 (Ph), 129.22 (Ph), 129.29 (Ph), 131.43 (Ph), 138.54 (Ph), 155.03 (N=**C**(CH$_3$)), 161.57 (Ph), 164.17 (**C**=OBoc), 173.56 (O–**C**NNC) ppm.

^{51}**V-NMR** (105 MHz, DMSO-d_6): $\delta =$ -532.23 ppm ($\nu_{1/2}$ = 720 Hz).

IR data $\tilde{\nu}$/cm^{-1}: 1616 (s, C=N–N=C), 949 (s, VO_2), 901 (s, VO_2).

UV/Vis (Acetonitrile solution, λ_{max} in nm (ε in 10^3 M^{-1} cm^{-1})): 211 (26), 271 (12.8), 366 (6). **UV/Vis** (MeOH solution, λ_{max} in nm (ε in 10^3 M^{-1} cm^{-1})): 291 (12.0), 361 (4.2).

ESI-MS (negative ion mode, in methanol): m/z = 478 ([VO_2(Mesalhybocphe)] – H^+).

NH_4[VO_2(MesalhyBocphe)] (12)

To a solution of MesalBocPheHy (230 mg, 0,58 mmol) in methanol (30 mL), NH_4VO_3 (75 mg, 0.64 mmol) was added. The mixture was heated at reflux for 1 hour yielding

a red-brown precibitate. The hot reaction mixture was filtrated, and the filtrate was allowed to evaporate slowly in air at room temperature. The separated brown solid was collected by filtration and dried in vacuum. mp 127 °C.

Total yield: 0.24 g (0.49 mmol, 83%).

Elemental analysis for $C_{22}H_{29}N_4O_6V$ (496.43 g/mol): calculated C: 53.23%, H: 5.89%, N: 11.29%; found C: 53.54%, H: 5.65%, N: 10.19%.

^{1}H-NMR (400 MHz, DMSO-d_6): $\delta =$ (s, 9H, C(C**H**$_3$)$_3$), 2.67 (s, 3H, C**H**$_3$), 2.85 – 3.11 (m, 2H, β-C**H**$_2$), 4.37 (m, 1H, α-C**H**), 6.78 (m, 2H, Ph), 6.96 (s, 1H, N**H**boc), 7.09 – 7.28 (m, 5H, Ph and NH_4^+), 7.69 – 7.71 (m, 1H, Ph) ppm.

^{13}C-NMR (100 MHz, DMSO-d_6): $\delta =$ 15.96 (**C**H$_3$), 28.16 (C(**C**H$_3$)$_3$), 38.17 (β-**C**H$_2$), 53.73 (α-**C**H), 77.64 (O**C**(CH$_3$)$_3$), 117.08 (Ph), 119.55 (Ph), 122.20 (Ph), 125.92 (Ph), 127.86 (Ph), 129.20 (Ph), 129.33 (Ph), 131.60 (Ph), 138.61 (Ph), 155.06 (Ph), 161.50 (**C**=N), 164.15 (**C**=OBoc), 173.6 (O–**C**NNC) ppm.

^{51}V-NMR (105 MHz, DMSO-d_6): $\delta =$ -546.58, -533.67 ppm.

IR data $\tilde{\nu}$/cm^{-1}: 1601 (s, C=N–N=C), 944 (s, VO_2), 873 (s, VO_2).

UV/Vis (DMF solution, λ_{max} in nm (ε in 10^3 M^{-1} cm^{-1})): 260 (10.6), 365 (3.3).

ESI-MS (negative ion mode, in methanol): m/z = 478 ([VO_2(MesalhyBocPhe)] – H^+).

2.6.10 Synthesis of monooxovanadium complexes with phenylalanine Schiff base ligands

VO(OiPr)(salhyBocphe) (13)

To a solution of HsalhyBocphe (0.3 g, 0.78 mmol) in 30 mL dryed iso-propanol [VO(OiPr)$_3$] (192 mg, 0.78 mmol) was added dropwise under an argon atmosphere. The reaction mixture was stirred under argon for 2 h yielding a brown solution. The solvent was removed under reduced pressure to obtain the product as a brown solid.

Total yield: 90 mg (0.18 mmol, 23.83%).

Elemental analysis for $C_{24}H_{30}N_3O_6V$ (507.5 g/mol): calculated C: 56.80%, H: 5.96%, N: 8.28%; found C: 56.85%, H: 5.55%, N: 8.97%.

VO(OiPr)(MesalhyBocphe) (**14**)

To a solution of MesalhyBocphe (0.5 g, 1.26 mmol) in 30 mL dried iso-propanol [$VO(OiPr)_3$] (0.31 g, 1.26 mmol) was added dropwise under an argon atmosphere. The reaction mixture was stirred under argon for 2 h yielding a brow solution. The solvent was removed under reduced pressure to obtain the product as a brown solid.

Total yield: 0.37 g (0.71 mmol, 56%).

Elemental analysis for $C_{25}H_{32}N_3O_6V$ (521.5 g/mol): calculated C: 57.58%, H: 6.19%, N: 8.06%; found C: 56.77%, H: 6.22%, N: 7.91%.

EI-MS (positive mode): m/z = 522 ($M + H^+$ 5%).

V_2O_3(MesalhyBocphe) (**15**)

To a suspension of VO(OiPr)(MesalhyBocphe) (0.11 g, 0.21 mmol) was added 10 mL distilled water, followed by 10 mL methanol. Nothing has dissolved. The solvent was removed under reduced pressure, and to the residue were added 10 mL aceton, and the mixture was heated slowly to 56 °C until complete dissolved. The brown solution was kept at 0 °C for several days, no precipitate formed. The solvent was removed slowly under reduced pressure, to obtain the brown solid, which was dried under vacuum.

Total yield: 0.73 g (0.78 mmol, 62%).

Elemental analysis for $C_{44}H_{50}N_6O_{11}V_2$ (940.8 g/mol): calculated C: 56.17%, H: 5.36%, N: 8.93%; found C: 55.61%, H 5.40%, N 8.84%.

EI-MS (negative mode): m/z = 940 ($M - H^+$ 20%).

2.6.11 Catalytic oxidative bromination of TMB/MCD

The bromination reaction was performed in acetonitrile solution, thermostat at 20 °C. For each complex, three standard solutions of the same concentration were prepared. All measurements were performed in triplicate. Typical procedure: The standard assay

mixture was prepared in an optical cuvette, covered with a teflon-cover, and contained: 0.24 mM sodium bromide (NaBr), 0.24 mM $HClO_4$, 0.12 mM TMB, 6 μM vanadium complex, 0.53 mM hydrogen peroxide (H_2O_2), and 0.05 μM MCD (final concentration in the cuvette). Total volume of the reaction mixture is 2 mL. Each compound was added in the following order: 1,3,5-trimethoxybenzene (TMB), monochlorodimedone (MCD) and NaBr were premixed in acetonitrile to have the concentrations of 0.27 mM, 0.114 mM and 0.54 mM, in ratio 3:3:9 respectively. 880 μL of this mixture was added to 12 μL of vanadium complex, followed by 100 μL of hydrogen peroxide (H_2O_2). The reaction was initiated by addition of 52 μL of $HClO_4$ and followed by UV at 258 nm.

2.6.12 General procedure for preparation of chiral sulfoxides:

Vanadium complex (0.02 mmol) was dissolved at room temperature in a mixture of CH_2Cl_2/CH_3OH 7:3 (20 mL) and 1,3,5-trimethoxybenzene (0.34 g, 2.0 mmol) as internal standard was added followed by (0.24 ml, 2.0 mmol) phenyl methyl sulfide. The resulting solution was cooled down on an ice-bath and H_2O_2 8.24 M (1.2 equiv., 0.31 mL, 2.5 mmol) was added dropwise. The reaction solution was warmed up to room temperature and stirred in a capped flask and monitored by thin-layer chromatography technique (Et_2O:*n*-hexane 9:1). After 1, and 3-hours reaction time, aliquots of the reaction solutions (2.0 mL) were quenched with ca. 5 mL of a stock solution of NaOH (0.1 M) and extracted with ethyl acetate (3×4 mL). The collected organic phases were removed completely to dryness and the residue was redissolved in deuterated chloroform (600 μL) and analyzed by ^{1}H–NMR to determine the yield. From this solution was then taken 60 μL of chloroform, removed the solvent to dryness and the residue redissolved in 2 mL dichlormethane and the enantiomeric excess was determined by chiral HPLC. HPLC retention times for the methylphenyl sulfoxides (R) = 21.17 min and (S) = 29.60 min (hexane:2-propanol, 95:5).

Chapter 3

Vanadium(v) complexes with free L-α-amino-acid residue ligands

Among the biological functions of vanadium, tyrosine and tyrosine derivative complexes play a distinctive role in physiological interactions involving vanadium in the oxidation states +v, +iv, +iii. A prominent example is the potential of tunichromes of vanadium sequestering sea squirts (*Ascidiaceae*) in the reduction of vanadate ($H_2VO_4^-$) to vanadyl (VO^{2+}) and V^{III} ($VO(OH)(H_2O)_4$).[100] Protein phosphatases and kinases are inhibited or stimulated by vanadate, and it has been proposed that this activity of vanadates is related to the presence of vanadium coordination to tyrosine (or serine or threonine) in the active site of these enzymes, a view which is corroborated by the structure of elucidation of a bovine low molecular weight phosphotyrosyl phosphatase,[33] in which vanadate is covalently attached to a serinate, giving rise to an overall trigonal bipyramidal coordination array. Further it has been suggested that the insulin–enhancing behavior of many vanadium compounds has been traced back to the inhibition of a protein tyrosine phosphatase.[101] Furthermore, based on the reported crystal structure of vanadium chloroperoxidase,[19] amino acid residues such as serine, lysine, histidine, arginine and aspartate are present at the active center.

Although many dioxovandium(v) complexes have been prepared, and characterized by X-Ray crystallography, the structure of *cis*-dioxovanadium complexes containing *N*-salicylidene amino acid hydrazide ligands have not been found. Herein we report the first examples of *cis*-dioxovanadium complexes with *N*-Salicylidene amino acid hydrazide

ligands. We have included tyrosine, phenylalanine and leucine in this chapter, in order to enhance the hydrogen bonding interaction of the prosthetic group of V-HPOs, and further to allow comparison of the halogenating properties of the *cis*-dioxovanadium(V) complexes with protected amino acid residue ligands, described in Chapter 2.

3.1 Synthesis and Reactions

To synthesize the Schiff base ligands two possible methods can be used. The first method was applied for the Schiff base ligands with phenylalanine residue, and involves the removal of the Boc protecting group from the Schiff base ligands containing protected phenylalanine, described in chapter 2. The most commonly reported method in the literature is the deprotection of Boc-group with trifluoroacetic acid (TFA), in CH_2Cl_2.[102–104]. In the present work the removal of the Boc group was performed with 20 equiv. of TFA in CH_2Cl_2 for 23–24 hours, followed by neutralization with a 20% aqueous solution of sodium hydrogen carbonate (see Figure 3.1). After working up the products were obtained in good yield 80–90%. Completion of the reaction was monitored by TLC (ethyl acetate/hexane 4:6) until the disappearance of starting material.

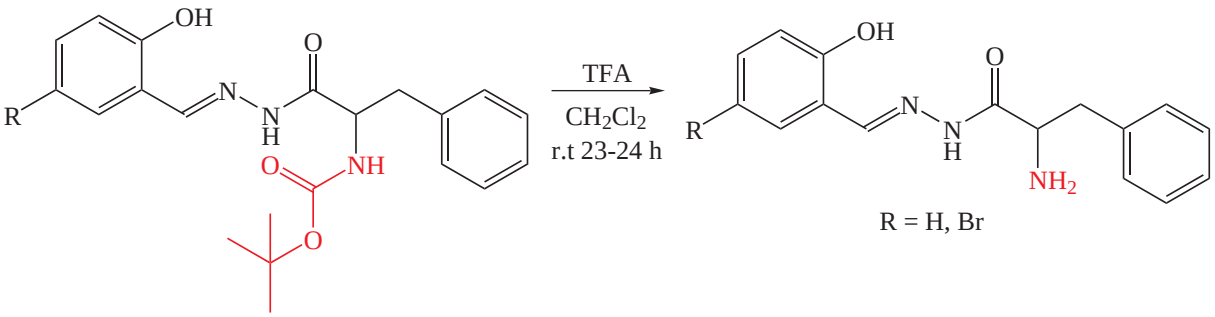

Figure 3.1: Synthesis of *N*-Salicylidenehydrazide ligands with phenylalanine residue by the removal of Boc group from the corresponding Schiff base ligand with protected phenylalanine.

The synthesis of *N*-salicylidene amino acid hydrazide ligands using the second method follows the pathway depicted in Figure 3.2. L-α-leucine, L-α-phenylalanine, and L-α-tyrosine were used as amino acids. Amino acid-methyl-ester-hydrochlorides were used as starting materials.

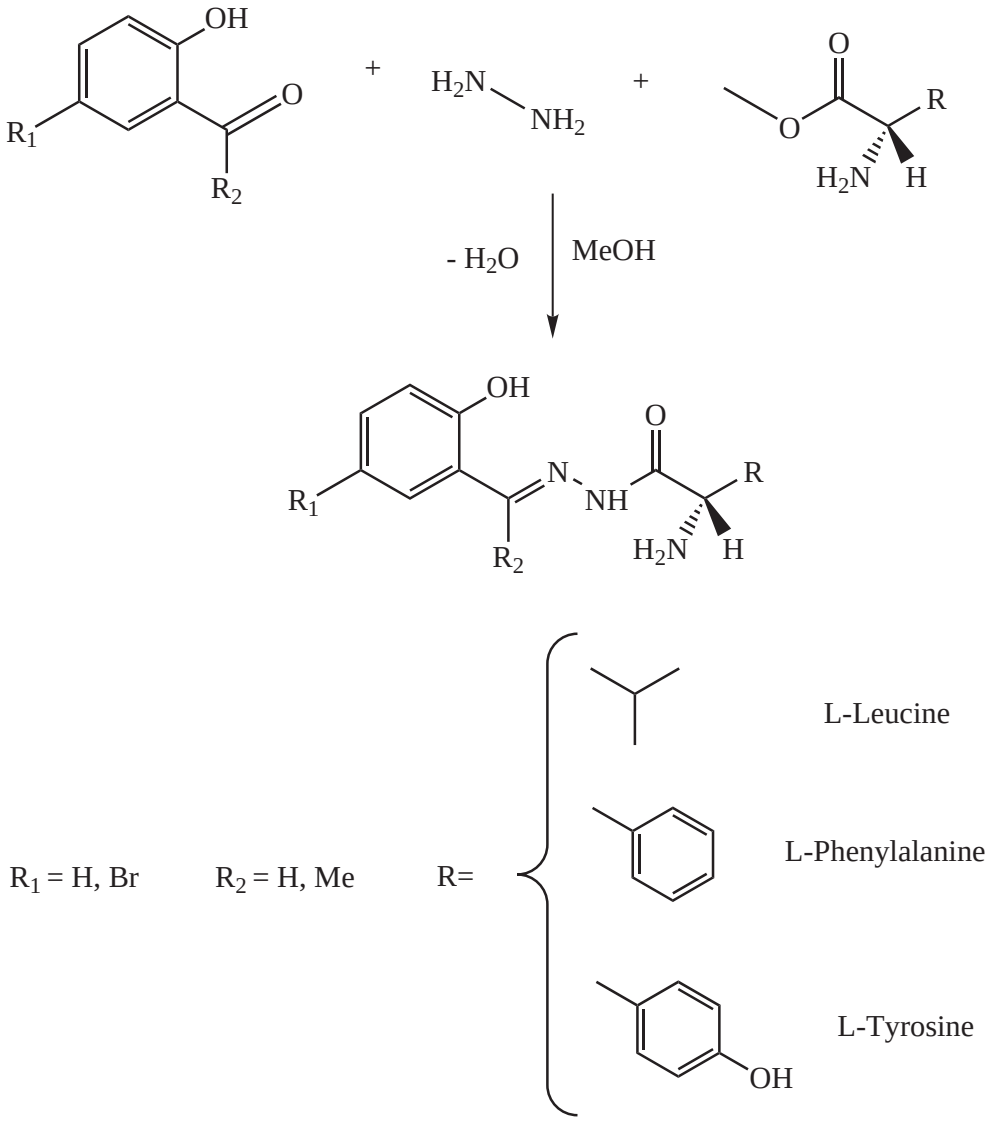

Figure 3.2: Schematic representation of the synthesis of *N*-Salicylidenehydrazide ligands with free amino acid substitutions.

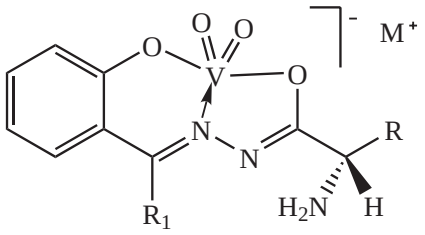

		R	R_1	M^+
Complex	**16**	$CH_2CH(CH_3)_2$	Me	$H^{+(a)}$
	17	$CH_2CH(CH_3)_2$	Me	K^+
	18	CH_2Ph	Me	$H^{+(a)}$
	19	CH_2Ph	Me	K^+
	20	CH_2PhOH	Me	$H^{+(a)}$

[(a)] neutral complex, with protonated amino group

Figure 3.3: Schematic representation of chiral *cis*-dioxo-vanadium(V) complexes with free amino acid residues.

In the case of leucine, the synthesis of leucine-hydrazide was straightforward, thus leucine methyl-ester-hydrochloride reacts with two equivalents of hydrazine monohydrate, in methanol solution at room temperature. When one equivalent of hydrazine was used the reaction time was prolonged. Hydrazide-hydrochloride can be separated from the leucine hydrazide by recrystallization from ethanol. In the case of phenylalanine and tyrosine the first step was removing of hydrochloric acid to obtain the free amino acid-methyl-esters.[105] These esters react then in the next step with two folds excess of hydrazine monohydrate resulting in the formation of the corresponding amino acid hydrazides, which were crystallized directly from the reaction mixture as colorless solids, and further purification was unnecessary. The excess of hydrazine remains in the solution. Subsequent reaction of amino acid hydrazides with salicylaldehyde (itself or one of its ring substituted derivative) results in the formation of the desired Schiff base ligands. Preparation of vanadium complexes were carried out with the vanadium precursor compounds ammonium vanadate (NH_4VO_3), potassium vanadate (KVO_3), vanadium sulfate tryhydrate, and triisopropoxyvanadium(V) oxide ($VO(OiPr)_3$).

Stoichiometric reaction of the ligands with ammonium metavanadate in refluxing methanol

solution, result in the formation of the neutral *cis*-dioxovanadium complexes $[VO_2(Mesalhyleu)]$ (**16**), $[VO_2(Mesalhyphe)]\cdot MeOH$ (**18**), $[VO_2(Mesalhytyr)]\cdot MeOH$ (**20**), and the ammonium salts of the anionic *cis*-dioxovanadium complexes $NH_4[VO_2(salhyCONH_2)]$ (**22**), and $NH_4[VO_2(BrsalhyCONH_2)]\cdot H_2O$ (**25**) (Figure 3.3; 3.5). Sodium salts of the anionic *cis*-dioxovanadium complexes $Na[VO_2(salhyCONH_2)]\cdot MeOH\cdot H_2O$ (**21**), and $Na[VO_2(BrsalhyCONH_2)]$ (**24**) were obtained when vanadyl sulfate trihydrate was used as the vanadium source, under basic conditions (at pH 12–13 using 0.1 M NaOH), in a methanol:water mixture at 65 °C (see Figure 3.5). During this reaction aerial oxygen acts as the oxidising agent in the oxidation of vanadium(VI) to (V). This method represents an alternative method to synthesize dioxovanadium complexes, but in comparison with he first method this has the disadvantage of longer reaction time.

In the case of the Schiff base ligand with tyrosine residue in an alternative way the ligand was allowed to react with tri-isopropylatvanadium(V) oxide ($VO(OiPr)_3$) in dry isopropanol under argon atmosphere. Our initially idea was to synthesize monooxo-

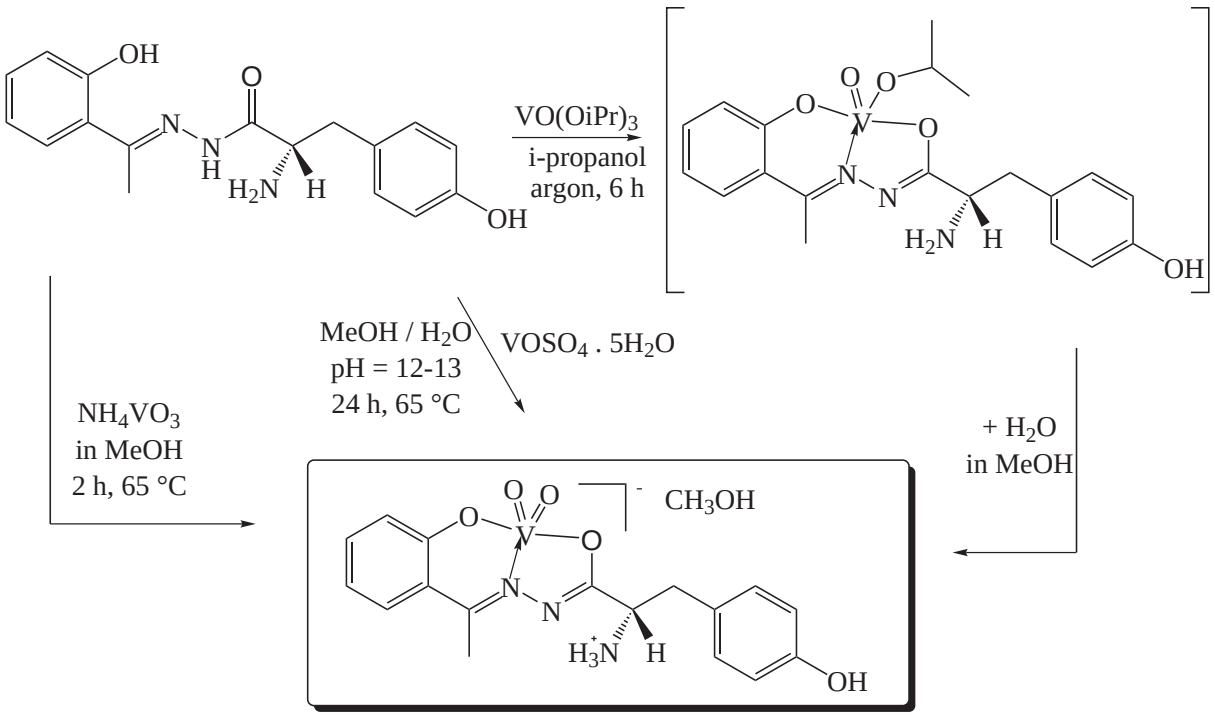

Figure 3.4: Schematic representation of chiral *cis*-dioxo-vanadium(V) complex **20** with tyrosine substituted ligand.

vanadium complex, but unfortunately we could not isolate this complex. An unidentified mixture of compounds was formed, which was converted to the neutral *cis*-dioxovanadium complex **20**, as a product of the hydrolization reaction by addition of water and methanol (Figure 3.4).

To synthesize the potassium salts of the anionic *cis*-dioxovanadium(V) complexes $K[VO_2(Mesalhyleu)]\cdot 5H_2O$ (**17**), $K[VO_2(Mesalhyphe)]$ (**19**), $K[VO_2(salhyCONH_2)]\cdot MeOH$ (**23**), and $K[VO_2(BrsalhyCONH_2)]\cdot H_2O$ (**26**) potassium vanadate reacts with the ligands in methanol solution heated at reflux (see Figure 3.3, 3.5).

The Schiff base ligands with salicylaldehyde, and its bromo substituted derivative, react with the above-mentioned vanadium sources in order to synthesize the corresponding *cis*-dioxovanadium complexes. Unfortunately, they were not able to give the desired complexes. Instead vanadium complexes **21** to **26** were obtained as the products of the oxidative removal of amino acid residues from the α-methyl groups, followed by oxidation of the C^{α}–C bond, leading to the formation of the α-ketoamides (see Figure 3.5). The unprecedented complexes thus formed, serve as very good catalyst for the oxidation reaction of C^{α}–C to C=O.

The sodium salts of the anionic *cis*-dioxovanadium complexes **21, 24** were obtained when $VOSO_4$ was used under basic conditions (0.1 M NaOH), the potassium salts of the anionic *cis*-dioxovanadium complexes **23, 26** were obtained using KVO_3, and the corresponding ammonium salt of the anionic *cis*-dioxovandium complexes **22, 25** were isolated using NH_4VO_3 as vanadium source. In another attempt we tried to prevent aerial oxygen which acts as the oxidising agent. Therefore the ligand Brsalhyphe was allowed to react with 1 equivalent of NH_4VO_3 in dry methanol under argon atmosphere. Again the C^{α}–C side chain of phenylalanine was oxidized generating the complex **25** with α-ketoamide ligand. The oxidative transformation of C^{α}–C side chain of an amino acid to a carbonyl (CO) function has been reported previously.[106] They report a novel strategy for the backbone modification at the α-carbon of serine and threonine residues in peptide, where Ru(VIII) was used as a powerful oxidizing agent. It is no wonder that there are only a few examples of backbone modifications at the α-carbon in peptides,[107,108] and our complexes described here are the first examples of the *cis*-dioxovanadium complexes which in *situ* generate the oxidative scission of the C^{α}–C side chain of an amino acid.

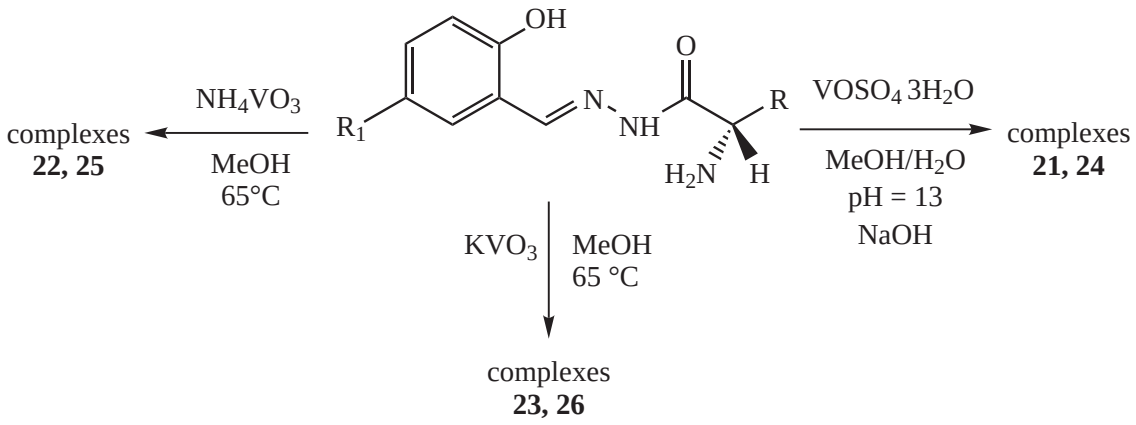

Complex		R_1	M^+
	21	H	Na
	22	H	NH_4
	23	H	K
	24	Br	Na
	25	Br	NH_4
	26	Br	K

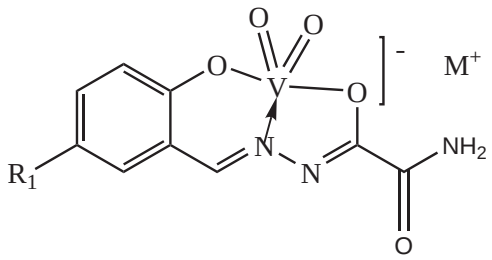

Figure 3.5: Unprecedent formation of *cis*-dioxovanadium(V) complexes from the Schiff base ligands with salicylaldehyde (R_1 = H), and its bromo substituted residue (R_1 = Br).

3.2 Structural characterization

3.2.1 Complexes with phenylalanine residue (18)

The molecular structure of the neutral *cis*-dioxovanadium(V) complex [VO_2(Mesalhyphe)] ·MeOH (**18**) together with the atom numbering scheme is shown in Figure 3.6, and selected bond lengths and angels in Table 3.1. The vanadium(V) atom is five coordinated by the phenolate oxygen atom O3, the imine nitrogen atom N1, amide oxygen atom O4 and the two oxo groups O1 and O2, in a square pyramidal coordinated environment. The ligand acts as a tridentate ligand. The aromatic ring of the aldehyde together with the hydrazide groups lye in the basal plane. Relative to the mean plane given by the ligand system (O3 N1 C8 O4), the vanadium atom is displaced toward the apical oxo group O1 by 40.2 pm, while the equatorial oxo group is slightly distorted on the opposite side by 27.0 pm. The τ value is 0.08 which is slightly distorted from the square-pyramidal

geometry (0 for ideal square-pyramidal and 1 for ideal bipyramidal arrangements.[83]).

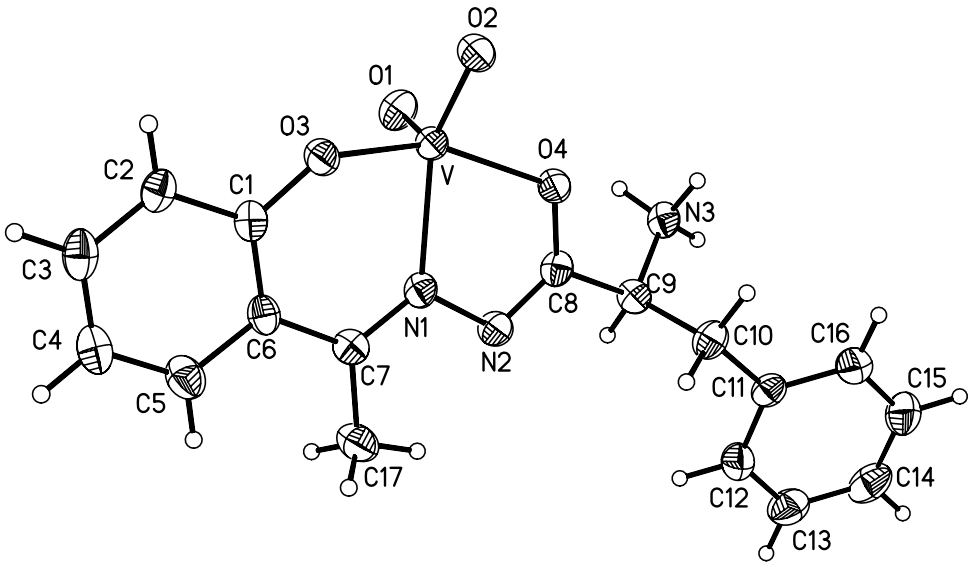

Figure 3.6: Molecular structure of $[VO_2(Mesalhyphe)]\cdot MeOH$ (**18**) (thermal ellipsoids are drawn at the 50% probability level).

The V=O distances V–O1 (161.7(18) pm) and V–O2 (165.8(17) pm) are typical for dioxo-vandium groups.[42,85] The angles in the basal plane of the distorted pyramid are O3–V–O4 149.3(8)° and O3–V–N1 81.9(8)°, which are quite similar to those previously reported for the *cis*-VO_2 moiety in other complexes.[39,42,84,86] The iminolate form of the ligand is consistent with the observed V–O4 and O4–C8 bond lengths. The O4–C8 bond distance, which is the most significant parameter for differentiating between the iminol and keto form of the amide functionality, exhibits value of 130.4(3) (pm) and is nearer to a C–O single bond than to a C–O double bond distance. The bond lengths N1–N2, N1–C7 of the coordinated ligand system are in good agreement with the data found for similar dioxovanadium complexes.[42,84] The adjacent C8–N2 bond display a typical double bond distance of 129.4(3) (pm), and a concomitant lengthening of the N2-N1 bond of 141.5(3) (pm) is also apparent. The N1–C7 bond distance of 131.8(11) (pm) is pretty close to the usual C=N length.[84] The protonated amino group compensates the negative charge of the vanadate moiety. Similar charge compensation is formed at the lysine residue in the vanadium dependent haloperoxidase enzymes, and the lysine is involved in strong hydrogen bonding interaction.

The complex crystallizes in the orthorhombic space group $P2_12_12_1$ with one methanol molecule as solvent of crystallization. An extensive hydrogen bonding interaction is observed, which involves particularly both double bonded oxo groups of the vanadate moiety, mimicking the environment found in the native enzyme (Figure 3.7). The apical oxygen atom O1 forms an intermolecular hydrogen bond with the methanol molecule of crystallization (O1···O1M 286.1(28) pm), which is involved in bifurcated hydrogen bonding interaction with the apical oxo group O1 and the protonated amino group (O1M···N3 280.1(33) pm). The oxygen atom O2 is in hydrogen bonding interactions with two protonated amino groups from two neighboring molecules (O2···N3A 281.5(28) pm, and O2···N3B 279.4(29) pm). A very important role in the native vanadium haloperoxidases is attributed to the lysine residue that is hydrogen bonded to the equatorial oxygen atoms of the vanadate as the prosthetic group V–O···NH_3^+.

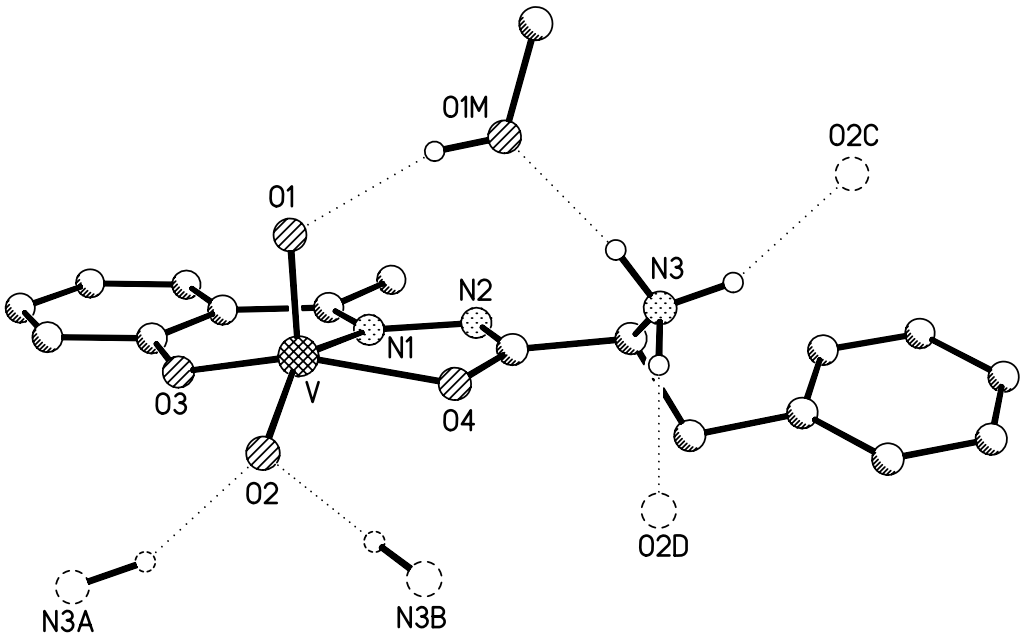

Figure 3.7: Representation of the hydrogen bonding interactions in crystals of complex $[VO_2(Mesalhyphe)]\cdot MeOH$ (**18**) (broken lines represent hydrogen bonds); relevant distances (in pm): N3···O2C 281.5(28), N3···O2D 279.4(29), N3···O1M 280.1(33), O1···O1M 286.1(28) (symmetry transformations: A: – 1 + x, y, z; B: $-\frac{1}{2}+$ x, $\frac{1}{2}-$ y, –z; C: 1 + x, y, z; D: $\frac{1}{2}+$ x, $\frac{1}{2}-$ y, –z).

A similar situation is found in the case of this complex, where the place of the lysine residue is taken by phenylalanine residue leading to a similar V–O···N bridge. Moreover the compensation of the negative charge on the vanadium center by protonated functionalities of the ligand is quite rare and only two more examples are known in the literature. These are the *cis*-dioxovanadium(V) complexes based on *N*-salicylidene hydrazides that contain an amino-functionalized aliphatic side chain,[41] and on *N*-salicylidene dimethylamino acetic hydrazide, which contain a substituted quaternary amino group.[109]

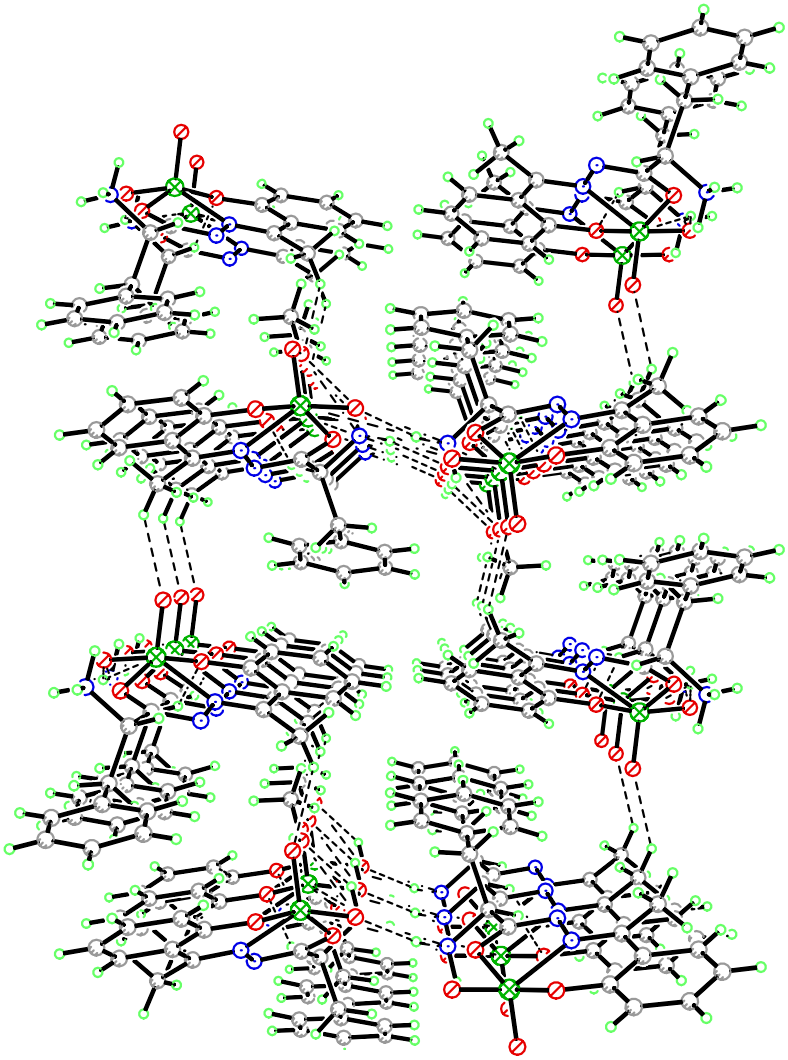

Figure 3.8: Representation of the two-dimensional hydrogen bonding interactions in crystals of complex $[VO_2(Mesalhyphe)]\cdot MeOH$ (**18**), as viewed along the [100] direction; broken lines represent hydrogen bonding interactions.

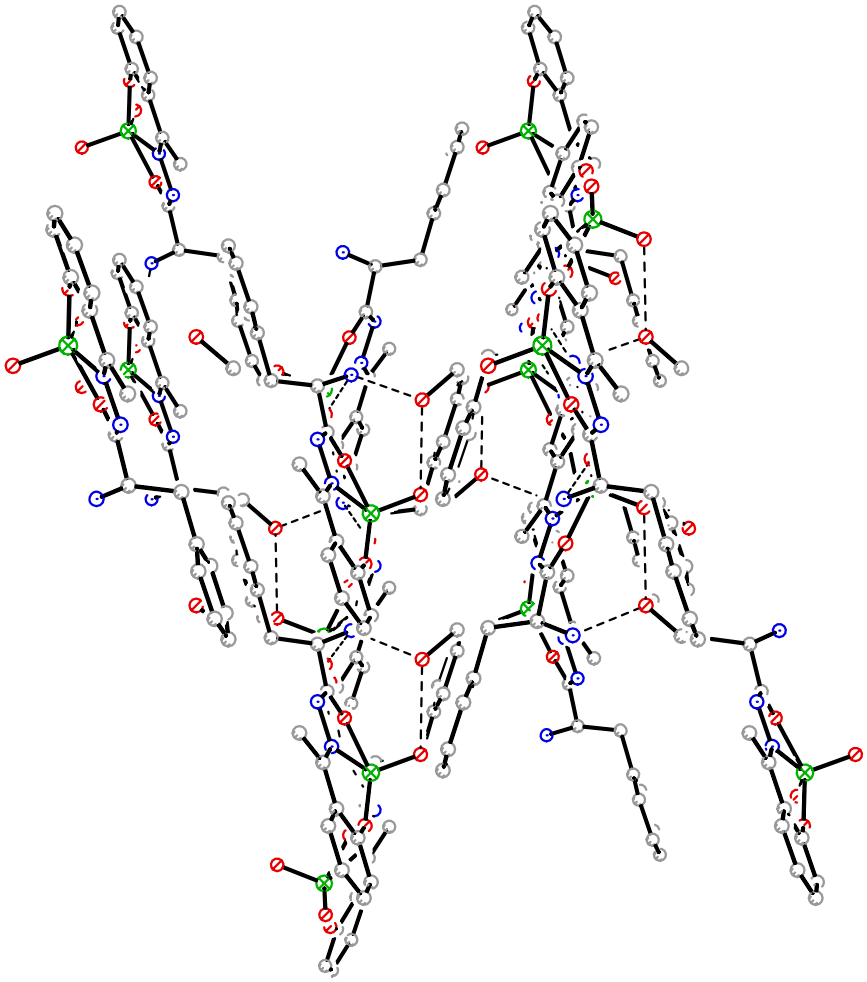

Figure 3.9: Representation of the two-dimensional hydrogen bonding interactions in crystals of complex $[VO_2(Mesalhyphe)]\cdot MeOH$ (**18**), as viewed along the [001] direction; broken lines represent hydrogen bonding interactions.

3.2.2 Complexes with tyrosine residue (20a and 20b)

According with the used synthesizing method and the solvent of crystallization, two types of crystals could be isolated. Crystallization from a 1:1 mixture of methanol-water, following the synthesizing method A, affords complex **20a** (see Figure 3.10), while crystallization from methanol, according with method B and C, leads to complex **20b** (see Figure 3.12). The first mentioned compound contains one methanol, and three water molecules of crystallization per formula unit. Molecular structure determination of complex **20a** shows two crystallographically independent *cis*-dioxovanadium moieties, which form a racemic mixture thus the chirality of the compound has a value of 0.59 (0 for chiral and 1 for no chiral molecules)

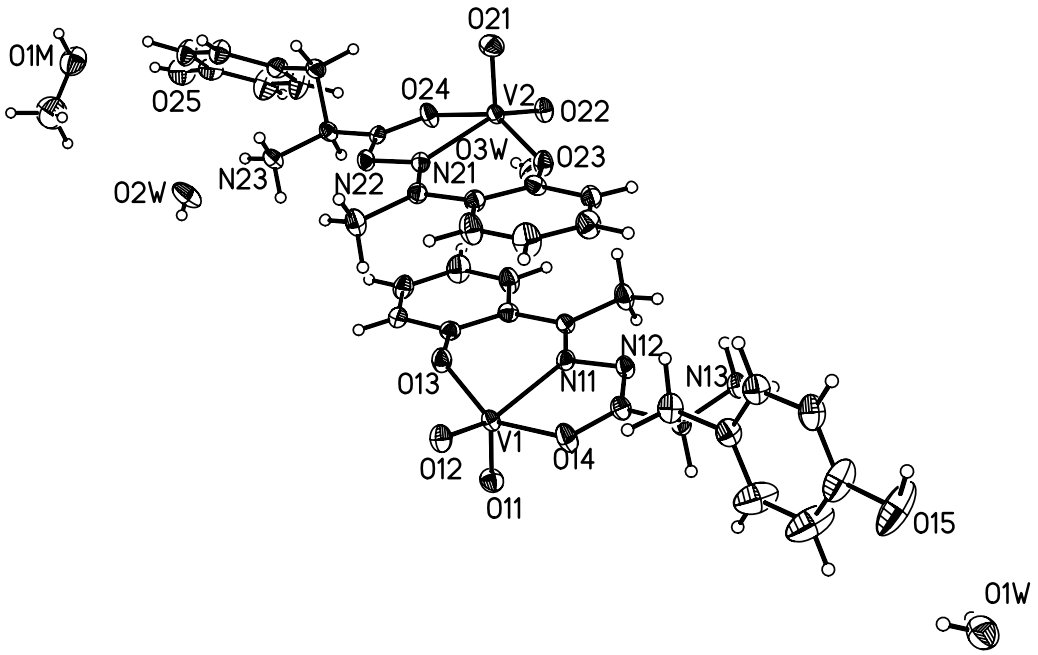

Figure 3.10: Molecular structure of $[VO_2(Mesalhytyr)]\cdot MeOH\cdot 3H_2O$ (**20a**) (thermal ellipsoids are drawn at the 50% probability level).

The complex crystallizes in the monoclinic space group $P2_1$. The vanadium atoms are five coordinated in a square pyramidal geometry with a τ value of 0.004 in the first molecule and, distorted square pyramidal geometry with a τ value of 0.09 in the second molecule. The protonated amino groups compensate the negative charges of the vanadate moieties similar to the lysine residue in the vanadium dependent haloperoxidase enzymes.

The tridentate chelate system coordinates through the phenolate (O13 and O23) and iminolate (O14 and O24) oxygen atoms, as well as the imine nitrogen atoms (N11 and N21). The bond lengths C18–O14 and C28–O24 of 131.1(4) and 129.7(4) respectively, are consistent with the enolized form of the amide functionality and in agrement with the observed V1–O14 and V2–O24 bond lengths of 198.5(3) and 198.3(2), respectively. The vanadium to oxo group bond lengths (V=O) of 162.2(3) pm and 162.4(3) pm, respectively, are similar to reported bond distances in *cis*-dioxovanadium(V) complexes, as well as the V–N and V–O bond lengths.[84,110] Selected bond lengths and angles are listed in Table 3.2.

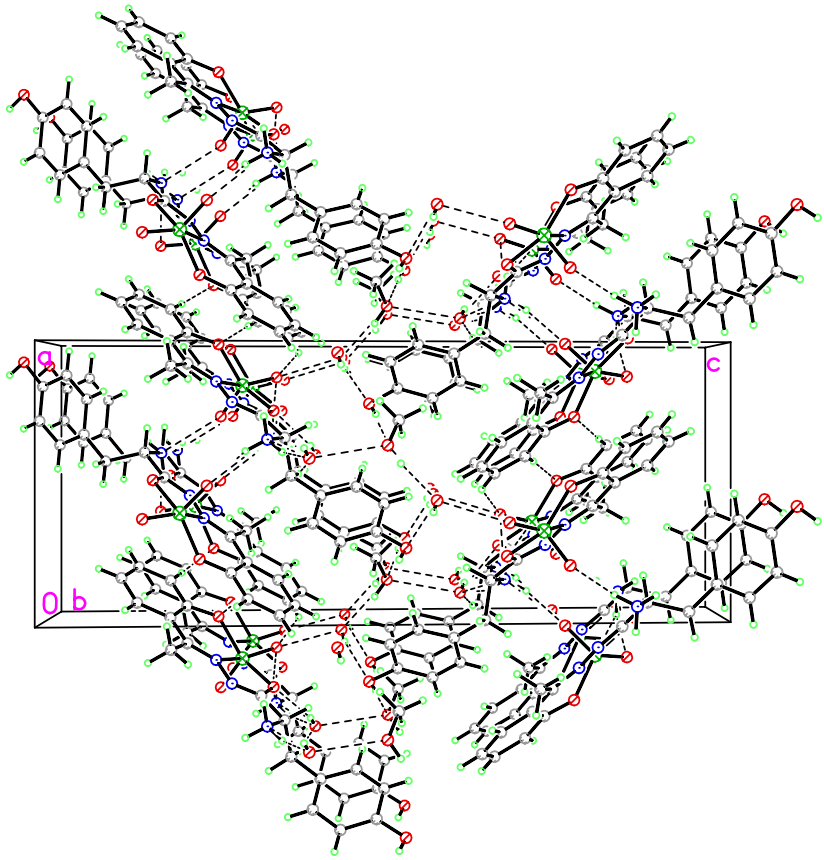

Figure 3.11: Representation of the hydrogen bonding interactions in crystals of complex $[VO_2(Mesalhytyr)]\cdot MeOH\cdot 3H_2O$ (**20a**).

The molecular structure of the neutral *cis*-dioxovanadium(V)-complex $[VO_2(Mesalhytyr)]\cdot MeOH$ (**20b**) given in Figure 3.12, also shows similarities with the corresponding phenylalanine substituted analog $[VO_2(Mesalhyphe)]\cdot MeOH$ (**18**). For the vanadium atom a

slightly distorted square pyramidal coordination is found with the equatorial plane formed by ONO donor atoms of the Schiff base ligand together with the oxo group O2. The apical position in the coordination polyhedron at the vanadium atom is occupied by the other oxo group O1 with a V=O1 bond distance of 161.0(18) pm. This bond distance is comparable with that of complex **18** described previously and within the reported range of vanadium to axial oxygen atom distances in *cis*-dioxovanadium(V) complexes.[39,90,111] The aromatic ring of the aldehyde together with the hydrazide groups lye in the mean plane. The vanadium atom is displaced from the mean plane given by the ligand system (O3 N1 C8 O4), toward the apical oxo group O1 by 33.6 pm, whereas the oxo group O2 is slightly distorted to the opposite side by 47.5 pm. This leads to a τ value of 0.09 which is as in the case of **18**, slightly distorted from the square pyramidal geometry.

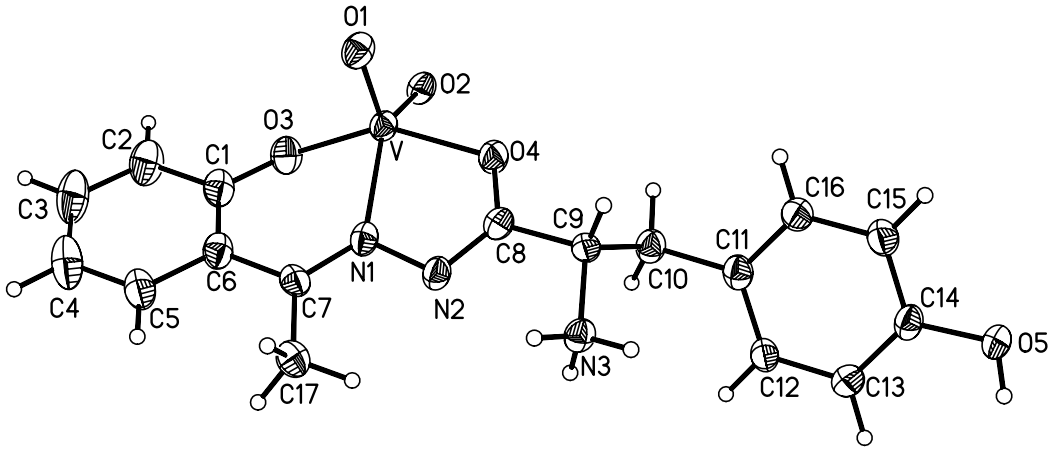

Figure 3.12: Molecular structure of $[VO_2(Mesalhytyr)]\cdot MeOH$ (**20b**) (thermal ellipsoids are drawn at the 50% probability level).

The important difference between the phenylalanine and tyrosine derivative is, that, the network observed for $[VO_2(Mesalhytyr)]\cdot MeOH$ (**20**) contains an additional donor group, namely the hydroxyl functionality which is in hydrogen bonding contact with the methanol molecule of one neighboring molecule (O5$\cdots$O1MD 276.8(1) pm), and the oxo group of another neighboring molecule O2D (O5$\cdots$O2D 264.0(2) pm). The compensation of the negative charge of the vanadate center, as in the case of the complex **18**, is done by the positively charged tyrosine functionality, which is involved in strong hydrogen bonding interactions (Figure 3.13). A vital role for the catalytic activity of vanadium

haloperoxidases enzyme has been attributed to histidine residue (His486 V-BPO and His496 V-CPO) as the single amino acid residue covalently bonded to the vanadium atom. The same situation is found in the described herein complex, where the apical oxygen atom O1 is hydrogen bonding contact to the protonated amino group of a neighboring molecule N3C (O1···N3C 279.3(1) pm) leading to a similar V–O···N bridge. The methanol molecule of crystallization establishes further an intermolecular hydrogen bonding interaction with the protonated amino group N3 (O1M···N3 276.5(1) pm), which is further involved in hydrogen bonding interaction with the equatorial oxo group O2 of a neighboring molecule (N3···O2B 280.0(1) pm).

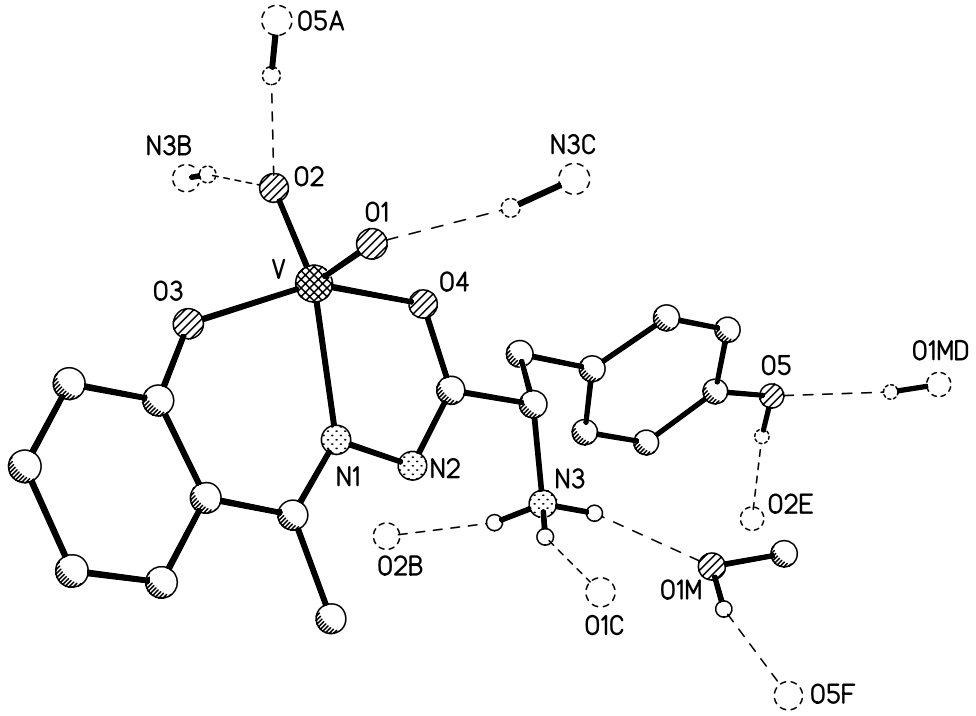

Figure 3.13: Representation of the hydrogen bonding interactions in crystals of complex $[VO_2(Mesalhytyr)]\cdot MeOH$ (**20b**). Only hydrogen atoms bonded to heteroatoms are shown, broken lines represent hydrogen bonds, dashed circles symmetry equivalent atoms; relevant distances (in pm): N3···O1C 279.3(1), N3···O2B 280.0(1), N3···O1M 276.5(1), O5···O1MD 276.8(1), O2···O5A 264.0(2) (symmetry operators: A: $-\frac{1}{2}+x, \frac{1}{2}+y, z$; B: $-x, y, -z$; C: $-x, y, 1-z$; D: $-\frac{1}{2}-x, -\frac{1}{2}+y, 1-z$; E: $-\frac{1}{2}+x, -\frac{1}{2}+y, z$; F: $-\frac{1}{2}-x, \frac{1}{2}+y, 1-z$;).

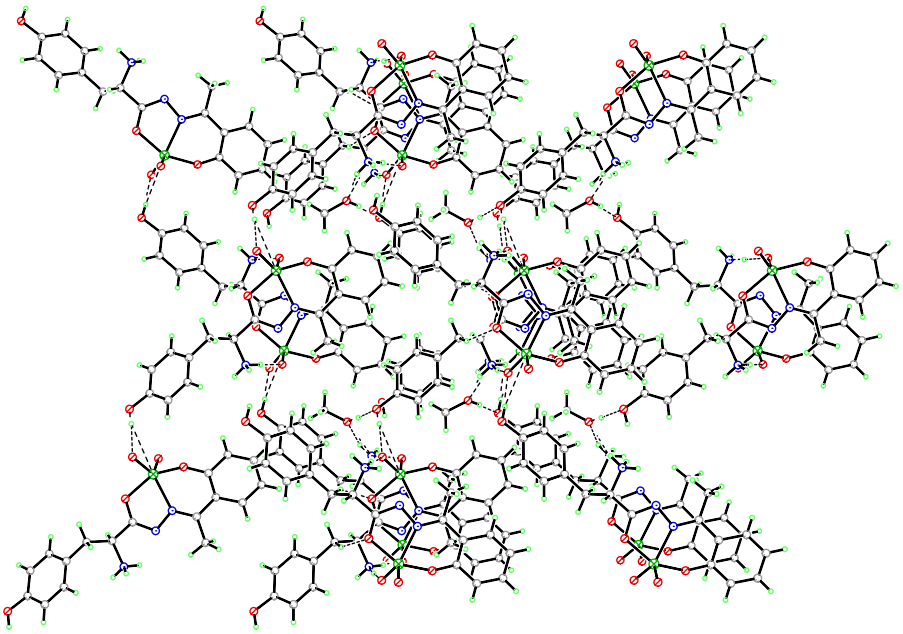

Figure 3.14: Representation of the two-dimensional hydrogen bonding interactions in crystals of complex $[VO_2(Mesalhytyr)]\cdot MeOH$ (**20b**), as viewed along the [001] direction; broken lines represent hydrogen bonding interactions.

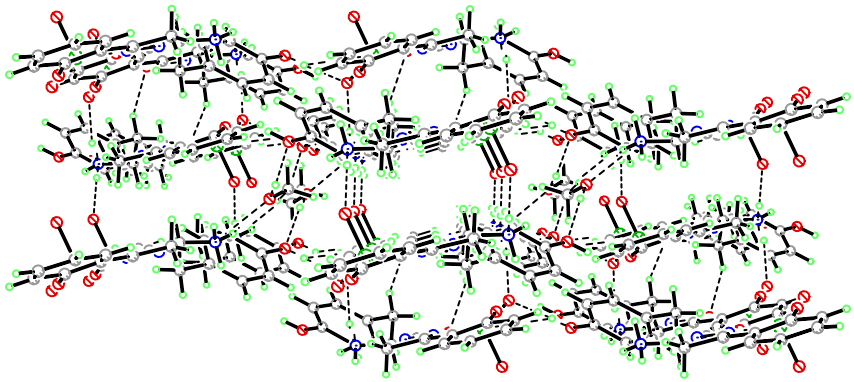

Figure 3.15: Representation of the two-dimensional hydrogen bonding interactions in crystals of complex $[VO_2(Mesalhytyr)]\cdot MeOH$ (**20b**), as viewed along the [010] direction; broken lines represent hydrogen bonding interactions.

3.2.3 Comparison of the structures 18 and 20b

At the first glance, the molecular structure of the neutral *cis*-dioxovanadium(V)-complex $[VO_2(Mesalhytyr)]\cdot MeOH$ (**20b**) shows high similarity with those observed for the corresponding phenylalanine substituted analog $[VO_2(Mesalhyphe)]\cdot MeOH$ (**18**). The overlay of the covalent parts of the two structures shown in Figure 3.16 confirms this. However, from Figure 3.16 it is also obvious, that there are significant differences regarding the orientation of the amino acid residue of the ligand system. This is illustrated by the torsion angle N2–C8–C9–N3 which has a value of 146.7° in complex **18** with the amino acid functionality orientated on the same side as with the vanadate center and phenylalanine residue on the opposite side; whereas in complex **20b** the tyrosine functionality is orientated on opposite direction with the torsion angle of 7.3°. The overlay of two molecular structures was done by method of least square refinement fitting the covalent parts of the two vanadium complexes except the functionalized amino acid residue.

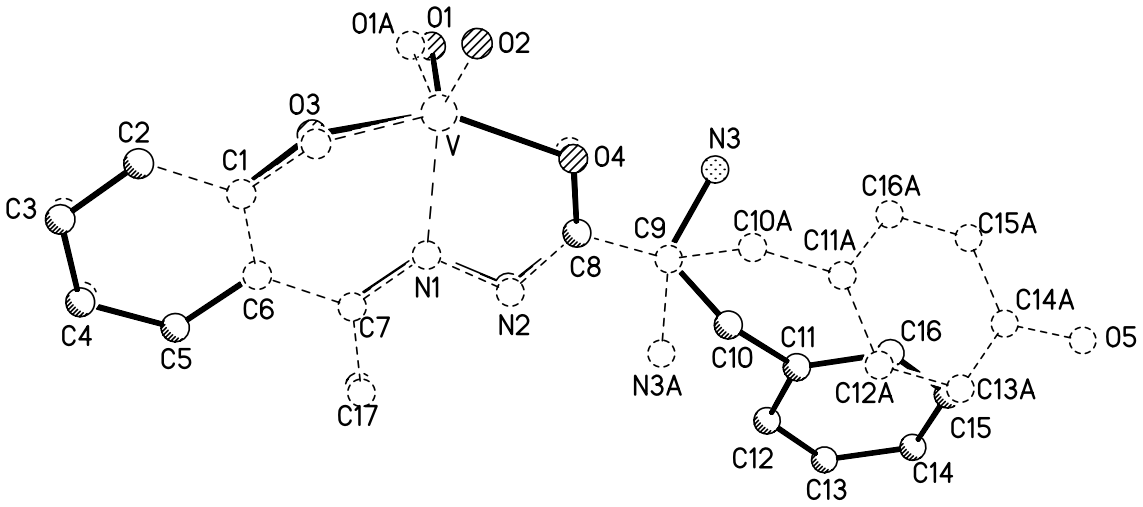

Figure 3.16: Overlay of the molecular structures of complex **18** (thick lines) and complex **20b** (atom numbering extension A, broken lines).

3.2.4 Unprecedented complex 21

The molecular structure of $Na[VO_2(salhyCONH_2)]\cdot MeOH\cdot H_2O$ (**21**) determined by X-ray crystallography features a dioxovanadium(V) moiety as depicted in Figure 3.17. In the

equatorial plane, the vanadium atom is coordinated by the oxo group O2 and the donor atoms N1, O3 and O4 of the tridentate chelate ligand. The apical position at the vanadium atom is occupied by the oxo group O1. The geometry around the vanadium center is, as in the case of complexes **18** and **21**, slightly distorted from the square pyramidal geometry, with the τ value of 0.13. The distances V–O1 162.9(19) pm, and V–O2 163.6(17) pm are well within the expected range and very similar with the corresponding bond lengths in two other complexes **18**, and **21**.

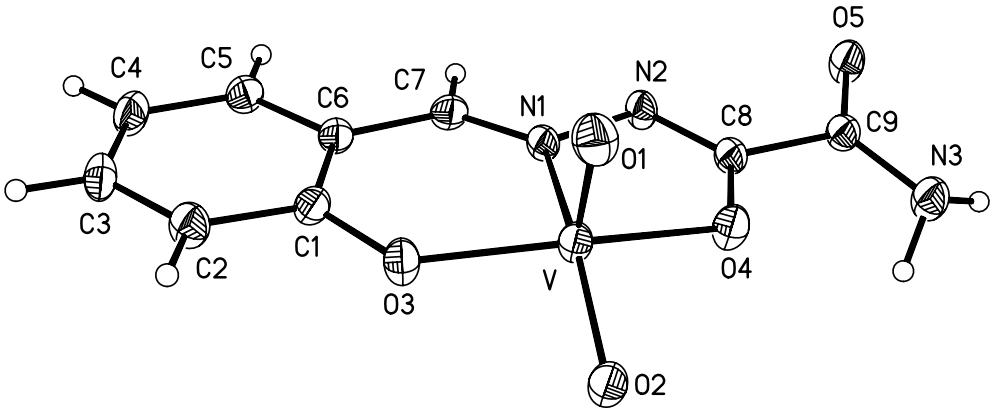

Figure 3.17: Molecular structure of $[VO_2(salhyCONH_2)]^-$ in crystals of $Na[VO_2(salhyCONH_2)]\cdot MeOH\cdot H_2O$ (**21**) (thermal ellipsoids are drawn at the 50% probability level).

Relevant bond distances and angles in complex **21** are listed in Table 3.1. The complex crystallizes in the monoclinic space group $P2_1/n$ with one methanol, and one water molecule as solvent of crystallization. An intramolecular hydrogen bonding interaction is established between the apical oxo group O1 and the methanol of crystallization (O1$\cdots$O1M 275.8(1) pm), and further to the water of one neighboring molecule (O1$\cdots$O1WC 290.0(1) pm) (Figure 3.18). The water molecule of crystallization establishes two hydrogen bonding interactions of which one is to the apical oxo group of one neighboring molecule O1C, and the other is to the oxygen atom O3 of another neighboring molecule O3B (O1W$\cdots$O3B 276.5(1) pm). The amino group is in hydrogen bonding interaction with the equatorial oxo group O2 of one neighboring molecule (N3$\cdots$O2A 298.8(1) pm), and the oxygen atom O5 of another neighboring molecule (N3$\cdots$O5D

286.8(1) pm). This situation is similar to the other complexes **18** and **20**, where the equatorial oxygen atom is hydrogen bonded to the protonated functionalities of the amino acid and moreover similar with the vanadium chloroperoxidase enzyme, where the lysine residue formes hydrogen bond to the equatorial oxygen atom of the prosthetic group. In the native form of vanadium-chloroperoxidase enzyme water molecules were found near the Ser402 residue as well as in the vicinity of the apical oxygen atom of the vanadate moiety.

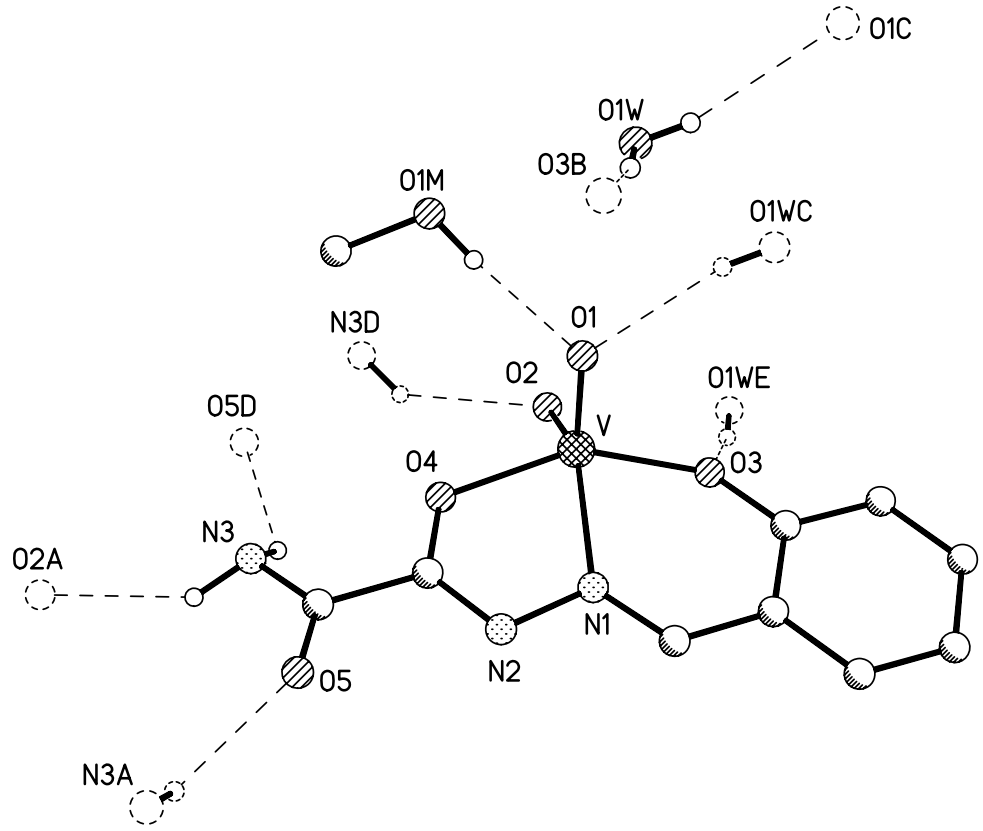

Figure 3.18: Representation of the hydrogen bonding interactions in crystals of complex $Na[VO_2(salhyCONH_2)]\cdot MeOH\cdot H_2O$ (**21**). Only hydrogen atoms bonded to heteroatoms are shown, broken lines represent hydrogen bonds, dashed circles symmetry equivalent atoms; relevant distances (in pm): O1···O1WA 290.0(1), O1···O1M 275.8(1), O1W···O3B 276.5(1), O2···N3D 298.8(1), N3···O5D 286.8(1) (symmetry operators: A: $-\frac{1}{2}+x, \frac{1}{2}-y, -\frac{1}{2}+z$; B: $-1+x, y, z$; C: $1-x, -y, 1-z$; D: $\frac{1}{2}+x, \frac{1}{2}-y, \frac{1}{2}+z$; E: $1+x, y, z$).

The solvent molecules in complex **21** form a long hydrogen bonding channel (Figure 3.19 and 3.20). Thus the complex **21** presents a similar hydrogen bonding network established between water, methanol molecules, and additionally it contains also sodium cations, coordinated to the water molecule of crystallization, methanol molecules and also to the the oxygen atom O5.

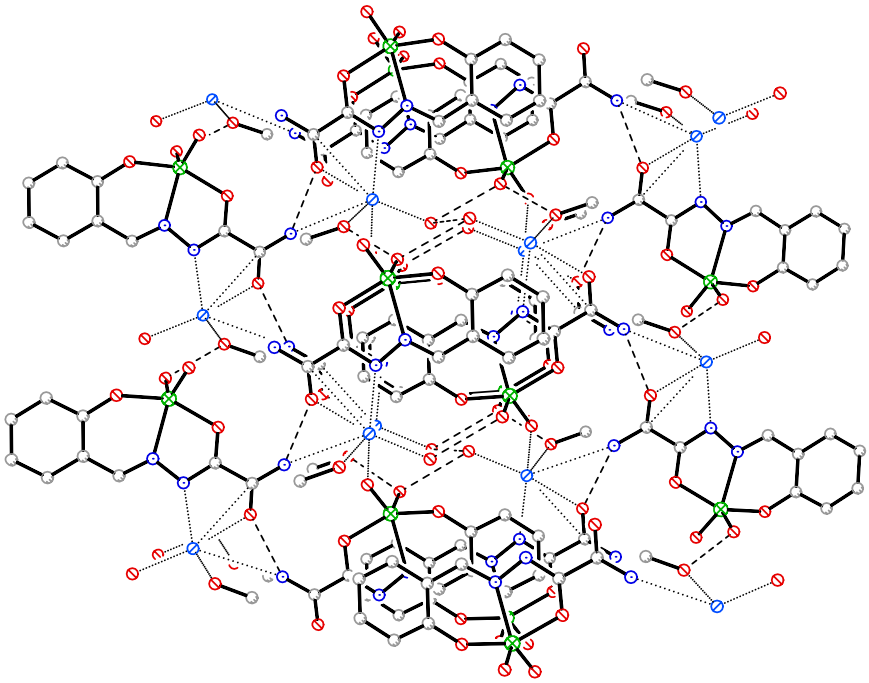

Figure 3.19: Representation of the two-dimensional hydrogen bonding interactions in crystals of complex $Na[VO_2(salhyCONH_2)]\cdot MeOH\cdot H_2O$ (**21**), as viewed along the [100] direction; broken lines represent hydrogen bonding interactions; dotted lines represent sodium contacts.

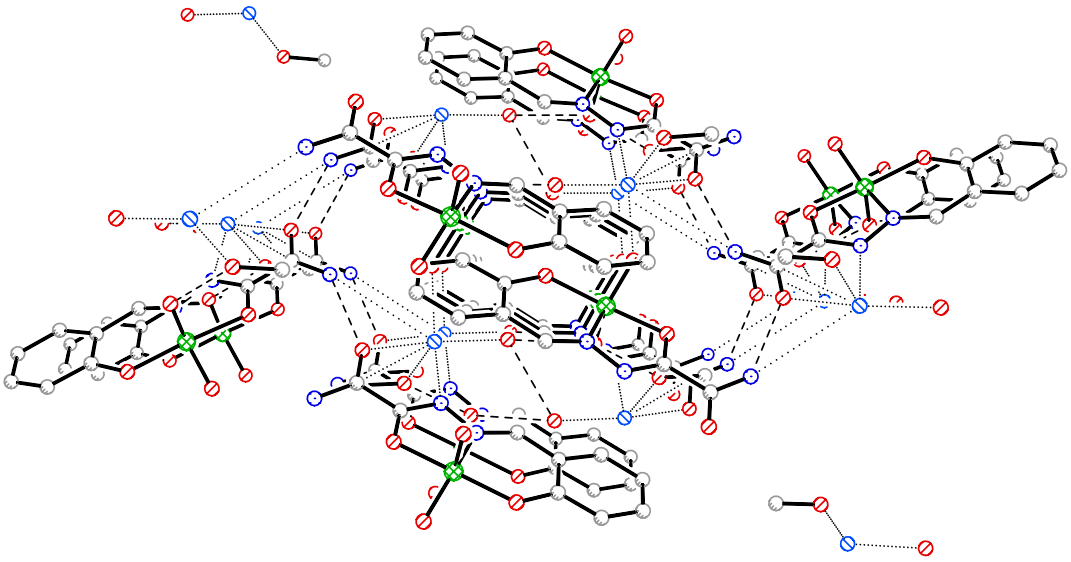

Figure 3.20: Representation of the two-dimensional hydrogen bonding interactions in crystals of complex $Na[VO_2(salhyCONH_2)]\cdot MeOH\cdot H_2O$ (**21**), as viewed along the [001] direction; broken lines represent hydrogen bonding interactions; dotted lines represent sodium contacts.

Table 3.1: Selected bond lengths (pm) and angles (°) for complexes **18**, **20b**, and **21**.

	18	**20b**	**21**
Bond lengths			
V–O1	161.7(18)	161.0(18)	162.9(19)
V–O2	165.8(17)	167.0(2)	163.6(17)
V–O3	187.3(17)	186.4(2)	190.0(16)
V–O4	197.5(18)	198.6(2)	197.1(16)
V–N1	214.6(2)	214.6(3)	215.0(2)
O4–C8	130.4(3)	129.6(4)	130.2(3)
N1–N2	141.5(3)	140.2(4)	141.0(3)
N1–C7	131.8(3)	131.1(4)	129.2(3)
N2–C8	129.4(3)	128.5(5)	129.5(3)
Bond angles			
O1–V–O2	110.2(10)	108.5(12)	108.97(10)
O1–V–O3	106.2(9)	102.7(12)	102.51(8)
O1–V–O4	99.0(9)	101.4(11)	100.39(8)
O2–V–O3	95.9(8)	96.1(3)	96.56(8)
O2–V–O4	91.4(8)	92.8(10)	92.65(8)
O3–V–O4	149.3(8)	149.9(10)	150.95(8)
O1–V–N1	104.1(9)	106.5(11)	107.06(9)
O2–V–N1	144.8(9)	144.5(10)	143.28(9)
O4–V–N1	75.2(8)	74.5(11)	74.01(7)
O3–V–N1	81.9(8)	81.4(10)	82.31(7)

Table 3.2: Selected bond lengths (pm) and angles (°) for complex **20a**.

Bond lengths			
V1−O11	162.3(3)	V2−O21	162.4(3)
V1−O12	166.2(2)	V2−O22	166.0(2)
V1−O13	185.4(3)	V2−O23	186.1(3)
V1−O14	198.5(3)	V2−O24	198.3(2)
V1−N11	216.8(3)	V2−N21	215.3(3)
O14−C18	131.1(4)	O24−C28	129.7(4)
N11−N12	140.5(4)	N21−N22	140.7(4)
N12−C18	130.8(3)	N22−C28	128.8(5)
Bond angles			
O11−V1−O12	107.55(13)	O21−V2−O22	107.13(13)
O11−V1−O13	105.64(13)	O21−V2−O23	107.26(13)
O12−V1−O13	98.36(12)	O22−V2−O23	97.43(12)
O11−V1−O14	102.70(14)	O21−V2−O24	104.04(13)
O12−V1−O14	89.93(12)	O22−V2−O24	89.21(11)
O13−V1−O14	146.36(12)	O23−V2−O24	144.36(11)
O11−V1−N11	104.48(12)	O21−V2−N21	102.49(13)
O12−V1−N11	146.63(12)	O22−V2−N21	148.91(12)
O13−V1−N11	81.62(11)	O23−V2−N21	82.41(11)
O14−V1−N11	74.02(10)	O24−V2−N21	74.49(10)

Table 3.3: Comparison of the bond lengths and C8–N2–N1 angle for complexes **18**, **20b**, and **21**

Complex	d(N1–N2) /pm	(C8–N2–N1) /°	d(C8–O4) /pm	d(C8–N2) /pm	d(V–O4) /pm
18	141.5	108.62	130.4	129.4	197.5
20b	140.2	109.13	129.6	128.5	198.6
21	141.0	107.80	130.2	129.5	197.1

3.3 Spectroscopic Characterization

The spectroscopic characterization of the complexes are consistent with the proposed structures (see Table 3.4). The IR spectra contain strong stretching vibration in the region 899–942 cm^{-1} for the anionic complexes and 862–951 cm^{-1} for the neutral complexes. These stretching vibrations were assigned to the *cis*-VO_2 moiety and the vibrations are similar with reported values for $\nu(VO_2^+)$ group[81,112,113]. The coordination mode of the Schiff base ligands are identical with our *cis*-dioxovanadium(V) complexes published previously.[82] The infrared spectra of the ligands exhibits a strong band in the 1654–1684 region due to ν(C=O) stretching vibrations, and a strong band at 1603–1623 cm^{-1} due to ν(C=N) stretches. These vibrations are absent in the IR spectra of the corresponding complexes. Instead a strong band is observed at around 1600–1617 cm^{-1} which can be attributed to the stretching vibration of the conjugate –C=N–N=C– grouping.[84] This band is characteristic for the coordination of the iminolate form of the ligand to the dioxovanadium(V) moiety. In the case of the complexes **21** to **26** a strong band is observed at 1685–1703 cm^{-1}, which is attributed to the carbonyl ν(C=O) stretching vibrations, confirming the transformation of C^{α}–C side chain of the amino acids to the carbonyl (CO) function. The IR spectra of the free ligands as well as those of the corresponding *cis*-dioxovanadium complexes exhibit a broad vibration in the region 3332–3447 cm^{-1} attributed to the amino functionality of the amino acids. The charac-

teristic ligand stretching vibrations at 3276–3132 cm^{-1} due to ν(O–H) were not observed in the IR spectra of the complexes, indicating the coordination of the ligands through the phenolate function. The presence of water and methanol molecules in the spectra of complexes is shown by broad bands at 3609 and 3634 cm^{-1}, for ν(O–H)–H_2O and ν(O–H)–MeOH, respectively.

Table 3.4: Characteristics IR bands [cm^{-1}] of the *cis*-dioxovanadium complexes with free amino acid residue ligands

Formula	Complex	ν(C=N–N=C)	$\nu(VO_2)$
$[VO_2$(Mesalhyleu)]	**16**	1607	951, 862
$K[VO_2$(Mesalhyleu)]·$5H_2O$	**17**	1606	951, 862
$[VO_2$(Mesalhyphe)]·MeOH	**18**	1600	940, 870
$K[VO_2$(Mesalhyphe)]	**19**	1601	942, 899
$[VO_2$(Mesalhytyr)]·MeOH	**20**	1617	927, 881
$Na[VO_2$(salhy$CONH_2$)]·MeOH·H_2O	**21**	1612	926
$NH_4[VO_2$(salhy$CONH_2$)]	**22**	1616	910
$K[VO_2$(salhy$CONH_2$)]·MeOH	**23**	1612	926
$Na[VO_2$(Brsalhy$CONH_2$)]	**24**	1617	929
$NH_4[VO_2$(Brsalhy$CONH_2$)]·H_2O	**25**	1616	916
$K[VO_2$(Brsalhy$CONH_2$)]·H_2O	**26**	1614	927

Further evidence for the coordination mode of the ligands was obtained from the ^{1}H– and ^{13}C–NMR spectra, and ^{51}V–NMR spectra of the complexes in DMSO-d_6, which are summarized in the experimental section. The ^{1}H–NMR integrations and signal multiplicities agree with the proposed formula. The ^{1}H–NMR spectra of the ligands with salicylaldehyde and its bromo substituted residue reveal the presence of two isomers in a ratio as given in the experimental section. When the metal is coordinated, the deshielding effect of the metal atom is apparent in some protons, causing a downfield shift of the corresponding ^{1}H–NMR peaks. A significant downfield shift of ca. 0.30 ppm for the

azomethine (CH=N) proton signal in the complexes with respect to the corresponding free ligands confirms the coordination of the azomethine nitrogen atom. The aromatic protons of ligands and complexes as well as the α-CH, β-CH_2, and hydroxy group of tyrosine residue, appear in the expected region, with slight shifts in their positions (see Experimental Section). In the case of the complexes **21**, to **26**, no signals are present for the α-CH, β-CH_2, and the aromatic protons of the amino acid residues. This is consistent with the oxidation of the C^{α}–C bond, and removing of the rest of amino acid residue. The ^{1}H–NMR spectra of the complex **20b** does not show any methanol molecule, instead a peak corresponding to the water molecule appears at 3.33 ppm. This was also confirmed by elemental analysis. Whereas the structure analyzes show one methanol molecule, per formula unit. This can be explained due to the fact that the X-ray analysis were performed on fresh crystals from the methanol solution, whereas for NMR and elemental analysis the sample was dried completely before analyzing. It seems that after drying methanol has been removed and water has been absorbed from the complex **20b**.

A broad resonance at ca. 7.22 ppm is observed in the ^{1}H–NMR spectra of the ammonium salt of the *cis*-dioxovanadium(V) complexes **22** and **25** and is attributed to NH_4^+ protons. This resonance is absent in the ^{1}H–NMR of the neutral, and potassium salts of the anionic *cis*-dioxo- complexes. The ^{1}H–NMR of the neutral complexes **16, 18** and **20** exhibit a broad band at ca. 8.15 ppm attributable to the protonated amino acid functionality NH_3^+, whereas the ^{1}H–NMR of the *cis*-dioxovanadium complexes **21** to **26**, formed by the oxidation of the C^{α}–C bond, gave two broad signals in range 7.50–7.80 ppm corresponding to the amino acid functionality NH_2. Furthermore temperature-dependent ^{1}H–NMR experiments of the complex Na[VO_2(BrsalhyCONH_2)] (**24**) were carried out at 400 MHz in DMSO-d_6 solution. Complex **24** exhibits two moderately broad singlets at room temperature, at 7.5 and 7.7 ppm, ca. 0.2 ppm apart from each other, corresponding to the two protons of the amide NH_2. These signals broaden further as the temperature increases, until they coalesce into a broad single signal at 353 K (Figure 3.21). On the basis of these data it could be inferred that the studied *cis*-dioxovanadium complexes **21** to **26**, formed by the oxidation of the C^{α}–C bond, prefer to attain a conformation where the two protons of the amide NH_2 functionality are not equivalent. When conformational interconversion is very slow on the NMR time scale, two broad signals are detected (at

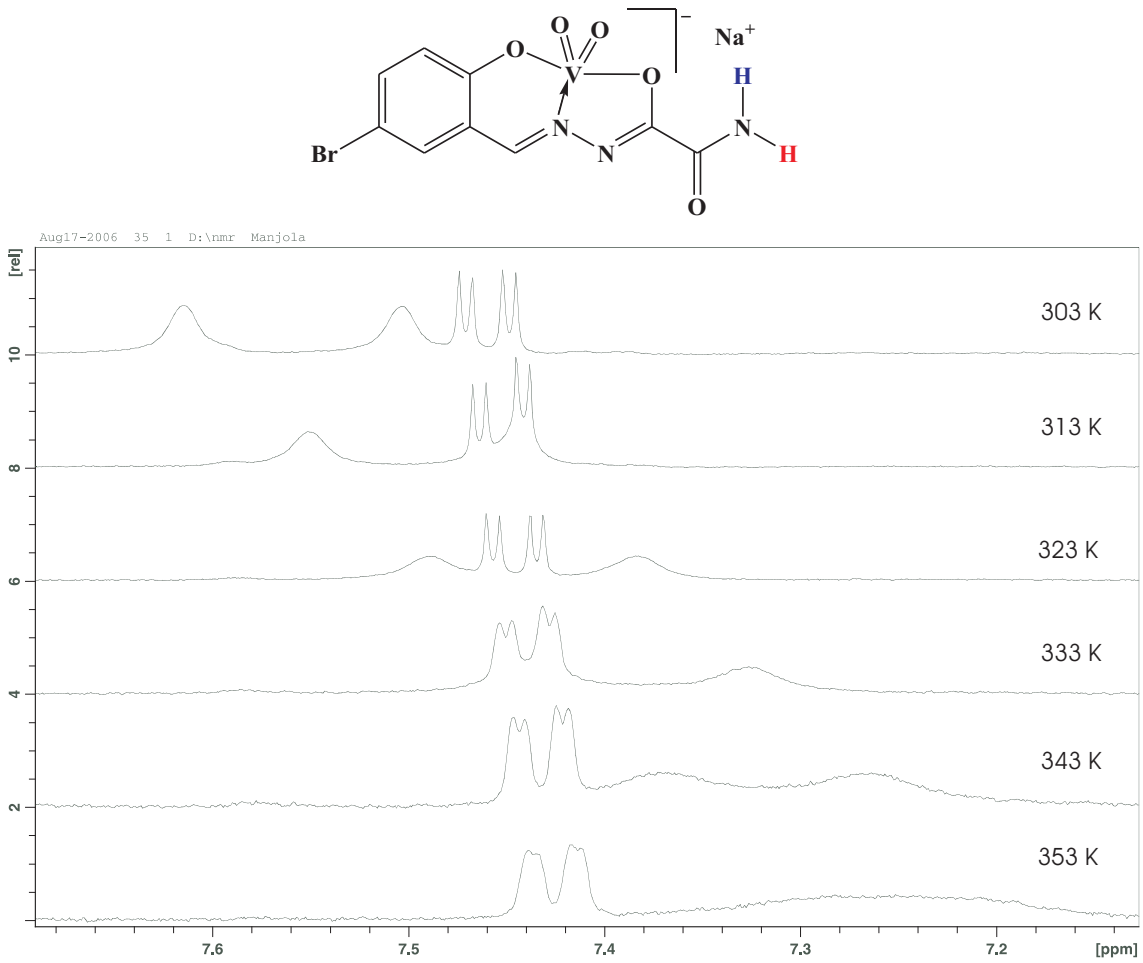

Figure 3.21: Temperature-dependent ^{1}H–NMR experiments of the complex Na[VO_2(BrsalhyCONH$_2$)] (**24**) carried out at 400 MHz in DMSO-d_6 solution

room temperature). As the temperature increases, the interconversion rate increases and the two signals broaden accordingly.

A comparison between the ^{13}C–NMR patterns of the free ligand and the corresponding ^{13}C–NMR spectra of complexes proved the coordination mode of the ligand. The most indicative resonance is the down field shift at 164 ppm of the imine carbon atom (*C*H=N) in the complex, that resonate around 148 – 158 ppm, respectively, in the free ligand as a consequence of the E-Z isomers.

A very good indication of the integrity of complexes in solution is represented by ^{51}V–NMR spectra. The *cis*-dioxovanadium(V) complexes in DMSO-d_6 solution, show one strong resonance at ca. -533 ppm, which is typical for the shift of dioxovanadium(V)

complexes containing a mixed O/N donor set.[10,84,90,91] The resonances have line widths at half-height between 757 and 1077 Hz.

3.4 Reactivity of the complexes

3.4.1 Oxidative bromination of 1,3,5-trimethoxybenzene/monochlordimedone

Following the procedure outlined in chapter 2, the *cis*-dioxovanadium(V) complexes with free amino acid residues described here, were also tested towards their capability to catalyze the oxidative bromination of 1,3,5-trimethoxybenzene (TMB) and monochlordimedone (MCD). The results are summarized in Table 3.5. The turnover frequencies reached by dioxovanadium(V) complexes described here, were compared with those found for $(nBu_4N)_2HVO_4$ published previously.[94] The bromination of TMB took about 480 s when the reaction was catalyzed by vanadate alone; this reaction time was shortened to 204 s (turn over = 350 $mol_{Br\text{-}TMB}h^{-1}mol^{-1}_{catalyst}$) in the presence of $[VO_2(Mesalhyleu)]$ (**16**), which indicates that the catalyst is 2.3 times more reactive with respect to the catalytic bromination of TMB.

Table 3.5: Catalytic oxidative bromination of TMB/MCD catalyzed by *cis*-dioxovanadium complexes with free amino acid residue ligands

Formula	Complex	Time (s)	TOF[(a)]
$[VO_2(Mesalhyleu)]$	**16**	204	350
$[VO_2(Mesalhyphe)]\cdot MeOH$	**18**	252	288
$[VO_2(Mesalhytyr)]\cdot MeOH$	**20**	240	297
$Na[VO_2(salhyCONH_3)]\cdot MeOH\cdot H_2O$	**21**	336	216

(a) Turnover frequencies ($mol_{Br\text{-}TMB}h^{-1}mol^{-1}_{catalyst}$) are calculated for each complex taking into account the completed bromination of TMB within the corresponding time.

The turnover frequencies lay in the range 216–350 $\mathrm{mol_{Br\text{-}TMB}h^{-1}mol^{-1}_{catalyst}}$. No big difference in activity was observed by changing the amino acid residues, but nevertheless a slightly increase in reactivity was observed in the direction Phe < Tyr < Leu. Thus the dioxovanadium complexes with leucine residue appear to be the most reactive catalysts. Moreover it is obviously that the *cis*-dioxovanadium(V) complexes with free amino acid residues react faster than those with Boc protected amino group, described in chapter 2.

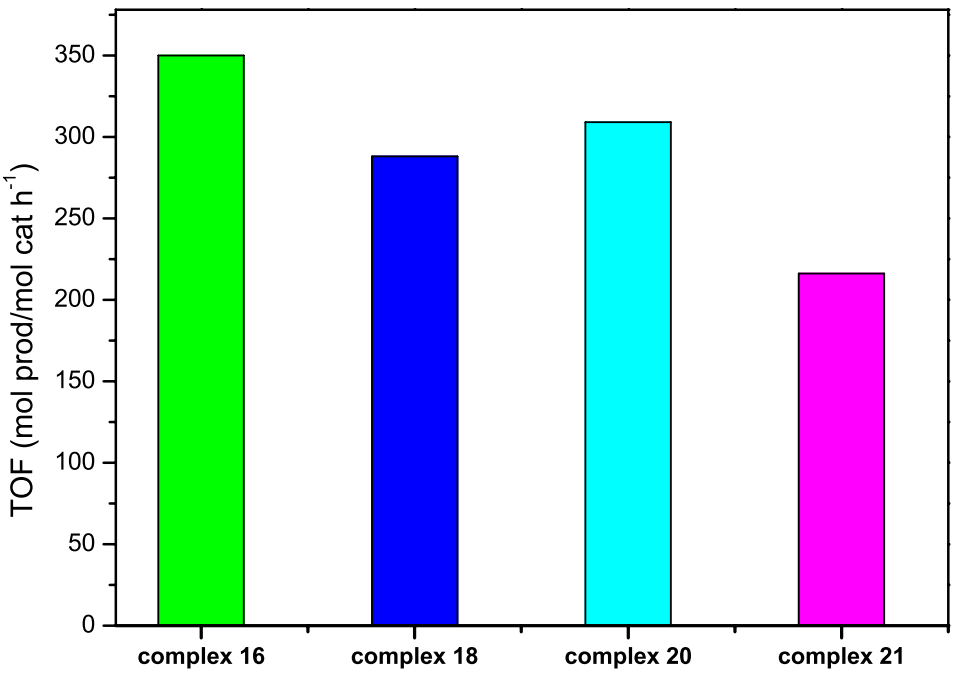

Figure 3.22: Comparison of the catalytic activity towards bromination of TMB/MCD for vanadium complexes, with free amino acid residues

3.4.2 Oxidation of sulfides catalyzed by *cis*-dioxovanadium complexes with free amino acid functionalized ligands

The new chiral *cis*-dioxovanadium complexes with free amino acid ligands, were also tested toward their capability to catalyze the oxidation of methyl phenyl sulfide, using hydrogen peroxide as oxidant. Following the typical procedure described in chapter 2, 1 mol-% catalyst has been used for the reaction and a slight excess (1.2 equivalents) of hydrogen peroxide, in a mixture CH_2Cl_2/CH_3OH 7:3. After defined intervals of time, aliquots were taken from the reaction mixture and the product analyzed by NMR (determination of the yield) and HPLC (determination of the ee). The outcomes of the catalytic reaction are summarized in Table 3.6 for the *cis*-dioxovanadium(V) complexes with free-amino acid residues. After 3 hours 72% of the corresponding sulfoxide was obtained when complex **16**, with leucine residue, was used as catalyst, whereas 75% conversion was established within the same time, by the catalyst **18** with phenylalanine residue. For the catalyst **20**, with tyrosine residue, after 1 hour 24% of sulfoxide was obtained, whereas 86% conversion was established within 3 hours, which is also the most efficient catalytic activity of the herein described complexes. This results are similar with the previous described vanadium complexes with Boc-amino acid ligands and also similar with reported capability of vanadium complexes to catalyze the sulfur oxidation reaction[95,96] where Salen-type oxovanadium(IV) complex which accomplished 80% conversion after two hours of reaction,[95] were reported as efficient vanadium-based catalyst for the sulfide oxidation reaction. The enantioselectivity of the *cis*-dioxovanadium(V) complexes with free amino acid residues, is very low, similar with the ee of the *cis*-dioxovanadium(V) complexes with with Boc-amino acid residue ligands. This indicates that the chiral center is too far away from the vanadate moiety.

Table 3.6: Catalyzed asymmetric oxidation of methyl phenyl sulfide using various complexes

Formula	Complex	Time (h)	Yield[a] (%)	ee [b] (%)	Configuration[c]
$[VO_2$(Mesalhyleu)]	**16**	1	6	13.7	S
$[VO_2$(Mesalhyleu)]	**16**	3	72	0.4	S
$[VO_2$(Mesalhyphe)]·MeOH	**18**	1	0	0	–
$[VO_2$(Mesalhyphe)]·MeOH	**18**	3	75	2	S
K$[VO_2$(Mesalhyphe)]	**19**	1	2	0.84	S
K$[VO_2$(Mesalhyphe)]	**19**	3	7	12	S
K$[VO_2$(Mesalhyphe)]	**19**	24	25	1.5	S
$[VO_2$(Mesalhytyr)]·MeOH	**20**	1	24	4.1	S
$[VO_2$(Mesalhytyr)]·MeOH	**20**	3	86	1.5	S

All reactions were carried out at 0 °C with vanadium complexes loading to 1 mol-% and (1.2 equivalents) of hydrogen peroxide (8.24 M), in a mixture CH_2Cl_2/CH_3OH 7:3. [a]yield determined by ^{1}H–NMR (400 MHz) using 1,3,5-trimethoxybenzene as internal standard. [b] Determined by HPLC using a (S,S)-WHELK-01 chiral column (25 cm × 4.6 mm). The column was eluted with hexane:2-propanol (90:10), at a flow rate of 2.0 mL/min. [c] Absolute configuration of the major product was determined to be S, by comparison of the chromatogram in HPLC with the authentic sample.

3.4.3 Spectrophotometric titration

The spectrophotometric titration of complex **18** was studied, in order to see the stability of complex in water. Therefore a 0.05 mM solution of complex in water was prepared, and titrated with a 10^{-2} M aqueous solution of HCl. The spectral studies shown that the complex slowly decompose in water. The hydrolyses of complex takes about 4 hours. During this period, a gradually loss in intensity of the bands at 260–280 nm due to the monomeric *cis*-dioxovanadium and their final disappearance is observed. The band at

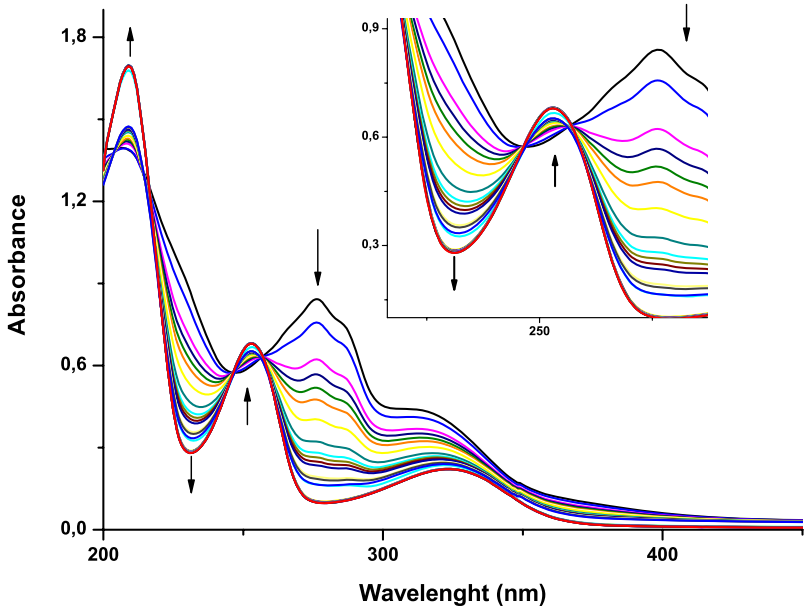

Figure 3.23: Spectrophotometric titration of $[VO_2(Mesalhyphe)]\cdot MeOH$ (**18**) with 0.01 M HCl. The spectra were recorded every 10 minutes after the addition of HCl to a 0.05 mM aqueous solution of **18**

210 nm increase its intensity. The spectrum exhibits further formation of the new band at ca. 250 nm due to the hydrolyzed product, with the isosbestic point clearly present (Figure 3.23).

3.5 Conclusions

New *cis*-dioxovanadium(V) complexes with *N*-salicylidene-amino-acid-hydrazides have been synthesized and fully characterized. This complexes are of interest due to the presence of free amino acid residues within vicinity of the vanadium atom. The importance of these residues are exemplified by the vast number of hydrogen bonding interactions observed, which are involved in pathways relevant to the enzymatic activity. The observed hydrogen bonding network of the complexes show similar features as the active site of V-HPO. The complexes are capable to oxidise bromide, to produce brominated 1,3,5-trimethoxybenzene (TMB)/ monochlorodimedone (MCD), thus modelling the cor-

responding enzyme reaction. Therefore, the herein described complexes can be regarded as both structural and functional model complexes for vanadium haloperoxidases. Moreover complexes showed significant capability for sulfide oxidation, where 86% conversion of thioanisole within three hours was observed using the dioxovanadium complex with tyrosine residue.

3.6 Experimental Section

3.6.1 Synthesis of the Schiff base ligands with L-α-leucine residue

L-α-Leucine hydrazide

To a solution of L-α-leucine-methyl-ester-hydrochloride (10.00 g, 55.05 mmol) in methanol (130 mL) was added dropwise with stirring hydrazine monohydrate (80 %) (5.37 mL, 3 eq.). The reaction mixture was stirred at room temperature for an overnight period. The solvent was removed to dryness to obtain a colorless viscous oil which was dried under strong vacuum and then solidified upon staying at room temperature. This was recrystallized from ethanol. Colorless needles were separated out, which were identified as hydrazide hydrochloride. From the ethanolic filtrate was isolated the right product as a colorless solid.

Total yield: 6.32 g (43.49 mmol, 79%).

^{1}**H-NMR** (400 MHz, $CDCl_3$): $\delta =$ 0.94 (m, 6H, (C**H**$_3$)$_2$), 1,5 (m, 1H, γ-C**H**), 1.64 (m, 2H, β-C**H**$_2$), 3.5 (t, ^{3}J = 7.32 Hz, 1H, α-C**H**), 5.61 (br, 4H, 2N**H**$_2$), 9.32 (br, 1H, N**H**) ppm.

^{13}**C-NMR** (50 MHz, $CDCl_3$): $\delta =$ 22.27, 22.66 (C(**C**H$_3$)$_2$), 23.96 (γ-**C**H), 42.78 (β-**C**H$_2$), 55.99 (α-**C**H), 171.87 (C=O) ppm.

N-Salicylidene-L-α-leucine-hydrazide (Hsalhyleu)

To a stirred solution of leucine-hydrazide (1.11 g, 7.66 mmol) in methanol (30 mL) was added dropwise salicylaldehyde (0.56 mL, 7.66 mmol). The resulting yellow solution

was stirred at room temperature for 6 hours. The volume of the filtrate solution was concentrated to about half under reduce pressure and left at room temperature when an yellow precipitate is formed overnight. The precipitate was collected and recrystallized from ethanol to obtain the product as an yellow solid. The NMR data confirm the presence of two isomers in ratio 1.7:1.

Total yield: 1.74 g (6.97 mmol, 91%).

^{1}**H-NMR** (200 MHz, DMSO-d_6): $\delta =$ 0.97 (m, 6H, (C**H**$_3$)$_2$), 1,59 (m, 3H, γ-C**H**, β-C**H**$_2$), 3.75, 4.54 (t, ^{3}J = 6.68 Hz, 1H, α-C**H**), 6.88 (m, 2H, Ph), 7.27 (m, 1H, Ph), 7.50—7.67 (m, 1H, Ph), 8.57, 8.68 (C**H**=N) ppm.

^{13}**C-NMR** (50 MHz, DMSO-d_6): $\delta =$ 22.13, 22.27, 22.65, 22.93, (C(**C**H$_3$)$_2$), 23.68, 23.89 (γ-**C**H), 40.78 (overlapped with deuterated solvent, β-**C**H$_2$), 48.41, 55.99 (α-**C**H), 116.36 (Ph), 118.64, 119.31, (Ph), 119.95, 125.45, (Ph), 128.92, 131.51 (Ph), 141.99, 147.87 (**C**H=N), 156.67, 157.36 (Ph), 167.55, 171.43 (C=O) ppm.

IR data (KBr disk, cm^{-1}): $\tilde{\nu}$ = 3334 (NH$_2$), 3151 (O–H), 1684 (C=O), 1623 (C=N).

o-Hydroxy-acetophenone-L-α-leucine-hydrazide (Mesalhyleu)

To a solution of leucine-hydrazide (2.77 g, 19.08 mmol) in methanol (30 mL) was added dropwise 2-hydroxy-acetophenone (1.95 mL, 19.08 mmol). The yellow reaction mixture obtained was heated at 40 °C for 22 hours. The resulting solution was evaporated to dryness under reduced pressure and the remaining yellow solid was dried under vacuo. m.p 108 °C.

Total yield: 4.99 g (18.95 mmol, 99.32%).

$[\alpha]_D^{22}$: + 17.5; c = 1 g in 100 mL solution 2.5 N HCl in methanol.

^{1}**H-NMR** (400 MHz, DMSO-d_6): $\delta =$ 0.98 (m, 6H, (C**H**$_3$)$_2$), 1,63 (m, 3H, γ-C**H**, β-C**H**$_2$), 3.17 (s, 3H, C**H**$_3$), 4.13 (t, ^{3}J = 6.68 Hz, 1H, α-C**H**), 6.89 (m, 2H, Ph), 7.31 (m, 1H, Ph), 7.61 (m, 1H, Ph), 7.89 (br, 2H, N**H**$_2$), 13.07 (O**H**) ppm.

^{13}**C-NMR** (100 MHz, DMSO-d_6): $\delta =$ 14.78 (**C**H$_3$), 22.67, 23.17, (C(**C**H$_3$)$_2$), 24.41 (γ-**C**H), 40.82 (β-**C**H$_2$), 50.78 (α-**C**H), 117.57 (Ph), 118.02 (Ph), 119.631 (Ph), 128.95 (Ph), 131.82 (Ph), 136.68 (Ph), 157.79 (**C**H=N), 159.03 (Ph), 168.61 (C=O) ppm.

IR data (KBr disk, cm^{-1}): $\tilde{\nu}$ = 3383 (NH$_2$), 3132 (O–H), 1684 (C=O), 1610 (C=N).

5-Bromo-2-hydroxy-salicylidene-L-α-leucine-hydrazide (Brsalhyleu)

To a solution of L-α-leucine-hydrazide (4.90 g, 33.75 mmol) in methanol (40 mL) was added slowly while stirring a solution of 5-bromo-2-hydroxy-benzaldehyde (6.80 g, 33.75 mmol) in methanol (140 mL) resulting in a clear yellow solution. The reaction mixture was stirred at room temperature overnight. The solvent was evaporated to dryness, and the yellow viscous oil was dried under strong vacuum to obtain the product as an yellow solid. The NMR data confirm the presence of two isomers in ratio 1.2:1.

Total yield: 10.75 g (32.75 mmol, 97.04%).

Elemental analysis for $C_{13}H_{18}BrN_3O_2$ (328.20 g/mol): calculated C: 47.57%, H: 5.53%, N: 12.80%; found C: 45.65%, H: 5.27%, N: 11.33%.

^{1}**H-NMR** (200 MHz, DMSO-d_6): $\delta =$ 0.93 (m, 6H, (C**H**$_3$)$_2$), 1.38–1,81 (m, 3H, γ-C**H**, β-C**H**$_2$), 3.40, 4.40 (t, ^{3}J = 6.68 Hz, 1H, α-C**H**), 6.81–6.92 (m, 1H, Ph), 7.38 (m, 1H, Ph), 7.76 (m, 1H, Ph), 8.28, 8.48 (C**H**=N) ppm.

^{13}**C-NMR** (50 MHz, DMSO-d_6): $\delta =$ 21.35, 21.95, 22.89, 23.15, (C(**C**H$_3$)$_2$), 23.88, 24.02 (γ-**C**H), 41.84, 42.98 (β-**C**H$_2$), 48.68, 51.85 (α-**C**H), 110.31, 110.60 (Ph), 118.64, 121.24, 122.49, 127.41, 130.15, 133.33, 133.47 (all Ph), 139.25, 144.98 (**C**H=N), 155.70, 156.36 (Ph), 170.76, 173.76 (C=O) ppm.

IR data (KBr disk, cm^{-1}): $\tilde{\nu}$ = 3336 (NH$_2$), 3153 (O–H), 1676 (C=O), 1617 (C=N).

3.6.2 Synthesis of the Schiff base ligands with L-α-phenylalanine residue

L-α-Phenylalanine methyl ester

To ethyl acetate (46 mL), water (35 mL), and L-α-phenylalanine-methyl-ester-hydrochloride (5.00 g, 23.0 mmol) in a 250 mL separatory funnel, (1 84 g, 13.0 mmol) of potassium carbonate was added gradually to pH 7.5. After each addition the mixture was shaken. At the end both layers became clear. The acetate layer was then separated

and the aqueous layer was extracted with ethyl acetate (3 x 100 mL). The organic phases were combined, dried over sodium sulfate, filtrated and the solvent was evaporated to obtain a pale yellow oil which was used in the next step without further purification.
Total yield: 3.44 g (22.7 mmol, 99%)

L-α-Phenylalanine-hydrazide

To a stirred solution of L-α-phenylalanine-methyl-ester (3.72 g, 25.00 mmol) in methanol (40 mL) was dropped (2.41 mL, 50 mmol) of hydrazine monohydrate (80 %). The pale yellow clear solution was stirred at room temperature. After 1 day a colorless precipitate was formed. The reaction mixture was stirred for an additional day. Then stopped the reaction, filtrated, and dried in air. A second part of the product was obtained by reducing the volume of the solvent from the filtrate. m.p 89 – 90 °C.
Total yield: 3.64 g (20.00 mmol, 81.2%).
Elemental analysis for $C_9H_{13}N_3O$ (179.22 g/mol): calculated C: 60.32%, H: 7.31%, N: 23.45%; found C: 60.18%, H: 7.25%, N: 23.29%.
^{1}**H-NMR** (400 MHz, DMSO-d_6): $\delta =$ 1.64 (br, 2H, N**H**$_2$), 2.57 – 2.63 (dd, ^{3}J = 8 Hz, ^{2}J = 13.32 Hz, 1H, β–C**H**$_2$), 2.85 – 2.90 (dd, ^{3}J = 4.76 Hz, ^{2}J = 13.32 Hz, 1H, β–C**H**$_2$), 3.37 (m, 1H, α–C**H**), 4.15 (br, 2H, N**H**$_2$), 7.16 – 7.28 (m, 5H, Ph), 8.93 (br, 1H, N**H**) ppm.
^{13}**C-NMR** (100 MHz, DMSO-d_6): $\delta =$ 40.62 (β-CH_2), 55.71 (α–CH), 126.48 (Ph), 128.52 (Ph), 129.72 (Ph), 139.27 (Ph), 174.05 (C=O) ppm.
EI-MS (positive ion mode, in methanol): m/z = 180 (70% [M^+]), 120 (100%).

N-Salicylidene-L-α-phenylalanine-hydrazide (Hsalhyphe)

Method 1 **Removing of the Boc group from the Schiff base ligand with protected phenylalanine HsalhyBocphe**

To a stirred solution of the ligand (1.789 g, 5.533 mmol) in 25 mL CH_2Cl_2, cooled to 0 °C was added trifluoroacetic acid (4.67 mL, 10 equiv.), and the mixture was stirred at room temperature for 23 h, until the TLC (ethyl acetate/hexane 4:6) does not show the

starting material. The reaction was then stopped and the pH of the solution was adjusted to 9–10 with a 20% aqueous solution of sodium hydrogen carbonate. The resulting biphasic mixture was transferred to a separatory funnel, and the organic and aqueous layers were separated. The product was extracted from the combined aqueous layers with chloroform (3 x 40 mL). All organic phases were combined, dried over sodium sulfate and concentrated in vacuum. The remaining yellow solid was recrystallized from ethanol to obtain the product as a yellow solid which was finally dried under vacuum.

Total yield: 1.42 g (5.03 mmol, 90%).

Method 2 **Starting from phenylalanine-hydrazide**

Following the procedure described for Hsalhyleu, L-α-phenylalanine-hydrazide (2.92 g, 16.30 mmol) was converted to the title compound as an yellowish white solid. The NMR data confirm the presence of two isomers in ratio 1:0.18. m.p 55 °C.

Total yield: 4.00 g (13.87 mmol, 85.1%)

Elemental analysis for $C_{16}H_{17}N_3O_2$ (283.33 g/mol): calculated C: 67.83%, H: 6.05%, N: 14.83%; found C: 67.90%, H: 6.04%, N: 14.67%.

^{1}**H-NMR** (400 MHz, DMSO-d_6): δ = 2.70 – 2.75 (dd, ^{3}J = 7.5 Hz, ^{2}J = 13.25 Hz, 1H, β-C**H**), 2.96 – 3.00 (dd, ^{3}J = 5.6 Hz, ^{2}J = 13.25 Hz, 1H, β-C**H**$_2$, 4.35 (dd, ^{3}J = 5.6, 7.5 Hz, 1H, α-C**H**), 6.86 (m, 3H, Ph), 7.24 (m, 5H, Ph), 7.42 (m, 1H, Ph), 7.72 (m, 1H, Ph), 8.20 and 8.40 (s, 1H, C**H**=N) ppm.

^{13}**C-NMR** (100 MHz, DMSO-d_6): δ = 41.15, 41.45 (β-**C**H$_2$), 52.95, 56.21 (α-**C**H), 116.63, 116.82 (Ph), 118.97, 119.07 (Ph), 119.74, 119.88 (Ph), 126.48, 126.64 (Ph), 128.45, 128.76 (Ph), 129.75, 129.91 (Ph), 131.44, 131.70 (Ph), 138.90, 139.27 (Ph), 147.99, 148.50 (Ph), 156.85, 157.83 (**C**H=N), 171.30, 176.22 (C=O) ppm.

EI–MS (positive mode, in methanol): m/z = 283 (30% [M$^+$]), 192 (42%), 120 (100%).

IR data (KBr disk, cm^{-1}): $\tilde{\nu}$ = 3361 (NH$_2$), 3209 (O–H), 1675 (C=O), 1622 (C=N).

o-Hydroxy-acetophenone-L-α-phenylalanine-hydrazide (Mesalhyphe)

Following the procedure described for Mesalhyleu, L-α-phenylalanine-hydrazide (1.41 g, 7.867 mmol) was converted to the title compound as an yellowish white solid, by heating

slowly at 65 °C for an overnight period. m.p 105 °C.

Total yield: 1.96 g (6.592 mmol, 84%).

Elemental analysis for $C_{17}H_{19}N_3O_2$ (297.35 g/mol): calculated C: 68.67%, H: 6.44%, N: 14.13%; found C: 68.76%, H: 6.58%, N: 13.89%.

$[\alpha]_D^{22}$: + 40°; c = 2 g in 100 mL solution 2.5 N HCl in methanol.

^{1}**H-NMR** (400 MHz, DMSO-d_6): δ = 2.28 (s, 3H, C**H**$_3$), 2.76 (dd, ^{3}J = 7.76 Hz, ^{2}J = 13.24 Hz, 1H, β–C**H**$_2$), 3.00 (dd, ^{3}J = 4.64 Hz, ^{2}J = 13.24 Hz, 1H, β–C**H**$_2$), 3.37 (br, 1H, N**H**), 3.74 (t, ^{3}J = 7.76 Hz, 1H, α-C**H**), 4.84 (br, 2H, N**H**$_2$), 6.86 – 6.90 (m, 2H, Ph), 7.20 – 7.30 (m, 6H, Ph), 7.58 (m, 1H, Ph), 13.17 (br, 1H, O**H**) ppm.

^{13}**C-NMR** (100 MHz, DMSO-d_6): δ = 13.72 (**C**H$_3$), 41.48 (β–**C**H$_2$), 55.43 (α-**C**H), 117.69 (Ph), 118.94 (Ph), 119.76 (Ph), 126.61 (Ph), 128.56 (Ph), 128.79 (Ph), 129.80 (Ph), 131.53 (Ph), 138.97 (Ph), 155.10 (C=N), 159 02 (Ph), 171.90 (C=O) ppm.

IR data (KBr disk, cm^{-1}): $\tilde{\nu}$ = 3398 (NH$_2$), 3297 (O–H), 1685 (C=O), 1603 (C=N).

5-Bromo-2-Hydroxy-salicyliden-L-α-phenylalanine-hydrazide (Brsalhyphe)

Method 1 **Removing of the Boc group from the ligand BrsalhyBocphe**

Following the *Method 1* described for Hsalhyphe, BrsalhyBocphe (520 mg, 1.125 mmol) was converted to Brsalhyphe as an yellow solid. The NMR data confirm the presence of two isomers in ratio 1:2.3.

Total yield: 0.310 g (0.856 mmol, 80%).

^{1}**H-NMR** (400 MHz, DMSO-d_6): δ = 2.70 – 2.75 (dd, ^{3}J = 7.6 Hz, ^{2}J = 13.6 Hz, 1H, β-C**H**), 2.96 – 3.00 (dd, ^{3}J = 5.6 Hz, ^{2}J = 13.48 Hz, 1H, β-C**H**$_2$), 4.34 (m, 1H, α-C**H**), 6.86 (m, 2H, Ph), 7.24 (m, 5H, Ph,), 7.42 (m, 1H, Ph), 7.72 (m, 1H, Ph), 8.20 and 8.40 (s, 1H, C**H**=N) ppm.

^{13}**C-NMR** (100 MHz, DMSO-d_6): δ = 40 (overlapping with DMSO-d_6), 41.42 (β-**C**H$_2$), 56.19, 56.50 (α-**C**H), 110.76, 111.08 (Ph), 118.93, 119.12 (Ph), 121.69, 123.26 (Ph), 126.53, 126.65 (Ph), 128.23, 128.45 (Ph) 128.54, 128.61 (Ph), 129.73, 129.75 (Ph), 130.88 (Ph), 133.57, 133.90 (Ph), 138.90 (Ph), 139.43, 145.38 (Ph), 156.07, 156.88 (**C**H=N), 171.47, 172.83 (C=O) ppm.

EI–MS (positive mode): m/z = 361 (36% [M^+]), 120 (100%).

Method 2 **Starting from phenylalanine-hydrazide**

Following the procedure described for Brsalhyleu, L-α-phenylalanine-hydrazide (2.53 g, 14.13 mmol) was converted to the title compound, which was precipitated from the reaction solution as an yellow solid. Additional material can be obtained by reduction under strong vacuum of the solution to about half of its original volume. The product was purified by recrystallization from ethanol. The NMR data confirm the presence of two isomers in ratio 1:2.4. m.p 65 °C.

Total yield: 3.70 g (10.24 mmol, 73%).

Elemental analysis for $C_{16}H_{16}N_3O_2Br$ (361.22 g/mol): calculated C: 53.05%, H: 4.45%, N: 11.60%; found C: 53.16%, H: 4.43%, N: 11.58%.

^{1}**H-NMR** (400 MHz, DMSO-d_6): δ = 2.63 – 2.75 (dd, ^{3}J = 6.76 Hz, ^{2}J = 13.48 Hz, 1H, β-C**H**), 2.92 – 3.00 (dd, ^{3}J = 6.76 Hz, ^{2}J = 13.48 Hz, 1H, β-C**H**$_2$), 3.52, 4.35 (m, 1H, α-C**H**), 6.86 (m, 1H, Ph), 7.24 (m, 5H, Ph), 7.42 (m, 1H, Ph), 7.72 (m, 1H, Ph), 8.20 and 8.40 (s, 1H, C**H**=N) ppm.

^{13}**C-NMR** (100 MHz, DMSO-d_6): δ = 41.31, 41.42 (β-**C**H$_2$), 53.15, 56.20 (α-**C**H), 111.05, 110.75 (Ph), 118.95, 119.12 (Ph), 121.70, 123.56 (Ph), 126.52, 126.64 (Ph), 128.53, 128.61 (Ph), 129.75, 130.87 (Ph), 133.56, 133.89, (Ph), 138.91, 139.45 (Ph), 145.39, 147.99, (Ph), 156.12, 156.91 (**C**H=N), 171.48, 176.46 (C=O) ppm.

IR data (KBr disk, cm^{-1}): $\tilde{\nu}$ = 3390 (NH_2), 3205 (O–H), 1675 (C=O), 1616 (C=N).

EI–MS (positive mode, in methanol): m/z = 361 (36% [M^+]), 120 (100%).

3.6.3 Synthesis of the Schiff base ligands with L-α-tyrosine residue

L-α-Tyrosine-ethyl ester

Using the method described for L-α-phenylalanine methyl-ester, L-α-tyrosine-ethyl-ester-hydrochloride (12.28 g, 0.05 mol), was converted to the title compound as a colorless

solid. m.p 103 °C.

Total yield: 8.9 g (0.043 mol, 85%).

Elemental analysis for $C_{11}H_{15}NO_3$ (209.14 g/mol): calculated C: 63.14%, H: 7.22%, N: 7.17%; found C: 63.38%, H: 7.33%, N: 6.70%.

^{1}**H-NMR** (400 MHz, DMSO-d_6): $\delta =$ 1.17 (m, 3H, C**H**$_3$-ester), 2.8 (m, 2H, β–C**H**$_2$), 3.59 (m, 2H, C**H**$_2$-ester), 4.09 (m, 1H, α-C**H**), 4.83 (s, 3H, N**H**$_2$ + O**H**), 6.69 (m, 2H, Ph-**H**^{B}), 6.98 (m, 2H, Ph-**H**^{A}) ppm.

^{13}**C-NMR** (100 MHz, DMSO-d_6): $\delta =$ 14.44 (**C**H$_3$-ester), 40.88 (β-**C**H$_2$), 56.78 (**C**H$_2$-ester), 61.92 (α-**C**H), 116.34 (Ph), 128.80 (**C**^{Ph}-β-CH$_2$), 131.37 (Ph), 157.46 (**C**^{Ph}-OH), 176.42 (C=O) ppm.

L-α-Tyrosine-hydrazide

Following the method described for L-α-phenylalanine hydrazide, L-α-tyrosine-ethyl-ester (6.5 g, 0.031 mol), was converted to the title compound as a colorless solid. m.p. 199 °C.

Total yield: 6.3 g (0.03 mol, 98%).

Elemental analysis for $C_9H_{13}N_3O_2$ (195.22 g/mol): calculated C: 55.37%, H: 6.71%, N: 21.25%; found C: 55.75%, H: 6.47%, N: 21.80%.

^{1}**H-NMR** (400 MHz, DMSO-d_6): $\delta =$ 2.5 (dd, ^{3}J = 7.8 Hz, ^{2}J = 13.3 Hz, 1H, β–C**H**$_2$), 2.75 (dd, ^{3}J = 5.6 Hz, ^{2}J = 13.3 Hz, 1H, β-C**H**$_2$), 3.23 (dd, ^{3}J = 5.6, 7.8 Hz, 1H, α-C**H**), 4.4 (br, s, 2H, N**H**$_2$), 6.43–6.65 (d, J$_{AABB}$ = 8.5 Hz, 2H, Ph), 6.94–7.01 (d, J$_{AABB}$ = 8.5 Hz, 2H, Ph), 9.13 (s, 1H, O**H**) ppm.

^{13}**C-NMR** (100 MHz, DMSO-d_6): $\delta =$ 40.75 (β-CH$_2$), 55.43 (α-CH), 55.45 (α-C**H**), 114.91 (Ph), 128.67 (**C**^{Ph}-β-CH$_2$), 130.11 (Ph), 155.64 (**C**^{Ph}-OH), 173.67 (C=O) ppm.

N-Salicylidene-L-α-tyrosine-hydrazide (Hsalhytyr)

Following the procedure described for Hsalhyleu, L-α-tyrosine-hydrazide (2.00 g, 11 mmol) was converted to the title compound as an yellowish–white solid, by heating at 40 °C overnight. The yellowish–white solid was recrystallized from ethanol to obtain the product as a colorless solid. The NMR data confirm the presence of two isomers in ratio

1:2.79. m.p 203 °C.

Total yield: 2.30 g (7.70 mmol, 70%).

Elemental analysis for $C_{16}H_{17}N_3O_3$ (299.33 g/mol): calculated C: 64.20%, H: 5.72%, N: 14.04%; found C: 64.38%, H: 5.81%, N: 13.92%.

^{1}H-NMR (400 MHz, DMSO-d_6): δ = 2.62 (dd, ^{3}J = 7.13 Hz, ^{2}J = 13.53 Hz, 1H, β-C**H**$_2$), 2.83 (dd, ^{3}J = 5.66 Hz, ^{2}J = 13.53 Hz, 1H, β-C**H**$_2$), 3.45 (dd, ^{3}J = 5.6, 7.13 Hz, 1H, α-C**H**), 6.63 – 6.68 (d, J_{AABB} = 8.50 Hz, 2H, Ph–tyr), 6.88 – 6.99 (m, 2H, Ph), 7,02 – 7,03 (d, J_{AABB} = 8.50 Hz, 2H, Ph–tyr), 7.22 – 7.27 (m, 1H, Ph), 7.44 – 7.47 (m, 1H, Ph), 8.18 and 8.42 (s, 1H, C**H**=N)ppm.

^{13}C-NMR (50 MHz, DMSO-d_6): δ = 40.73 (β-**C**H$_2$), 53.09, 56.43 (α-**C**H), 115.29, 115.46 (Ph), 116.63, 116.83 (Ph), 119.07, 119.73 (Ph), 119.87, 120.64 (Ph), 126.88, 128.78 (Ph), 129.13 (Ph), 129.45, 129.54 (Ph), 129.93, 130.63 (Ph), 131.43, 131.69 (Ph), 141.36, 147.95 (**C**H=N), 154.87, 156.23 (Ph), 156.88, 157.84 (Ph), 171.45, 176.30 (C=O) ppm.

IR data (KBr disk, cm^{-1}): $\tilde{\nu}$ = 3421 (NH_2), 3218 (O–H), 1654 (C=O), 1612 (C=N) ppm.

o-Hydroxy-acetophenone-L-α-tyrosine-hydrazide (Mesalhytyr)

Following the procedure described for Mesalhyleu, L-α-tyrosine-hydrazide (2.00 g, 11 mmol) was converted to the title compound as an yellowish–white solid, by refluxing at 65 °C for 7 hours. The volume of the solution was reduced to about 50 mL. Upon cooling to room temperature a yellow precipitate formed, which was collected by filtration, washed repeatedly with cold methanol, and dried under vacuum. m.p. 208 °C.

Total yield: 3.32 g (10.6 mmol, 97.3%).

Elemental analysis for $C_{17}H_{19}N_3O_3$ (313.1 g/mol): calculated C: 65.16%, H: 6.11%, N: 13.41%; found C: 65.27%, H: 6.40%, N: 13.31%.

^{1}H-NMR (400 MHz, DMSO-d_6): δ = 2.27 (s, 3H, C**H**$_3$), 2.63 (dd, ^{3}J = 7.13 Hz, ^{2}J = 13.53 Hz, 1H, β-C**H**$_2$), 2.83 (dd, 1H, ^{3}J = 5.66 Hz, ^{2}J = 13.53 Hz, β-C**H**$_2$), 3.63 (dd, 1H, ^{3}J = 5.7, 7.13 Hz, α-C**H**), 4.8 (br, 2H, N**H**$_2$–amino acid), 6.63 – 6.67 (d, 2H, J_{AABB} = 8.50 Hz, Ph–tyr), 6.8 – 6.9 (m, 2H, Ph), 7,01 – 7,03 (d, 2H, J_{AABB} = 8.50 Hz, Ph–tyr), 7.24 – 7.29 (m, 1H, Ph), 7.55 – 7.57 (m, 1H, Ph), 8.85 (br, 1H, N**H**), 9.13 (s, br, O**H**–amino acid), 13.16 (s, br, 1H, Ph–O**H**) ppm.

^{13}C-NMR (50 MHz, DMSO-d_6): δ = 13.20 (**C**H_3), 40.73 (β-**C**H_2), 55.23 (α-**C**H), 114.91 (Ph), 117.21 (Ph), 118.46 (Ph), 119.28 (Ph), 128.35 (Ph), 128.34 (Ph), 130.20 (Ph), 131.05 (Ph), 155.51 (Ph), 155.75 (Ph), 158.54 (**C**=N), 172.48 (C=O) ppm.

IR data (KBr disk, cm^{-1}): $\tilde{\nu}$ = 3389 (NH_2), 3222 (O–H), 1664 (C=O), 1653 (C=N) ppm.

5-Bromo-2-Hydroxy-salicyliden-L-α-tyrosine-hydrazide (Brsalhytyr)

Following the procedure described for Brsalhyleu, L-α-tyrosine-hydrazide (1.31 g, 6.72 mmol) was converted to the title compound, which was precipitated from the reaction solution as an yellow solid. Additional material can be obtained by reduction under strong vacuum of the solution to about half of its original volume. The NMR data confirm the presence of two isomers in ratio 1:4.05.

Total yield: 2.50 g (6.63 mmol, 98.75%).

Elemental analysis for $C_{16}H_{16}BrN_3O_3$ (378.22 g/mol): calculated C: 50.81%, H: 4.26%, N: 11.11%; found C: 50.60%, H: 4.28%, N: 11.23%.

^{1}H-NMR (400 MHz, DMSO-d_6): δ = 2.62 (dd, ^{3}J = 7.13 Hz, ^{2}J = 13.53 Hz, 1H, β-C**H**$_2$), 2.83 (dd, ^{3}J = 5.66 Hz, ^{2}J = 13.53 Hz, 1H, β-C**H**$_2$), 3.63 (dd, ^{3}J = 5.66, 7.13 Hz, 1H, α-C**H**), 6.63 – 6.67 (d, J_{AABB} = 8.50 Hz, 2H, Ph–tyr), 6.8 – 6.9 (m, 1H, Ph), 7,01 – 7,03 (d, J_{AABB} = 8.50 Hz, 2H, Ph–tyr), 7.32 – 7.41 (m, 1H, Ph), 7.68 (m, 1H, Ph), 8.18 and 8.38 (s, 1H, C**H**=N)ppm.

^{13}C-NMR (50 MHz, DMSO-d_6): δ = 40.73 (β-**C**H_2), 48.57, 55.33 (α-**C**H), 110.19, 110.47 (Ph), 114.82, 114.97 (Ph), 118.51, 118.65 (Ph), 121.21, 122.81 (Ph), 127.74, 128.24 (Ph), 128.34 (Ph), 128.84 (Ph), 130.13, 130.40 (Ph), 133.05, 133.38 (Ph), 138.40, 144.90 (**C**H=N), 155.65, 155.74 (Ph), 156.49 (Ph), 171.07, 176.00 (C=O) ppm.

IR data (KBr disk, cm^{-1}): $\tilde{\nu}$ = 3332 (NH_2), 3276 (O–H), 1675 (C=O), 1615 (C=N) ppm.

ESI-MS (negative ion mode): (**MeOH**) m/z = 379 [M–H^+].

3.6.4 Synthesis of *cis*-dioxovanadium(v)-complexes with L-α-leucine residue ligands

[VO_2(Mesalhyleu)] (16)

Method A (**16**·H_2O): To a solution of Schiff base ligand Mesalhyleu (0.41 g, 1.56 mmol) in methanol (30 mL) was added NH_4VO_3 (0.18 g, 1.56 mmol). The reaction mixture was heated at 65°C. In 30 minutes a yellow precipitate was formed. The reaction was continued for another 2 hours. The hot reaction mixture was filtrated, and the yellow product was dried under vacuum.

Total yield: 0.37 g (1.02 mmol, 65%).

Elemental analysis for $C_{14}H_{22}N_3O_5V$ (363.28 g/mol): calculated C: 46.29%, H: 6.10%, N: 11.57%; found C 45.67%, H: 5.75%, N: 12.11%.

^{1}**H-NMR** (400 MHz, DMSO-d_6): $\delta =$ 0.93 (m, 6H, (C**H**$_3$)$_2$), 1.57–1.79 (m, 3H, γ-C**H**, β-C**H**$_2$), 2.76 (s, 3H, C**H**$_3$), 3.33 (br, 2H, **H**$_2$O), 3.92 (t, ^{3}J = 5.49 Hz, 1H, α-C**H**), 6.79 (m, 2H, Ph), 7.31 (m, 1H, Ph), 7.73 (m, 1H, Ph), 8.15 (br, 3H, N**H**$_3^+$) ppm.

^{13}**C-NMR** (100 MHz, DMSO-d_6): $\delta =$ 16.58 (**C**H$_3$), 22.59, 22.84, (C(**C**H$_3$)$_2$), 24.40 (γ-**C**H), 40.91, (β-**C**H$_2$), 50.57 (α-**C**H), 117.64 (Ph), 120.50 (Ph), 122.37 (Ph), 130.11 (Ph), 132.51 (Ph), 163.76 (**C**H=N), 164.82 (Ph), 170.70 (C=O) ppm.

^{51}**V-NMR** (105 MHz, DMSO-d_6): $\delta =$ -533.71 ppm ($\nu_{1/2}$ = 827 Hz).

IR data (KBr disk, cm^{-1}): 3447 (br, NH_3^+), 1607 (s, C=N–N=C), 951 (s, VO_2), 862 (s, VO_2).

ESI-MS (negative ion mode): (**MeOH**) m/z = 344 ([VO_2(Mesalhyleu)] – H^+).

Method B (**16**): The pH of a solution of vanadyl sulfate trihydrate (0.23 g, 1.01 mmol) in water (40 mL) was adjusted to pH = 13.5 by adding a 0.10 M solution of NaOH (25 mL). Upon addition of sodium hydroxide to the blue vanadyl sulfate solution in water, it turned dark gray. The ligand, Mesalhyleu, solution (0.28 g, 1.01 mmol), in methanol (40 mL), was added to the aqueous solution of vanadyl sulfate, which changed further color to green brown. The reaction mixture was refluxed at 65°C. In 1 hour a yellow precipitate was formed. After 24 hours the precipitate formed, was filtrated, dried and recrystallized

from methanol.

Total yield: 0.18 g (0.52 mmol, 51.5%).

Elemental analysis for $C_{14}H_{20}N_3O_4V$ (345.27 g/mol): calculated C: 48.70%, H: 5.84%, N: 12.17%; found C 48.25%, H: 5.91%, N: 11.97%.

^{1}**H-NMR** (400 MHz, DMSO-d_6): $\delta =$ 0.94 (m, 6H, (C**H**$_3$)$_2$), 1.58–1.77 (m, 3H, γ-C**H**, β-C**H**$_2$), 2.76 (s, 3H, C**H**$_3$), 3.92 (t, ^{3}J = 5.49 Hz, 1H, α-C**H**), 6.78 (m, 2H, Ph), 7.31 (m, 1H, Ph), 7.74 (m, 1H, Ph), 8.15 (br, 3H, N**H**$_3^+$) ppm.

^{13}**C-NMR** (100 MHz, DMSO-d_6): $\delta =$ 16.58 (**C**H$_3$), 22.59, 22.84, (C(**C**H$_3$)$_2$), 24.39 (γ-**C**H), 41.84, (β-**C**H$_2$), 50.58 (α-**C**H), 117.63 (Ph), 120.49 (Ph), 122.37 (Ph), 130.11 (Ph), 132.51 (Ph), 163.76 (**C**H=N), 164.82 (Ph), 170.72 (C=O) ppm.

^{51}**V-NMR** (105 MHz, DMSO-d_6): $\delta =$ -533.04 ppm ($\nu_{1/2}$ = 862 Hz).

IR data (KBr disk, cm^{-1}): 3447 (br, NH_3^+), 1607 (s, C=N–N=C), 951 (s, VO_2), 862 (s, VO_2).

UV/Vis (DMF solution, λ_{max} in nm (ε in 10^3 M^{-1} cm^{-1})): 288 (14.1), 376 (6.9).

ESI-MS (negative ion mode): (**MeOH**) m/z = 346 ([VO_2(Mesalhyleu)] – H^+).

K[VO_2(Mesalhyleu)]·5H_2O (17)

To a solution of Schiff base ligand Mesalhyleu (0.36 g, 1.37 mmol) in methanol (30 mL) was added KVO_3 (0.19 g, 1.37 mmol). The reaction mixture was heated at reflux yielding red-brown colored solution. In 1 hour a yellow precipitate was separated out. It was filtrated and air dried.

Total yield: 0.27 g (0.57 mmol, 42%).

Elemental analysis for $C_{14}H_{29}KN_3O_9V$ (473.43 g/mol): calculated C: 35.52%, H: 6.17%, N: 8.26%; found C 34.23%, H: 4.08%, N: 8.41%.

^{1}**H-NMR** (400 MHz, DMSO-d_6): $\delta =$ 0.93 (m, 6H, (C**H**$_3$)$_2$), 1.59–1.75 (m, 3H, γ-C**H**, β-C**H**$_2$), 2.77 (s, 3H, C**H**$_3$), 3.33 (s, 10H, **H**$_2$O), 3.92 (br, 1H, α-C**H**), 6.78 (m, 2H, Ph), 7.32 (m, 1H, Ph), 7.75 (m, 1H, Ph), 8.15 (br, 2H, N**H**$_2$) ppm.

^{13}**C-NMR** (100 MHz, DMSO-d_6): $\delta =$ 16.58 (**C**H$_3$), 22.59, 22.84, (C(**C**H$_3$)$_2$), 24.40 (γ-**C**H), 40.93, (β-**C**H$_2$), 59.07 (α-**C**H), 117.63 (Ph), 120.49 (Ph), 122.37 (Ph), 130.11 (Ph), 132.51 (Ph), 163.76 (**C**H=N), 164.82 (Ph), 170.72 (C=O) ppm.

^{51}**V-NMR** (105 MHz, DMSO-d_6): $\delta =$ -533.54 ppm ($\nu_{1/2}$ = 790 Hz).

IR data (KBr disk, cm^{-1}): 3398 (br, NH_2), 1607 (s, C=N–N=C), 951 (s, VO_2), 862 (s, VO_2).

3.6.5 Synthesis of *cis*-dioxovanadium(v)-complexes with L-α-phenylalanine residue ligands

[VO_2(Mesalhyphe)]·MeOH (18)

Method A: To a solution of the Schiff base ligand Mesalhyphe (145.00 mg, 0.488 mmol) in methanol (20 mL) was added NH_4VO_3 (57.00 mg, 0.488 mmol). The reaction mixture was heated at reflux for 5 hours yielding a red-brown colored solution. The hot reaction mixture was filtrated to remove small amounts of unreacted NH_4VO_3. Upon standing at 5 °C yellow colored single crystals suitable for X-ray studies formed within two weeks. The same crystals were formed from the methanolic solution of the complex at room temperature for 1 day.

Total yield: 95 mg (0.14 mmol, 60%).

Elemental analysis for $C_{18}H_{22}N_3O_5V$ (411.33 g/mol): calculated C: 52.56%, H: 5.39%, N: 10.22%; found C: 51.72%, H: 5.19%, N: 10.55%.

IR data (KBr disk, cm^{-1}): 3407 (br, NH_3^+), 1600 (s, C=N–N=C), 940 (s, VO_2), 870 (s, VO_2).

UV/Vis (DMF solution, λ_{max} in nm (ε in 10^3 M^{-1} cm^{-1})): 298 (7.9), 376 (4.8). **UV/Vis** (Acetonitrile solution, λ_{max} in nm (ε in 10^4 M^{-1} cm^{-1})): 210 (27.9), 260 (17.2), 362 (4.9).

ESI-MS (negative ion mode): (**MeOH**) m/z = 378 ([VO_2(Mesalhyphe)] – H^+).

Method B: The pH of a solution of vanadyl sulfate trihydrate (0.23 g, 1.01 mmol) in water (40 mL) was adjusted to pH = 13.5 by adding a 0.10 M solution of NaOH (25 mL). Upon addition of sodium hydroxide to the blue vanadyl sulfate solution in water, it turned dark gray. The ligand (Mesalhyphe) solution (0.30 g, 1.01 mmol), in methanol (40 mL), was added to the aqueous solution of vanadyl sulfate, which changed further color to green brown. The reaction mixture was refluxed for 24 hours resulting in a clear yellow-orange

solution. The volume of the solution was reduced to half of its original volume and allowed to stand at 0 °C. An orange precipitate is formed, which is filtrated, dried and recrystallized from methanol to afford yellow crystals suitable for X-Ray measurement.

Total yield: 0.193 g (0.467 mmol, 46.2%).

Elemental analysis for $C_{18}H_{22}N_3O_5V$ (411.33 g/mol): calculated C: 52.56%, H: 5.39%, N: 10.22%; found C 52.36%, H: 5.25%, N: 10.29%.

^{1}H-NMR (400 MHz, DMSO-d_6): $\delta =$ 2.62 (s, 3H, C**H**$_3$), 3.06 – 3.08 (dd, ^{3}J = 6.4 Hz, ^{2}J = 13.6 Hz, 1H, β–C**H**$_2$), 3.16 – 3.22 (m, 2H, β–C**H**$_2$ overlapping with C**H**$_3$OH), 4.08 (br, 1H, CH$_3$O**H**), 4.18 (t, ^{3}J = 6.4 Hz, 1H, α-C**H**), 6.78 (m, 2H, Ph), 7.25 (m, 6H, Ph), 7.70 (d, ^{2}J = 7.60 Hz, 1H, Ph), 8.26 (s, 3H, NH_3^+) ppm.

^{13}C-NMR (100 MHz, DMSO-d_6): $\delta =$ 16.09 (**C**H$_3$), 39.96 (β–**C**H$_2$), 48.59 (**C**H$_3$OH), 52.74 (α-**C**H), 117.16 (Ph), 120.03 (Ph), 121.81 (Ph), 126.87 (Ph), 128.35 (Ph), 129.61 (Ph), 132.11 (Ph), 135.57 (Ph), 138.97 (Ph), 164.30 (C=N), 163.56 (Ph), 169.00 (C=O) ppm.

^{51}V-NMR (105 MHz, DMSO-d_6): $\delta =$ -533.56 ppm ($\nu_{1/2}$ = 919 Hz).

IR data (KBr disk, cm^{-1}): 3634 (MeOH), 3399 (br, NH_3^+), 1600 (s, C=N–N=C), 941 (s, VO_2), 870 (s, VO_2).

K[VO$_2$(Mesalhyphe)] (**19**)

To a solution of the Schiff base ligand Mesalhyphe (0.107 g, 0.360 mmol) in methanol (20 mL) was added KVO_3 (49.67 mg, 0.360 mmol). The reaction mixture was heated at reflux for 5 days yielding a clear yellow colored solution. The hot reaction mixture was filtrated to remove small amounts of unreacted KVO_3. Upon standing at room temperature a yellow precipitate was formed, which was filtrated, and air dried.

Total yield: 107 mg (0.256 mmol, 71%).

Elemental analysis for $C_{17}H_{17}KN_3O_4V$ (417.37 g/mol): calculated C: 48.92%, H: 4.11%, N: 10.07%; found C: 49.07%, H: 4.28%, N: 9.31%.

^{1}H-NMR (400 MHz, DMSO-d_6): $\delta =$ 2.64 (s, 3H, C**H**$_3$), 2.77 – 2.88 (dd, ^{3}J = 7.6 Hz, ^{2}J = 13.6 Hz, 1H, β–C**H**$_2$), 2.99 – 3.01 (dd, ^{3}J = 6.4 Hz, ^{2}J = 13.6 Hz, 2H, β–C**H**$_2$), 3.66 (br, 1H, α-C**H**), 6.78 (m, 2H, Ph), 7.25 (m, 6H, Ph), 7.70 (m, 1H, Ph) ppm.

^{13}**C-NMR** (100 MHz, DMSO-d_6): δ = 22.44 (**C**H_3), 39.96 (β–**C**H_2), 52.74 (α-**C**H), 116.82 (Ph), 119.88 (Ph), 122.26 (Ph), 126.18 (Ph), 128.08 (Ph), 129.41 (Ph), 132.16 (Ph), 138.01 (Ph), 139.04 (Ph), 161.30 (C=N), 163.00 (Ph), 164.00 (C=O) ppm.

^{51}**V-NMR** (105 MHz, DMSO-d_6): δ = -532.51 ppm ($\nu_{1/2}$ = 659 Hz).

IR data (KBr disk, cm^{-1}): 3370 (br, NH_2), 1601 (s, C=N–N=C), 942 (s, VO_2), 899 (s, VO_2).

3.6.6 Synthesis of *cis*-dioxovanadium(v)-complexes with L-α-tyrosine residue ligands

[VO_2(Mesalhytyr)]·MeOH (**20**)

Method A **20**·H_2O: The pH of a solution of vanadyl sulfate trihydrate (0.36 g, 1.7 mmol) in water (60 mL) was adjusted to pH = 13.5 by adding a 0.10 M solution of NaOH. Upon addition of sodium hydroxide to the blue vanadyl sulfate solution in water it turned dark gray. The ligand Mesalhytyr solution (0.54 g, 1.7 mmol) in methanol (30 mL) was added to the aqueous solution of vanadyl sulfate, which changed further color to green brown. The reaction mixture was refluxed for 24 hours resulting in a yellow-orange solution. The volume of the solution was reduced to half of its original volume and allowed to stand at 0 °C. Yellow crystals were formed in less than one week, which were big enough for X-ray analyses. After drying in air, crystals were transformed to a powder material; methanol has been removed from the complex and water has been absorbed, as shown from the following analyses.

Total yield: 0.35 g (0.9 mmol, 53%).

Elemental analysis for $C_{17}H_{20}N_3O_6V$ (413.30 g/mol): calculated C: 49.40%, H: 4.88%, N: 10.17%; found C: 49.32%, H: 4.87%, N: 10.12%.

^{1}**H-NMR** (200 MHz, DMSO-d_6): δ = 2.65 (s, 3H, C**H**$_3$), 2.96 (dd, ^{3}J = 6.0 Hz, ^{2}J = 14.0 Hz, 1H, β–C**H**$_2$), 3.10 (dd, ^{3}J = 6.8 Hz, ^{2}J = 14.0 Hz, 1H, β–C**H**$_2$), 3.33 (s, 2H, **H**$_2$O), 4.1 (dd, ^{3}J = 6.0, 6.8 Hz, 1H, α–C**H**), 6.64 (d, J_{AABB} = 8.5 Hz, 2H, Ph–Tyr), 6.79 (m, 2H, Ph), 7.03 (m, 2H, Ph), 7.3 (m, 1H, Ph), 7.7 (d, J_{AABB} = 7.6 Hz, 1H, Ph–Tyr),

8.04 (br, 3H, N$\mathbf{H}_3^+$), 9.5 (s, 1H, O**H**–amino acid) ppm.

^{13}**C-NMR** (50 MHz, DMSO-d_6): δ = 16.12 (**C**H_3), 36.12 (β–**C**H_2), 52.96 (α-**C**H), 115.17 (Ph), 117.14 (Ph), 120.04 (Ph), 121.84 (Ph), 125.37 (Ph), 129.66 (Ph), 130.61 (Ph), 132.07 (Ph), 156.31 (Ph), 163.50 (Ph), 164.31, (**C**=N), 169.20 (O–**C**NNC) ppm.

^{51}**V-NMR** (105 MHz, DMSO-d_6): δ = −533.6 ppm ($\nu_{1/2}$ = 986 Hz).

IR data (KBr disk, cm^{-1}): $\tilde{\nu}$ = 3609 (O–H (H_2O)), 3369 (br; NH_3^+), 1617 (s, C=N–N=C) 927 (s, VO_2), 881 (s, VO_2).

UV/Vis (Acetonitrile solution, λ_{max} in nm (ε in 10^3 M^{-1} cm^{-1})): 215 (14.1), 260 (7.8), 312 (4).

ESI-MS (negative ion mode, in methanol): m/z = 394 ([VO_2(Mesalhytyr)] – H^+).

Method B **20**·H_2O: To a solution of Mesalhytyr (0.5 g, 1.6 mmol) in 50 mL dried isopropanol are added dropwise under an argon atmosphere [VO(OiPr)$_3$] (0.39 g, 1.6 mmol). The color of the reaction mixture became brown once the [VO(OiPr)$_3$] was added. The reaction mixture was stirred under argon for 6 hours yielding a brown precipitate. The Schlenk tube was kept overnight at 0 °C. The precipitate thus obtained was filtrated under argon, and dried under vacuum. To the crude mass of precipitate was added 10 mL water forming red-brown suspension. Ethanol was then added 10 mL resulting in a yellow-green solution. The solvent was removed under reduced pressure to obtain the product as a yellow greenish solid, which is dried under vacuum. Recrystallization from methanol afford yellow crystals suitable for X-ray measurement.

Total yield: 0.13 g (0.33 mmol, 21%).

Elemental analysis for $C_{17}H_{20}N_3O_6V$: (413.30 g/mol) calculated C: 49.40%, H: 4.88%, N: 10.17%; found C: 49.75%, H: 5.08%, N: 9.64%.

^{1}**H-NMR** (400 MHz, DMSO-d_6): δ = 2.66 (s, 3H, C**H**$_3$), 2.96 (dd, ^{3}J = 6.0 Hz, ^{2}J = 14.0 Hz, 1H, β–C**H**$_2$), 3.10 (dd, ^{3}J = 6.8 Hz, ^{2}J = 14.0 Hz, 1H, β–C**H**$_2$), 3.33 (s, 2H, **H**$_2$O), 4.1 (br, 1H, α–C**H**), 6.64 (m, 2H, Ph), 6.79 (d, J_{AABB} = 8.0 Hz, 2H, Ph–tyr), 7.03 (m, 2H, Ph), 7.3 (m, 1H, Ph), 7.7 (d, J_{AABB} = 8.0 Hz, 2H, Ph–tyr), 8.04 (br, 3H, N$\mathbf{H}_3^+$), 9.3 (s, 1H, O**H**–amino acid) ppm.

^{13}**C-NMR** (100 MHz, DMSO-d_6): δ = 16.1 (**C**H_3), 36.15 (β–**C**H_2), 52.99 (α-**C**H), 115.14 (Ph), 117.11 (Ph), 120.03 (Ph), 121.82 (Ph), 125.41 (Ph), 129.62 (Ph), 130.58

(Ph), 132.05 (Ph), 156.27 (Ph), 163.42 (Ph), 164.29 (**C**=N), 169.25 (O–**C**NNC) ppm.

^{51}**V-NMR** (105 MHz, DMSO-d_6): δ = -533.40 ppm ($\nu_{1/2}$ = 1036 Hz).

IR data (KBr disk, cm^{-1}): ν = 3370 (s, br; NH_3^+), 1602 (s, br; C=N–N=C), 921 (s, VO_2), 872 (s, VO_2).

ESI-MS (negative ion mode, in methanol): m/z = 394 ([VO_2(Mesalhytyr)]–H^+).

Method C **20**·H_2O: To a solution of Schiff base ligand Mesalhytyr (0.23 g, 0.93 mmol) in methanol (20 mL) was added NH_4VO_3 (0.11 g, 0.93 mmol). The reaction mixture was heated at reflux for 3.5 hours yielding a red-brown colored solution. The hot reaction mixture was filtrated to remove small amounts of unreacted NH_4VO_3. The solution was kept at room temperature to evaporate the solvent to dryness and the residue as a dark brown solid was recrystallized from methanol. Upon standing at room temperature yellow colored single crystals suitable for X-ray studies formed within two days.

Total yield: 0.35 g (0.9 mmol, 53%).

Elemental analysis for $C_{17}H_{20}N_3O_6V$ (413.1 g/mol): calculated C: 49.40%, H: 4.88%, N: 10.17%; found C: 49.24%, H: 4.98%, N: 10.09%.

^{1}**H-NMR** (400 MHz, DMSO-d_6): δ = 2.66 (s, 3H, C**H**$_3$), 2.97 (dd, ^{3}J = 6.0 Hz, ^{2}J = 14.0 Hz, 1H, β–C**H**$_2$), 3.10 (dd, ^{3}J = 6.8 Hz, ^{2}J = 14.0 Hz, 1H, β–C**H**$_2$), 3.33 (s, 2H, **H**$_2$O), 4.07 (br, 1H, α–C**H**), 6.64 (d, J_{AABB} = 7.6 Hz, 2H, Ph–tyr), 6.79 (m, 2H, Ph), 7.04 (m, 2H, Ph), 7.31 (m, 1H, Ph), 7.72 (d, J_{AABB} = 7.6 Hz, 2H, Ph–tyr), 8.04 (br, 3H, N**H**$_3^+$), 9.25 (s, 1H, O**H**–amino acid) ppm.

^{13}**C-NMR** (100 MHz, DMSO-d_6): δ = 16.08 (**C**H$_3$), 36.10 (β–**C**H$_2$), 52.94 (α-**C**H), 115.14 (Ph), 117.10 (Ph), 120.00 (Ph), 121.81 (Ph), 125.36 (Ph), 129.60 (Ph), 130.56 (Ph), 132.03 (Ph), 156.27 (Ph), 163.42 (Ph), 164.28 (**C**=N), 169.14 (O–**C**NNC) ppm.

^{51}**V-NMR** (105 MHz, DMSO-d_6): δ = -532.82 ppm ($\nu_{1/2}$ = 1077 Hz).

IR data (KBr disk, cm^{-1}): ν = 3599 (O–H H_2O), 3367 (s, br; NH_3^+), 1602 (s, br; C=N–N=C), 927 (s, VO_2), 878 (s, VO_2).

ESI-MS (negative ion mode, in methanol): m/z = 394 ([VO_2(Mesalhytyr)] – H^+).

3.6.7 Unprecedented obtaining complexes

$Na[VO_2(salhyCONH_2)]\cdot MeOH\cdot H_2O$ (21)

The pH of a solution of vanadyl sulfate trihydrate (0.39 g, 1.15 mmol) in water (50 mL) was adjusted to pH = 13.5 by adding a 0.10 M solution of NaOH (40 mL). Upon addition of sodium hydroxide to the blue vanadyl sulfate solution in water, it turned dark gray. The ligand salhytyr (or salhyphe or salhyleu) solution (1.01 mmol), in methanol (100 mL), was added to the aqueous solution of vanadyl sulfate, which changed further color to green brown. The reaction mixture was refluxed for 19 hours resulting in a clear yellow-orange solution. The volume of the solution was reduced to dryness and the residue yellow solid was recrystallized from methanol to afford yellow crystals suitable for X-Ray measurement.

Total yield: 130 mg (0.36 mmol, 31%).

Elemental analysis for $C_{10}H_{13}NaN_3O_7V$ (361.16 g/mol): calculated C: 33.26%, H: 3.63%, N: 11.63%; found C: 33.38%, H: 3.20%, N: 11.81%.

^{1}H-NMR (400 MHz, DMSO-d_6): $\delta =$ 3.16 (d, 3H, ^3J = 5.20 Hz, C**H**$_3$OH), 3.32 (s, 2H, **H**$_2$O), 4.08 (q, 1H, ^3J = 5.60 Hz, CH$_3$O**H**), 6.81 (m, 2H, Ph), 7.36 (m, 1H, Ph), 7.37 (m, 1H, Ph), 7.53 (m, 1H, Ph), 7.59 (s, 1H, N**H**$_2$), 7.70 (s, 1H, N**H**$_2$), 8.99 (s, 1H, C**H**=N) ppm.

^{13}C-NMR (100 MHz, DMSO-d_6): $\delta =$ 48.5 (**C**H$_3$OH), 116.91 (Ph), 119.37 (Ph), 119.78 (Ph), 132.97 (Ph), 134.00 (Ph), 158.91 (C=N), 162.37 (Ph), 164.71 (C=O), 165.15 (C=O) ppm.

^{51}V-NMR (105 MHz, DMSO-d_6): $\delta =$ -529.76 ppm ($\nu_{1/2}$ = 757 Hz).

IR data (KBr disk, cm^{-1}): 3413 (br, NH_2), 1695 (s, C=O), 1612 (s, C=N–N=C), 926 (br, VO_2).

$NH_4[VO_2(salhyCONH_2)]$ (22)

To a solution of Schiff base ligand Hsalhyphe (or Hsalhytyr, or Hsalhyleu) (0.495 mmol) in methanol (30 mL) was added NH_4VO_3 (58 mg, 0.495 mmol). The reaction mixture

was heated at reflux for 3 hours yielding a red-brown colored solution. The hot reaction mixture was filtrated to remove small amounts of unreacted NH_4VO_3. Upon standing at 0 °C a yellow precipitate was formed. The same precipitate was formed from the methanolic solution of the complex at room temperature for 1 day.

Total yield: 40 mg (0.13 mmol, 26%).

Elemental analysis for $C_9H_{11}N_4O_5V$ (306.15 g/mol): calculated C: 35.31%, H: 3.62%, N: 18.30%; found C: 34.83%, H: 3.83%, N: 16.76%.

IR data (KBr disk, cm^{-1}): 3459 (br, NH_3^+), 1685 (s, C=O), 1616 (s, C=N–N=C), 910 (br, VO_2).

ESI-MS (negative ion mode, in methanol): m/z = 288 ($[VO_2(salhyCONH_2)] - H^+$).

K[VO_2(salhyCONH$_2$)]·MeOH (**23**)

To a solution of Schiff base ligand Hsalhyphe (Hsalhytyr or Hsalhyleu) (1.24 mmol) in methanol (30 mL) was added KVO_3 (173 mg, 1.24 mmol). The reaction mixture was heated at reflux for 3 days yielding a red-brown colored solution. The hot reaction mixture was filtrated to remove small amounts of unreacted KVO_3. The volume of the solution was reduced slowly at room temperature when a yellow precipitate was formed.

Total yield: 70 mg (0.19 mmol, 15.7%).

Elemental analysis for $C_{10}H_{11}KN_3O_6V$ (359.25 g/mol): calculated C: 33.43%, H: 3.09%, N: 11.70%; found C: 34.08%, H: 2.89%, N: 10.59%

^{1}**H-NMR** (400 MHz, DMSO-d_6): $\delta =$ 3.16 (d, 3H, ^3J = 5.20 Hz, C**H**$_3$OH), 4.08 (q, 1H, ^3J = 5.60 Hz, CH$_3$O**H**), 6.79 (m, 2H, Ph), 7.37 (m, 1H, Ph), 7.57 (m, 2H, Ph + NH from N**H**$_2$), 7.76 (s, 1H, N**H**$_2$), 8.98 (s, 1H, C**H**=N) ppm.

^{13}**C-NMR** (50 MHz, DMSO-d_6): $\delta =$ 48.5 (**C**H$_3$OH), 114.95 (Ph), 119.42 (Ph), 119.75 (Ph), 133.03 (Ph), 134.01 (Ph), 158.86 (C=N), 162.30 (Ph), 164.70 (C=O), 165.09 (C=O) ppm.

^{51}**V-NMR** (105 MHz, DMSO-d_6): $\delta =$ -529.72 ppm ($\nu_{1/2}$ = 947 Hz).

IR data (KBr disk, cm^{-1}): 3413 (br, NH_2), 1695 (s, C=O), 1612 (s, C=N–N=C), 926 (br, VO_2).

ESI-MS (negative ion mode, in methanol): m/z = 288 ($[VO_2(salhyCONH_2)] - H^+$).

Na[VO_2(BrsalhyCONH$_2$)] (**24**)

Following the procedure described for complex **21**, the ligand (Brsalhyphe or Brsalhytyr, or Brsalhyleu) (1.01 mmol) was converted to the title compound as an yellow solid.

Total yield: 58 mg (0.15 mmol, 15%).

Elemental analysis for $C_9H_6BrN_3NaO_5V$: (390.00 g/mol): calculated C: 27.72%, H: 1.55%, N: 10.77%; found C: 28.20%, H: 1.81%, N: 10.07%.

^{1}**H-NMR** (400 MHz, DMSO-d_6): $\delta =$ 6.77 (m, 1H, Ph), 7.45 (m, 1H, Ph), 7.50 (s, 1H, N**H**$_2$), 7.62 (s, 1H, N**H**$_2$), 8.97 (s, 1H, C**H**=N) ppm.

^{13}**C-NMR** (100 MHz, DMSO-d_6): $\delta =$ 107.08 (Ph), 121.126 (Ph), 122.13 (Ph), 134.39 (Ph), 136.00 (Ph), 157.65 (C=N), 162.10 (Ph), 164.08 (C=O), 165.28 (C=O) ppm.

^{51}**V-NMR** (105 MHz, DMSO-d_6): $\delta =$ -529.98 ppm ($\nu_{1/2}$ = 950 Hz).

IR data (KBr disk, cm^{-1}): 3440 (br, NH_2), 1700 (s, C=O), 1617 (s, C=N–N=C), 929 (br, VO_2).

NH_4[VO_2(BrsalhyCONH$_2$)]·H_2O (**25**)

Following the procedure described for complex **22** the ligand Brsalhyphe (or Brsalhytyr, or Brsalhyleu) (0.488 mmol) was converted to the title compound as an yellow precipitate.

Total yield: 75 mg (0.19 mmol, 38%).

Elemental analysis for $C_9H_{12}BrN_4O_6V$: (403.06 g/mol): calculated C: 26.82%, H: 3.00%, N: 13.90%; found C: 26.91%, H: 2.40%, N: 10.38%.

^{1}**H-NMR** (400 MHz, DMSO-d_6): $\delta =$ 3.33 (s, 2H, **H**$_2$O), 6.76 (m, 1H, Ph), 7.22 (br, 4H, NH_4^+), 7.46 (m, 1H, Ph), 7.52 (s, 1H, N**H**$_2$), 7.63 (s, 1H, N**H**$_2$), 8.96 (s, 1H, C**H**=N) ppm.

^{13}**C-NMR** (100 MHz, DMSO-d_6): $\delta =$ 107.11 (Ph), 121.26 (Ph), 122.10 (Ph), 134.40 (Ph), 136.00 (Ph), 157.61 (C=N), 162.06 (Ph), 164.08 (C=O), 165.24 (C=O) ppm.

^{51}**V-NMR** (105 MHz, DMSO-d_6): $\delta =$ -530.75 ppm ($\nu_{1/2}$ = 825 Hz).

IR data (KBr disk, cm^{-1}): 3437 (br, NH), 1701 (s, C=O), 1616 (s, C=N–N=C), 916 (br, VO_2).

K[VO_2(BrsalhyCONH_2)]·H_2O (26)

Following the procedure described for complex **23** the ligand Brsalhyphe (or Brsalhytyr, or Brsalhyleu) (1.41 mmol) was converted to the title compound as an yellow solid.

Total yield: 0.27 g (0.64 mmol, 46%).

Elemental analysis for $C_9H_8BrKN_3O_6V$ (424.12 g/mol): calculated C: 25.49%, H: 1.90%, N: 9.22%; found C: 25.56%, H: 1.68%, N: 7.49%.

^{1}**H-NMR** (400 MHz, DMSO-d_6): $\delta =$ 3.33 (s, 2H, **H_2**O), 6.85 (m, 1H, Ph), 7.37 (m, 1H, Ph), 7.66 (s, 1H, N**H_2**), 7.80 (s, 1H, N**H_2**), 8.98 (s, 1H, C**H**=N) ppm.

^{13}**C-NMR** (100 MHz, DMSO-d_6): $\delta =$ 107.17 (Ph), 121.27 (Ph), 122.14 (Ph), 134.40 (Ph), 136.05 (Ph), 157.72 (C=N), 162.12 (Ph), 164.09 (C=O), 165.23 (C=O) ppm.

^{51}**V-NMR** (105 MHz, DMSO-d_6): $\delta =$ -531.68 ppm ($\nu_{1/2}$ = 987 Hz).

IR data (KBr disk, cm^{-1}): 3635 (O–H H_2O), 3432 (br, NH_2), 1730 (s, C=O), 1614 (s, C=N–N=C), 927 (br, VO_2).

3.6.8 Catalytic oxidative bromination of TMB/MCD

The bromination reaction was performed in acetonitrile solution, thermostat at 20 °C. For each complex two standard solutions of the same concentration were prepared. All measurements were performed in triplicate. Typical procedure: The standard assay mixture was prepared in an optical cuvette, covered with a teflon-cover, and contained 0.24 mM sodium bromide (NaBr), 0.24 mM $HClO_4$, 0.12 mM TMB, 6 μM vanadium complex, 0.53 mM hydrogen peroxide (H_2O_2), and 0.05 μM MCD (final concentration in the cuvette). Total volume of the reaction mixture is 2 mL. Each compound was added in the following order: 1,3,5-trimethoxybenzene (TMB), monochlorodimedone (MCD) and NaBr were premixed in acetonitrile to have the concentrations of 0.27 mM, 0.114 mM and 0.54 mM, in ratio 3:3:9 respectively. 880 μL of this mixture was added to 12 μL of vanadium complex, followed by 100 μL of hydrogen peroxide (H_2O_2). The reaction was initiated by addition of 52 μL of $HClO_4$ and followed by UV at 258 nm.

3.6.9 Catalytic oxidation of methyl phenyl sulfide:

The vanadium complex (0.02 mmol) was dissolved at room temperature in a mixture of CH_2Cl_2/CH_3OH 7:3 (20 mL) and 1,3,5-trimethoxybenzene (0.34 g, 2.0 mmol) as internal standard was added followed by (0.24 ml, 2.0 mmol) phenyl methyl sulfide. The resulting solution was cooled down on an ice-bath and H_2O_2 8.24 M (1.2 equiv., 0.31 mL, 2.5 mmol) was added dropwise. The reaction solution was warmed up to room temperature and stirred in a capped flask and monitored by thin-layer chromatography technique (Et_2O:*n*-hexane 9:1). After 1, 3, and 24-hours reaction time, alliquots of the reaction solutions (2.0 mL) were quenched with ca. 5 mL of a stock solution of NaOH (0.1 M) and extracted with ethyl acetate (3×4 mL). The collected organic phases were removed completely to dryness and the residue was redissolved in deuterated chloroform (600 μL) and analyzed by ^{1}H-NMR to determine the yield. From this solution was then taken 60 μL of chloroform, removed the solvent to dryness and the residue redissolved in 2 mL dichlormethane and the enantiomeric excess was determined by chiral HPLC. HPLC retention times for the methylphenyl sulfoxides (R) = 21.17 min and (S) = 29.60 min (hexane:2-propanol, 95:5).

Chapter 4

Vanadium(v) complexes with L-β-alanine residue ligands

Based on the reported crystal structure of vanadium chloroperoxidase, amino acid residues such as serine, lysine, histidine, arginine and aspartate are present at the active center,[19] and stabilize the vanadate moiety by hydrogen bonding interactions. A vital role for the catalytic reaction of V-HPOs has been attributed to Lys353, an amino acid bonded to one of the equatorial oxygen atom of the prosthetic group.[114,115] In order to model unspecific vanadium binding to proteins, the complexation behaviour of vanadate to protein fragments is of interest. The vanadium binding to L-α-alanyl-L-histidine, has been published.[116] Although much knowledge is available about the complex formation between vanadium and amino acids,[40,46–58] no work has been reported on the complexation of dioxovanadium(V) complexes with *N*-Salicylidene β-alanine hydrazide ligands. The interesting information found in the literature is represented by similar described *cis*-dioxovanadium(V) complexes based on *N*-salicylidene hydrazides that contain an amino-functionalized aliphatic side chain.[41]

This chapter describes the synthesis and characterization of *cis*-dioxovanadium(V) complexes which contain a β-alanine ligand. Introducing of a β-alanine has been achieved in order to design a new ligand system capable of mimicking the hydrogen bonding interaction of vanadate moiety from the natural system with lysine residue. Therefore this ligand seemed to be suitable for the synthesis of *cis*-dioxovanadium(V) complexes, which would be potentially interesting as oxidation catalyst.

4.1 *cis*-Dioxovanadium complexes derived from *N*-salicylidene Boc-L-β-alanine hydrazide ligands

The synthesis of the Schiff base ligand involves, in the first step, the esterification of Boc-L-β-alanine, in DMF solution, using methyl-iodite, giving the corresponding methyl-ester. The second step is the reaction between ester and two equivalent of hydrazine hydrate. The reaction was performed in methanol solution at room temperature, under continuous stirring, to form the Boc-L-β-alanine hydrazide. Afterwards the Schiff base condensation with salicylaldehyde affords *N*-salicylidene-Boc-L-β-alanine hydrazide, which exists in two tautomeric forms. The schematic representation of the synthesis pathway is depicted in Figure 4.1.

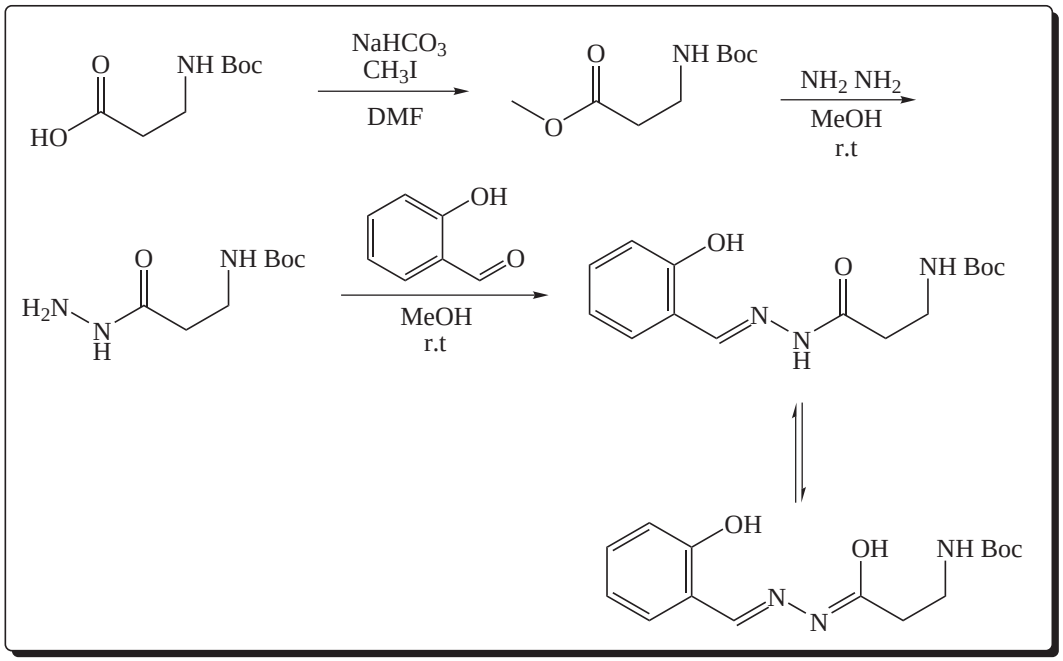

Figure 4.1: Schematic representation of the synthesis of *N*-Salicylidene-hydrazide ligand with Boc-L-β-alanine residue.

The stoichiometric reactions of these new Schiff base ligand with ammonium or potassium vanadate as vanadium sources in refluxing methanol results in the formation of the corresponding neutral complex **27**, and the potassium salt of the anionic *cis*-dioxovanadium(V) complex **28**. The synthesis pathway is depicted in Figure 4.2 and is similar with the pre-

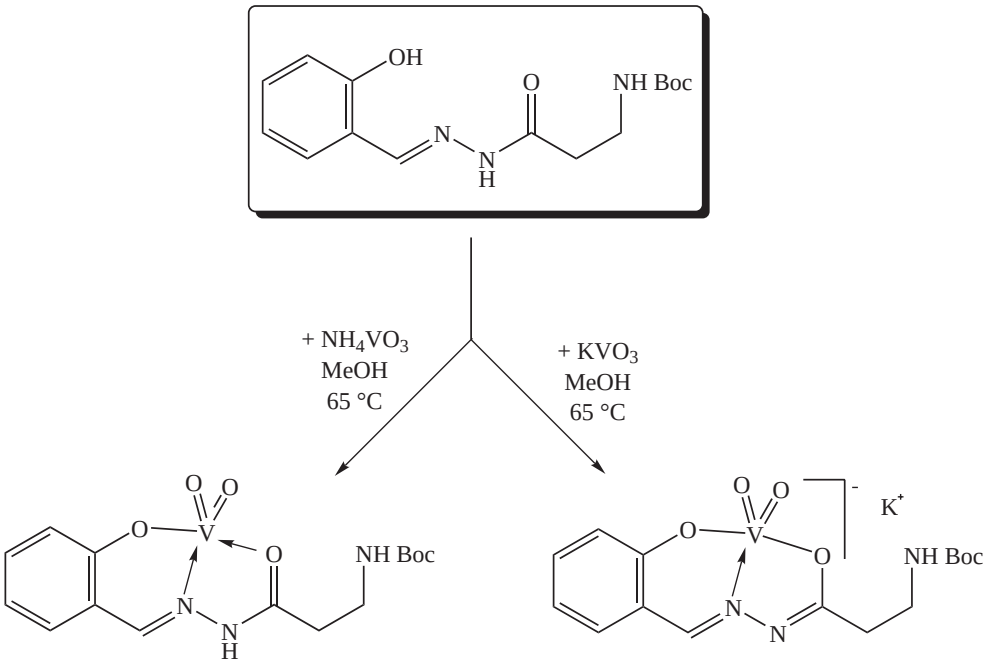

Figure 4.2: Synthesis of *cis*-dioxovanadium complexes containing β-alanine; complexes **27** left, and **28** right.

viously described procedures outlined in chapter 2.

4.1.1 Spectroscopic Characterization

The infrared spectrum of the Schiff base ligand HsalhyBocβala recorded using a KBr disc shows an absorption at 1651 cm^{-1}, which is attributed to a C=O stretching vibration[117]. This band is shifted at 1615 cm^{-1} upon complexation in the neutral *cis*-dioxovanadium complex **27** and disappears in the IR spectra of the potassium salt of the corresponding anionic complex **28**. The IR spectra of the potassium salt shows instead a strong band at 1613 cm^{-1}, attributed to the stretching vibration of the conjugate HC=N–N=C group[118,119] a characteristic IR feature of vanadium complexes with the enolized form of *N*-salicylidenehydrazide ligands.[42,82] A broad O–H stretching vibration for the free ligand, is observed at 3180 cm^{-1}. This is an indication for hydrogen bonding, because the normal position for free O–H is in the range 3730–3520 cm^{-1}.[117] This band is not present in the IR spectra of both *cis*-dioxo complexes, indicating deprotonation of the phenol group on coordination of the metal center. A strong band at ca. 3350 cm^{-1},

attributed to the stretching vibration N–H-Boc is present in the IR spectra of the free ligand as well as in the IR spectra of both complexes. A strong C=N stretching vibration band is observed at 1664 cm^{-1}. A band at 1533 cm^{-1} may be assigned to C=C stretching vibration.[117] The formation of the *cis*-dioxovanadium complexes is confirmed by strong IR vibrations corresponding to the $\nu(VO_2^+)$ group, which are observed at 908 and 966 cm^{-1} in the neutral complexes **27**, and 908 and 947 cm^{-1} in the anionic complexes **28**. These stretching vibrations are similar with those found for the previously described *cis*-dioxovanadium complexes with α-amino acid residue ligands, and moreover comparable with the stretching vibrations of reported values for $\nu(VO_2^+)$ group.[81,82,84,112,113]

Solution characterization of the complexes has been achieved through ^{1}H–, ^{13}C–NMR and ^{51}V–NMR measurements. The ^{1}H–NMR data for the novel *cis*-dioxovanadium(V) complexes are consistent with the proposed structures and exhibit shifted resonances in comparison with the corresponding proton resonances of the free ligands. In particular, the full deprotonation of the free *N*-salicylidene hydrazide ligands in the anionic complexes **28** is confirmed by the absence of the downfield ^{1}H–NMR resonance corresponding to the O−H proton. Moreover, the ^{1}H–NMR spectra of the Schiff base ligand shows two sets of resonances at 8.25 and 8.33 ppm, attributable to the azomethine (-CH=N) proton due to the E-Z isomerism. The azomethine bond is stabilized through vanadium coordination proved by an observed deshielded resonance of its singlet at 8.75 ppm in the ^{1}H–NMR of the complex (see Experimental part). The aromatic protons of the ligand and the complex as well as the α-CH, and β-CH_2 protons of alanine residue, appear in the expected region, with slight shifts in their positions.

A comparison between the ^{13}C–NMR patterns of the free ligand and the corresponding ^{13}C–NMR spectra of complexes proved the coordination mode of the ligand. The most indicative resonance is the down field shift at 155 ppm of the imine carbon atom (*C*H=N), that resonate around 140 – 147 ppm, respectively in the free ligand as a consequence of the E-Z isomers.

Furthermore, ^{51}V–NMR is indicative of the *cis*-VO_2^+ formation. ^{51}V–NMR performed in DMSO-d_6 shows one resonance for the potassium salt of *cis*-dioxovanadium(V) complex **28** at -534 ppm, which is certainly specific for *cis*-dioxovanadium(V) complexes with this type of ligand, and also similar with the resonances of the complexes with

α-amino acid residue ligands, described in the previous chapters.

4.1.2 Reactivity of the complexes

Bromination reaction of TMB/MCD

Vanadium bromoperoxidases, isolated mainly from marine organism catalyze the oxidation of bromide[120] and iodide[4] by hydrogen peroxide. The oxidized halide species can subsequently react with appropriate organic substrates to yield halogen-containing derivates.[23,121] Many covalent vanadate complexes functionally mimic vanadium bromoperoxidases (V-BPO).[1,92,122–124] The first functional mimic of the V-BPO enzyme is represented by ammonium vanadate.[93] This is able to catalyze the peroxidative halogenation of 1,3,5-trimetoxybenzene (TMB) in acidified DMF solution with a maximum turnover frequency of 15 $\mathrm{mol_{Br\text{-}TMB}h^{-1}mol^{-1}_{catalyst}}$.[93,125] V-BPO enzymes have been reported to catalyze the same reaction with a turnover frequency of $4.7{\times}10^5$ $\mathrm{mol_{Br\text{-}TMB}h^{-1}mol^{-1}_{enzyme}}$ at pH 6.5 in water.[120,126,127] Contrary to the native enzyme, all the reported functional vanadium complexes catalyze the oxidation of bromide at lower pH, with turnover rates 10^4 times slower then the native enzyme.[79] Recently the catalytic activity of vanadate is enhanced by changing water for acetonitrile, using 1,3,5-trimethoxybenzene (TMB) and monochlorodimedone (MCD) as organic substrate.[128,129] The herein reported *cis*-dioxovanadium(V) complex **28** has been also tested towards its capability to catalyze the oxidative bromination of TMB/MCD using hydrogen peroxide as oxidant and $HClO_4$ as acid.

The competitive bromination of 1,3,5-trimethoxybenzene TMB/MCD was performed in acetonitrile. Therefore stock solutions of 1 mM MCD, 4 mM TMB, 10.6 mM H_2O_2, 9.21 mM $HClO_4$ in acetonitrile and 1 mM catalyst in MeCN/MeOH (95:5) and 8 mM NaBr in MeCN/H_2O (99:1) were prepared. The final concentrations in the cuvette were 6 μM catalyst, 0.05 mM MCD, 0.12 mM TMB, 0.24 mM NaBr and 0.53 mM H_2O_2 in 2 ml MeCN. The reaction was initiated by addition of $HClO_4$ (at least 0.24 mM) and followed by UV at 258 nm (characteristic absorption of MCD). When the bromination of TMB was completed, MCD was brominated as indicated by the decreasing UV intensity.

The period until decreasing of the intensity corresponds to the total reaction time of TMB bromination (T_{TMB} in the Figure 4.3).

The bromination of TMB catalyzed by *cis*-dioxovandium complex with β-alanine ligand, took 277 s. This corresponds to a turn over of 260 $mol_{Br\text{-}TMB}h^{-1}mol^{-1}_{catalyst}$, whereas the same reaction catalyzed by vanadate standard $(nBu_4N)_2HVO_4$), took 480 s,[94] which corresponds to a turn over of 150 $mol_{Br\text{-}TMB}h^{-1}mol^{-1}_{catalyst}$. This is the first example where the *cis*-dioxovanadium complexes containing β-amino acid residue catalyze bromination of both substrates (TMB/MCD) and moreover with a high turnover frequency.

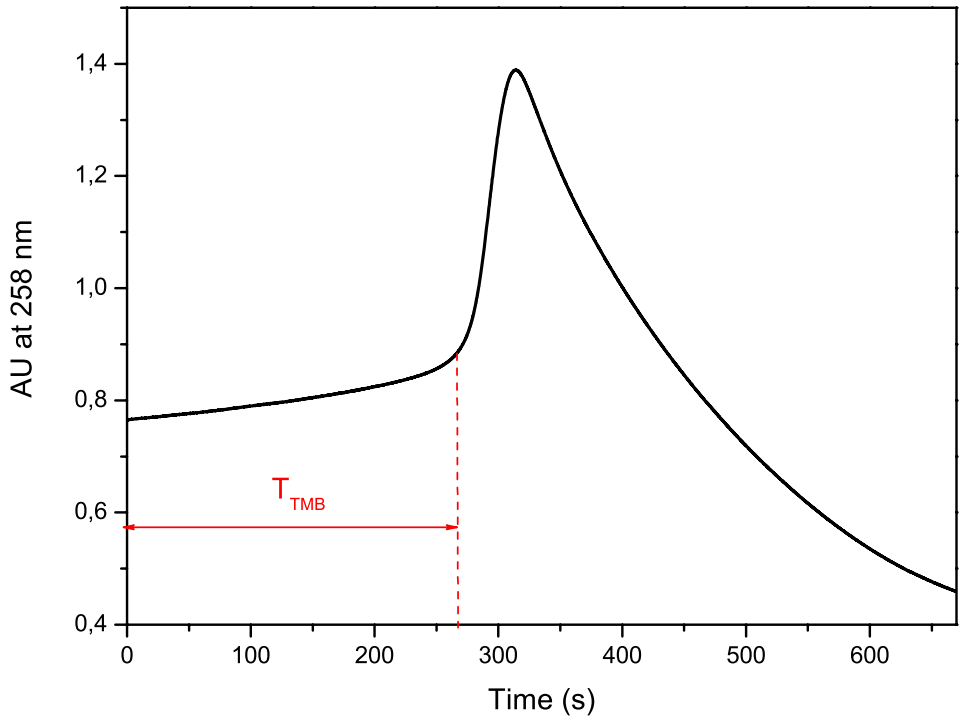

Figure 4.3: Competitive catalytic bromination of TMB/MCD, followed by UV at 258 nm. Reaction conditions: 6 μM vanadate, 0.05 mM MCD, 0.12 mM TMB, 0.53 mM H_2O_2, 0.24 mM NaBr and 0.24 mM $HClO_4$.

Oxidation of sulfides catalyzed by *cis*-dioxovanadium complexes with β-alanine functionalized ligands

The catalytic properties of the complex **28** was examined in the oxidation of organic sulfides to the corresponding sulfoxide (Figure 4.4). This is another important reaction catalyzed by vanadium haloperoxidases,[26,28] as well as by vanadium complexes.[95,96] 1 mol-% catalyst was used and the reaction was performed in a mixture of CH_2Cl_2/ CH_3OH 7:3, at 0 °C. As oxidant was used 1.2 equivalents of a 8.24 M solution of hydrogen peroxide. 1,3,5-trimethoxybenzene (2.0 mmol) was used as internal standard. After defined intervals of time, aliquots were taken from the reaction mixture and the product analyzed by NMR (determination of the yield) and HPLC (determination of the ee). With the *cis*-dioxovanadium complex **28**, the reaction seems to be very fast. Oxidation of methyl phenyl sulfide, afforded methyl phenyl sulfoxide, in 68% yield, within 1 hour, while the reaction was completed in 3 hours giving the corresponding sulfoxide in 100% yield and 0.83% ee (S). The results are comparable with those of vanadium complexes described in two previous chapters 2 and 3.

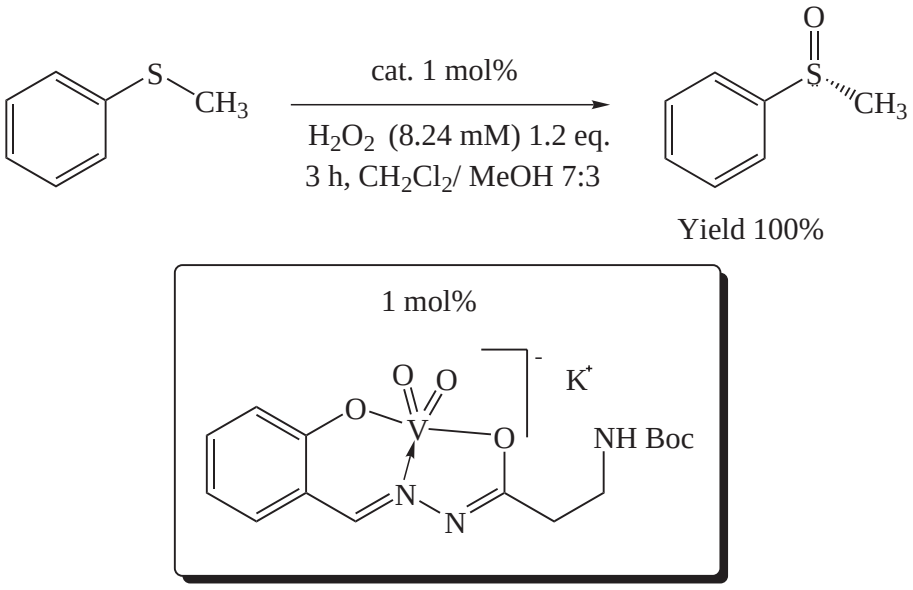

Figure 4.4: Catalytic oxidation of sulfide to sulfoxides promoted by Schiff base-vanadium(V) complex derived from β-alanine.

4.2 Complexation studies using free β-alanine ligand

Catalytic data showed that the vanadium complex with Boc-β-alanine, described in this chapter, reacts faster towards bromination of TMB/MCD, as well as the oxidation of methyl phenyl sulfide, comparing with the data of vanadium complexes containing Boc-α-amino acid ligands, described in chapter 2. Moreover comparing the catalytic data of the vanadium complexes with free and Boc-α-amino acid ligands, showed that the complexes with free-α-amino acid residue ligands react faster than the corresponding complexes with Boc-α-amino acid residue. Based on this information, we are focused on the synthesis of the *cis*-dioxovanadium complexes which contain a free β-alanine ligand, which we expect to have higher catalytic activity. Similar complexes, with *N*-salicylidene hydrazide ligands that contain an amino-functionalized aliphatic side chain, have been prepared recently in our research group.[41]

The synthesis of the Schiff base ligands with unprotected β-alanine residue follows the pathway depicted in Figure 4.5 analogously to literature,[41] with some differences, for example preventing heating under reflux, and some other differences.

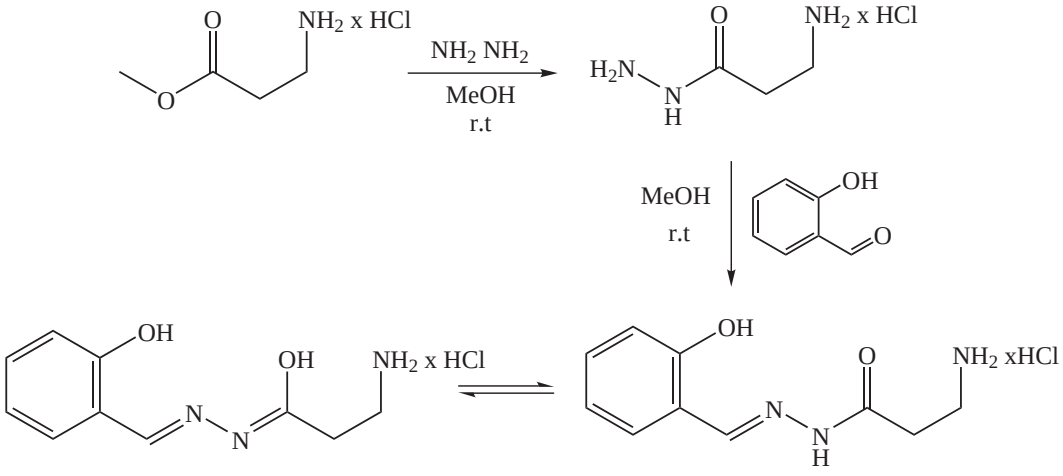

Figure 4.5: Synthesis of Schiff base ligand with free β-alanine.

Thus β-alanine methyl ester as hydrochloride salt reacts with two equivalents of hydrazine hydrate, in methanol solution, under stirring at room temperature, resulting in the formation of β-alanine hydrazide hydrochloride. Reaction of equivalent amounts of this product and salicylaldehyde, in methanol (stirring) overnight at room tempera-

ture gives a yellow suspension, from which the yellow precipitate was characterized as disalicylidene-hydrazide. The ligand was isolated from the filtrate by evaporation of the solvent. After purification by recrystallization from ethanol, the ligand was obtained in 43% yield.

Two attempts were made to synthesize *cis*-dioxovanadium(V) complexes from the Schiff base ligand with free β-alanine, but unfortunately no well defined products were obtained. Ammonium and potassium vanadate were used as vanadium sources and the reactions were performed in refluxing methanol. In both attempts to synthesis the *cis*-dioxovanadium(V) complexes, after slow evaporation of the solvent a dark brown powder was obtained. Isolated products were characterized using ^{1}H– and ^{51}V–NMR spectroscopy, IR spectroscopy, UV-Vis, and elemental analysis. ^{51}V–NMR spectrum in DMSO-d_6 shows one resonance at -532 pm, which is similar to the value found for the other amino acid dioxovanadium complexes. Infrared spectroscopy experiments revealed the presence of *cis*-dioxovanadium species, since sharp signals were found in the region 969 and 909 cm^{-1}. Furthermore ^{1}H–NMR shows some minor impurities. On the other hand the UV spectrum recorded in acetonitrile displays a band a 278 nm ($\varepsilon = 10{\cdot}10^3$ M^{-1} cm^{-1}), assuming that the complex is monomeric, and a small shoulder at 407 nm ($\varepsilon = 2{\cdot}10^3$ M^{-1} cm^{-1}). Attempts to purify the product by recrystallization from alcohol (MeOH, EtOH) were unsuccessful. Although again a brown solid was obtained, unfortunately no well defined complexes were isolated according to ^{1}H–NMR. Nevertheless, according to the elemental analysis the *cis*-dioxovanadium complex K[VO_2(salhyβalaCl)]·H_2O was formed.

4.3 Conclusions

In this chapter the synthesis of new *cis*-dioxovanadium(V) complexes **27** and **28** is described, based on *N*-salicylidene Boc-β-alanine hydrazide ligand which is easily obtainable. The complex **28** was examined in bromination reaction of TMB/MCD, and the results were compared with those obtained for the *cis*-dioxovanadium(V) complexes with α-amino acids described in chapters 2 and 3. For the herein described complex the best results were obtained, it appeared to be the more active catalyst with a turnover number of 260 $mol_{\text{Br-TMB}}h^{-1}mol^{-1}_{\text{catalyst}}$.

The catalyst was also tested on its ability to oxidise the organic sulfides to the corresponding sulfoxides. The results showed that the reaction was completed in 3 hours giving the corresponding sulfoxide in 100% yield.

The ligand with free β-alanine is inappropriate for the synthesis of *cis*-dioxovanadium(V) complexes, since no well characterized complexes were isolated. Using modified procedures, there were indications that vanadium ions were coordinated to the ligand system, but mixture of products were obtained, that were difficult to characterize. The attempts to purify the products were unsuccessful.

4.4 Experimental part

4.4.1 Synthesis of Schiff base ligand with Boc-L-β-alanine

Boc-L-β-alanine-methyl-ester (Boc-β-alaOMe)

To a suspension of $NaHCO_3$ (1.50 g, 17.4 mmol, 1.1 eq.) in 30 ml dry DMF was added Boc-L-β-alanine (3 g, 15.9 mmol, 1 eq.) and methyl iodide (1.10 mL, 17.9 mmol, 1.1 eq). The mixture was stirred at room temperature under argon atmosphere for 20 hours. Distilled water (50 mL) was added and the product extracted with ethyl acetate (3 x 50 mL). The combined organic layers were washed with distilled water and than dried over Na_2SO_4, and concentrated in vacuum to obtain the product as yellow-orange oil. This is purified by column chromatography (eluent hexan/ethyl acetate 1:1) to obtain yellow oil product.

Total yield: 1.4 g (6.9 mmol, 44%).

^{1}**H-NMR** (200 MHz, DMSO-d_6): δ = 1.36 (s, 9H, C(C**H**$_3$)$_3$), 2.41 (t, ^{3}J = 6.96 Hz, 2H, α-C**H**$_2$), 3.14 (q, ^{2}J = 6.70 Hz, 2H, β–C**H**$_2$), 3.57 (s, 3H, C**H**$_3$–ester), 6.81 (t, ^{3}J = 6.96 Hz, 1H, N**H**Boc) ppm.

^{13}**C-NMR** (50 MHz, DMSO-d_6): δ = 28.11(C(**C**H$_3$)$_3$), 34.06 (α-**C**H$_2$), 36.04 (β-**C**H$_2$), 51.20 (**C**H$_3$ ester), 77.63 (O**C**(CH$_3$)$_3$), 155.40 (NH**C**=OBoc), 171.61 (O=**C**NHN) ppm.

Boc-L-β-alanine-hydrazide (Bocβalahy)

To a solution of BocβalaOMe (1.28 g, 6.3 mmol) in methanol (30 mL) was added slowly dropwise hydrazine monohydrate (0.92 mL, 18.9 mmol) (100%). The clear colorless reaction mixture was stirred at room temperature for 30 hours. After removing of the solvent, the product was recrystallized from ethyl acetate, and dried under vacuum. The product was obtained as a colorless crystalline solid. m.p. 116–118°C.

Total yield: 1.23 g (6.05 mmol, 96%).

Elemental analysis for $C_8H_{17}N_3O_3$ (203.24 g/mol): calculated C: 47.28%, H: 8.43%, N: 20.68%; found C: 47.52%, H: 8.30%, N: 20.56%.

^{1}**H-NMR** (200 MHz, DMSO-d_6): $\delta =$ 1.35 (s, 9H, C(C**H**$_3$)$_3$), 2.14 (t, ^{3}J = 7.39 Hz, 2H, α-C**H**$_2$), 3.14 (q, ^{2}J = 6.70 Hz, 2H, β–C**H**$_2$), 4.14 (s, 2H, N**H**$_2$), 6.61 (t, ^{3}J = 7.39 Hz, 1H, N**H**Boc), 8.94 (s, 1H, N**H**–NH$_2$) ppm.

^{13}**C-NMR** (50 MHz, DMSO-d_6): $\delta =$ 28.21 (C(**C**H$_3$)$_3$), 33.92 (α-**C**H$_2$), 36.71 (β-**C**H$_2$), 77.56 (O**C**(CH$_3$)$_3$), 155.40 (NH**C**=OBoc), 169.72 (O=**C**NHN) ppm.

N-Salicylidene-Boc-L-β-alanine-hydrazide (HsalhyBocβala)

Salicylaldehyde (0.23 mL, 3.026 mmol) was slowly added dropwise to a solution of Boc-L-β-alanine-hydrazide (Bocβalahy) (0.62 g, 3.3.026 mmol) in 20 mL methanol. The reaction mixture turns its color to pale yellow once the salicylaldehyde is added. The mixture was stirred at room temperature for 24 hours. The product was obtained as a colorless solid. (The reaction was followed by TLC). The NMR data confirm the presence of two isomers in ratio 1:1.75. m.p 170 °C.

Total yield: 1.12 g (2.68 mmol, 85.5%).

Elemental analysis for $C_{15}H_{23}N_3O_4$ (307.34 g/mol): calculated C: 58.62%, H: 6.89%, N: 13.67%; found C: 58.40%, H: 7.09%, N: 13.57%.

^{1}**H-NMR** (400 MHz, DMSO-d_6): δ = 1.36 (s, 9H, C(C**H**$_3$)$_3$), 2.37 (t, ^{2}J = 7.06 Hz, 2H, α-C**H**$_2$), 2.20 (t, ^{3}J = 7.06 Hz, 2H, β-C**H**$_2$), 6.76 (bs, 1H, N**H**–Boc), 6.81 – 6.90 (m, 2H, Ph), 7.19 – 7.28 (m, 1H, Ph), 7.48–7.68 (m, 1H, Ph), 8.25, 8.33 (s, 1H, C**H**=N), 10.05, 11.12(s, 1H, O**H**, N**H**), 11.24 and 11.61 (s, 1H, O**H**) ppm.

^{13}C-NMR (100 MHz, DMSO-d_6): $\delta =$ 28.15 (C(**C**H_3)$_3$), 32.58, 34.41 (α-**C**H_2), 35.81, 36,33 (β-**C**H_2), 77.47, 77.59, (O**C**(CH$_3$)$_3$), 116.02, 116.26 (Ph), 118.48, 119.18 (Ph), 119.29, 120.00 (Ph), 126.69, 129.41 (Ph), 130.81, 131.10 (Ph), 140.89, 146.65 (**C**H=N), 155.45, 156.26, (Ph), 157.26 (**C**=OBoc), 166.59, 172.19 (O=**C**) ppm.

MS (FAB$^+$, nba): m/z = 307 (70% [M$^+$]), 251 (100%).

Selected IR data (cm^{-1}): $\tilde{\nu}$ = 3351 (N–H), 3180 (O–H), 1664 (C=N), 1657 (C=O).

4.4.2 Synthesis of vanadium complexes with Boc-L-β-alanine

[VO_2(HsalhyBocβala)]·MeOH (27)

To a solution of Schiff base ligand HsalhyBocβala (0.10 g, 0.325 mmol) in methanol (20 mL) was added NH_4VO_3 (41.8 mg, 0.325 mmol). The reaction mixture was heated at reflux for 3 hours yielding a red-brown colored solution. The hot reaction mixture was filtrated, the solvent was removed to dryness and the residue is recrystallized from ethanol to obtain the product as a brown solid.

Total yield: 61.5 mg (0.146 mmol, 45%).

Elemental analysis: for $C_{16}H_{23}N_3O_7V$ (420.31 g/mol) calculated C: 45.72%, H: 5.52%, N: 10.00%; found C: 45.85%, H: 6.22%, N: 11.09%.

Selected IR data (cm^{-1}): $\tilde{\nu}$ = 3340 (s, br; N–H), 1615 (s, C=O), 966 (s, VO_2), 908 (s, VO_2).

K[VO_2(salhyBocβala)]·H_2O (28)

To a solution of salhyBocβala (0.10 g, 0.33 mmol) in 30 mL methanol was added KVO_3 (44.86 mg, 0.33 mmol). The resulting reaction mixture was heated under reflux with continuous stirring for 24 hours till all vanadate was reacted. The clear yellow reaction mixture was filtrated, and allowed to evaporate slowly at room temperature. The product was precipitated as a yellow solid, which is filtrated, and dried under vacuum. m.p 221–225 °C.

Total yield : 103 mg (0.23 mmol, 70%).

Elemental analysis: for $C_{15}H_{21}N_3O_7VK$ (445.38 g/mol) calculated C: 40.45%, H: 4.75%, N: 9.43%; found C: 40.52%, H: 4.72%, N: 9.41%.

^{1}H-NMR (400 MHz, DMSO-d_6): $\delta =$ 1.37 (s, 9H, C(C**H**$_3$)$_3$), 2.37 (m, 2H, α-C**H**$_2$), 3.19 (m, 2H, β-C**H**$_2$), 3.32 (s, 2H, **H**$_2$O), 6.74 (m, 2H, Ph + N**H**Boc), 7.28 (m, 1H, Ph), 7.48 (m, 1H, Ph), 8.75 (s, 1H, C**H**=N) ppm.

^{13}C-NMR (100 MHz, DMSO-d_6): $\delta =$ 28.23 (C(**C**H$_3$)$_3$), 32.70 (β-**C**H$_2$), 37.39 (α-**C**H$_2$), 77.59, (O**C**(CH$_3$)$_3$), 116.49 (Ph), 119.41 (Ph), 119.69 (Ph), 132.37 (Ph), 132.83 (Ph), 154.69 (**C**H=N), 155.37 (Ph), 157.26 (**C**=OBoc), 164.42, (NH**C**=OBoc), 174.05 (O–**C**NNC) ppm.

^{51}V-NMR (105 MHz, DMSO-d_6): $\delta =$ -533.67 ppm.

Selected IR data (cm^{-1}): $\tilde{\nu}$ = 3357 (s, br; N–H), 1613 (s, C=N–N=C), 947 (s, VO_2), 908 (s, VO_2).

UV/Vis (MeOH solution, λ_{max} in nm (ε in 10^4 M^{-1} cm^{-1})): 214 (21.5), 272 (10.9), 384 (5.9).

ESI-MS (negative ion mode): **(MeOH)** m/z = 388 ([VO_2(salhyBocβala)] – H^+).

4.4.3 Synthesis of Schiff base ligand with L-β-alanine

β-Alanine-hydrazide hydrochloride

To a solution of β-alanine-methylester-hydrochloride (3.02 g, 21.63 mmol) in methanol (80 mL), hydrazine monohydrate (2.10 mL, 43.3 mmol) (100%) was added under continuous stirring. The resulting solution was stirred at room temperature overnight, until the TLC (methanol/hexan 2:1, visualized by vanillin/H_2SO_4) didn't show any starting material. The solvent was removed to dryness and the remaining viscous oil was dried under strong vacuum, and recrystallized from methanol, to obtain the product as a colorless solid. m.p 188–191 °C.

Total yield : 1.92 g (13.75 mmol, 64%).

Elemental analysis: for $C_3H_{10}ClN_3O$ (139.58 g/mol) calculated C: 25.81%, H: 7.22%,

N: 30.10%; found C: 24.53%, H: 6.94%, N: 30.80%.

^{1}H-NMR (200 MHz, DMSO-d_6): $\delta =$ 1.38 (m, 2H, α-C**H**$_2$), 3.75 (m, 2H, β-C**H**$_2$), 4.34 (br, 2H, N**H**$_2$), 8.24 (br, 2H, N**H**$_2$), 9.58 (br, 1H, N**H**) ppm.

^{13}C-NMR (50 MHz, DMSO-d_6): $\delta =$ 17.20 (β-**C**H$_2$), 47.00 (α-**C**H$_2$), 168.45 (**C**=O) ppm.

N-Salicylidene-L-β-alanine-hydrazide-hydrochloride (Hsalhyβala×HCl)

To a solution of β-alanine-hydrazide hydrochloride (1.19 g, 8.53 mmol) in methanol (60 mL), salicylaldehyde (1.04 g, 8.53 mmol) was added dropwise. The resulting yellow solution was stirred at room temperature for 2 days. A yellow solid was separated out, which was filtrated and characterized as disalicylidene-hydrazide. The filtrate was concentrated to dryness and the residue is recrystallized from ethanol to obtain the product as a colorless solid. The NMR data confirm the presence of two isomers in ratio 1:2. m.p 197–205 °C.

Total yield : 0.94 g (3.86 mmol, 43%).

Elemental analysis: for $C_{10}H_{14}ClN_3O_2$ (243.69 g/mol) calculated C: 49.29%, H: 5.79%, N: 17.24%; found C: 49.84%, H: 5.69%, N: 17.05%.

^{1}H-NMR (200 MHz, DMSO-d_6): $\delta =$ 1.45 (m, 3H, α-C**H**$_2$, β-C**H**), 3.98 and 4.5 (s, 1H, β-C**H**), 6.85 (m, 2H, Ph), 7.29 (m, 1H, Ph), 7.66 (m, 1H, Ph), 8.36 (br, 3H, N**H**$_3^+$Cl$^-$), 8.38 and 8.52 (s, 1H, C**H**=N), 10.14, 10.84 (s, 1H, N**H**), 11.75, 12.45 (s, 1H, O**H**) ppm.

^{13}C-NMR (50 MHz, DMSO-d_6): $\delta =$ 15.83, 17.00 (β-**C**H$_2$), 46.54, 57.52 (α-**C**H$_2$), 116.37, 118.67 (Ph), 119.34, 119.91 (Ph), 125.72, 128.70 (Ph), 131.63, 133.00 (Ph), 142.16, 147.81 (**C**H=N), 156.65, 157.30 (Ph), 158.53, 162.51 (Ph), 165.84, 170.53 (**C**=O) ppm.

Selected IR data (cm^{-1}): $\tilde{\nu} = 3461$ ($NH_3^+Cl^-$), 3169 (NH), 1703 (C=O), 1683 (C=N).

4.4.4 Attempted synthesis of vanadium complexes with L-β-alanine

K[VO_2(salhyβalaCl)]·H_2O (29)

To a solution of Schiff base ligand Hsalhyβala×HCl (0.47 g, 1.93 mmol) in methanol (30 mL) was added KVO_3 (0.26 g, 1.93 mmol). The resulting reaction mixture was heated under reflux with continuous stirring for 3.5 hours till all vanadate was reacted. The red-brown reaction mixture was filtrated. The volume of the solution was concentrated to about half under reduce pressure and left at room temperature when a brown precipitate is formed overnight. The resulting precipitate was filtrated off and the solution volume removed under reduce pressure for additional material. m.p 360 °C.

Total yield : 0.64 g (1.76 mmol, 43%).

Elemental analysis: for $C_{10}H_{14}ClKN_3O_5V$ (381.73 g/mol) calculated C: 31.46%, H: 3.70%, N: 11.01%; found C: 31.97%, H: 3.31%, N: 9.59%.

^{1}**H-NMR** (400 MHz, DMSO-d_6): $\delta =$ 1.52 (m, 3H, α-C**H**$_2$, β-C**H**), 3.33 (s, 2H, **H**$_2$O), 3.68 (m, 1H, β-C**H**), 6.85 (br, 3H, NH_3^+), 6.95 (m, 2H, Ph), 7.32 (m, 2H, Ph), 8.99 (s, 1H, C**H**=N) ppm.

^{51}**V-NMR** (105 MHz, DMSO-d_6): $\delta =$ -532 ppm.

Selected IR data (cm^{-1}): $\tilde{\nu}$ = 3400 (s, NH_3^+), 1608 (br, -C=N-N=C-), 969 and 909 (s, VO_2).

UV/Vis (acetonitrile solution, λ_{max} in nm (ε in 10^4 M^{-1} cm^{-1})): 278 (10), 407 (2).

[VO_2(salhyβala)]·H_2O (30)

To a solution of Schiff base ligand-Hsalhyβala×HCl (0.47 g, 1.93 mmol) in methanol (50 mL) was added NH_4VO_3 (0.23 g, 1.93 mmol). The resulting mixture was refluxed for 24 hours, till all vanadate was reacted, filtrated, and the solution was allowed to stand at room temperature, to evaporate slowly the solvent to obtain the dark brown solid which was collected by filtration, and dried in air.

UV/Vis (acetonitrile solution, λ_{max} in nm (ε in 10^4 M^{-1} cm^{-1})): 272 (10.4), 316 (6.7),

399 (2.7).

4.4.5 Catalytic oxidative bromination of TMB/MCD

The bromination reaction was performed in acetonitrile solution, thermostat at 20 °C. For each complex three standard solutions of the same concentration were prepared. All measurements were performed in triplicate. Typical procedure: The standard assay mixture was prepared in an optical cuvette, covered with a teflon-cover, and contained: 0.24 mM sodium bromide (NaBr), 0.24 mM $HClO_4$, 0.12 mM TMB, 6 μM vanadium complex, 0.53 mM hydrogen peroxide (H_2O_2), and 0.05 μM MCD (final concentration in the cuvette). Total volume of the reaction mixture is 2 mL. Each compound was added in the following order: 1,3,5-Trimethoxybenzene (TMB), monochlorodimedone (MCD) and NaBr were premixed in acetonitrile to have the concentrations of 0.27 mM, 0.114 mM and 0.54 mM, in ratio 3:3:9 respectively. 880 μL of this mixture was added to 12 μL of vanadium complex, followed by 100 μL of hydrogen peroxide (H_2O_2). The reaction was initiated by addition of 52 μL of $HClO_4$ and followed by UV at 258 nm.

4.4.6 Catalytic oxidation of methyl phenyl sulfide

Vanadium complex (0.02 mmol) was dissolved at room temperature in a mixture of CH_2Cl_2/CH_3OH 7:3 (20 mL) and 1,3,5-trimethoxybenzene (0.34 g, 2.0 mmol) as internal standard was added followed by (0.24 ml, 2.0 mmol) phenyl methyl sulfide. The resulting solution was cooled down on an ice-bath and H_2O_2 8.24 M (1.2 equiv., 0.31 mL, 2.5 mmol) was added dropwise. The reaction solution was warmed up to room temperature and stirred in a capped flask and monitored by thin-layer chromatography technique (Et_2O:*n*-hexane 9:1). After 1, and 3-hours reaction time, aliquots of the reaction solutions (2.0 mL) were quenched with ca. 5 mL of a stock solution of NaOH (0.1 M) and extracted with ethyl acetate (3×4 mL). The collected organic phases were removed completely to dryness and the residue was redissolved in deuterated chloroform (600 μL) and analyzed by ^{1}H-NMR to determine the yield. From this solution was then taken 60 μL of chloroform, removed the solvent to dryness and the residue redissolved in 2 mL dichlormethane

and the enantiomeric excess was determined by chiral HPLC. HPLC retention times for the methylphenyl sulfoxides (R) = 21.17 min and (S) = 29.60 min (hexane:2-propanol, 95:5).

Chapter 5

Molybdenum(VI) complexes with Boc-L-amino acid residue ligands

The coordination chemistry of molybdenum(VI) has assumed special importance due to its biochemical significance[60,130,131] as well as for the involvement of Mo(VI) compounds as catalysts in several industrial processes such as amoxidation of propene,[132] epoxidation of olefins,[133] olefin metathesis and isomerization of allylic alcohols.[134] In order to mimic the biological systems, a number of dioxomolybdenum complexes have been synthesized and characterized[62,135–137] Here we describe the preparation and characterization of a series of mononuclear *cis*-dioxo molybdenum(VI) complexes, containing the tridentate Schiff base ligands derived from salicylaldehyde itself or one of its ring substituted derivative, and Boc-amino acid hydrazides. The oxidation catalysis are also reported. As far as we are aware no structures of this type of ligands have been described in the literature.

The synthesis of the Schiff base ligands were performed according to the procedure described in chapter 2 and 3 for Boc-α and β amino acid respectively, where the same ligands were used to synthesize *cis*-dioxovanadium complexes. The reactions of $MoO_2(acac)_2$ with tridentate Schiff bases in appropriate solvent results in the formation of corresponding *cis*-dioxo molybdenum(VI) complexes. The complexes are yellow solids and in the case of β amino acid could be crystallized from methanol to obtain single crystals suitable for X-Ray analysis.

5.1 Molecular structure of complex 36

The reaction of $MoO_2(acac)_2$ with ligand HsalhyBocala, the Schiff base ligand with Boc-β-alanine residue in refluxing methanol, were accompanied by an immediate change of the solution color to yellow-orange. After reducing the volume of the solution, yellow colored single crystal were formed at -28 °C, within two weeks. The complex crystallizes in the monoclinic space group $P2_1/n$, with two methanol molecules as solvent of crystallization. The molecular structure and the atom numbering scheme for the complexes **36** is shown in Figure 5.1, with the relevant bond distances and angles collected in Table 5.1. The coordination geometry around molybdenum atom can be described as distorted octahedral where the ligand dianion acts in tridentate manner forming one five-membered and another six-membered metallo-cycle involving the $MoO_2{}^{2+}$ moiety.

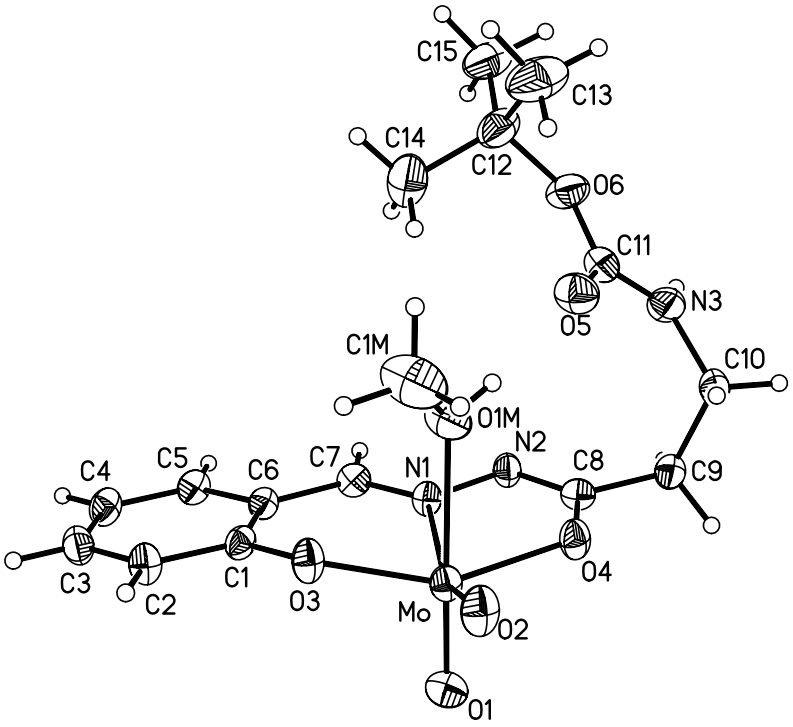

Figure 5.1: Molecular structure of $[MoO_2(salhyBocala)(MeOH)]$ in crystals of $[MoO_2(salhyBocala)(MeOH)]\cdot 2MeOH$ (**36**) (thermal ellipsoids are drown at the 50% probability level).

As expected the Schiff base ligand is coordinated in the deprotonated iminolate form, through the phenolate oxygen atom O3, the imine nitrogen atom N1, amide oxygen atom

O4. The Mo atom has two additional oxo groups O1 and O2. One methanol molecule completes the distorted octahedral coordination sphere which lies *trans* to oxo group O1. The molybdenum atom is significantly displaced from the plane, formed by the ligand, toward the apical oxygen atom O1 by 31.3 pm. The ring system and the hydrazide group lie in the mean plane. The alanine residue raises out of the mean plane by a torsion angle (C9–C10–N3–C11) of 96.1 °. Both Mo=O distances, ranging from 169.6(3) to 169.8(2) pm, and the O=Mo=O angle of 105.6 °, are in the usual range for *cis*-MoO_2 complexes.[45, 138, 139] The Mo - O1M bond of 233.6(2) pm, is significantly longer than the other Mo - O bonds from 169.6(3) to 202.1(2) pm, indicating that the alcohol molecule is weakly bonded to the $MoO_2{}^{2+}$-core.

Table 5.1: Selected bond lengths (pm) and angles (°) for complex **36**.

Bond lengths			
Mo−O1	169.6(3)	Mo−O1M	233.6(2)
Mo−O2	169.8(2)	Mo−N1	224.6(3)
Mo−O3	192.8(2)	C8−N2	128.9(5)
Mo−O4	202.1(2)	C8−O4	132.3(4)
Bond angles			
O1−Mo−O2	105.56(12)	O2−Mo−O3	102.72(11)
O1−Mo−O3	100.37(12)	O2−Mo−N1	157.97(12)
O1−Mo−O4	96.46(11)	O2−Mo−O4	97.31(10)
O1−Mo−N1	94.71(11)	O2−Mo−O1M	83.99(2)
O1−Mo−O1M	169.76(2)	O4−Mo−N1	71.44(10)
O3−Mo−N1	81.57(9)	O4−Mo−O1M	78.37(1)
O3−Mo−O4	149.18(10)	O3−Mo−O1M	80.68(1)

The complex crystallizes with two methanol molecules which form hydrogen bonding interactions. Thus the coordinated methanol molecule is involved in intermolecular hydrogen bonding with the oxygen atom of the Boc group O5 (O5···O1M 263.2 pm). The oxo group O1 forms hydrogen bonding with a second methanol molecule of one neighboring molecule (O1···H2MA 275.5 pm). The hydrazide nitrogen atom N2 forms intermolecular hydrogen bonding interaction with a second methanol molecule (N2···O2M 280.7) which is further involved in bifurcated bonding interaction with the third methanol molecule of a neighboring molecule O3MB (O2M···O3MB 270.1 pm). The amino functionality of alanine forms intermolecular hydrogen bond with a third methanol molecule (N3···O3M 287.4 pm), which is further hydrogen bonded to one methanol molecule of another neighboring molecule (see Figure 5.2).

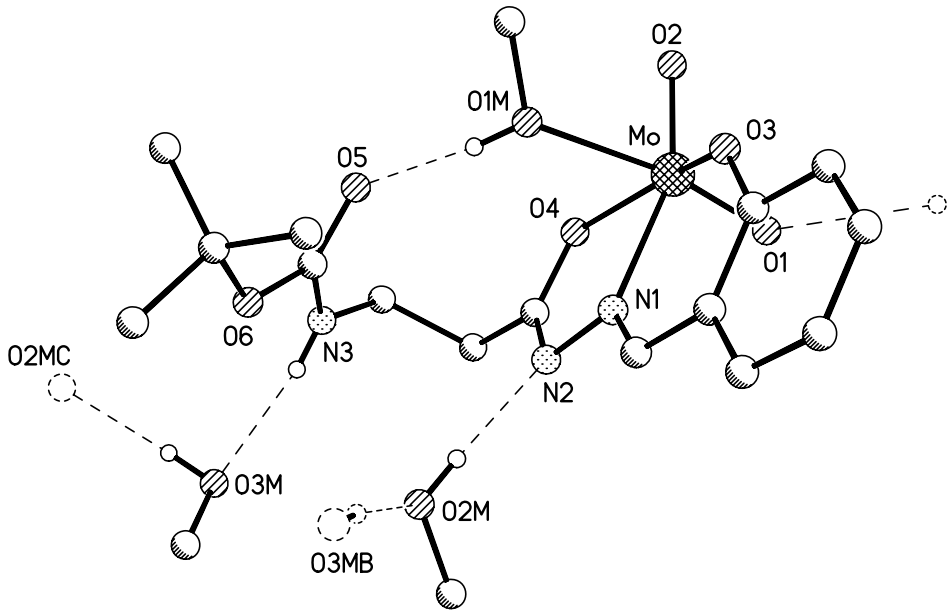

Figure 5.2: Representation of the hydrogen bonding interactions in crystals of $[MoO_2(salhyBocala)(MeOH)]\cdot 2MeOH$ (**36**). Only hydrogen atoms bonded to heteroatoms are shown, broken lines represent hydrogen bonds, dashed circles symmetry equivalent atoms; relevant distances (in pm): O1···H2MA 275.5, N3···O3M 287.4, O5···O1M 263.2, N2···O2M 280.7, O2M···O3MB 270.1 (symmetry operators: A: 1 – x, 1 – y, – z; B: $\frac{3}{2}$ – x, $\frac{1}{2}$ + y, $\frac{1}{2}$ – z; C: $\frac{3}{2}$ – x, – $\frac{1}{2}$ + y, $\frac{1}{2}$ – z.

5.2 Spectroscopic Characterization

Selected spectroscopic data of the complexes are summarized in Table 5.2. In all of them, the ligand is found to coordinate through the deprotonated phenolate oxygen, enolate oxygen, and the azomethine nitrogen atoms. The IR spectra of the complexes do not exhibit the ligand bands at ca. 3477 cm^{-1} [ν(OH)], and 3209 cm^{-1} [ν(NH)].[117,140] Characteristic strong bands at 1661–1675 cm^{-1} due to the carbonyl moiety ν(C=O) stretching vibrations of the ligands[117,140,141] are not observed any more in the spectra of the complexes. Instead a strong band is observed at around 1617 cm^{-1} which can be attributed to the stretching vibration of the conjugate –C=N–N=C– grouping.[84] This band is characteristic for the coordination of the iminolate form of the ligand to the dioxo molybdenum(VI) moiety. The Mo=O stretching modes occur as a pair of sharp strong peaks in the 946 –908 cm^{-1} range,[45,131,142–144], the higher frequency band originating from the antisymmetric while the lower one from the symmetric stretching mode, thus confirming the formation of mononuclear molybdenum(VI) complexes.

Table 5.2: Characteristics IR bands [cm^{-1}] for the complexes.

Formula	Complex	ν(C=N–N=C)	ν(MoO_2)
[MoO_2(salhyBocser)]	**31**	1617	944, 911
[MoO_2(salhyBoctrp)]·Et_2O	**32**	1615	944, 910
[MoO_2(salhyBocphe)]	**33**	1618	942, 910
[MoO_2(BrsalhyBocphe)]	**34**	1621	946, 914
[MoO_2(MesalhyBocphe)]	**35**	1601	941, 908
[MoO_2(salhyBocala)(MeOH)]·2MeOH	**36**	1616	942, 912

The formation of the *cis*-dioxomolybdenum complexes has been also confirmed by ^{1}H– and ^{13}C–NMR. The ^{1}H–NMR spectra of all complexes are in agreement with the proposed formula, they confirm the dianionic coordination of the ligands by the loss of the signals for the OH and NH protons. The azomethine proton (–CH=N) is upfield shifted by

around 0.4 ppm, with respect to the corresponding free ligands. The aromatic protons, as well as the α-CH, β-CH_2, and hydroxy group of serine amino acid, appear in the expected region, with slight shifts in their positions. The ^{1}H–NMR spectra of complex **36** and the elemental analysis show 0.88 methanol molecule per formula unit, which does not agree with the crystal structure analysis. This can be explained due to the fact that the X-ray analysis were performed on fresh crystals from methanol solution, whereas for NMR and elemental analysis the sample was dried completely before analysis, which results in the loss methanol molecules of crystallization, only the coordinated methanol is retained.

A comparison between the ^{13}C–NMR patterns of the free ligands and the corresponding ^{13}C–NMR spectra of complexes proved the coordination mode of the ligands. The most indicative resonance is the down field shift at 156 ppm of the imine carbon atom (*C*H=N), that resonate around 140 – 147 ppm, respectively in the free ligands. The presence of ether molecule in complex **32** is confirmed by the resonances of the CH_3 protons at 1.09 ppm, of the CH_2 protons at 3.48 ppm, and the ^{13}C resonances at 15.12 and 64.88 ppm for the CH_3 and CH_2 carbons respectively. Whereas the presence of the coordinated methanol in complex **36** is confirmed by the specific resonances of the CH_3 protons at 3.15 – 3.18 ppm and 4.06 ppm for the OH proton with the ^{13}C resonance at 42.6 ppm.

5.3 Oxidation of sulfides catalyzed by dioxomolybdenum complexes with Boc-amino acid functionalized ligands

Complexes were examined as catalysts in the oxidation reaction of methyl phenyl sulfide using hydrogen peroxide as oxidant. Details about the conditions applied are given in the experimental section. Results are shown in Table 5.3. Despite having different amino acid residues, complexes with Boc-α-amino acid residues show a similar catalytic activity. There is a strong decrease in activity on going from α to β-amino acids. Accordingly, the lowest activity is found for catalyst **32**, after 3 hours of the reaction time 82% yield can

Table 5.3: Catalyzed asymmetric oxidation of methyl phenyl sulfide using various complexes

Formula	Complex	Time (h)	Yield[a] (%)	ee [b] (%)	Configuration[c]
$[MoO_2(salhyBocser)]$	**31**	1	58	1.62	S
$[MoO_2(salhyBocser)]$	**31**	3	90	0.22	S
$[MoO_2(salhyBoctrp)]\cdot Et_2O$	**32**	1	45	n.d[d]	n.d
$[MoO_2(salhyBoctrp)]\cdot Et_2O$	**32**	3	82	n.d	n.d
$[MoO_2(BrsalhyBocPhe)]$	**34**	1	40	n.d	n.d
$[MoO_2(BrsalhyBocPhe)]$	**34**	3	91	n.d	n.d
$[MoO_2(MesalhyBocPhe)]$	**35**	1	55	3.02	S
$[MoO_2(MesalhyBocPhe)]$	**35**	3	98	1.97	S
$[MoO_2(salhyBocala)]$	**36**	1	99	0.12	S

All reactions were carried out at 0 °C with vanadium complexes loading to 1 mol-% and (1.2 equivalents) of hydrogen peroxide (8.24 M), in a mixture CH_2Cl_2/CH_3OH 7:3. [a] isolated yield determined by ^{1}H–NMR (400 MHz) using 1,3,5-trimethoxybenzene as internal standard. [b] Determined by HPLC using a (S,S)-WHELK-01 chiral column (25 cm × 4.6 mm). The column was eluted with hexane:2-propanol (90:10), at a flow rate of 2.0 mL/min. [c] Absolute configuration of the major product was determined to be S, by comparison of the chromatogram in HPLC with the authentic sample. [d] n.d. not determined.

be obtained, while 99% were reached after 1 hour, when the catalyst **36** was used (see Figure 5.3).

The haloperoxidase activity of the *cis*-dioxomolybdenum complexes has been performed following the procedure described for vanadium complexes in chapters 2 and 3. Unfortunately no catalytic activity of the molybdenum complexes has been found towards the peroxidative bromination of 1,3,5-trimethoxybenzene/monochlorodimedone,

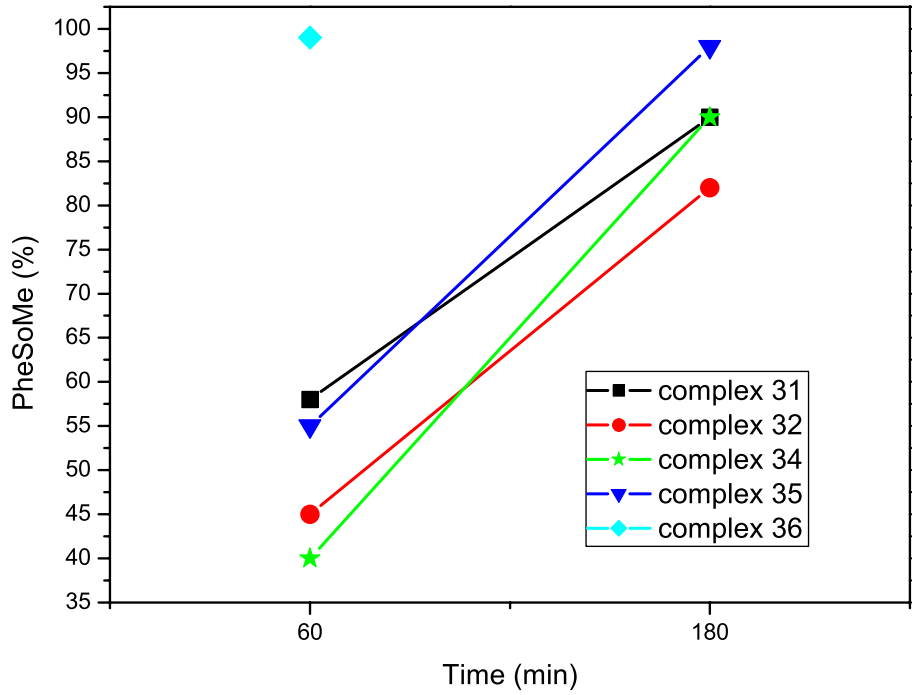

Figure 5.3: Oxidation of methyl phenyl sulfide catalyzed by molybdenum complexes with Boc-amino acid ligands.

although the ligand system is capable to coordinate molybdenum in a similar manner with vanadium complexes. This observation is in agreement with the results reported for vanadium haloperoxidase enzyme where the molybdate bonded enzyme was reported as inactive.[18] Compared to the inorganic molybdate and vanadate, were the molybdate proved to be an efficient catalyst of the haloperoxidase reaction, the replacement of vanadate with molybdate in this case did not afford the same positive effect.

5.4 Conclusions

In this chapter the synthesis of a series of new *cis*-dioxomolybdenum complexes is described, based on the tridentate Schiff base ligands derived from salicylaldehyde itself or one of its ring substituted derivative, and Boc-amino acid hydrazides. Boc-α-serine, tryptophan, phenylalanine and Boc-β-alanine were used as amino acids. The catalysts were tested on the ability to catalyze the oxidative bromination of TMB/MCD by hydrogen

peroxide, but they are not suitable for such catalytic reaction, they show no catalytic activity, contrary to the corresponding *cis*-dioxovanadium(V) complexes described in chapters 2 and 3. The complexes were also examined as catalyst in sulfoxidation reaction of sulfides to corresponding sulfoxides and the results were compared. All types of catalysts showed high activity. The best results were obtained using *cis*-dioxomolybdenum complex **31** with Boc-β-alanine residue ligand. It appeared to be the most active catalyst, which accomplished 99% conversion after one hour of reaction.

5.5 Experimental part

5.5.1 $[MoO_2(salhyBocser)]$ (31)

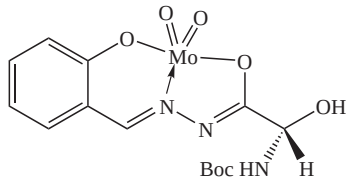

To a solution of the ligand HsalhyBocser (0.17 g, 0.52 mmol) in methanol (20 mL) was added $MoO_2(acac)_2$ (0.17 g, 0.52 mmol). The reaction mixture was heated at reflux for 35 minutes yielding a clear yellow solution. The hot solution was cooled down to room temperature and the solvent removed slowly at room temperature to obtain a yellow solid, which was dried in air.

Total yield: 0.20 g (0.42 mmol, 80.7%).

Elemental analysis for $C_{16}H_{23}MoN_3O_8$ (481.31 g/mol): calculated C: 39.93%, H: 4.82%, N: 8.73%; found C: 39.60%, H: 4.95%, N: 8.31%.

^{1}**H-NMR** (400 MHz, DMSO-d_6): $\delta =$ 1.39 (s, 9H, C(C**H**$_3$)$_3$), 3.33 (s, **H**$_2$O), 3.56 – 3.62 (m, 2H, β-C**H**$_2$), 4.31 (s, 1H, α-C**H**), 4.88 (s, 1H, O**H**–Amino acid), 6.88 – 6.94 (m, 2H, Ph), N**H**Boc), 7.00 – 7.07 (m, 1H, Ph), 7.45 – 7.54 (m, 1H, Ph), 7.65 – 7.70 (m, 1H, Ph), 8.78 (s, 1H, C**H**=N) ppm.

^{13}**C-NMR** (100 MHz, DMSO-d_6): $\delta =$ 31.42 (C(**C**H$_3$)$_3$), 54.18 (α-**C**H), 62.00 (β-**C**H$_2$), 78.30 (O**C**(CH$_3$)$_3$), 118.61 (Ph), 120.21 (Ph), 121.54 (Ph), 134.32 (Ph), 134.92 (Ph),

155.27 (Ph), 156.05 (**C**=N), 159.53 (**C**=OBoc), 173.30 (O–**C**NNC) ppm.

Selected IR data (cm^{-1}): $\tilde{\nu}$ = 3365 (s, br; O–H), 1617 (s, br; C=N–N=C), 944 (s, MoO_2), 911 (s, MoO_2).

5.5.2 $[MoO_2(salhyBoctrp)]\cdot Et_2O$ (32)

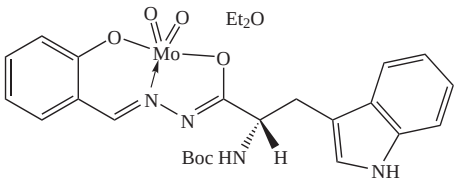

To a solution of Schiff base ligand HsalhyBoctrp (158 mg, 0.374 mmol) in 50 mL methanol was added $MoO_2(acac)_2$ (119.7 mg, 0.374 mmol). The resulting orange reaction mixture was heated under reflux for 4 hours when a clear orange solution was obtained. The hot solution was filtrated off, reduced the volume to $\sim$ 5 mL and allowed to cool down to room temperature. Diethyl ether was added which results in the precipitation of the yellow-orange solid, which was filtrated and air dried.

Total yield: 0.16 g (0.257 mmol, 68.7%)

Elemental analysis for $C_{27}H_{34}MoN_4O_7$ (622.52 g/mol): calculated C: 52.09%, H: 5.51%, N: 9.00%; found C: 53.07%, H: 5.48%, N: 9.24%.

^{1}H-NMR (400 MHz, DMSO-d_6): δ = 1.09 (t, ^{3}J= 7 Hz, 3H, Et_2O), 1.31 (s, 9H, C(C**H**$_3$)$_3$), 3.02 (m, 2H, β-C**H**$_2$), 3.48 (q, ^{3}J = 7 Hz, 2H, Et_2O), 4.45 (m, 1H, α-C**H**), 6.90 (s, 1H, N**H**Boc), 6.94 – 7.06 (m, 5H, Ph), 7.14 (m, 1H, Ph), 7.31 (m, 1H, Ph), 7.50 (m, 2H, Ph), 7.65 (m, 1H, Ph), 8.40 (s, 1H, C**H**=N), 10.80 (s, 1H, N**H**) ppm.

^{13}C-NMR (50 MHz, DMSO-d_6): δ = 15.12 (Et_2O), 28.00 (C(**C**H$_3$)$_3$), 30.65 (β-**C**H$_2$), 52.31 (α-**C**H), 64.88 (Et_2O), 78.00 O(**C**(CH$_3$)$_3$), 110.00 (Ph), 111.33 (Ph), 116.31 (Ph), 118.09 (Ph), 118.33 (Ph), 118.50 (Ph), 120.08 (Ph), 120.85 (Ph), 121.41 (Ph), 123.58 (Ph), 127.54 (Ph), 134.17 (Ph), 134.81 (Ph), 136.02 (Ph), 155.04 (Ph), 156.06 (**C**H=N), 159.36 (**C**=OBoc), 174.34 (O–**C**NNC) ppm.

Selected IR data (cm^{-1}): ν = 3412 (br, NH), 1695 (C=O-Boc), 1615 (C=N–N=C), 944 (s, MoO_2), 910 (s, MoO_2).

MS (FAB$^+$, nba): m/z = 548 (8% $[M]^+$).

5.5.3 [MoO_2(salhyBocphe)] (33)

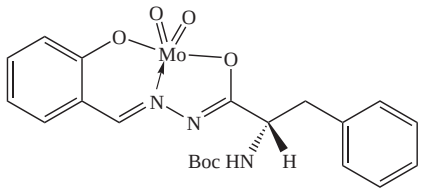

To a solution of Schiff base ligand HsalhyBocphe (0.77 g, 2.00 mmol) in 10 mL methanol was added $MoO_2(acac)_2$ (0.66 g, 2.00 mmol). The resulting orange reaction mixture was stirred at room temperature for 15 hours when a clear orange solution was obtained. The volume of this dark orange solution was then reduced to 5 ml. On standing at room temperature, the solution deposited orange precipitate, which was collected by rapid filtration, washed well with cold methanol and dried in vacuo. m.p 167 °C

Total yield: 0.61 g (1.2 mmol, 60%).

^{1}**H-NMR** (200 MHz, DMSO-d_6): $\delta =$ 1.30 (s, 9H, C(C**H**$_3$)$_3$), 2.82 – 3.02 (m, 2H, β-C**H**$_2$), 4.44 (m, 1H, α-C**H**), 6.83 – 7.08 (m, 2H, Ph), 7.17 – 7.30 (m, 6H, Ph, N**H**Boc), 7.50 (m, 1H, Ph), 7.70 (m, 1H, Ph), 8.78 (1H, s, C**H**=N) ppm.

^{13}**C-NMR** (50 MHz, DMSO-d_6): $\delta =$ 28.16 (C(**C**H$_3$)$_3$), 38.25 (β-**C**H$_2$), 52.92 (α-**C**H), 78.04 (O**C**(CH$_3$)$_3$), 118.51 (Ph), 120.05 (Ph), 121.44 (Ph), 126.30 (Ph), 128.07 (Ph), 129.20 (Ph), 134.23 (Ph), 134.87 (Ph), 137.78 (Ph), 155.03 (**C**H=N), 156.14 (Ph), 159.34 (**C**=OBoc), 173.99 (O–**C**NNC) ppm.

Selected IR data (cm^{-1}): $\nu = 3340$ (br, NH), 1662 (C=O-Boc), 1618(C=N–N=C), 942 (s, MoO_2), 910 (s, MoO_2).

5.5.4 [MoO_2(BrsalhyBocphe)] (34)

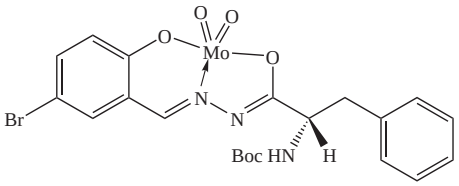

To a solution of Schiff base ligand BrsalhyBocphe (0.51 g, 1.11 mmol) in 30 mL methanol was added $MoO_2(acac)_2$ (0.36 g, 1.11 mmol). The resulting orange reaction mixture was heated under reflux for 21 hours when a clear orange solution was obtained. The hot solution was filtrated, reduced the volume to $\sim$ 10 mL and allowed to cool down to room temperature. An orange solid was precipitated, which was filtrated, dried and recrystallized from a CH_2Cl_2/hexane mixture, to obtain the product as a yellow solid.

Total yield: 0.18 g (0.31 mmol, 28%).

^{1}**H-NMR** (400 MHz, DMSO-d_6): $\delta =$ 1.38 (s, 9H, C(C**H**$_3$)$_3$), 2.86 (m, 2H, β-C**H**$_2$), 4.43 (m, 1H, α-C**H**), 6.88 (m, 1H, Ph), 7.23 (m, 6H, Ph + N**H**Boc), 7.48 (m, 1H, Ph), 7.93 (m, 1H, Ph), 8.75 (s, 1H, C**H**=N) ppm.

^{13}**C-NMR** (100 MHz, DMSO-d_6): $\delta =$ 28.13 (C(**C**H$_3$)$_3$), 37.61 (β-**C**H$_2$), 52.94 (α-**C**H), 78.05 (O**C**(CH$_3$)$_3$), 112.07 (Ph), 1210.83 (Ph), 121.99 (Ph), 126.27 (Ph), 129.00 (Ph), 129.59 (Ph), 135.73 (Ph), 136.87 (Ph), 137.96 (Ph), 154.98 (**C**H=N), 158.50 (Ph), 163.51 (**C**=OBoc), 174.61 (O–**C**NNC) ppm.

Selected IR data (cm^{-1}): ν = 3340 (br, NH), 1621 (s, C=N–N=C), 946 (s, MoO_2), 914 (s, MoO_2).

EI-MS (negative ion mode,
in methanol): m/z = 592 ([MoO_2(BsalhyBocphe)] – H^+).

5.5.5 [MoO_2(MesalhyBocphe)] (35)

The Schiff base ligand MesalhyBocphe (0.61 g, 1.5 mmol) was dissolved in methanol (30 mL) by heating slowly on a water bath and $MoO_2(acac)_2$ (0.5 g, 1.5 mmol) was

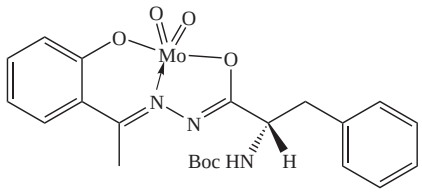

added to the resultant solution and the mixture stirred at room temperature for 4 hours and then filtrated. Slow evaporation of the orange filtrate over 3 days produced dark orange precipitate, which was filtrated, and dried in air. m.p 86 °C

Total yield: 0.5 g (0.96 mmol, 64%).

Elemental analysis for $C_{22}H_{25}MoN_3O_6$ (523.39 g/mol): calculated C: 50.49 %, H: 4.81 %, N: 8.03 %; found C: 50.69 %, H: 5.50 %, N: 7.78 %.

^{1}**H-NMR** (400 MHz, DMSO-d_6): $\delta =$ 1.32 (s, 9H, C(C**H**$_3$)$_3$), 2.71 (3H, s, C**H**$_3$), 2.84 – 3.06 (m, 2H, β-C**H**$_2$), 4.5 (m, 1H, α-C**H**), 6.90 – 7.08 (m, 2H, Ph), 7.17 – 7.30 (5H, m, Ph; 1H, N**H**Boc), 7.55 (1H, m, Ph) ppm.

^{13}**C-NMR** (50 MHz, DMSO-d_6): $\delta =$ 16.56 (**C**H$_3$), 28.18 (C(**C**H$_3$)$_3$), 38.25 (β-**C**H$_2$), 53.42 (α-**C**H), 78.00 (O**C**(CH$_3$)$_3$), 118.58 (Ph), 121.52 (Ph), 122.65 (Ph), 126.23 (Ph), 129.18 (Ph), 130.86 (Ph), 131.39 (Ph), 136.23 (Ph), 138.04 (Ph), 155.37 (N=**C**(CH$_3$)), 159.96 (Ph), 164.06 (**C**=OBoc), 173.54 (O–**C**NNC) ppm.

Selected IR data (cm^{-1}): ν = 3330 (br, NH), 1601 (s, C=N–N=C), 941 (s, MoO_2), 908 (s, MoO_2).

MS (FAB$^+$, nba): m/z = 523 (40% [M]$^+$).

5.5.6 [MoO_2(salhyBocala)(MeOH)]·2MeOH (36)

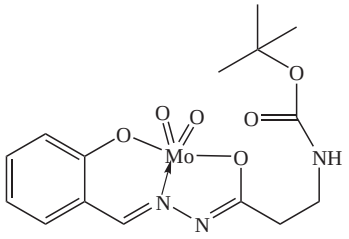

To a solution of HsalhyBocala (0.16 g, 0.52 mmol) in 20 mL methanol was added

$MoO_2(acac)_2$ (0.17 g, 0.52 mmol). The reaction mixture changed color to orange. The resulting mixture was heated at 65°C with continuous stirring. In 30 minutes all molybdate was reacted. The mixture was heated for an additional 40 minutes, then the volume of the solution was reduced to about 5 mL, and left at -28°C. Yellow colored single crystals suitable for X-ray studies formed within two weeks. m.p 130–135 °C, Elemental analysis and NMR show 0.88 MeOH

Total yield: 65 mg, (0.123 mmol, 76.9%).

Elemental analysis for $C_{18}H_{31}MoN_3O_9$ (529.39 g/mol): calculated C: 40.84%, H: 5.90%, N: 7.94%; found C: 40.80%, H: 4.94%, N: 8.82%.

^{1}**H-NMR** (400 MHz, DMSO-d_6): $\delta =$ 1.37 (s, 9H, C(C**H**$_3$)$_3$), 2.37 (m, 2H, α-C**H**$_2$), 3.18 (m, 2H, β-C**H**$_2$ overloaded with MeOH), 4.06 (s, 1H, MeO**H**), 6.79 (br, 1H, N**H**–Boc), 6.88 (m, 1H, Ph), 7.00 (m, 1H, Ph), 7.49 (m, 1H, Ph), 7.68 (m, 1H, Ph), 8.30 (s, 1H, C**H**=N) ppm.

^{13}**C-NMR** (100 MHz, DMSO-d_6): $\delta =$ 28.23 (C(**C**H$_3$)$_3$), 32.70 (β-**C**H$_2$), 38.65 (α-**C**H$_2$), 42.45 (MeOH), 77.78 (O**C**(CH$_3$)$_3$), 118.48 (Ph), 120.02 (Ph), 121.41 (Ph), 134.16 (Ph), 134.74 (Ph), 155.40 (**C**H=N), 155.42 (Ph), 159.29 (**C**=OBoc), 173.64 (O–**C**NNC) ppm.

Selected IR data (cm^{-1}): $\nu = 3362$ (s, br; N–H), 1674 (C=O-Boc), 1616 (s, C=N–N=C), 942 (s, MoO_2), 912 (s, MoO_2).

5.5.7 Catalytic oxidation of methyl phenyl sulfide:

Molybdenum complex (0.02 mmol) was dissolved at room temperature in a mixture of CH_2Cl_2/CH_3OH 7:3 (20 mL) and 1,3,5-trimethoxybenzene (0.34 g, 2.0 mmol) as internal standard was added followed by (0.24 ml, 2.0 mmol) phenyl methyl sulfide. The resulting solution was cooled down on an ice-bath and H_2O_2 8.24 M (1.2 equiv., 0.31 mL, 2.5 mmol) was added dropwise. The reaction solution was warmed up to room temperature and stirred in a capped flask and monitored by thin-layer chromatography technique (Et_2O:*n*-hexane 9:1). After 1, and 3-hours reaction time, aliquots of the reaction solutions (2.0 mL) were quenched with ca. 5 mL of a stock solution of NaOH (0.1 M) and extracted with ethyl acetate (3×4 mL). The collected organic phases were removed completely to dryness and the residue was redissolved in deuterated chloroform (600 μL) and analyzed

by ^{1}H-NMR to determine the yield. From this solution was then taken 60 μL of chloroform, removed the solvent to dryness and the residue redissolved in 2 mL dichlormethane and the enantiomeric excess was determined by chiral HPLC as described in chapter 2.

Chapter 6

Molybdenum(VI) complexes with free L-α-amino acid residue ligands

The present chapter investigates the synthesis, spectral and structural characterization of *cis*-dioxomolybdenum(VI) complexes of the tridentate Schiff base ligands containing free amino acid residues. The oxidation catalysis are also reported. Although, many *cis*-dioxomolybdenum(VI) complexes have been synthesized and characterized previously, as far as we are aware no molybdenum complexes with amino acid hydrazide ligands have been reported.

The Schiff base ligands were prepared following the procedure described in Chapter 3. In order to prepare dioxomolybdenum(VI) complexes (**37** − **42**), the Schiff base ligands were allowed to react with $MoO_2(acac)_2$ in 1:1 molar proportion in methanol (Figure 6.1). The mixture was heated under reflux. This reaction leads to the formation of two types of products; the first one is the desired *cis*-dioxomolybdenum complex signed as **I** formed in high yield. The second product **II** was formed by condensation of the amino acid functionality with the acac (acetylacetonate) group of the $MoO_2(acac)_2$, in a low yield. All of them are dark yellow–orange crystalline solids. The complexes **I** are air sensitive and have a very good solubility in polar organic solvents like DMSO or methanol, whereas the complexes of type **II** are little soluble in these solvents. This makes possible the separation of the two products, by crystallization of **II** out of the methanolic solution. The decomposition of all types of complexes occurs slowly in solution and the color changes from yellow to green in the presence of moisture. Dioxomolybdenum(VI) complexes of type **I**

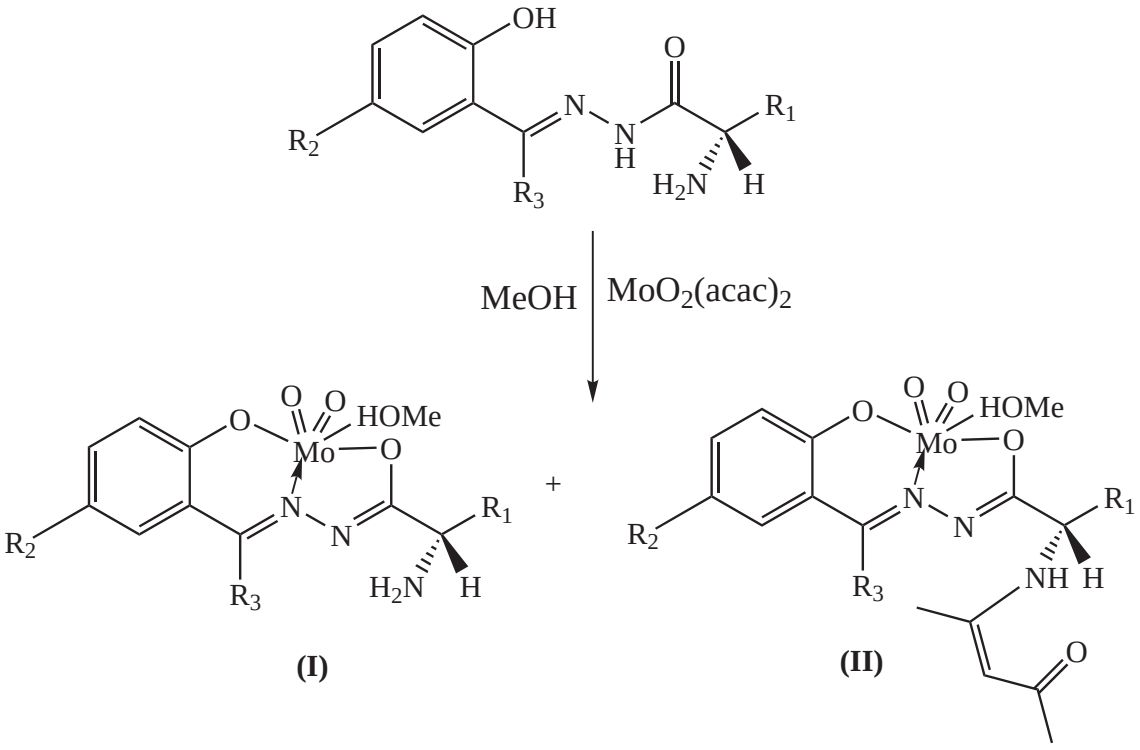

	R_1	R_2	R_3
37 (II)	$CH_2CH(CH_3)_2$	Br	H
38 (I)	CH_2Ph	H	Me
39 (II)	CH_2Ph	H	Me
40 (I)	CH_2Ph	Br	H
41 (I)	CH_2PhOH	Me	H
42 (II)	CH_2PhOH	Me	H

Figure 6.1: Schematic representation of the synthesis of *cis*-dioxomolybdenum complex with free amino acid functionalized ligands

could be more successfully obtained by the use of $NaMoO_4 \cdot 2H_2O$ instead of $MoO_2(acac)_2$.

6.1 Structural characterization

6.1.1 Mo-complex with leucine residue (37)

Yellow crystals of complex **37** suitable for X-Ray analysis were obtained by slow evaporation at room temperature of a methanol solution. The crystal structure is shown in Figure 6.2, and the selected bond distances and angles in Table 6.1. The molybdenum center

is coordinated with two oxo groups in *cis* position, the phenolate oxygen atom O3, the imine nitrogen atom N1, and amide oxygen atom O4 of the tridentate ligand. The sixth coordination site around Mo is occupied by a solvent (MeOH) molecule, thereby providing a distorted octahedral coordination environment around Mo in which the coordinated MeOH lies *trans* to oxo group O1.

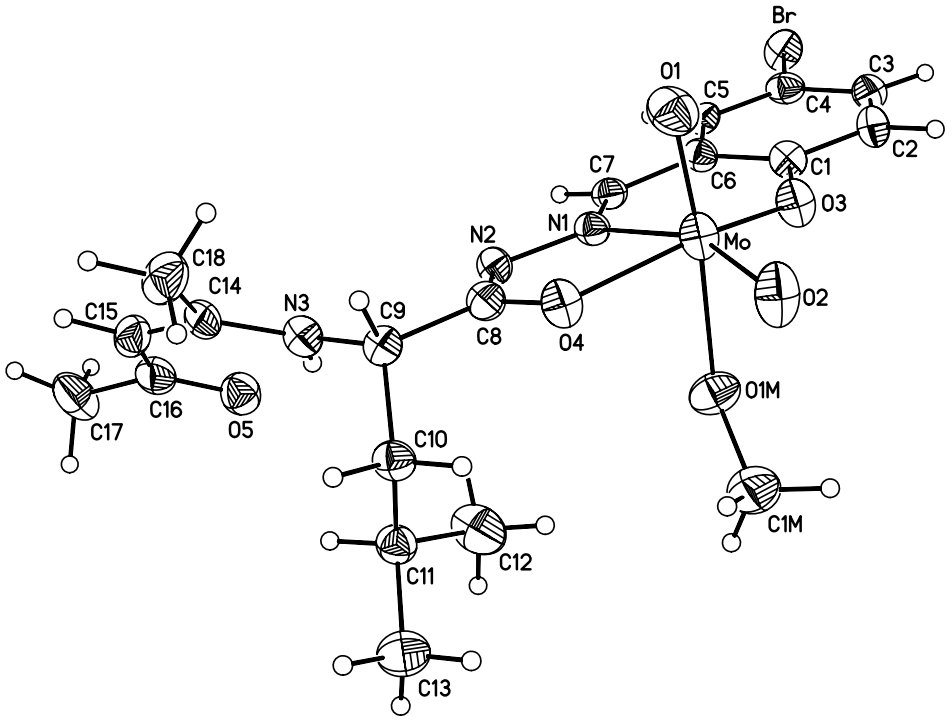

Figure 6.2: Molecular structure of [MoO_2(Brsalhyleuacac)(MeOH)] (**37**) (thermal ellipsoids are drawn at the 50% probability level)

The Mo=O bond distances [168.8(3) and 169.3(3) pm], and the average O=Mo=O bond angle are very common for *cis*-dioxomolybdenum(VI) complexes,[45,131,138,145,146] and also not significant different from those observed in $Mo^{VI}O_2$ complex with β-alanine residue ligand presented in chapter 5 [169.6(3)–169.8(2) pm, and 105.56 °]. The imine nitrogen and methanol oxygen atoms, which are *trans* to the terminal oxo-groups, are bound to Mo^{VI} ions at distance of 224.0(4) pm for nitrogen and 233.1(3) pm for oxygen, respectively. The *cis* angles around Mo ranges from 71.48(12) ° for N1–Mo–O4 to 105.86(16) ° for O1–Mo–O2, while the two *trans* angles vary from 170.04(14) ° for O1–Mo–O1M, to 149.81(13) ° for O3–Mo–O4. The C8–N2 bond distance is 128.0(5) pm, which is pretty

close to the usual C=N length.[147] The molybdenum atom is significantly displaced from the plane, formed by the ligand aromatic part, toward the apical oxygen atom O1 by 30.2 pm. The ring system and the hydrazide group lie in the mean plane. The leucine residue raises out of the mean plane, towards the apical oxo group O1 by an torsion angle (C9–C10–N3–C11) of 81.9 °, whereas the amino functionality of the leucine together with the acac group deviate by an torsion angle (C8–C9–N3–C14) of 145.2 °.

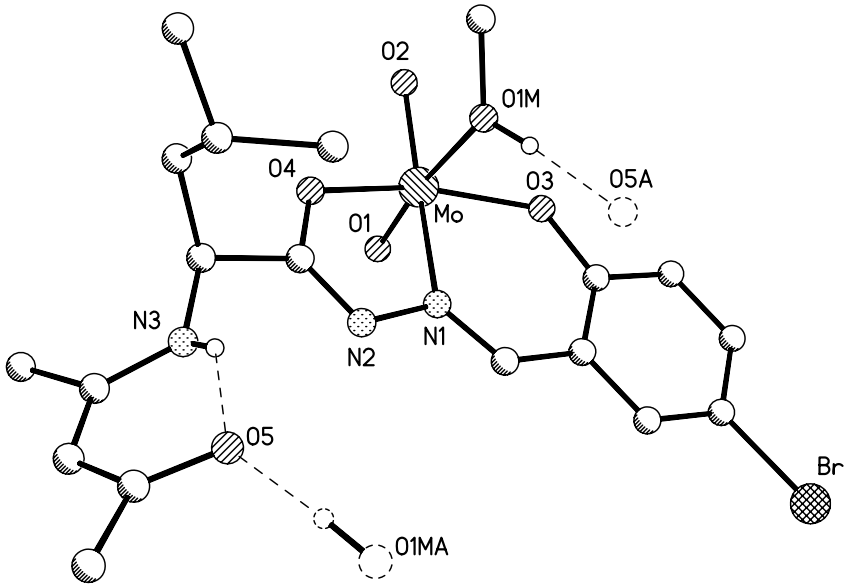

Figure 6.3: Representation of the hydrogen bonding interactions in crystals of complex $[MoO_2(Brsalhyleuacac)(MeOH)]$ (**37**) (broken lines represent hydrogen bonds); relevant distances (in pm): O5···O1MA 262.7, O5···N3 271.4 (symmetry transformations: A: – x, y, 1 – z).

The hydrogen bonding interactions in complex **37** were also observed with involvement of different donor patterns. The coordinated methanol molecule is in hydrogen bonding interaction with the oxygen atom O5 of the acac group of the neighboring molecule (O1M···O5A 262.7 pm). An intermolecular hydrogen bond interaction was found, which involved the nitrogen atom N3 of the leucine functionality, and the oxygen atom of the acac group O5 (N3···O5 271.4 pm).

6.1.2 Mo-complex with phenylalanine residue (39)

The molecular structures of complex **39** is shown in Figure 6.4, with the relevant bond distances and angles collected in Table 6.1. The coordination geometry around the Mo^{VI} atom is quite similar with the other studied Mo complexes. The Schiff base ligand is bonded to the *cis*-$Mo^{VI}O_2^{2+}$ ion in an xy-plane through the phenolate oxygen atom O3, the imine nitrogen atom N1, amide oxygen atom O4 of the tridentate ligand, and the two oxo groups O1 and O2.

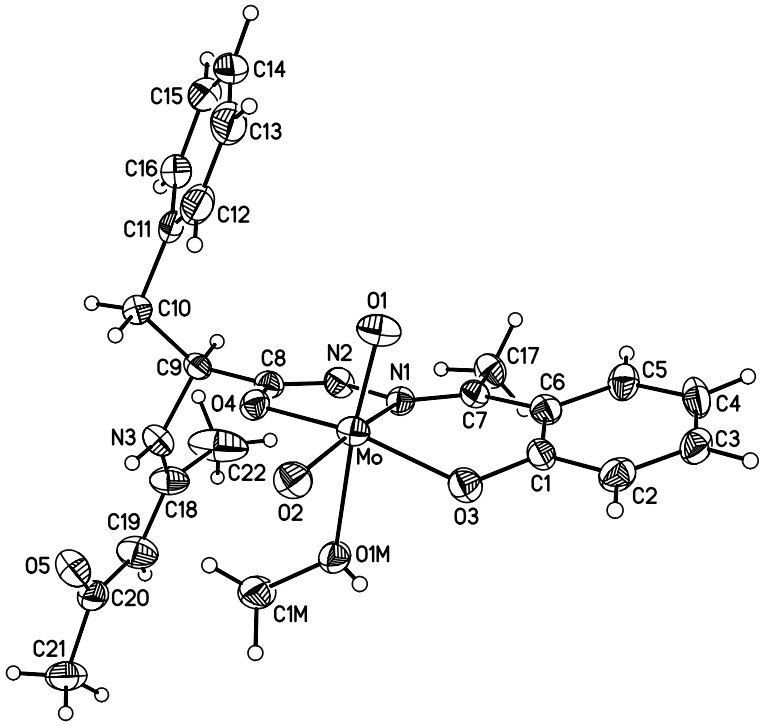

Figure 6.4: Molecular structure of $[MoO_2(Mesalhypheacac)(MeOH)]\cdot 2MeOH$ (**39**) (thermal ellipsoids are drawn at the 50% probability level)

A methanol molecule completes the distorted octahedral coordination sphere and is *trans* to the oxo group O1. The O=Mo=O angle of 105.74(18) ° and the Mo=O distances (168.7(2)-170.2(3) pm) are typical for *cis*-dioxomolybdenum complexes.[45, 131, 138, 145, 146] The imine nitrogen and methanol oxygen atoms, which are *trans* to the terminal oxo groups, bond to Mo^{VI} ions with distances of 225.7(3) pm for nitrogen and 233.3(3) for oxygen, respectively. On the whole the structure of complex **39** is very similar to those of dioxomolybdenum(VI) complexes described previously.

Complex crystallizes in the monoclinic space group $C2$, with two additional methanol molecules as solvent of crystallization. An intermolecular hydrogen bonding interaction is established between two uncoordinated methanol molecules (O2M···O3M 270.2 pm), from which one is hydrogen bonded to the methanol molecule of the neighboring molecule O1MB (O2M···O1MB 266.7 pm), and the other to the oxygen atom of the acac group of another neighboring molecule O5C (O3M···O5C 162.2 pm) (Figure 6.5).

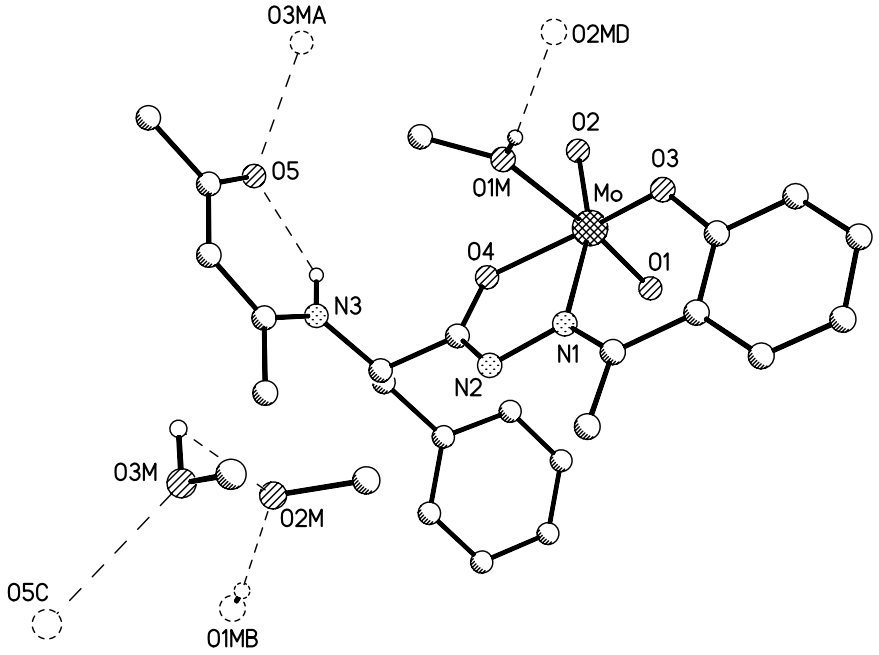

Figure 6.5: Representation of the hydrogen bonding interactions in crystals of complex $[MoO_2(Mesalhypheacac)(MeOH)]\cdot 2MeOH$ (**39**) (broken lines represent hydrogen bonds); relevant distances (in pm): N3···O5 266.0, O1M···O2MD 266.7, O2M···O3M 270.2, O5···O3MA 262.2; (symmetry transformations: A: 1 – x, 1 + y, 1 – z; B: x, – 1 + y, z; C: 1 – x, – 1 + y, 1 – z; D: x, 1 + y, z).

An intermolecular hydrogen bond interaction is established between the nitrogen atom N3 of the phenylalanine functionality, and the oxygen atom of the acac group O5 (N3···O5 266.0 pm). The hydrogen bonding interaction established in the crystal packing of *cis*-dioxomolybdenum complex **39** results in the formation of layered polymeric structure (Figure 6.6).

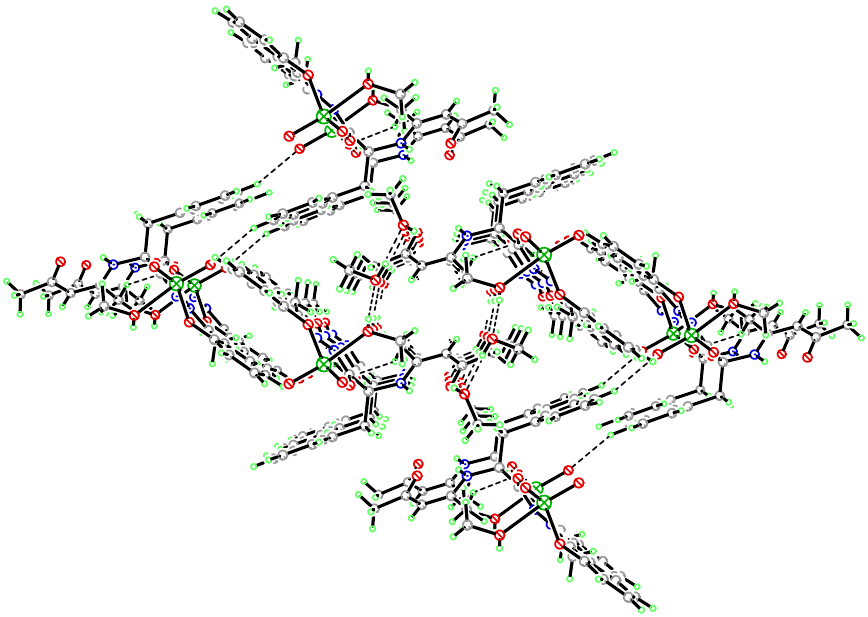

Figure 6.6: Representation of the two-dimensional hydrogen bonding interactions in crystals of complex $[MoO_2(Mesalhypheacac)(MeOH)]\cdot 2MeOH$ (**39**), as viewed along the [010] direction; broken lines represent hydrogen bonding interactions.

6.1.3 Mo-complex with tyrosine residue (42)

Good quality crystals of **42** were obtained from methanol solution. The X-ray crystallographic study revealed that the Mo^{VI} center is present in a distorted octahedral donor environment consisting of *cis*-oxo atoms O1 and O2, *trans*-phenolate and iminolate oxygen atoms O3 and O4, which are *cis* to O1 and O2, and an imine nitrogen atom N1 (Figure 6.7). The sixth weaker coordination comes from the solvent molecule methanol. The atoms O2, N1, O3 and O4 show a high degree of planarity from the equatorial base, the metal ion is displaced by approximately 34 pm towards the apical oxo group O1 from this plane and the O1M is *trans* to O1. The Mo=O1 and Mo=O2 bonds of MoO_2 group are equal 170.3(3) pm, they are somewhat longer than those in $Mo^{VI}O_2$ complexes with other amino acid residue ligands described previously, but still within reported ranges.[45, 131, 138, 145, 146, 148] The Mo-N1 and more so the Mo-O1M bonds are the longest in the coordination polyhedron (see Table 6.1). The longest bond from the methanol coordination indicates that the alcohol molecule is weakly bonded to the $MoO_2{}^{2+}$-core.

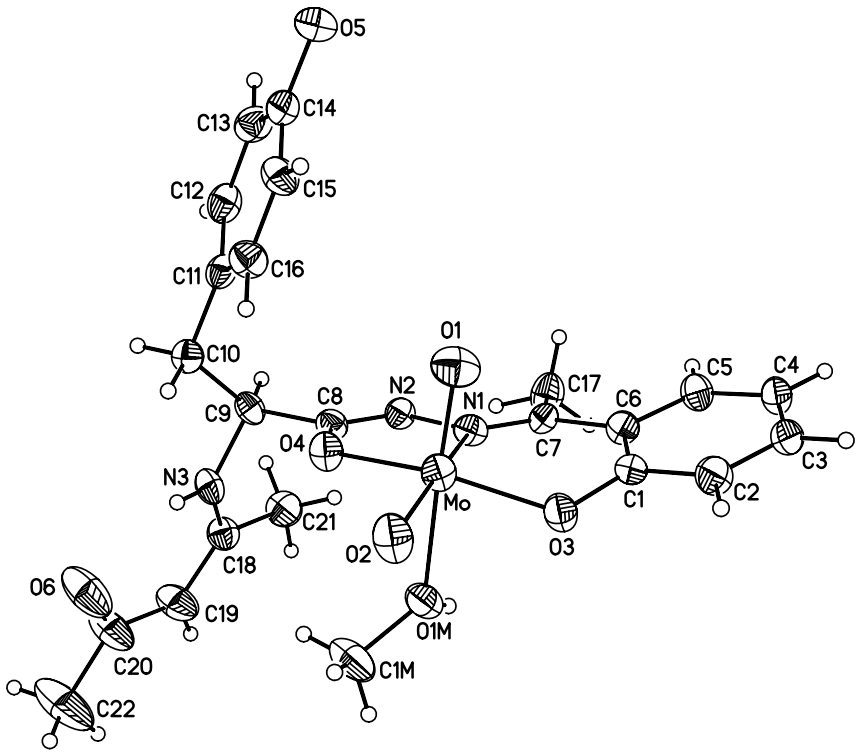

Figure 6.7: Molecular structure of $[MoO_2(Mesalhytyracac)(MeOH)]\cdot 2MeOH\cdot Et_2O$ (**42**) (thermal ellipsoids are drawn at the 50% probability level)

The O=Mo=O angle of 106.10(15) ° is very similar to those of dioxomolybdenum(VI) complexes described previously. Complex crystallizes in the orthorhombic space group $P2_12_12_1$, with two additional methanol molecules and one diethylether molecule as solvent of crystallization, which are involved in hydrogen bonding interaction. An intermolecular hydrogen bonding is established between the coordinated methanol molecule O1M and the second methanol molecule O2M (O1M···O2M 265.3 pm), which is further hydrogen bonded to the oxygen atom of the ether molecule from the neighboring molecule (O2M···O1EC 277.3 pm). Another intermolecular hydrogen bonding is observed, which involves the nitrogen atom of the tyrosine functionality N3 and the oxygen atom of the acac group (N3···O6 263.6). The same situation was found in two other *cis*-dioxomolybdenum complexes with leucine and phenylalanine residue ligands, described previously. Further the third methanol molecule is hydrogen bonded to the oxygen atom of the acac group of one neighboring molecule (O3M···O6B 265.0 pm).

Thy hydrogen bonding interaction established in the crystal packing of *cis*-dioxomolybden-

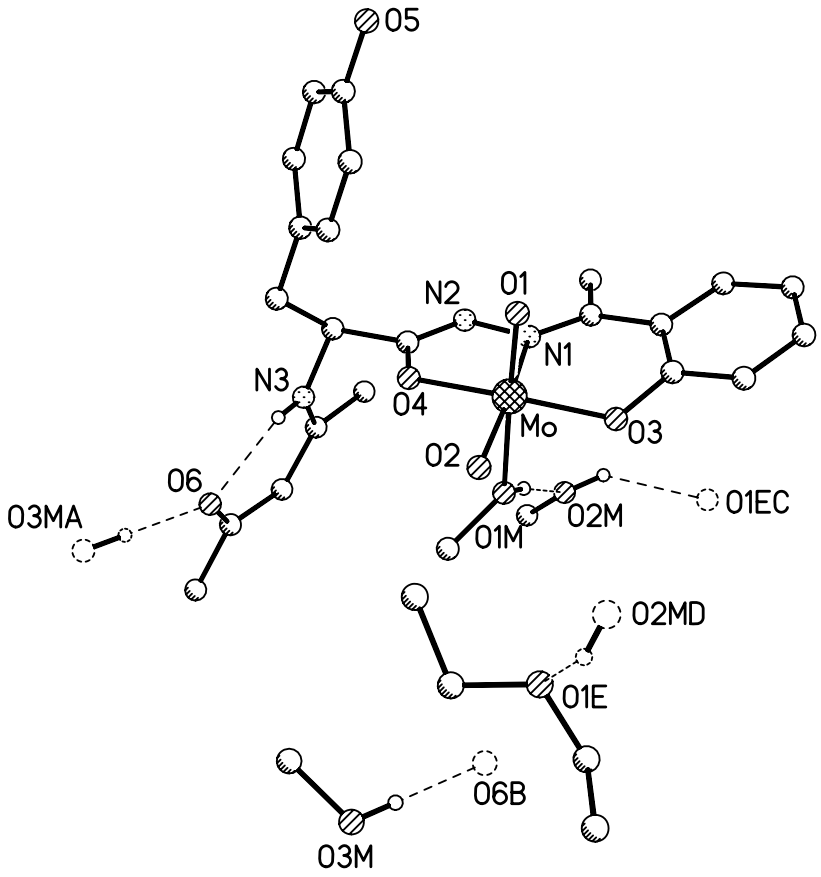

Figure 6.8: Representation of the hydrogen bonding interactions in crystals of complex $[MoO_2(Mesalhytyracac)(MeOH)]\cdot 2MeOH\cdot Et_2O$ (**42**) (broken lines represent hydrogen bonds); relevant distances (in pm): N3···O6 263.6, O1M···O2M 265.3, O6···O3MA 265.0, O1E···O2MD 277.3; (symmetry transformations: A: 1 + x, y, z; B: – 1 + x, y, z; C: 1 – x, $-\frac{1}{2}$ + y, $\frac{1}{2}$ – z; D: 1 – x, $-\frac{1}{2}$ + y, $\frac{1}{2}$ – z).

um complex **42** results in the formation of layered polymeric structure (Figure 6.9).

Moreover, at first sight the molecular structure of $[MoO_2(Mesalhytyracac)(MeOH)]\cdot 2MeOH\cdot Et_2O$ (**42**) shows high similarity with that observed for $[MoO_2(Mesalhypheacac)(MeOH)]\cdot 2MeOH$ (**39**). The overlay of the covalent parts of the two structures shown in Figure 6.10 confirms this. The aromatic ring of the amino acid residue deviates from the mean plane by a torsion angle (C9–C10–C11–C12) of 80.0° in complex **39**, whereas this deviation in complex **42** is 80.6° which shows no significant differences. Nevertheless, a slight different orientation of the acac group has been observed in complex **39** by comparison to the complex **42**. This is illustrated by the torsion angle C18–N3–C9–C8

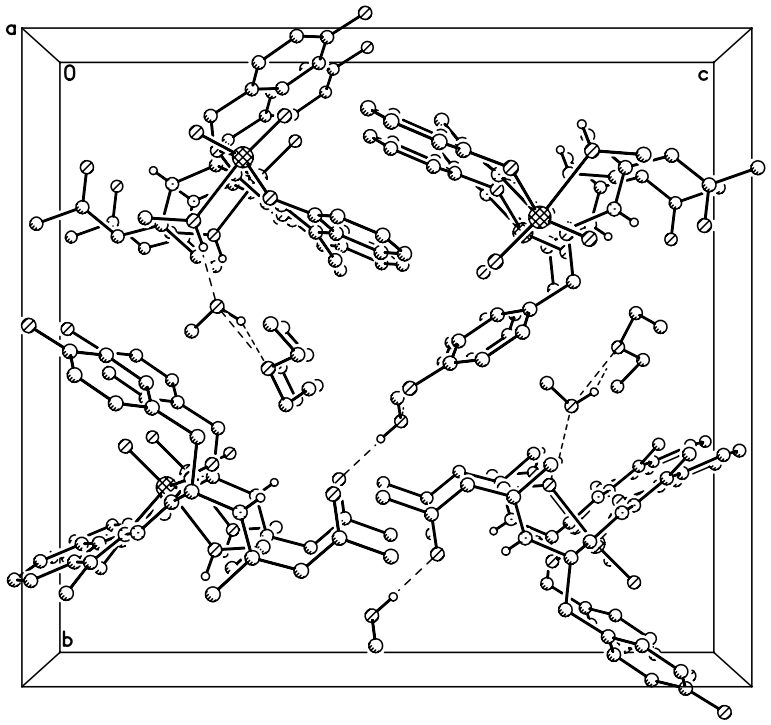

Figure 6.9: Representation of the two-dimensional hydrogen bonding interactions in crystals of complex $[MoO_2(Mesalhytyracac)(MeOH)]\cdot 2MeOH\cdot Et_2O$ (**42**), as viewed along the [100] direction; broken lines represent hydrogen bonding interactions.

which has a value of 96.6° in complex **39** with phenylalanine residue, whereas in complex **42** the acac group is orientated with the torsion angle of 84.5°.

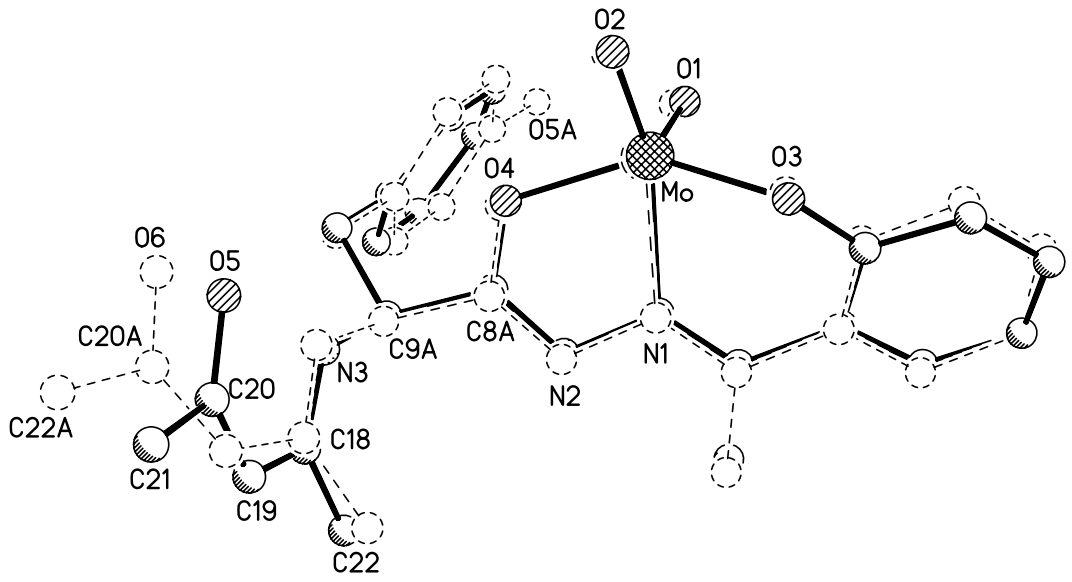

Figure 6.10: Overlay of the molecular structures of complex **39** with phenylalanine side chain (thick lines) and complex **42** with tyrosine side chain (atom numbering extension A, broken lines).

Table 6.1: Selected bond lengths (pm) and angles (°) for complexes **37**, **39**, and **42**.

	37	**39**	**42**
Bond lengths			
Mo–O1	168.8(3)	168.7(2)	170.3(3)
Mo–O2	169.3(3)	170.2(3)	170.3(3)
Mo–O3	193.5(3)	192.1(3)	192.0(3)
Mo–O4	199.9(4)	200.1(3)	200.3(2)
Mo–O1M	233.1(3)	233.3(3)	233.1(2)
Mo–N1	224.0(4)	225.7(3)	225.0(3)
O4–C8	131.0(6)	132.7(5)	132.8(4)
N1–N2	141.6(5)	142.3(4)	141.6(4)
N1–C7	128.9(5)	130.5(5)	131.4(5)
N2–C8	128.0(5)	129.5(5)	128.9(5)
Bond angles			
O1–Mo–O2	105.86(16)	105.74(18)	106.10(15)
O1–Mo–O3	98.72(15)	99.66(13)	99.37(14)
O1–Mo–O4	97.40(15)	100.64(16)	99.34(14)
O1–Mo–O1M	170.04(14)	168.64(16)	171.1(2)
O2–Mo–O3	103.78(15)	104.53(14)	103.16(13)
O2–Mo–O4	96.08(14)	95.61(11)	96.03(12)
O2–Mo–O1M	84.05(15)	85.61(16)	82.73(1)
O3–Mo–O4	149.81(13)	146.18(12)	148.20(12)
O1–Mo–N1	94.38(15)	91.50(16)	93.22(13)
O2–Mo–N1	157.62(15)	160.65(15)	159.14(13)
O3–Mo–N1	81.97(13)	80.58(11)	80.83(11)
O3–Mo–O1M	79.53(13)	76.64(11)	78.85(1)
O4–Mo–N1	71.48(12)	72.15(12)	72.65(11)
O4–Mo–O1M	80.19(12)	78.16(14)	78.71(1)

6.2 Spectroscopic Characterization

The infrared spectra of complexes **37** to **42** (see Table 6.2) exhibit, beside typical ligand vibrations, two strong absorptions at 903–914 and 922–941 cm^{-1} which are attributed to the symmetric and asymmetric ν(Mo=O) vibrations of the *cis*- MoO_2^{2+} groups, respectively, thus confirming the formation of mononuclear molybdenum(VI) complexes in chapter 5. This stretching vibrations are similar with those found for the previous described *cis*-dioxomolybdenum complexes with amino acid residue ligands. Coordination of the imine group through nitrogen is seen in the ν(C=N–N=C) at 1598-1604 cm^{-1}, which is slightly lower than in uncoordinated bases. Characteristic strong bands at 1654–1684 cm^{-1} due to the carbonyl moiety ν(C=O) stretching vibrations of the ligands[117,140,141] are not observed any more in the spectra of the complexes. The coordination of the ligands through the phenolate function is confirmed for all complexes by the disappearance of the ν(O–H) vibration in comparison to the spectra of free ligands. The ^{1}H–NMR spectra of the complexes are indicative of binding of the ligands through the deprotonated phenolate oxygen, enolate oxygen, and the azomethine nitrogen atoms. Coordination from the imine nitrogen is reflected in the downfield shift of about 0.5 ppm of the CH=N proton in the NMR spectra of the complexes **37** and **40**. The aromatic protons of ligands and complexes as well as the α-CH, β-CH_2, and hydroxy group of tyrosine amino acid, appear in the expected region, with slight shifts in their positions (see Experimental Section). The presence of acac group in the spectra of complexes **37**, **39** and **42** is shown by singlet signals at 1.89 and 1.96 ppm for the CH_3 protons and 4.91 ppm for CH proton. The ^{1}H–NMR spectra of the complexes also showed a doublet (3.2 ppm, CH_3) and quartet (4.1 ppm, OH) of coordinated methanol. In addition, in the case of complexes **40** and **41** the presence of water molecules are confirmed by the specific resonance at 3.3 ppm. The ^{1}H–NMR spectra of complex **42** shows only three methanol molecules, but does not show any diethyl ether molecule, and moreover the elemental analyzes confirm this. Whereas the structure analyzes show also one diethyl ether molecule, per formula unit. This can be explained due to the fact that the X-ray analysis were performed on

fresh crystals from the solution, whereas for NMR and elemental analysis the sample was dried completely before analyzing. It seems that after drying diethyl ether is removed.

Table 6.2: Characteristics IR bands [cm^{-1}] for the complexes

Formula	Complex	ν(C=N–N=C)	$\nu(MoO_2)$
$[MoO_2$(Brsalhyleuacac)(MeOH)]	**37**	1598	937, 914
$[MoO_2$(Mesalhyphe)]	**38**	1603	934, 908
$[MoO_2$(Mesalhypheacac)(MeOH)]·2MeOH	**39**	1603	938, 908
$[MoO_2$(Brsalhyphe)(MeOH)]·H_2O	**40**	1602	941, 907
$[MoO_2$(Mesalhytyr)]·$2H_2O$	**41**	1604	922, 903
$[MoO_2$(Mesalhytyracac)(MeOH)]·2MeOH·Et_2O	**42**	1601	939, 911

6.3 Oxidation of sulfides catalyzed by dioxomolybdenum complexes with Boc-amino acid functionalized ligands

The new *cis*-dioxomolybdenum complexes with free amino acid ligands, were also tested toward their capability to catalyze the oxidation of methyl phenyl sulfide, using hydrogen peroxide as oxidant. Following typical procedure described in chapter 2, 1 mol-% catalyst has been used for the reaction and a slight excess (1.2 equivalents) of hydrogen peroxide, in a mixture CH_2Cl_2/CH_3OH 7:3. After defined intervals of time, aliquots were taken from the reaction mixture and the product analyzed by NMR (determination of the yield) and HPLC (determination of the ee). The outcomes of the catalytic reaction are summarized in Table 6.3 for the *cis*-dioxomolybdenum(VI) complexes with free-amino acid residues. After 1 hour of the reaction time 100% of the corresponding sulfoxide was obtained when complex **37**, with leucine residue, was used as catalyst, which is also the most efficient catalyst of the herein described molybdenum complexes (see Figure 6.11).

Table 6.3: Catalyzed asymmetric oxidation of methyl phenyl sulfide using various complexes

Formula	Complex	Time (h)	Yield[a] (%)	ee [b] (%)	Configuration[c]
$[MoO_2(Brsalhyleuacac)(MeOH)]$	**37**	1	100	n.d[d]	–
$[MoO_2(Mesalhyphe)]$	**38**	1	61	2.92	S
$[MoO_2(Mesalhyphe)]$	**38**	3	94	2.34	S
$[MoO_2(Mesalhytyr)]\cdot 2H_2O$	**41**	1	61	2.61	S
$[MoO_2(Mesalhytyr)]\cdot 2H_2O$	**41**	3	80.4	0.79	S
$[MoO_2(Mesalhytyracac)(MeOH)]$ $\cdot 2MeOH\cdot Et_2O$	**42**	1	86	2.75	S

All reactions were carried out at 0 °C with vanadium complexes loading to 1 mol-% and (1.2 equivalents) of hydrogen peroxide (8.24 M), in a mixture CH_2Cl_2/CH_3OH 7:3. [a] isolated yield determined by ^{1}H–NMR (400 MHz) using 1,3,5-trimethoxybenzene as internal standard. [b] Determined by HPLC using a (S,S)-WHELK-01 chiral column (25 cm × 4.6 mm). The column was eluted with hexane:2-propanol (90:10), at a flow rate of 2.0 mL/min. [c] Absolute configuration of the major product was determined to be S, by comparison of the chromatogram in HPLC with the authentic sample. [d] n.d. not determined.

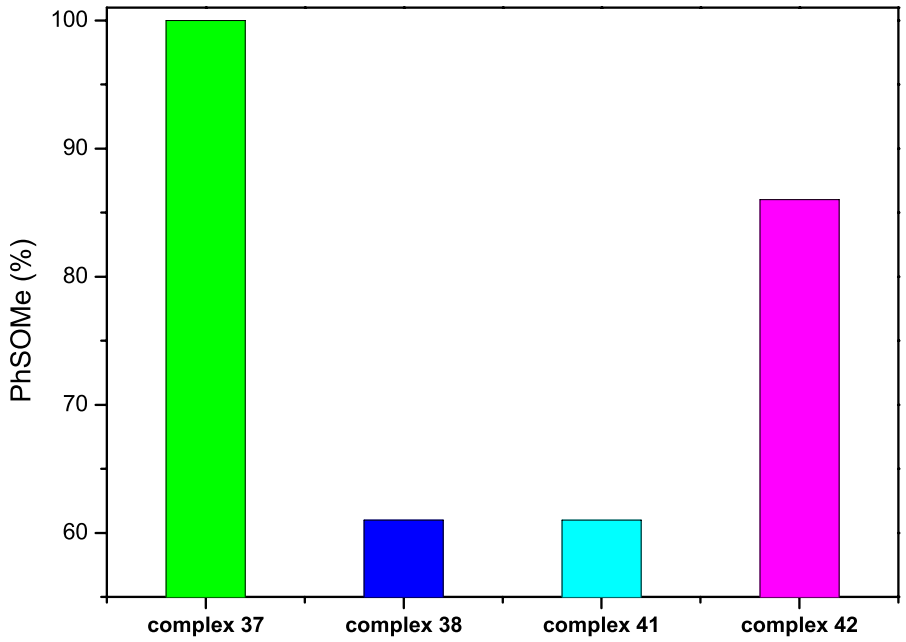

Figure 6.11: Oxidation of methyl phenyl sulfide catalyzed by molybdenum complexes with free-amino acid ligands. The conversions in % were reached after 1 hour of the reaction time

6.4 Conclusions

The synthesis of new *cis*-dioxomolybdenum complexes(VI) **37** to **42** is described based on free amino acid residue ligands. The main product was the desired *cis*-dioxomolybdenum complexe(VI). This was accompanied by the second product formed by condensation of the amino acid functionality with the acac (acetylacetonate) group of the $MoO_2(acac)_2$, in a low yield. The complexes were examined as catalyst in the sulfoxidation reaction of methyl phenyl sulfide to the corresponding sulfoxide. There are no significant differences in the catalytic activity. All types of catalysts showed high activity, but unfortunately, the ee values were two low, which can be explained as in the case of the corresponding dioxovanadium complexes with the fact that, the chiral center is far away from the dioxo molybdenum(VI) moiety. Nevertheless, these complexes are more reactive than the corresponding dioxovanadium complexes.

6.5 Experimental part

6.5.1 [MoO_2(Brsalhyleuacac)(MeOH)] (37)

To a solution of Schiff base ligand Brsalhyleu (0.82 g, 2.5 mmol) in methanol (30 mL) was added $MoO_2(acac)_2$ (0.82 g, 2.5 mmol). The green brown reaction mixture was stirred at room temperature for 3 days, when a yellow solution was formed. The solution was filtrated, to remove small amounts of unreacted molybdate, the volume of the filtrate was reduced to about 5 mL, and left at room temperature when an yellow precipitate is formed. The resulting precipitate was filtrated, recrystallized from methanol, and kept in an open flask at room temperature. After slow evaporation of the solvent suitable crystals for X-ray measurement were isolated.

Total yield: 0.57 g (1.00 mmol, 40%).

Elemental analysis for $C_{19}H_{26}BrMoN_3O_6$ (568.27 g/mol): calculated C: 40.16%, H: 4.61%, N: 7.39%; found C: 39.85%, H: 4.84%, N: 7.12%.

^{1}**H-NMR** (400 MHz, DMSO-d_6): $\delta =$ 0.95 (m, 6H, (C**H**$_3$)$_2$), 1.65 (m, 3H, γ-C**H**, β-C**H**$_2$), 1.89 (s, 3H, C**H**$_3$(acac)), 1.96 (s, 3H, C**H**$_3$(acac)), 3.16 (s, 3H, MeOH), 4.01 (s, 1H, MeOH), 4.42 (m, 1H, α-C**H**), 4.91 (s, 1H, C**H**(acac)), 6.90 (m, 1H, Ph), 7.66 (m, 1H, Ph), 7.94 (s, 1H, Ph), 8.82 (s, 1H, C**H**=N), 10.84 (br, 1H, N**H**) ppm.

^{13}**C-NMR** (100 MHz, DMSO-d_6): $\delta =$ 19.06 (**C**H$_3$(acac)), 22.62, 22.82, (C(**C**H$_3$)$_2$), 24.83 (γ-**C**H), 29.21 (**C**H$_3$(acac)), 42.53 (β-**C**H$_2$), 49.06 (MeOH), 52.30 (α-**C**H), 95.62 (**C**H(acac)), 112.76 (Ph), 121.36 (Ph), 122.36 (Ph), 136.38 (Ph), 137.59 (Ph), 156.07 (**C**H=N), 158.88 (Ph), 162.32 (**C**=N), 174.55 (**C**H=O), 194.60 (**C**H=Oacac), ppm.

MS (FAB$^+$, nba): m/z = 536 [30% M + H$^+$], 410 (80%), 307 (100%), 289 (70%).

Selected IR data (cm^{-1}): ν = 1598 (s, C=N–N=C), 937 (s, MoO_2), 914 (s, MoO_2).

6.5.2 [MoO_2(Mesalhyphe)] (38)

Method A To a solution of Mesalhyphe (0.12 g, 0.40 mmol) in 20 mL methanol was added $MoO_2(acac)_2$ (0.13 g, 0.40 mmol). The reaction mixture changed color to orange. The resulting mixture was heated under reflux with continuous stirring. In a few minutes a yellow precipitate is formed. The mixture was heated for an additional 2 hours, then the

yellow precipitate was filtrated, and dried in air. m.p 240°C

Total yield: 0.15 g (0.354 mmol, 88.5%).

Elemental analysis for $C_{17}H_{17}MoN_3O_4$ (423.3 g/mol): calculated C: 48.24%, H: 4.02%, N: 9.93%; found C: 47.00%, H: 3.85%, N: 9.59%.

^{1}**H-NMR** (200 MHz, DMSO-d_6): $\delta =$ 2.67 (s, 3H, C**H**$_3$), 2.80 (m, 1H, β–C**H**$_2$), 2.97 (m, 1H, β–C**H**$_2$), 3.78 (br, 1H, α-C**H**), 6.88 (m, 1H, Ph), 7.04 (m, 1H, Ph), 7.18 (m, 5H, Ph), 7.57 (m, 1H, Ph), 7.82 (m, 1H, Ph) ppm.

^{13}**C-NMR** (50 MHz, DMSO-d_6): $\delta =$ 16.58 (**C**H$_3$), 38.25 (β–**C**H$_2$), 54.11 (α-**C**H), 118.63 (Ph), 121.46 (Ph), 122.59 (Ph), 126.10 (Ph), 128.00 (Ph), 129.41 (Ph), 130.84 (Ph), 133.46 (Ph), 138.37 (Ph), 159.82 (Ph), 163.84 (C=N), 174.36 (C=O) ppm.

Selected IR data (cm^{-1}): $\nu = 3321$, 3257 (s, NH), 1603 (s, C=N–N=C), 934 (s, MoO_2), 908 (s, MoO_2).

Method B To a solution of the ligand Mesalhyphe (0.25 g, 0.84 mmol) in 30 mL methanol was added $NaMoO_4 \cdot 2H_2O$ (0.20 g, 0.84 mmol). The reaction mixture was stirred at room temperature for 30 minutes followed by heating under reflux for 1 hour till all molybdate was reacted. The volume of the yellow clear solution was reduced to about half of its original volume and left at room temperature when a yellow precipitate is formed. The resulting precipitate was filtrated and dried in air.

Total yield: 0.20 g (0.47 mmol, 56%).

^{1}**H-NMR** (400 MHz, DMSO-d_6): $\delta =$ 2.27 (s, 3H, C**H**$_3$), 2.72 (m, 1H, β–C**H**$_2$), 2.97 (m, 1H, β–C**H**$_2$), 3.78 (m, 1H, α-C**H**), 6.88 (m, 1H, Ph), 7.04 (m, 1H, Ph), 7.18 (m, 5H, Ph), 7.57 (m, 1H, Ph), 7.82 (m, 1H, Ph) ppm.

^{13}**C-NMR** (100 MHz, DMSO-d_6): $\delta =$ 13.23 (**C**H$_3$), 38.25 (β–**C**H$_2$), 55 (α-**C**H), 117.22 (Ph), 118.33 (Ph), 119.27 (Ph), 126.08 (Ph), 128.04 (Ph),128.27 (Ph), 129.31 (Ph), 130.98 (Ph), 138.54 (Ph), 155.54 (Ph), 158.69 (C=N), 171.54 (C=O) ppm.

6.5.3 [MoO_2(Mesalhypheacac)(MeOH)]·2MeOH (39)

The yellow crystals of this type of complex were obtained and isolated from the concentrated solution of the filtrate from complex **38** when kept at -28°C for 3 days.
mp 185–192°C.

Total yield: 28 mg (0.046 mmol, 11.5%).

Elemental analysis for $C_{24}H_{31}MoN_3O_7$ (569.46 g/mol): calculated C: 50.62%, H: 5.49%, N: 7.38%; found C:51.18%, H: 4.66%, N: 8.03%.

Selected IR data (cm^{-1}): ν = 3400 (s, NH), 1603 (s, C=N–N=C), 938 (s, MoO_2), 908 (s, MoO_2).

6.5.4 $[MoO_2(Brsalhyphe)(MeOH)]\cdot H_2O$ (40)

To a solution of the ligand Brsalhyphe (0.190 g, 0.520 mmol9 in 20 mL methanol was added $MoO_2(acac)_2$ (0.170 g, 0.520 mmol). The reaction mixture changed color from yellow to orange. The mixture was heated under reflux for 30 minutes, when all molybdate was reacted. The volume of the solution was reduced to half of its original volume, and left at room temperature when a yellow precipitate is formed. The resulting precipitate was filtrated and dried in air.

Total yield: 0.31 g (0.50 mmol, 96%).

Elemental analysis for $C_{22}H_{26}MoN_3O_7$ (620.30 g/mol): calculated C: 42.60%, H: 4.22%, N: 6.77%; found C: 42.184%, H: 3.94%, N: 6.54%.

^{1}**H-NMR** (400 MHz, DMSO-d_6): δ = 1.89 (s, 3H, C$\mathbf{H}_3$(acac)), 1.96 (s, 3H, C$\mathbf{H}_3$(acac)), 2.98 (m, 2H, β-C$\mathbf{H}_2$), 3.16 (s, 3H, MeOH), 3.33 (s, 3H, C**H**(acac) overlapping with H_2O), 4.51 (m, 1H, α-C**H**), 6.90 (m, 1H, Ph), 7.25 (m, 6H, Ph), 7.62–7.91 (m, 1H, Ph), 8.76 (s, 1H, C**H**=N), 10.89 (s, 1H, N**H**) ppm.

^{13}**C-NMR** (50 MHz, DMSO-d_6): δ = 23.37 (**C**H_3(acac)), 33.60 (**C**H_3(acac)), 45.50 (β-**C**H_2), 48.59 (MeOH), 53.46 (α-**C**H), 100.75 (Ph), 117.16 (Ph), 125.78 (Ph), 126.75 (Ph), 131.63 (Ph), 133.15 (Ph), 134.23 (Ph), 134.70 (Ph), 140.81 (Ph), 141.23 (Ph), 142.04 (Ph), 160.56 (**C**H=N), 163.30 (Ph), 166.45 (**C**=N), 178.07 (**C**=O), 195.00 (**C**=O) ppm.

Selected IR data (cm^{-1}): ν = 1602 (s, C=N–N=C), 941 (s, MoO_2), 907 (s, MoO_2).

6.5.5 $[MoO_2(Mesalhytyr)]\cdot 2H_2O$ (41)

To a solution of Mesalhytyr (439 mg, 1.40 mmol) in 60 mL hot methanol was added $MoO_2(acac)_2$ (450 mg, 1.40 mmol). The reaction mixture changed color to orange. The resulting yellow solution was heated under reflux with continuous stirring. In a few

minutes a yellow precipitate is formed. The mixture was heated for an additional 1 hour, then the yellow precipitate was filtrated, and dried in air.

Total yield: 0.35 g (0.74 mmol, 53%).

Elemental analysis for $C_{17}H_{21}MoN_3O_7$ (475.30 g/mol): calculated C: 42.96%, H: 4.45%, N: 8.84%; found C: 43.00%, H: 3.91%, N: 8.88%.

^{1}**H-NMR** (200 MHz, DMSO-d_6): $\delta =$ 2.68 (s, 3H, C**H**$_3$), 2.83–2.93 (m, 2H, β–C**H**$_2$), 3.33 (s, 2H, **H**$_2$O), 3.72 (m, 1H, α–C**H**), 6.64 (m, 2H, Ph), 6.91 (m, 2H, Ph), 7.03 (m, 2H, Ph), 7.50 (m, 1H, Ph), 7.78 (m, 1H, Ph), 8.04 (br, 1H, O**H**–amino acid) ppm.

^{13}**C-NMR** (50 MHz, DMSO-d_6): $\delta =$ 16.6 (**C**H$_3$), 38.15 (β–**C**H$_2$), 54.22 (α-**C**H), 114.87 (Ph), 118.61 (Ph), 121.47 (Ph), 122.30 (Ph), 129.45 (Ph), 130.31 (Ph), 130.85 (Ph), 132.90 (Ph), 155.73 (Ph), 159.81 (Ph), 163.12 (**C**=N), 170.93 (O–**C**NNC) ppm.

Selected IR data (cm^{-1}): $\nu = 3503$ (s, br; O–H), 3316 (s, N–H), 1604 (s, br; C=N–N=C), 922 (s, MoO_2), 903 (s, MoO_2).

EI-MS (negative ion mode, in methanol): m/z = 442 ([MoO_2(Mesalhytyr)] – H^+ 10%), 335.9 (100%).

6.5.6 [MoO_2(Mesalhytyracac)(MeOH)]·2MeOH·Et_2O (42)

To a solution of Mesalhytyr (304 mg, 0.97 mmol) in 40 mL methanol was added $MoO_2(acac)_2$ (311 mg, 0.97 mmol). The reaction mixture changed color to orange. The resulting mixture was heated under reflux with continuous stirring for 4 hours. Then the volume of the solution was reduced to about 5 mL, diethyl ether was added which results in the formation of a slurry solution, which left at -28°C. Yellow colored single crystals suitable for X-ray studies formed within two weeks.

Total yield: 62 mg (0.100 mmol, 10.4%).

Elemental analysis for $C_{25}H_{35}MoN_3O_9$ (617.50 g/mol): calculated C: 48.63%, H: 5.71%, N: 6.80%; found C: 47.41%, H: 5.42%, N: 7.06%.

^{1}**H-NMR** (400 MHz, DMSO-d_6): $\delta =$ 1.73 (s, 3H, C**H**$_3$(acac)), 1.86 (s, 3H, C**H**$_3$(acac)), 2.71 (s, 3H, C**H**$_3$), 2.81–2-87 (dd, ^{3}J = 8.21, ^{2}J = 13.72 Hz, 1H, β–C**H**$_2$), 3.02–3-03 (dd, ^{3}J = 5.61, ^{2}J = 13.72 Hz, β–C**H**$_2$), 3.16 (d, ^{3}J = 5.20 Hz, C**H**$_3$OH), 3.32 (s, 4H, Et_2O), 4.91 (s, 1H, C**H**(acac)), 6.61 (m, 1H, Ph), 6.91 (m, 1H, Ph), 7.05 (m, 3H, Ph), 7.48 (m,

1H, Ph), 7.87 (m, 1H, Ph), 9.21 (s, 1H, OH), 10.93 (br, 1H, N**H**(acac)) ppm.

^{13}**C-NMR** (50 MHz, DMSO-d_6): δ = 18.47 (**C**H_3), 28.70 (**C**H_3(acac)), 29.21 (**C**H_3(acac)), 40.75 (β–**C**H_2), 48.58 (MeOH), 55.56 (α-**C**H), 95.62 (**C**H(acac)), 115.02 (Ph), 118.65 (Ph), 121.65 (Ph), 122.43 (Ph), 126.60 (Ph), 130.46 (Ph), 131.01 (Ph), 133.71 (Ph), 156.03 (Ph), 159.75 (Ph), 164.69 (**C**=N), 170.97 (O–**C**NNC), 193.73 (**C**=O(acac)) ppm.

Selected IR data (cm^{-1}): ν = 3368 (s, br; N–H), 1601 (s, C=N–N=C), 939 (s, MoO_2), 911 (s, MoO_2).

6.5.7 Catalytic oxidation of methyl phenyl sulfide

Molybdenum complex (0.02 mmol) was dissolved at room temperature in a mixture of CH_2Cl_2/CH_3OH 7:3 (20 mL) and 1,3,5-trimethoxybenzene (0.34 g, 2.0 mmol) as internal standard was added followed by (0.24 ml, 2.0 mmol) phenyl methyl sulfide. The resulting solution was cooled down on an ice-bath and H_2O_2 8.24 M (1.2 equiv., 0.31 mL, 2.5 mmol) was added dropwise. The reaction solution was warmed up to room temperature and stirred in a capped flask and monitored by thin-layer chromatography technique (Et_2O:*n*-hexane 9:1). After 1, and 3-hours reaction time, aliquots of the reaction solutions (2.0 mL) were quenched with ca. 5 mL of a stock solution of NaOH (0.1 M) and extracted with ethyl acetate (3×4 mL). The collected organic phases were removed completely to dryness and the residue was redissolved in deuterated chloroform (600 μL) and analyzed by ^{1}H–NMR to determine the yield. From this solution was then taken 60 μL of chloroform, removed the solvent to dryness and the residue redissolved in 2 mL dichlormethane and the enantiomeric excess was determined by chiral HPLC as described in chapter 2.

Chapter 7

Summary

Amino acids occupy a special place in the coordination chemistry of transition metal ions. Since amino acids are the constituents from which proteins are built, the complexes formed by metal ions and amino acids have served as model systems for metalloprotein studies.[149] A knowledge of the interaction between vanadium and amino acids is of significance for the understanding of biological action of the metal. For example: (1) vanadium(IV) and (V) are thought to be bound to the serum protein transferrin via amino acids as ligands, (2) the tunichromes are catechol derivatives thought to play an important role in the accumulation and storage of vanadium by marine organisms tunicats, (3) the interaction of vanadium with tyrosine is thought to be responsible for the insulin enhancing effects of vanadate, and (4) vanadium is known to have a function in various enzymes of plants and organisms (Butler and Carrano, 1991; Kendrick et al., 1992).

After vanadium haloperoxidase had been found in various enzymes as an essential part, the focus on the structure and function of vanadium-dependent haloperoxidases has increased. Hydrogen bonding plays an important role in both the fixation of vanadate in the active site and in the activation of a peroxide substrate.

The objective of the present work was to synthesize chiral *cis*-dioxovanadium(V) complexes, which model the active site and catalytic function of vanadium haloperoxidases. To the best of our knowledge, no data on the formation of *cis*-dioxovanadium(V) complexes with *N*-salicylidene-amino-acid-hydrazide ligands have been reported. Therefore vanadium(V) complexes with the Schiff bases derived from salicylaldehyde itself or

one of its ring substituted derivative and amino acid hydrazides were prepared. Starting from protected amino acids, free (unprotected amino group of the amino acids) different amino acids were used. By this we propose to probe the role of the amino acid residues involved in the hydrogen bonding network of the protein bound vanadate in haloperoxidases.

The synthesis of *cis*-dioxovandium complexes with protected amino acids such as Boc-L-α-serine, Boc-L-α-histidine, Boc-L-α-tryptophan, and Boc-L-α-phenylalanine were described in chapter 2. Preparations were carried out with potassium or ammonium vanadate as vanadium sources. The resulting complexes were characterized and in the case of Boc-L-α-serine residue the complex has been structurally characterized by X-ray diffraction analysis, which showed the vanadium atom in a distorted square pyramidal coordination environment. Their oxidizing properties were studied in competitive bromination of 1,3,5-trimetoxybenzene (TMB) and monochlordimedone (MCD), in acetonitrile solution, using hydrogen peroxide as oxidant. The results showed that they are good catalysts. The best results were obtained with the serine residue vanadium complexes with bromo-substituted aldehyde $NH_4[VO_2(BrsalhyBocser)]\cdot MeOH$ (**4**). They are often almost as active or even more active than the vanadate standard $(nBu_4N)_2HVO_4$.

The capability of the new chiral *cis*-dioxovanadium(V) complexes to function as catalysts for the oxidation reaction of methyl phenyl sulfide by hydrogen peroxide was also investigated. The best results were obtained with complexes derived from Boc-L-α-serine, the reaction was completed in less than three hours, thus they have the highest efficient catalytic activity of the herein described complexes with Boc-amino acid residues. The enantioselectivity of the *cis*-dioxovanadium(V) complexes was very low. This indicates that the chiral center is too far away from the vanadate moiety.

In order to see the influence of the amino acids protecting group on the catalytic activity of vanadium complexes, free amino acids were introduced as described in chapter 3. The synthesis of *cis*-dioxovanadium complexes followed the same procedure as in the case of protected ones, in addition vanadyl sulfate was used as an alternative method to synthesize the neutral complexes. The Schiff base ligands with hydroxy acetophenone proved to be successful to incorporate vanadium in the desired manner. X-ray crystal structures revealed the vanadium atom in a slightly distorted square pyramidal, where

the protonated amino acids functionality compensate the negative charge of the vanadate moiety, similar to the lysine residue in the vanadium dependent haloperoxidase enzymes.

The Schiff base ligands with salicylaldehyde, and its bromo substituted derivative, were not able to give the desired complexes. Instead vanadium complexes **21** to **26** were obtained as the products of the oxidative removal of amino acid residues from the α-methyl groups, followed by oxidation of the C^{α}–C bond, leading to the formation of the α-ketoamides. The unprecedented complexes thus formed, serve as very good catalyst for the oxidation reaction of C^{α}–C to C=O. The *cis*-dioxovanadium(V) complexes with free amino acid residues, described in chapter 3 were also tested towards their capability to catalyze the oxidative bromination of TMB/MCD. The results showed that they react faster than those with Boc protected described in chapter 2. The complexes showed also high efficient capability in catalyzing the oxidation of sulfide when H_2O_2 was used as oxidizing agent, comparable with the results found from the vanadium complexes with protected amino acid residue ligands.

In order to see the influence of β-amino acids on the catalytic activity, Boc-L-β-alanine was introduced as described in chapter 4. Therefore, a new ligand system was designed which proved to be successful to incorporate vanadium(V), capable of mimicking the hydrogen bonding interactions of vanadate moiety from the natural system with lysine residue. Complex $K[VO_2(salhyBoc\beta ala)]\cdot H_2O$ (**28**) was tested for its catalytic activity in the reaction where TMB/MCD were used as substrate and hydrogen peroxide as the oxidant. It was found a good active catalyst. The results are comparable with those obtained for *cis*-dioxovanadium complexes with α-amino acids, even more active than vanadium complexes with protected α-amino acids. Therefore it could serve as a functional mimic for vanadium bromoperoxidase.

The catalyst **28** was also tested on its ability to oxidise the organic sulfides to the corresponding sulfoxides. The results showed that the reaction was completed in 3 hours giving the corresponding sulfoxide in a very high yield.

Based on the results of both catalytic reactions, attempts were made to synthesize *cis*-dioxovanadium complexes which contain a free β-alanine ligand, which we expect to have higher catalytic activity. Unfortunately, the ligand with free β-alanine was inappropriate for the synthesis of *cis*-dioxovanadium(V) complexes, since no well characterized

complexes were isolated.

The replacement of vanadate from vanadium haloperoxidase with molybdate or tungstate yielded an inactive enzyme.[14] Therefore, *cis*-dioxomolybdenum(VI) complexes based on *N*-salicylidene amino acid hydrazides were also obtained in order to address the question whether a synthetic molybdenum complex can catalyze the bromoperoxidase reaction. Molybdenum complexes which contain protected amino acid were described in chapter 5, whereas those with unprotected ones in chapter 6. But, however they showed no bromoperoxidase activity, in contrary to the corresponding *cis*-dioxovanadium(V) complexes. Instead, they served as very good catalyst in sulfoxidation reaction. Within the protected amino acid group there was a strong decrease in activity on going from α- to β-amino acids. Furthermore, *cis*-dioxomolybdenum(VI) which contain unprotected amino acid, turned out to be even more active.

Zusammenfassung

Aminosäuren nehmen einen speziellen Platz in der Koordinationsschemie der Übergangsmetalle ein. Da sie die Bausteine der Proteine sind, können Komplexe aus Metallionen und Aminosäuren als Modellsystheme für die Untersuchung von Metalloproteinen dienen. Das Wissen über die Wechselwirkung zwischen Vanadium und Aminosäuren kann für das Verständnis der biologischen Aktivität des Metalls von Bedeutung sein. Zum Beispiel: (1) Man nimmt an, dass Vanadium(IV) und (V) an das Serumprotein, Transferrin, durch Aminosäuren als Liganden gebunden sind, (2) dass in Tunikaten, maritimen Organismen, Catecholderivate, so genannte Tunichrome, eine wichtige Rolle bei der Aufnahme und Speicherung von Vanadium tragen, (3) die Wechselwirkung von Vanadium mit Tyrosin für den insulinmimetischen Effekt des Vanadates verantwortlich ist und (4) Vanadium eine Funktion in verschiedenen Enzymen in Pflanzen und Organismen trägt (Butler und Carrano, 1991; Kendrick et al., 1992).

Nachdem Vanadium in verschiedenen Organismen, z.B. in Haloperoxidasen, als ein essentieller Bestandteil gefunden wurde hat sich der Blick auf die Struktur und Funktion vanadium-abhängiger Enzyme verstärkt. Wasserstoffbrückenbindungen spielen dabei eine wichtige Rolle, zum einen bei der Fixierung des Vanadates im aktiven Zentrum und auch bei der Aktivierung des Peroxidsubstrates.

Das Ziel der vorliegenden Arbeit war es chirale *cis*-Dioxovanadium(V)-Komplexe zu synthetisieren, die das aktive Zentrum und die katalytische Funktion der Vanadiumhaloperoxidase nachbilden. Nach unserem Kenntnisstand wurden bisher keine Daten über die Bildung von *cis*-Dioxovanadium(V)-Komplexen mit *N*-Salicyliden-aminosäurehydrazidliganden veröffentlicht. Daher wurden Vanadium(V) Komplexe mit Schiffschen Basen ausgehend von Salicylaldehyd selbst oder eines seiner ringsubstituierten Derivate und Aminosaurehydraziden hergestellt. Ausgehend von geschützten Aminosäuren wurden verschiedene freie Aminosäuren schrittweise eingeführt. Dies dient dazu die Bedeutung der Aminosäurereste, welche über Wasserstoffbrückenbindungen mit dem äquatorialen Sauerstoffatom der prosthetischen Gruppe in der vanadiumhaltigen Haloperoxidase in Wechselwirkung stehen, zu untersuchen.

Die Synthese der *cis*-Dioxovandiumkomplexe mit den geschützten Aminosäuren Boc-L-α-Serin, Boc-L-α-Histidin, Boc-L-α-Tryptophan und Boc-L-α-Phenylalanin wird

in Kapitel 2 beschrieben. Die Darstellungen wurden mit Kalium oder Ammoniumvanadat als Vanadiumquelle durchgeführt. Die gebildeten Komplexe wurden charakterisiert und im Falle des Boc-L-α-Serinerestes strukturell durch eine Kristallstrukturanalyse untersucht, wobei das Vanadiumatom in einer verzerrt quadratisch pyramidalen Koordinationsumgebung vorliegt. Ihre Oxidationseigenschaften wurden bei der Bromierung von 1,3,5-Trimetoxybenzen (TMB) und Monochlordimedon (MCD) in Acetonitril, mit Wasserstoffperoxid als Oxidationsmittel, untersucht. Die Ergebnisse zeigen, dass sie sehr gute Katalysatoren sind. Die besten Ergebnisse wurden mit dem Vanadiumkomplexe mit Serinrest und Brom-substituierten Aldehyd $NH_4[VO_2(BrsalhyBocser)]\cdot MeOH$ (**4**) erzielt. Oftmals sind die Kompelxe fast so aktiv oder aktiver als der Vanadatstandard $(nBu_4N)_2HVO_4$.

Die Vermögen der neuen chiralen *cis*-Dioxovanadium(V)-Komplexe als Katalysator für die Oxidation von Methylphenylsulfid mittels Wasserstoffperoxid zu dienen wurde ebenfalls untersucht. Die besten Ergebnisse wurden mit den Komplexen die sich von Boc-L-α-Serin ableiten, erreicht. Die Reaktion war in weniger als drei Stunden abgeschlossen, also haben sie die größte katalytische Aktivität der hier beschriebenen Komplexe mit Boc-Aminosäureresten. Die Enantioselektivität der *cis*-Dioxovanadium(V) Komplexe ist sehr gering, was darauf zurück-zuführen ist, dass das chirale Zentrum weit vom Vanadatzentrum entfernt liegt.

Um den Einfluss der Aminosäureschutzgruppe auf die katalytische Aktivität des Vanadiumkomplexes zu untersuchen, werden in Kapitel 3 freie Aminosäuren vorgestellt. Die Synthese der *cis*-Dioxovanadiumkomplexe folgt dem selben Schema wie bei den geschützten Komplexen, zusätzlich wurde Vanadylsulfat-Trihydrat als eine alternative Methode der Komplexbildung verwendet. Die Schiff Base Liganden mit Hydroxyacetophenon erwiesen sich als geeignet um das Vanadium in der gewünschten Art und Weise zu koordinieren. Die Kristallstrukturanalyse zeigt wieder das Vanadium in einer leicht verzerrten quadratisch pyramidalen Koordination, wobei die protonierten Aminosäurefunktionalitäten die negative Ladung des Vanadats ausgleichen, ähnlich wie bei dem Lysinrest im vanadiumabhängigen Haloperoxidase-Enzym.

Mit den Schiff Base Liganden von Salicylaldehyd und seines bromsubstituierten Derivates konnten nicht die gewünschten Komplexe gebildet werden. Die beispiellose

Bildung der Vanadiumkomplexe **21**–**26** resultiert aus der oxidativen Abspaltung des Aminosäurerestes von der β-Methylgruppe, gefolgt von der Oxidation dieser C–C-Bindung. Die *cis*-Dioxovanadium(V)-Komplexe mit freien Aminosäureresten, die im Kapitel 3 beschrieben sind wurden auch auf ihre Fähigkeit zur Katalyse der oxidativen Bromierung von TMB/MCD getestet. Es zeigt sich, dass die Komplexe schneller reagieren als die in Kapitel 2 beschriebenen Boc-geschützten. Sie zeigten auch bei der katalytischen Oxidation von Sulfiden mit H_2O_2 Aktivität, vergleichbar mit der welche für die Vanadiumkomplexe mit geschützten Aminosäureresten am Liganden gefunden wurde.

Um den Auswirkung von β-Aminosäuren auf die katalytische Aktivität zu zeigen, wird in Kapitel 4 Boc-β-Alanin vorgestellt. Deshalb wurde ein neues Ligandensystem designed, welches sich als erfolgreich für die Koordination von Vanadium(V) erwies und fähig ist die Wasserstoffbrückenbindungen der Vanadatumgebung des natürlichen Systems mit Lysinrest nachzubilden. Es wurde anhand der Reaktion mit TMB/MCD als Substrat und Wasserstoffperoxid als Oxidationsmittel untersucht ob der Komplex K[VO_2(salhyBocβala)]·H_2O (**28**) als ein funktioneller Imitator für die Vanadiumbromoperoxidase dient. Es erwies sich als guter Katalysator, was vergleichbar mit den für die *cis*-Dioxovanadiumkomplexe mit α-Aminosäuren erhaltenen Werten ist, und er war aktiver als die Vanadiumkomplexe mit geschützten α-Aminosäuren.

Der Komplex **28** wurde auch auf die Eignung zur Oxidation von organischen Sulfiden zu den korrespondierenden Sulfoxiden untersucht. Die Reaktion war in 3 Stunden beendet.

Ausgehend von den Resultaten der beiden katalytischen Reaktionen, wurden Versuche unternommen einen *cis*-Dioxovanadiumkomplex mit einem freien β-Alaninliganden herzustellen, für welchen eine höhere katalytisch Aktivität erwartet werden würde. Bedauerlicherweise war der Ligand mit freiem β-Alanine ungeeignet für die Synthese von *cis*-Dioxovanadium(V)-Komplexen, da keine charakterisierbaren Komplexe isoliert werden konnten.

Der Ersatz von Vanadat in Vanadiumhaloperoxidasen mit Molybdat oder Wolframat führte zu inaktiven Enzymen. Deshalb wurden auch *cis*-Dioxomolybdän(VI)-Komplexe basierend auf *N*-Salicylidenaminosäurehydraziden synthetisiert um die Frage zu beantworten, ob synthetische Molybdänkomplexe die Bromoperoxidasereaktion kataly-

sieren können. Die Molybdänkomplexe mit geschützten Aminosäuren werden in Kapitel 5 beschrieben, und die ungeschützten in Kapitel 6. Allerdings zeigten sie keine Bromoperoxidaseaktivität, im Gegensatz zu den korrespondierenden *cis*-Dioxovanadium(V)-Komplexen. Sie dienen aber als sehr gute Katalysatoren für die Sulfoxidation, wobei bei den geschützten Aminosäuren eine große Abnahme der Aktivität von α- zu β-Aminosäuren zu verzeichnen war. Des Weiteren stellte sich heraus, dass die *cis*-Dioxomolybdän(VI)-Komplexe mit ungeschützter Aminosäure noch aktiver sind.

Chapter 8

Characterization techniques

8.1 Elemental analyses

Carbon, hydrogen and nitrogen contents were determined at the "Institut für Organiche und Makromolekulare Chemie", Friedrich-Schiller University, Jena using LECO CHN/932 and VARIO EL III elemental analyzers.

8.2 NMR spectroscopy

^{1}H, ^{13}C, ^{51}V NMR, ^{1}H{^{1}H} COSY and ^{1}H{^{13}C} heteronuclear correlation NMR spectra were recorded on Bruker Avance 200 and 400 MHz spectrometers.

8.3 Mass spectrometry

Mass spectrometry analysis were conducted on a MAT95XL Finnigan instrument, using electron spray ionization, negative and positive mode.

8.4 Infrared spectroscopy

IR spectra were recorded on Bruker IFS55/Equinox spectrometer on samples prepared as KBr pellets.

8.5 UV-Vis measurements

The principal method used for catalytic bromination reactions was UV/Vis-spectroscopy. All photometric measurements were carried with a Varian Cary 5000 UV/Vis/NIR spectrophotometer using solvents of high purity. The spectrophotometer was equipped with dual cell peltier accessory, which offered a continuous stirring and temperature control.

8.6 HPLC analyses

HPLC data were recorded using Jasco HPLC instrument equipped with UV-diode array detector, with a (S,S)-WHELK-01 chiral column (25 cm × 4.6 mm). The Borwin program was used to evaluate peak areas. The column was eluted with hexane:2-propanol (90:10), at a flow rate of 2.0 mL/min.

8.7 Crystal structure analyses

The crystallographic data were collected on a Nonius KappaCCD difractometer, using graphite-monochromated Mo-Kα radiation of 71.073 pm. A summary of crystallographic data and data collection for all complexes is given in the last part of the thesis. The structures were solved by direct methods (SHELXT) and subsequent least square refinement. All non-hydrogen atoms were refined by using anisotropic displacement parameters, while the hydrogen atoms were fixed and refined including their isotropic displacement parameters.

The reactions carried out under argon were made by using standard Schlenk line technique.

8.8 General Remarks:

All solvents and chemicals were reagent grade and used without further purifications unless otherwise specified: NH_4VO_3, KVO_3, $VOSO_4 \cdot 3H_2O$, Boc-L-α-amino acids, L-α-amino acid methylester hydrochloride were purchased from Fluka. $MoO_2(acac)_2$ were purchased from Aldrich. Acetonitrile was purchased from Merck and was of the purest grade.

For catalytic reaction: A 30% (8.24 M) hydrogen peroxide solution, purchased from Merck, was standardized by titrating with a 0.02 M solution of $KMnO_4$, and the solution was fresh prepared for each measurement. The concentration of a 60% (9.10 M) solution of $HClO_4$ was determined by titration with a 1 M solution of NaOH.

Part I

Crystallographic data

Table 8.1: Crystallographic data and structure refinemend for $K[VO_2(BrsalhyBocser)]\cdot 2H_2O$ (**3**)

Empirical formula	$C_{15}H_{21}BrKN_3O_9V$
Molecular mass, g/mol	557.30
Temperature, K	183(2)
Wavelength, pm	71.073
Crystal system, Space group	orthorhombic, $P2_12_12_1$
Unit cell dimensions,	
a, pm; α, °	672.96(7), 90
b, pm; β, °	1146.27(9), 90
c, pm; γ, °	2825.2(3) 90
Cell volume, nm^3	2.1793(4)
Z	4
Calculated density, g/cm^3	1.689
Absorbtion coefficient, mm^{-1}	2.530
F(000)	1112
Crystal size, mm	0.03 x 0.03 x 0.02
θ range for data collection, °	1.92 – 27.49
Flack parameter	0.02(2)
Index ranges	$-8 \leq h \leq 7$,$-13 \leq k \leq 14$,
	$-32 \leq l \leq 36$
Reflection collected	7133
Independent reflections	3220 ($R_{int} = 0.0731$)
R indices	$R_1 = 0.095$, $\omega R_2 = 0.1968$

Table 8.2: Crystallographic data and structure refinemend for $[VO_2(Mesalhyphe)]\cdot MeOH$ (**18**)

Empirical formula	$C_{18}H_{22}N_3O_5V$
Molecular mass, g/mol	411.33
Temperature, K	183(2)
Wavelength, Å	0.71073
Crystal system, Space group	orthorhombic, $P2_12_12_1$
Unit cell dimensions,	
a, pm; α, °	782.38(3), 90
b, pm; β, °	1309.77(4), 90
c, pm; γ, °	1820.94(6), 90
Cell volume, pm^3,	1865.99(11) x 10^6
Z	4
Calculated density, g/cm^3	1.464
Absorbtion coefficient, mm^{-1}	0.566
F(000)	856
Crystal size, mm	0.05 x 0.05 x 0.04
θ range for data collection, °	2.83 – 27.48
Flack parameter	0.03(2)
Index ranges	$-10 \leq h \leq 10$,$-17 \leq k \leq 16$,
	$-23 \leq l \leq 22$
Reflection collected	4270
Independent reflections	3348 ($R_{int} = 0.0775$)
R indices	$R_1 = 0.067$, $\omega R_2 = 0.086$

Table 8.3: Crystallographic data and structure refinemend for 2[VO_2(Mesalhytyr)]·MeOH·2H_2O (**20a**)

Empirical formula	$C_{35}H_{26}N_6O_{14}V_2$
Molecular mass, g/mol	876.66
Temperature, K	183(2)
Wavelength, Å	0.71073
Crystal system, Space group	monoclinic, $P2_1$
Unit cell dimensions,	
a, pm; α, °	7446.30(10), 90
b, pm; β, °	1046.97(2), 95.36(10)
c, pm; γ, °	2579.15(6), 90
Cell volume, pm^3,	2001.93(7) x 10^6
Z	2
Calculated density, g/cm^3	1.454
Absorbtion coefficient, mm^{-1}	0.540
F(000)	912
Crystal size, mm	0.04 x 0.04 x 0.03
θ range for data collection, °	2.51 – 27.85
Index ranges	$0 \leq h \leq 9$,-13 $\leq k \leq 13$,
	-33 $\leq l \leq$ 33
Flack parameter	0.59(2)
Reflection collected	8982
Independent reflections	3510 (R_{int} = 0.0516)
R indices	R_1 = 0.064, ωR_2 = 0.1379

Table 8.4: Crystallographic data and structure refinemend for $[VO_2(Mesalhytyr)]\cdot MeOH$ (**20b**)

Empirical formula	$C_{18}H_{22}N_3O_6V$
Molecular mass, g/mol	427.33
Temperature, K	183(2)
Wavelength, Å	0.71073
Crystal system, Space group	monoclinic, $C2$
Unit cell dimensions,	
a, pm; α, °	2107.74(15), 90
b, pm; β, °	1279.48(8), 91.93(4)
c, pm; γ, °	738.50(3), 90
Cell volume, pm^3,	1990.5(2) x 10^6
Z	4
Calculated density, g/cm^3	1.426
Absorbtion coefficient, mm^{-1}	0.537
F(000)	888
Crystal size, mm	0.03 x 0.03 x 0.02
θ range for data collection, °	1.86 – 27.46
Index ranges	$-27 \leq h \leq 24$,$-14 \leq k \leq 16$, $-9 \leq l \leq 9$
Flack parameter	0.01(2)
Reflection collected	4144
Independent reflections	3510 ($R_{int} = 0.0993$)
R indices	$R_1 = 0.061$, $\omega R_2 = 0.0919$

Table 8.5: Crystallographic data and structure refinemend for $Na[VO_2(salhyCONH_3)]\cdot H_2O\cdot MeOH$ (**21**)

Empirical formula	$C_{10}H_{14}N_3NaO_7V$
Molecular mass, g/mol	362.17
Temperature, K	183(2)
Wavelength, Å	0.71073
Crystal system, Space group	monoclinic , $P2_1/n$
Unit cell dimensions,	
a, pm; α, °	736.39(2), 90
b, pm; β, °	2350.31(9), 112.43(2)
c, pm; γ, °	886.87(4), 90
Cell volume, pm^3,	1418.86(9) x 10^6
Z	4
Calculated density, g/cm^3	1.695
Absorbtion coefficient, mm^{-1}	0.769
F(000)	740
Crystal size, mm	0.04 x 0.04 x 0.04
θ range for data collection, °	2.63 – 27.48
Index ranges	$-8 \leq h \leq 9$,$-27 \leq k \leq 30$, $-11 \leq l \leq 9$
Reflection collected	3105
Independent reflections	2397 ($R_{int} = 0.1056$)
R indices	$R_1 = 0.060$, $\omega R_2 = 0.097$

Table 8.6: Crystallographic data and structure refinemend for $[MoO_2(salhyBocala)(MeOH)]\cdot 2MeOH$ (**36**)

Empirical formula	$C_{18}H_{31}N_3O_9Mo$
Molecular mass, g/mol	529.40
Temperature, K	183(2)
Wavelength, Å	0.71073
Crystal system, Space group	monoclinic, $P2_1/n$
Unit cell dimensions,	
a, pm; α, °	1070.90(4), 90
b, pm; β, °	998.79(5), 95.154(3)
c, pm; γ, °	2294.81(9), 90
Cell volume, pm^3,	2444.61(18) x 10^6
Z	4
Calculated density, g/cm^3	1.438
Absorbtion coefficient, mm^{-1}	0.585
F(000)	1096
Crystal size, mm	0.03 x 0.03 x 0.03
θ range for data collection, °	2.03 – 27.48
Index ranges	$-13 \leq h \leq 13, -12 \leq k \leq 12,$ $-27 \leq l \leq 29$
Flack parameter	xx
Reflection collected	5568
Independent reflections	3537 ($R_{int} = 0.1041$)
R indices	$R_1 = 0.0470$, $\omega R_2 = 0.0880$

Table 8.7: Crystallographic data and structure refinemend for $[MoO_2(Brsalhyleuacac)]\cdot MeOH$ (**37**)

Empirical formula	$C_{19}H_{26}BrN_3O_6Mo$
Molecular mass, g/mol	568.28
Temperature, K	183(2)
Wavelength, Å	0.71073
Crystal system, Space group	monoclinic , $C2_c$
Unit cell dimensions,	
a, pm; α, °	2223.95(12), 90
b, pm; β, °	782.34(6), 108.47(4)
c, pm; γ, °	264.83(2), 90
Cell volume, pm^3,	4370.4(5) x 10^6
Z	8
Calculated density, g/cm^3	1.727
Absorbtion coefficient, mm^{-1}	2.469
F(000)	2288
Crystal size, mm	0.04 x 0.04 x 0.03
θ range for data collection, °	2.78 – 27.47
Index ranges	$-27 \leq h \leq 27$,$-10 \leq k \leq 8$, $-26 \leq l \leq 34$
Flack parameter	x
Reflection collected	4770
Independent reflections	3015 ($R_{int} = 0.103$)
R indices	$R_1 = 0.0471$, $\omega R_2 = 0.086$

Table 8.8: Crystallographic data and structure refinemend for $[MoO_2(Mesalhypheacac)(\cdot MeOH)]\cdot 2MeOH$ (**39**)

Empirical formula	$C_{25}H_{35}N_3O_8Mo$
Molecular mass, g/mol	601.50
Temperature, K	183(2)
Wavelength, Å	0.71073
Crystal system, Space group	monoclinic , $C2$
Unit cell dimensions,	
a, pm; α, °	3190.35(16), 90
b, pm; β, °	849.18(4), 94.224(3)
c, pm; γ, °	1043.82(4), 90
Cell volume, pm^3,	2820.2(2) x 10^6
Z	4
Calculated density, g/cm^3	1.417
Absorbtion coefficient, mm^{-1}	0.515
F(000)	1248
Crystal size, mm	0.04 x 0.04 x 0.03
θ range for data collection, °	3.13 – 27.46
Index ranges	$-36 \leq h \leq 41$,$-11 \leq k \leq 10$, $-13 \leq l \leq 11$
Flack parameter	0.10
Reflection collected	6055
Independent reflections	5001 ($R_{int} = 0.063$)
R indices	$R_1 = 0.043$, $\omega R_2 = 0.081$

Table 8.9: Crystallographic data and structure refinemend for [MoO_2(Mesalhytyracac)(·MeOH)] ·2MeOH·Et_2O (**42**)

Empirical formula	$C_{29}H_{44}N_3O_{10}Mo$
Molecular mass, g/mol	690.61
Temperature, K	183(2)
Wavelength, Å	0.71073
Crystal system, Space group	orthorhombic, $P2_12_12_1$
Unit cell dimensions,	
a, pm; α, °	833.45(2), 90
b, pm; β, °	1919.70(6), 90
c, pm; γ, °	2127.62(6), 90
Cell volume, pm^3,	3404.14(16) x 10^6
Z	4
Calculated density, g/cm^3	1.348
Absorbtion coefficient, mm^{-1}	0.515
F(000)	0.440
Crystal size, mm	0.04 x 0.04 x 0.03
θ range for data collection, °	2.12 – 27.47
Index ranges	$-10 \leq h \leq 10$,$-24 \leq k \leq 23$, $-26 \leq l \leq 27$
Flack parameter	0.00(4)
Reflection collected	7744
Independent reflections	5886 ($R_{int} = 0.0776$)
R indices	$R_1 = 0.0486$, $\omega R_2 = 0.0917$

Part II

Abbreviations

ala	alanine
br	brout
Br-TMB	1-bromo-2,4,6-trimethoxybenzene
ClPOs	chloroperoxidases
DMF	N,N-dimethylformamid
DMSO	dimethylsulfoxid
EtOH	ethanol
Hacac	acetylalcetone
His	histidine
Leu	leucine
Lys	lysine
MCD	monochlordimedone
Me	methyl
MeCN	acetonitrile
MeOH	methanol
$MoO_2(acac)_2$	bis (acetylacetonato) dioxomolybdenum(VI)
MS	mass spectrometry
NMR	nuclear magnetic resonance
Ph	phenyl Phe phenylalanine
q	quartet (NMR)
s	singlet (NMR)
Ser	serine
t	triplet (NMR)
TFA	trifluoro acetic acid
TLC	thin layer chromatography
TMB	1,3,5-trimethoxybenzene
TOF	turnover frequences
Trp	tryptophan
Tyr	tyrosine
UV-Vis	ultraviolet visible (spectroscopy)
V-BrPOs	vanadium-bromoperoxidases

V-ClPOs	vanadium-chloroperoxidase
V-HPOs	vanadium haloperoxidases

Bibliography

[1] D. Rehder, The coordination chemistry of vanadium as related to its biological functions, *Coord. Chem. Rev.* **1999**, *182*, 297–322.

[2] R. J. Lancashire, *http://wwwchem.uwimona.edu.jm/courses/vanadium.html* .

[3] R. E. Eady, Amavadin, the vanadium compound of Amanitae, in H. Sigel, A. Sigel (Editors) *Metals ions in biological systems 31*, 364–405, Marcel Dekker, Inc., New York **1995**.

[4] H. Vilter, Peroxidases from phaeophyceae: A vanadium(V)-dependent peroxidase from Ascophyllum nodosum, *Phytochem.* **1984**, *23*, 1387–1390.

[5] N. Itoh, Y. Izumi, H. Yamata, Purification of Bromoperoxidase form Corallina Pilijlifera, *Biochem. Biophys. Res. Commun.* **1985**, *131*, 428–435.

[6] R. Wever, W. Hemrika, Vanadium haloperoxidases, in A. Messerschmidt, R. Huber, T. Poulos, K. Wieghardt (Editors) *Handbook of Metalloproteins 2*, 1417–1428, John Wiley & Sons Ltd., Chichester **2001**.

[7] E. Bayer, H. Kneifel, Isolation of amavadin, a vanadium compound occurring in Amanita muscaria., *Z. Naturforsch. B* **1972**, *27*, 207.

[8] A. Butler, C. Carrano, Coordination Chemistry of Vanadium in Biological systems, *Coord. Chem. Rev.* **1991**, *109*, 61–105.

[9] E. Heath, O. Howarth, Vanadium–51 and Oxygen–17 Nuclear Magnetic Resonance Study of Vanadate(V) Equilibra and Kinetics, *J. Chem. Soc., Dalton Trans.* **1981**, 1105–1110.

[10] D. Rehder, C. Weidemann, A. Duch, W. Priebsch, ^{51}V Shielding in Vanadium(V) Complexes: A Reference Scale for Vanadium Binding Sites in Biomolecules, *Inorg. Chem.* **1988**, *27*, 584–587.

[11] W. Wiesner, K. H. V. Pée, F. Lingens, Purification and Characterization of a Novel Bacterial Non-heme Chloroperoxidase from Pseudomonas pyrrocinia, *J. Biol. Chem* **1988**, *263*, 13725–13732.

[12] L. P. Hager, D. R. Morris, F. S. Brown, H. Eberwein, Chloroperoxidase .2. Ultilization of Halogen Anions, *J. Biol. Chem.* **1966**, *241*, 1769–1777.

[13] J. Zeng, R. E. Fenna, X-ray Crystal Structuroe of Canine Myeloperoxidase at 3 Å Resolution, *J. Mol. Biol.* **1992**, *226*, 185–207.

[14] E. de Boer, K. Boon, R. Wever, Electron-paramagnetic resonance studies on conformational states and metal-ion exchange properties of vanadium bromoperoxidase, *Biochemistry* **1988**, *27*, 1629–1635.

[15] J. M. Arber, E. de Boer, C. D. Garner, S. S. Hasnain, R. Wever, Vanadium K-Edge X-ray Absorption Spectroscopy of Bromoperoxidase from Ascoph yllum nodosum, *Biochemistry* **1989**, *28*, 7968–7973.

[16] J. W. P. M. V. Schijndel, P. Barnett, J. Roelse, E. G. M. Vollenbroek, R. Wever, The stability and steady-state kinetics of vanadium chloroperoxidase from the fungus Cuwularia inaequalis, *Eur. J. Biochem* **1994**, *225*, 151–157.

[17] D. OHagan, C. Schaffrath, S. L. Cobb, J. T. G. Hamilton, C. D. Murphy, *Nature* **2002**, *416*, 279.

[18] A. Messerschmidt, R. Wever, X-ray structures of apo and tungstate derivatives of vanadium chloroperoxidase from the fungus Curvularia inaequalis, *Inorg. Chim. Acta* **1998**, *273*, 160–166.

[19] A. Messerschmidt, R. Wever, X-ray structure of a vanadium-containing enzyme: Chloroperoxidase from the fungus Curvularia inaequalis, *Proc. Natl. Acad. Sci. U.S.A.* **1996**, *93*, 392–396.

[20] A. Messerschmidt, L. Prade, R. Wever, Implications for the catalytic mechanism of the vanadium-containing enzyme chloroperoxidase from the fungus Curvularia inaequalis by X-ray structures of the native and peroxide form, *Biol. Chem.* **1997**, *378*, 309–315.

[21] A. Butler, J. V. Walker, Marine Haloperoxidases, *Chem. Rev.* **1993**, *93*, 1937–1944.

[22] A. Butler, Mechanistic considerations of the vanadium haloperoxidases, *Coord. Chem. Rev.* **1999**, *187*, 17–35.

[23] A. Butler, C. J. Carrano, Coordination chemistry of vanadium in biological systems, *Coord. Chem. Rev.* **1991**, *109*, 61–105.

[24] B. F. Sels, D. E. D. Vos, M. Buntinx, P. A. Jacobs, Transition metal anion exchanged layered double hydroxides as a bioinspired model of vanadium bromoperoxidase, *Journal of Catalysis* **2003**, *216*, 288–297.

[25] M. Andersson, A. Willetts, S. Allenmark, Asymmetric Sulfoxidation Catalyzed by a Vanadium-Containing Bromoperoxidase, *J. Org. Chem.* **1997**, *62*, 8455–8458.

[26] H. B. ten Brink, A. Tuynman, H. L. Dekker, W. Hemrika, Y. Izumi, T. Oshiro, H. E. Schoemaker, R. Wever, Enantioselective Sulfoxidation Catalyzed by Vanadium Haloperoxidases, *Inorg. Chem.* **1998**, *37*, 6780–6784.

[27] M. A. Andersson, S. G. Allenmark, Asymmetric sulfoxidation catalyzed by a vanadium-containing bromoperoxidase: Substrate requirements of the catalyst, *Tetrahedron* **1998**, *54*, 15293–15304.

[28] H. B. ten Brink, H. E. Schoemaker, R. Wever, Sulfoxidation mechanism of vanadium bromoperoxidase from Ascophyllum nodosum-Evidence for direct oxygen transfer catalysis, *Eur. J. Biochem.* **2001**, *268*, 132–138.

[29] J. S. Martinez, G. L. Carroll, R. A. Tschirret-Guth, G. Altenhoff, R. D. Little, A. Butler, On the Regiospecificity of Vanadium Bromoperoxidase, *J. Am. Chem. Soc.* **2001**, *123*, 3289–3294.

[30] M. Weyand, H.-J. Hecht, M. Kiess, M.-F. Liaud, H. Vilter, D. Schomburg, X-ray Structure Determination of a Vanadium-dependent Haloperoxidase from Ascophyllum nodosum at 2.0 *Å* Resolution, *J. Mol. Biol.* **1999**, *293*, 595–611.

[31] O. Herzberg, P. Reddy, S. Sutrina, J. M. H. Saier, J. Reizer, G. Kapadia, *Proc. Natl. Acad. Sci. USA* **1992**, *89*, 2499–2503.

[32] J. M. Denu, D. L. Lohse, J. Vijayalakshmi, M. A. Saper, J. E. Dixon, Visualization of intermediate and transition-state structures in protein-tyrosine phosphatase catalysis, *Proc. Natl. Acad. Sci. U.S.A.* **1996**, *93*, 2493–2498.

[33] M. Zhang, M. Zhou, R. L. V. Etten, C. V. Stauffacher, Crystal structure of bovine low molecular weight phosphotyrosyl phosphatase complexed with the transition state analog vanadate, *Biochemistry* **1997**, *36*, 15–23.

[34] Y. Lindqvist, G. Schneider, P. Vihko, Crystal-structures of rat acid-phosphatase complexed with the transition-state analogs vanadate and molybdate-implications for the reaction-mechanism, *Eur. J. Biochem.* **1994**, *221*, 139–142.

[35] D. Rehder, C. Schulzke, H. Dau, C. Meinke, J. Hanss, M. Epple, Water and bromide in the active center of vanadate-dependent haloperoxidases, *J. Inorg. Biochem.* **2000**, *80*, 115–121.

[36] H. Schmidt, I. Andersson, D. Rehder, L. Pettersson, Speciation in the vanadatealanylhistidineperoxide system, *J. Inorg. Biochem.* **2000**, *80*, 149–151.

[37] C. Slebodnick, B. J. Hamstra, V. L. Pecoraro, Modeling the Biological Chemistry of Vanadium, in *Structure and Bonding, Vol. 89*, 78–94, Springer Verlag, Berlin **1997**.

[38] N. Julien-Caitol, E. Rose, J. Vaisserman, D. Rehder, An unusual anionic oxo-(μ-oxo)-vanadium(V) network interlinked by cationic sodium chains, *J. Chem. Soc., Dalton Trans.* **1996**, 2111–2115.

[39] P. Noblia, E. J. Baran, L. Otero, P. Draper, H. Cerecetto, M. Gonzalez, O. E. Piro, E. E. Castellano, T. Inohara, Y. Adachi, H. Sakurai, D. Gambino, New Vanadium(V) Complexes with Salicylaldehyde Semicarbazone Derivatives: Synthesis, Characterization, and in vitro Insulin-Mimetic Activity Crystal Structure of [V(V)O_2(salicylaldehyde semicarbazone)], *Eur. J. Inorg. Chem.* **2004**, 322–328.

[40] V. Vergopoulos, W. Priebsch, M. Fritzsche, D. Rehder, Binding of L-Histidine to Vanadium. Structure of exo-[VO_2N-(2-oxidonaphthal)-His, *Inorg. Chem.* **1993**, *32*, 1844–1849.

[41] S. Nica, *Bioinspired Model Complexes For Vanadium Haloperoxidases*, Ph.D. thesis, Friedrich-Schiller Universität Jena, Jena **2005**.

[42] A. Pohlmann, S. Nica, T. K. K. Luong, W. Plass, Dioxovanadium(V) complexes with side chain substituted *N*-salicylidenehydrazides modelling supramolecular interactions in vanadium haloperoxidases, *Inorg. Chem. Comm.* **2005**, *8*, 289–292.

[43] M. Casny, D. Rehder, Towards hydroperoxovanadium complexes: the X-ray crystal structure of a peroxovanadium(V) complex containing a V(O_2)(RCO_2H)(H_2O)$_2$ cluster with hydrogen bond inter-linkages, *Chem. Commun. (Cambridge, U. K.)* **2001**, 921–922.

[44] C. Kimblin, X. Bu, A. Butler, Modeling the Catalytic Site of Vanadium Bromoperoxidase: Synthesis and Structural Characterization of Intramolecularly H-bonded Vanadium(V) Oxoperoxo Complexes, $[VO(O_2)(NH_2pyg_2)]K$ and $[VO(O_2)(BrNH_2pyg_2)]K$, *Inorg. Chem.* **2002**, *41*, 161–163.

[45] A. Pohlmann, *Wasserstoffbrückenbindungen in Übergangsmetallkomplexen*, Ph.D. thesis, Universität Siegen, Siegen **2002**.

[46] K. Nakajima, M. Kojima, K. Toriumi, K. Saito, J. Fujita, Crystal Structures of [VO(sal-L-ala)$(OCH_3)(CH_3OH]$(sal-L-ala= *N*-salicylidene-L-alaninate) and $[VO(sal\text{-}L\text{-}ala)]_2O_2$. $2CH_2Cl_2$, and the Catalytical Activity of These and Related Complexes on Asymmetric Oxidation of Methyl Phenyl Sulfide with *t*-Butyl Hydroperoxide, *Bull. Chem. Soc. Jpn.* **1989**, *62*, 760–767.

[47] R. Hämäläinen, U. Turpeinen, A. M., Structure of Aquaoxo(*N*-salicylidene-L-alaninato) vanadium(IV), *Acta Crystallogr., Sect. C,* **1985**, *41*, 1726–1728.

[48] I. Cavaco, J. C. Pessoa, S. M. Luz, M. T. Duarte, *N*-SalicylideneAmino-acidate complexes of oxovandium (IV). Synthesis, characterization and deamination of an *N*-salicylideneglycylglycinato complex., *Polyhedron* **1995**, *14*, 429–439.

[49] I. Cavaco, J. C. Pessoa, M. T. Duarte, R. T. Henriques, P. M. Matias, R. D. Gillard, Crystal and molecular structure of $[V_2O_3(sal\text{-}L\text{-}Val)_2(H_2)]$ (sal-L-val=*N*-salicylidene-L-valinate) and spectroscopic properties of related complexes, *J. Chem. Soc., Dalton Trans.* **1996**, 1989–1996.

[50] I. Cavaco, J. C. Pessoa, M. T. Duarte, R. D. Gillard, P. Matias, Molecular structure of [VO(sal-D,L-Asn)(py)(H_2O)]and reaction to produce coumarin-3-carboxamide, *Chem. Commun. (Cambridge, U. K.)* **1996**, 1365–1367.

[51] W. Chen, S. Gao, S.-X. Liu, Monooxovanadium(V) complexes with bidentate N-phenylbenzohydroxamate, *Acta Crystallogr., Sect. C: Cryst. Struct. Commun.* **1999**, *55*, 531–533.

[52] J. C. Pessoa, I. Cavaco, I. Correia, M. T. Duarte, R. D. Gillard, R. T. Henriques, F. J. Higes, C. Madeira, I. Tomaz, Preoaration and characterization of new oxovanadium(IV) Schiff base complexes derived from amino acids and aromatic *o*-hydroxyaldehydes, *Inorg. Chim. Acta* **1999**, *293*, 1–11.

[53] J. C. Pessoa, I. Cavaco, I. Correia, D. Costa, R. T. Henriques, R. D. Gillard, Preparattion and characterization of new oxovanadium (IV) Schiff base complexes derived from salicylaldehyde and simple dipeptides, *Inorg. Chim. Acta* **2000**, *305*, 7–13.

[54] S. Mondal, P. Ghosh, A. Chakravorty, A Family of α-Amino Acid Salicylaldiminates Incorporating the Binuclear $V_2O_3^{3+}$ Core: Electrosynthesis, Structure, and Metal Valence, *Inorg. Chem.* **1997**, *36*, 59–63.

[55] S. Mondal, S. P. Rath, K. K. Rajak, A. Chakravorty, A Family of (N-Salicylidene-α-amino acidato)vanadate Esters Incorporating Chelated Propane-1,3-diol and Glycerol: Synthesis, Structure, and Reaction, *Inorg. Chem.* **1998**, *37*, 1713–1719.

[56] S. W. Hon, C. H. Li, J. H. K. Kuo, N. B. Barhate, Y. H. Liu, Y. Wang, C. T. Chen, Catalytic Asymmetric Coupling of 2-Naphthols by Chiral Tridentate Oxovanadium(IV) Complexes, *Org. Lett.* **2001**, *3*, 869–872.

[57] J. C. Pessoa, M. T. Duarte, R. D. Gillard, C. Madeira, P. M. Matias, I. Tomaz, Preparation of [VO(sal-L-Trp)(H_2O)] (sal-L-Trp = *N*-salicylidene- L-tryptophanate) and characterisation of an unusual product obtained from its solutions in waterpyridine, *J. Chem. Soc., Dalton Trans.* **1998**, 4015–4020.

[58] M. Ebel, D. Rehder, Vanadium complexes with enamines having tyrosine constituents, *Inorg. Chim. Acta* **2003**, *356*, 210–214.

[59] C. D. Crans, H. Holst, D. A. Keramidas, D. Rehder, A Slow Exchanging Vanadium(V) Peptide Complex: Vanadium(V)-Glycine- Tyrosine, *Inorg. Chem.* **1995**, *34*, 2524–2534.

[60] R. Hille, *Chem. Rev.* **1996**, *96*, 2757–2816.

[61] J. B. Howard, D. C. Rees, Structural Basis of Biological Nitrogen Fixation, *Chem. Rev.* **1996**, *96*, 2965–2982.

[62] R. H. Holm, The Biologicaly relevant Oxygen Atom Transfer Chemistry of Molybdenum from Synthetic Analogue, *Coord. Chem. Rev.* **1990**, *100*, 183–221.

[63] R. H. Holm, P. Kennepohl, E. I. Solomon, Structural and Functional Aspects of Metal Sites in Biology, *Chem. Rev.* **1996**, *96*, 2239–2314.

[64] J.-M. Bregeault, Transition-metal complexes for liquid-phase catalytic oxidation: some aspects of industrial reactions and of emerging technologies, *Dalton Trans.* **2003**, 3289–3302.

[65] K. A. Jorgensen, Transition-Metal-Catalyzed Epoxidation, *Chem. Rev.* **1989**, *89*, 431–458.

[66] S. N. Rao, K. N. Munshi, N. N. Rao, Catalytic oxidation of styrene using *cis*-MoO_2(L)(solv) [L = salicylidene salicyloyl hydrazine] and its zeolite composite as catalysts in the presence of molecular oxygen, *J. Mol. Cat. A: Chem.* **2000**, *156*, 205–211.

[67] J. A. Brito, M. Gomez, G. Muller, H. Teruel, J.-C. Clinet, E. Dunach, M. A. Maestro, Structural Studies of Mono- and Dimetallic Mo^{VI} Complexes – A New Mechanistic Contribution in Catalytic Olefin Epoxidation Provided by Oxazoline Ligands, *Eur. J. Inorg. Chem.* **2004**, 4278–4285.

[68] S. Campestrini, V. Conte, F. D. Furia, G. Modena, Metal Catalysis in Oxidation by Peroxides. Electrophilic Oxygen Transfer from Anionic, Coordinatively Saturated Molybdenum Peroxo Complexes, *J. Org. Chem.* **1988**, *53*, 5721–5724.

[69] B. Meunier, *Metal-Oxo and Metal-Peroxo Species in Catalytic Oxidations*, Springer, Berlin **2000**.

[70] L. Stelzig, S. Kötte, B. Krebs, Molybdenum complexes with tridentate NS_2 ligands. Synthesis, crystal structures and spectroscopic properties, *Dalton Trans.* **1998**, 2921–2926.

[71] R. Dinda, P. Sengupta, H. Mayer-Figge, W. S. Sheldrick, A family of mononuclear molybdenum-(VI), and -(IV) oxo complexes with a tridentate (ONO) ligand, *J. Chem. Soc., Dalton Trans.* **2002**, 4434–4439.

[72] C. L. Copper, E. Koubek, Kinetics of the molybdate and tungstate catalyzed oxidation of iodide by hydrogen peroxide, *Inorg. Chim. Acta* **1999**, *288*, 229–232.

[73] G. E. Meister, A. Butler, Molybdenum(VI)- and Tungsten(VI)-Mediated Biomimetic Chemistry of Vanadium Bromoperoxidase, *Inorg. Chem.* **1994**, *33*, 3269–3275.

[74] M. S. Reynolds, K. J. Babinski, M. C. Bouteneff, J. L. Brown, R. E. Campbell, M. A. Cowan, M. R. Durwin, T. Foss, P. O'Brien, H. R. Penn, Kinetics of bromide oxidation by peroxo complexes of molybdenum(VI) and tungsten(VI), *Inorg. Chim. Acta* **1997**, *263*, 225–230.

[75] C. P. Rao, A. Sreedhara, P. V. Rao, M. B. Verghese, K. Rissanen, E. Kolehmainen, N. K. Lokanath, M. A. Sridhar, J. S. Prasad, Syntheses, structure, reactivity and species recognition studies of oxo-vanadium(V) and molybdenum(VI) complexes, *J. Chem. Soc., Dalton Trans.* **1998**, 2383–2393.

[76] H. Yu, J. W. Whittaker, Vanadate Activation of Bromoperoxidase from Corallina officinalis, *Biochem. Biophys. Res. Commun.* **1989**, *160*, 87–92.

[77] A. Butler, M. J. Clague, G. E. Meister, Vanadium Peroxide Complexes, *Chem. Rev.* **1994**, *94*, 625–638.

[78] C. J. Carrano, C. M. Nunn, R. Quan, J. A. Bonadier, V. L. Pecoraro, Coordination Chemistry of Zirconium Tetrachloride. Crystal Structure of the 1:2 Adduct with Pinacolone, *Inorg. Chem.* **1990**, *29*, 944–951.

[79] M. J. Clague, N. L. Keder, A. Butler, Biomimics of Vanadium Bromoperoxidase: Vanadium(V)- Schiff Base Catalyzed Oxidation of Bromide by Hydrogen Peroxide, *Inorg. Chem.* **1993**, *32*, 4754–4761.

[80] G. J. Colpas, B. J. Hamstra, J. W. Kampf, V. L. Pecoraro, Preparation of $V0^{3+}$ and VO^{2+} Complexes Using Hydrolytically Stable, Asymmetric Ligands Derived from Schiff Base Precursors, *Inorg. Chem.* **1994**, *33*, 4669–75.

[81] B. J. Hamstra, G. J. Colpas, V. L. Pecoraro, Reactivity of Dioxovanadium(V) Complexes with Hydrogen Peroxide: Implications for Vanadium Haloperoxidase, *Inorg. Chem.* **1998**, *37*, 949–955.

[82] W. Plass, Supramolecular interactions of vanadate species: vanadium(V) complexes with *N*-salicylidenehydrazides as versatile models, *Coord. Chem. Rev.* **2003**, *237*, 205–212.

[83] C. R. Cornman, K. M. Geiser-Bush, S. P. Rowley, P. D. Boyle, Reactivity of Dioxovanadium(V) Complexes with Hydrogen Peroxide: Implications for Vanadium Haloperoxidase, *Inorg. Chem.* **1997**, *36*, 6401–6408.

[84] W. Plass, H.-P. Yozgatli, Synthesis, Reactivity, and Structural Characterization of Dioxovanadium(V) Complexes with Tridentate Schiff Base Ligand: Vanadium Complexes in Supramolecular Networks, *Z. Anorg. Allg. Chem.* **2003**, *629*, 65–70.

[85] G. Asgedom, A. Sreedhara, J. Kivikoski, E. Kolehmainen, C. P. Rao, Structure, characterization and photoreactivity of monomeric dioxovanadium(V) Schiff-base complexes of trigonal-bipyramidal geometry, *J. Chem. Soc., Dalton Trans.* **1996**, 93–97.

[86] M. Melchior, K. H. Thompson, J. M. Jong, S. J. Rettig, E. Shuter, V. G. Yuen, Y. Zhou, J. H. McNeill, C. Orvig, Vanadium Complexes as Insulin Mimetic Agents: Coordination Chemistry and in Vivo Studies of Oxovanadium(IV) and Dioxovanadate(V) Complexes Formed from Naturally Occurring Chelating Oxazolinate, Thiazolinate, or Picolinate Units, *Inorg. Chem.* **1999**, *38*, 2288–2293.

[87] W. John, J. Ledbetter, Infrared Spectra of *N*-Aryl Imines of o-Hydroxybenzaldehyde between 2000 and 1500 cm^{-1}, *J Phys. Chem.* **1977**, *81*, 54–59.

[88] L. Casella, M. Gullotti, Coordination Modes of Histidine. Stereochemistry of the Reaction between Histidine Derivatives and Pyridoxal Analogues. Conformational Properties of Zinc(II) Complexes of Histidine Schiff Bases, *J. Am. Chem. Soc.* **1981**, *103*, 6338.

[89] A. D. Keramidas, A. B. Papaioannou, A. Vlahos, T. A. Kabanos, G. Bonas, A. Makriyannis, C. P. Rapropoulou, A. Terzis, Model Investigations for Vanadium-Protein Interactions. Synthetic, Structural, and Physical Studies of Vanadium(III) and Oxovanadium(IV/V) Complexes with Amidate Ligands, *Inorg. Chem.* **1996**, *35*, 357–367.

[90] M. R. Maurya, S. Khurana, C. Schulzke, D. Rehder, Dioxo- and Oxovanadium(V) Complexes of Biomimetic Hydrazone *ONO* Donor Ligands: Synthesis, Characterisation, and Reactivity, *Eur. J. Inorg. Chem.* **2001**, 779–788.

[91] M. R. Maurya, S. Khurana, W. Zhang, D. Rehder, Vanadium(IV/V) Complexes Containing $[VO]^2$, $[VO]^3$, $[VO_2]$ and $[VO(O_2)]$ Cores with Ligands Derived from 2-Acetylpyridine and S-Benzyl- or S-Methyldithiocarbazate, *Eur. J. Inorg. Chem.* **2002**, 1749–1760.

[92] A. Butler, A. H. Baldwin, Vanadium Bromoperoxidase and Functional Mimics, in *Structure and Bonding, Vol. 89*, 109–132, Springer Verlag, Berlin, Heidelberg **1997**.

[93] R. I. de la Rosa, M. J. Clague, A. Butler, A Functional Mimic of Vanadium Bromoperoxidase, *J. Am. Chem. Soc.* **1992**, *114*, 760–761.

[94] X. Zhang, W.-D. Woggon, A Supramolecular Fluorescence Sensor for Pyrovanadate as a Functional Model of Vanadium Haloperoxidase, *J. Amer. Chem. Soc.* **2005**, *127*, 14138–14139.

[95] J. Sun, C. Zhu, Z. Dai, M. Yang, Y. Pan, H. Hu, Efficient Asymmetric Oxidation of Sulfides and Kinetic Resolution of Sulfoxides Catalyzed by a Vanadium-Salan System, *J. Org. Chem.* **2004**, *69*, 8500–8503.

[96] N. N. Karpyshev, O. D. Yakovleva, E. P. Talsi, K. P. Bryliakov, O. V. Tolstikova, A. G. Tolstikov, Effect of portionwise addition of oxidant in asymmetric vanadium-catalyzed sulfide oxidation, *J. Mol. Cat. A: Chem.* **2000**, *157*, 91–95.

[97] C. Bolm, F. Bienewald, Asymmetrische Sulfid-Oxidation mit Vanadium-Katalysatoren und H2O2, *Angew. Chem.* **1995**, *107*, 2883–2385.

[98] C. Bolm, T. K. K. Luong, K. Harms, Bis-[2-oxazolinyl phenolato] oxovanadium(IV) complexes: synthesis, crystal stuctures and catalyses, *Chem. Ber.* **1997**, *130*, 887–890.

[99] T. S. Smith, V. L. Pecoraro, Oxidation of Organic Sulfides by Vanadium Haloperoxidase Model Complexes, *Inorg. Chem.* **2002**, *41*, 6754–6760.

[100] S. W. Taylor, B. Kammerer, E. Bayer, New Perspectives in the Chemistry and Biochemistry of the Tunichromes and Related Compounds, *Chem. Rev.* **1997**, *97*, 333–346.

[101] A. S. Tracey, J. M. Gresser, J. Michael, Interaction of Vanadate with Phenol and Tyrosine: Implication for the Effects of Vanadate on Systems Regulated by Tyrosine Phosphorylation, *Proc. Natl. Acad. Sci. U.S.A.* **1986**, *83*, 609–613.

[102] L. A. Carpino, M. E. E.-S. Mansour, A. El-Faham, Bis(Boc) Amino Acid Fluorides as Reactive Peptide Coupling Reagents, *Adv. Synth. Catal.* **1993**, *58*, 4162–4164.

[103] J. T. Su, P. Vachal, E. N. Jacobsen, Practical Synthesis of a Soluble Schiff Base Catalyst for the Asymmetric Strecker Reaction, *Adv. Synth. Catal.* **2001**, *343*, 197–200.

[104] R. Braslau, M. O. Anderson, F. Rivera, A. Jimenez, T. Haddad, J. R. Axon, Acyl hydrazines as precursors to acyl radicals, *Tetrahedron* **2002**, *58*, 5513–5523.

[105] M. Dymicky, Preparation of Carbobenzoxy-L-Tyrosine Methyl and Ethyl Esters and of the corresponding Carbobenzoxy Hydrazides., *Organic Preparations and Procedures Int.* **1989**, *21*, 83–90.

[106] D. Ranganathan, N. K. Vaish, K. Shah, Protein Backbone Modification by Novel C^{α}–C Side-Chain Scission, *J. Amer. Chem. Soc.* **1994**, *116*, 6545–6557.

[107] U. Schmidt, A. Lieberknecht, J. Wild, Didehydroamino Acids (DDAA) and Didehydropeptides (DDP), *Synthesis* **1988**, 159–172.

[108] G. Jung, Lantibiotics-Ribosomally Synthesized Biologically Active Polypeptides containing Sulfide Bridges and α, β-Didehydroamino Acids, *Angew. Chem., Int. Ed. Engl.* **1991**, *30*, 1051–1068.

[109] X. Wang, X. M. Zhang, H. X. Liu, Synthesis, characterisation and crystal structure of two *cis*-dioxo vanadium(V) complexes of monoanionic tridentate Schiff base ligands, *Inorg. Chim. Acta* **1994**, *223*, 193–197.

[110] W. Plass, A. Pohlmann, H.-P. Yozgatli, *N*-Salicylidenehydrazides as versatile tridentate ligands for dioxovanadium(V) complexes, *J. Inorg. Biochem.* **2000**, *80*, 181–183.

[111] M. Casný, D. Rehder, Molecular and supramolecular features of oxo-peroxovanadium complexes containing O3N, O2N2 and ON3 donor sets, *Dalton Trans.* **2004**, 839–846.

[112] M. R. Maurya, S. Agarwal, C. Bader, M. Ebel, D. Rehder, Synthesis, characterisation and catalytic potential of hydrazonatovanadium(V) model complexes with $[VO]^{3+}$and $[VO_2]^{+}$ cores., *Dalton Trans.* **2005**, 537–544.

[113] M. R. Maurya, S. Agarwal, C. Bader, D. Rehder, Dioxovanadium(V) Complexes of ONO Donor Ligands Derived from Pyridoxal and Hydrazides: Models of Vanadate-Dependent Haloperoxidases, *Eur. J. Inorg. Chem.* **2005**, 147–157.

[114] S. Macedo-Ribeiro, W. Hemrika, R. Renirie, R. Wever, A. Messerschmidt, X-ray crystal structures of active site mutants of the vanadium-containing chloroperoxidase from the fungus Curvularia inaequalis, *J. Biol. Inorg. Chem.* **1999**, *4*, 209–219.

[115] W. Hemrika, R. Renirie, S. Macedo-Ribeiro, A. Messerschmidt, R. Wever, Heterologous Expression of the Vanadium-containing Chloroperoxidase from Curvularia inaequalis in Saccharomyces cerevisiae and Site-directed Mutagenesis of the Active Site Residues His496, Lys353, Arg360, and Arg490, *J. Biol. Chem.* **1999**, *274*, 23820–23827.

[116] H. Schmidt, I. Andersson, D. Rehder, L. Pettersson, A Potentiometric and ^{51}V NMR Study of the Aqueous $H^{+}/H_2VO_4^{-}/H_2O_2$ /L-α-Alanyl-L-histidine System, *Chem. Eur. J.* **2001**, *7*, 251–257.

[117] G. Socrates, *Infrared and Raman Characteristic Group Frequnecies*, John Wiley and Sons Ltd., Chichester **2001**.

[118] L. E. Sayed, M. F. Iskander, Coordination compounds of hydrazine derivatives with transition metals. The reaction of aroyl hydrazones with Ni(II) and Cu(II) salts, *J. Inorg. Nucl. Chem.* **1971**, *33*, 435–443.

[119] M. F. Iskander, L. E. Sayed, N. M. H. Salem, W. Haase, H. J. Linder, S. Foro, Synthesis, characterization and magnetochemical studies of some copper(II) complexes derived from n-salicylidene-n-alkanoylhydrazins: X-ray crystal and molecular structure of bis [monochloro-(-n-salicylidenemyristoylhydrazine)ono(-1)] dicopper(II), *Polyhedron* **2004**, *23*, 23–31.

[120] R. R. Everett, H. S. Soedjak, A. Butler, Mechanism of Dioxygen Formation Catalyzed by Vanadium Bromoperoxidase, *J. Biol. Chem.* **1990**, *265*, 15671–15679.

[121] A. Butler, J. Carter, M. Simpson, *Handbook on Metallproteins*, Marcel Dekker, Inc., New York-Basel **2001**.

[122] A. G. J. Ligtenbarg, R. Hage, B. L. Feringa, Catalytic oxidations by vanadium complexes, *Coord. Chem. Rev.* **2003**, *237*, 89–101.

[123] G. J. Colpas, B. J. Hamstra, J. W. Kampf, V. L. Pecoraro, Functional Models for Vanadium Haloperoxidase: Reactivity and Mechanism of Halide Oxidation, *J. Am. Chem. Soc.* **1996**, *118*, 3469–3478.

[124] V. Conte, O. Bortolini, M. Carraro, S. Moro, Models for the active site of vanadium-dependent haloperoxidases: insight into the solution structure of peroxo vanadium compounds, *J. Inorg. Biochem.* **2000**, *80*, 41–49.

[125] M. J. Clague, A. Butler, On the Mechanism of cis-Dioxovanadium(V)-Catalyzed Oxidation of Bromide by Hydrogen Peroxide: Evidence for a Reactive, Binuclear Vanadium(V) Peroxo Complex, *J. Am. Chem. Soc.* **1995**, *117*, 3475–3484.

[126] H. S. Soedjak, A. Butler, Chlorination Catalyzed by Vanadium Bromoperoxidase, *Inorg. Chem.* **1990**, *29*, 5015–17.

[127] R. R. Everett, J. R. Kanofskyen, A. Butler, Mechanistic Investigations of the Novel Nonheme Vanadium Bromoperoxidases, *J. Biol. Chem.* **1990**, *265*, 4908–4914.

[128] C. Slebodnick, V. L. Pecoraro, Solvent effects on $^{5}1$V NMR chemical shifts: characterization of vanadate and peroxovanadate complexes in mixed water/acetonitrile solvent, *Inorg. Chim. Acta* **1998**, *283*, 37–43.

[129] X. an Zhang, W.-D. Woggon, A Supramolecular Fluorescence Sensor for Pyrovanadate as a Functional Model of Vanadium Haloperoxidase, *J. Am. Chem. Soc.* **2005**, *127*, 14138–14139.

[130] D. Collison, C. D. Garner, J. A. Joule, The Structure and Mode of Action of the Cofactor of the Oxomolybdoenzymes, *Chem. Soc. Rev.* **1996**, *25*.

[131] J. Liimatainen, A. Lehtonen, R. Sillanpaa, *cis*-Dioxomolybdenum(VI) complexes with tridentate and tetradentate Schiff base ligands. Preparation, structures and inhibition of aerial oxidation of aldehydes, *Polyhedron* **2000**, *19*, 1133–1138.

[132] R. K. Grasselli, Advances and future trends in selective oxidation and ammoxidation catalysis, *Catal. Today* **1999**, *49*, 141–153.

[133] R. J. Cross, P. D. Newman, R. D. Peacock, D. Stirling, Chiral phosphinoylalcohol complexes of monooxobis(peroxo)molybdenum(VI) and their use as asymmetric oxidants, *J. Mol. Catal. A* **1999**, *144*, 273–284.

[134] J. Belgacem, J. Kress, J. A. Osborn, On the Allylic Rearrangements in Metal Oxo Complexes: Mechanistic and Catalytic Studies on $MoO_2(allyloxo)_2(CH_3CN)_2$ alogous Complexes, *J. Am. Chem. Soc.* **1992**, *114*, 1501–1502.

[135] B. E. Schultz, R. H. Holm, Kinetics of oxygen-atom transfer in an analog reaction system of the molybdenum oxotransferase, *Inorg. Chem.* **1993**, *32*, 4244–4248.

[136] C. Lorber, M. R. Plutino, L. I. Elding, E. Nordlander, Kinetics of oxygen-atom transfer reactions involving molybdenum dithiolene complexes, *J. Chem. Soc., Dalton Trans.* **1997**, 3997–4003.

[137] H. Oku, N. Ueyama, M. Kondo, A. Nakamura, Oxygen Atom Transfer Systems in Which the (p-Oxo)dimolybdenum(V) Complex Formation Does Not Occur: Syntheses, Structures, and Reactivities of Monooxomolybdenum(IV) Benzenedithiolato Complexes as Models of Molybdenum Oxidoreductases, *Inorg. Chem.* **1994**, *33*, 209–216.

[138] J. M. Berg, R. H. Holm, A model for the active-sites of oxo-transfer molybdoenzymes – reactivity, kinetics, and catalysis, *J. Am. Chem. Soc.* **1985**, *107*, 925–932.

[139] J. M. Berg, R. H. Holm, A Model for the Active Sites of Oxo-Transfer Molybdoenzymes: Synthesis, Structure, and Properties, *J. Am. Chem. Soc.* **1985**, *107*, 917–925.

[140] S. Ghosh, T. K. Bandyopadhyay, P. K. Ray, M. S. Mitra, Ligational Behavior of a Novel Biologically Active Donor Toward Cu(II) and Ni(II) Ions and Potentiation of Its Antibacterial Activity by Chelation with Metal Ions, *J. Inorg. Biochem.* **1984**, *20*, 79–86.

[141] N. S. Biradar, B. R. Havinale, Dimeric Square Planar Complexes of Cu(II) with Aroyl Hydrazones, *Inorg. Chim. Acta* **1976**, *17*, 157–160.

[142] S. Purohit, A. P. Koley, L. S. Prasad, P. T. Manoharan, S. Ghosh, Chemistry of Molybdenum with Hard-Soft Donor Ligands. 2.[1] Molybdenum(VI), -(V), and -(IV) Oxo Complexes with Tridentate Schiff Base Ligands, *Inorg. Chem.* **1989**, *28*, 3735–3745.

[143] F. J. Arnaiz, R. Aguado, M. R. Podrosa, A. D. Cian, J. Fischer, Synthesis, characterization and catalytic activity of addition compounds of dioxomolybdenum(VI) pyridine-2,6-dicarboxylate. Crystal structure of $MoO_2(dipic)(L)$ (L = DMF, DMSO, $OPPh_3$), *Polyhedron* **2000**, *19*, 2141–2147.

[144] A. Rana, R. Dinda, P. Sengupta, L. R. Falvello, S. Ghosh, Synthesis, characterisation and crystal structure of *cis*-dioxomolybdenum(VI) complexes of some potentially pentadentate but functionally tridentate (ONS) donor ligands, *Polyhedron* **2002**, *21*, 1023–1030.

[145] I. Buchanan, M. Minelli, M. Ashbya, J. King, J. Enemark, C. Garner, Crystal Structure and Spectroscopic Studies of $[MoO_2(L\text{-}cys0Me)_2]$, *Inorg. Chem.* **1984**, *23*, 495–500.

[146] S. K. Dutta, D. B. McConville, W. J. Youngs, M. Chaudhury, Reactivity of Mo-Ot Terminal Bonds toward Substrates Having Simultaneous Proton- and Electron-Donor Properties: A Rudimentary Functional Model for Oxotransferase Molybdenum Enzymes, *Inorg. Chem.* **1997**, *36*, 2517–2522.

[147] C. Bustos, O. Burckhardt, R. Schrebler, D. Carrillo, A. M. Arif, A. H. Cowley, C. M. Nunn, Synthesis, Characterization, and Electrochemistry of cis-Dioxomolybdenum(VI) Complexes of Schiff Bases Derived from Carbohydrazide, Thiocarbohydrazide, and Salicylaldehyde. Crystal Structures of [MoO_2(o-OC_6H_4CH=NN=CSNHN=CHC_6H_4OH-o)Me_2SO] and [$(MoO_2)_2$(o-OC_6H_4CH=NN=CONN=CHC_6H_4O-o) $(Me_2SO)_2$]·0.5Me_2S0, *Inorg. Chem.* **1990**, *29*, 3996–4001.

[148] G. Cliff, B. Fallon, K. Gathouse, P. Murray, P. Newman, Structure and Spectral and Redox Properties of a Dioxomolybdenum(VI) Chelate of *N*-Methyl-p-tolylthiohydroxamic Acid, a Complex Containing a $0_2Mo0_2S_2$ Donor Set, *Inorg. Chem.* **1980**, *19*, 773–775.

[149] E. Farkas, I. Sovago, Metal Complexes of Amino Acids and Peptides, in *Amino Acids, Peptides and Proteins*, volume 33, 295–364, The Royal Society of Chemistry **2002**.

Selbständigkeitserklärung

Ich erkläre, dass ich die vorliegende Arbeit selbständig und unter Verwendung der angegebenen Hilfsmittel, persönlichen Mitteilungen und Quellen angefertigt habe.

Ort, Datum Unterschrift des Verfassers/der Verfasserin

CURRICULUM VITAE

MANJOLA MANCKA
Am Herrenberge 11/517, D-07745 Jena, Germany
☎ +49 – (0)174 4492 161
Mancka.M@uni-jena.de

Civil status: married
Date of birth: 17.04.1978
Place of birth: Devoll-Albania
Nationality: Albanian

	SCHOOL
09/1984 – 06/1992	Elementary School in Devoll-Albania
09/1992 – 07/1996	Professional School "Food Chemistry" in Elbasan-Albania
	HIGH EDUCATION
09/1996 – 02/2002	Food Chemistry-Natural Science Faculty, University of Tirana; Bachelor of Science, Tirana-Albania
	Diploma-Food-Chemist
February 2002	*Final examination-Diploma*
04/2001 – 12/2001	Diploma Work in department of analytic chemistry at the University of Siegen, thesis: "Extraction of ß-carotenes from different plants and determination by spectrophotometry and high-pressure-liquid-chromatography (HPLC)" under the supervision of Prof. Dr. B. Wenclawiak, • Extraction of ß-carotenes with different extraction methods: Soxhlet, Ultrasonic extraction, Supercritical Fluid Extraction (SFE), and analyses with HLPC and UV-measurements.
Since 10/2002	University of Siegen, and Friedrich-Schiller University of Jena-Germany **Ph.D.** Scientific co-worker in the Institute of Inorganic Chemistry at the University of Siegen, and in the Institute of Analytic and Inorganic Chemistry at Friedrich-Schiller University of Jena, working group of Prof. Dr. W. Plass **Ph.D. thesis**: "Vanadium and Molybdenum Complexes with Amino Acid Functionalized Ligands" • Chemical syntheses of new cis-dioxovanadium, and cis-dioxomolybdenum complexes with amino acid

functionalized ligands, as model systems for the active centre of haloperoxidase enzymes
- Characterization of compounds using NMR, MS, UV-VIS, and IR techniques
- Characterization of structures with single crystal analysis
- Catalytic activity of these complexes towards oxidation of bromide by hydrogen peroxide, mimicking therefore, the biomimetic reaction of the enzymatic system (vanadium-containing haloperoxidases)
- Catalytic activity towards oxidation of organic sulfides. Design of chiral vanadium and molybdenum complexes for asymmetric catalytic oxidation of organic sulfides

POSITIONS, RESPONSIBILITIES & EXPERIENCE

Since 10/2002	Scientific co-worker in the Institute of Inorganic Chemistry at the University of Siegen, and Institute for Analytic and Inorganic Chemistry at Friedrich-Schiller University of Jena, Jena-Germany
06/2002 – 10/2002	Scientific assistant in the Institute of Analytic Chemistry at the University of Siegen, Siegen-Germany
03/2002 – 06/2002	Scientific co-worker in the Department of Biochemistry and Biophysics, Institute of Biological Research, Tirana-Albania
04/2001 – 12/2001	Scientific co-worker in the Institute of Analytic Chemistry at the University of Siegen, Siegen-Germany
01/2001	Theoretical Course on "Malting and Brewing Science" Delivered at the Faculty of Natural Science, University of Tirana by Prof. Dr. G. Derdelinckx from the Catholic University of Lueven-Belgium
09/2000	"Thermo-Fluid Dynamics", Summer Academy Ohrid 2000, in cooperation with the University of Erlangen-Nuremberg, and Augsburg, Ohrid-Macedonia

KNOWLEDGE

Computer Application	MS-Office XP, Origin, CS Chem. Draw, Corel Draw, Diamond, Latex, etc. Databases: CA, Beilstein-crossfire, Scie-Finder
Language	Albanian: mother tongue English: fluent (in spoken und written) German: good (in spoken und written) Italian: good (in spoken und written)
Hobby	Traveling and foreign cultures, Literature

Publications

1) M. Mancka, A. Buchholz und W. Plass,
Synthesis, Characterization, and Reactivity of Dioxo-Vanadium(V) Complexes with Free Amino Acid Functionalized Ligands.
Inorg. Chem. in preparation

2) M. Mancka, A. Buchholz and W. Plass,
Dioxo-Vanadium(V) Complexes with Protected Amino Acid Functionalized Ligands: Synthesis, Characterization, and Reactivity
Dalton Trans. in preparation.

3) M. Mancka, R. Debel and W. Plass,
Dioxo-Vanadium(V) Complexes with ß-alanine Functionalized Ligands as Model System for Vanadium Haloperoxidase Enzymes.
In preparation.

4) M. Mancka, and W. Plass,
Structural characterization and sulfoxidation reactions of dioxomolybdenum complexes with protected amino acid residue ligands.
In preparation.

5) M. Mancka and W. Plass,
Molybdenum(VI) dioxo complexes with amino acid side chain substituted N-salicylidenehydrazides: Synthesis and reactivity.
In preparation

Conferences

1) EURACHEM/D, GDCH, Siegen 2001, Germany (participate)

2) Wilnewski S., Mancka M., Pól J., Wenclawiak B.W., Extraction of Beta-Carotinoids from Vegetables (poster).
EuroConference: Modern Analytical Methods for Food and Beverage Authentication, Lednice, Czech Republic, August 29-31, 2002.

3) Mitteldeutsches Anorganiker Nachwuchssymposium (MANS);
Leipzig 2005, Germany (participate)

4) The 3*rd* international SFB Conference 2005 *Metal mediated reactions modeled after natyre*; September 2005, Jena- Germany (participate)

5) 2. Koordinationchemikertreffen Februar 2006, Göttingen-Germany. (oral presentation). *Vanadium complexes with amino acid functionalized ligands*

Place, Date Signature